



HAL
open science

Biotechnological Routes for obtaining high-added value compounds from residual biomass

Marcelo Avelar Do Nascimento

► **To cite this version:**

Marcelo Avelar Do Nascimento. Biotechnological Routes for obtaining high-added value compounds from residual biomass. Other. Centrale Lille Institut; Universidade federal do Rio de Janeiro, 2023. English. NNT : 2023CLIL0036 . tel-04609506

HAL Id: tel-04609506

<https://theses.hal.science/tel-04609506>

Submitted on 12 Jun 2024

HAL is a multi-disciplinary open access archive for the deposit and dissemination of scientific research documents, whether they are published or not. The documents may come from teaching and research institutions in France or abroad, or from public or private research centers.

L'archive ouverte pluridisciplinaire **HAL**, est destinée au dépôt et à la diffusion de documents scientifiques de niveau recherche, publiés ou non, émanant des établissements d'enseignement et de recherche français ou étrangers, des laboratoires publics ou privés.

CENTRALE LILLE

THESE

Présentée en vue
d'obtenir le grade de

DOCTEUR

En

Spécialité: Chimie Theorique, Physique, Analytique

Par

Marcelo AVELAR DO NASCIMENTO

DOCTORAT DELIVRE PAR CENTRALE LILLE

ET UNIVERSIDADE FEDERAL DO RIO DE JANEIRO

Biotechnological Routes for Obtaining High-Added Value Compounds from
Residual Biomass

Voies biotechnologiques pour l'obtention de composés à haute valeur
ajoutée à partir de la biomasse résiduelle

Soutenue le 29 novembre 2023 devant le jury d'examen:

Président: Mme Andreea Pasc, Professeur Université de Lorraine – France.

Rapporteur: Mme Viridiana Santana Ferreira Leitao, Professeur, National Institute of Technology, INT - Rio de Janeiro - Brazil.

Membres: M. Raoni Schroeder Borges Gonçalves, Professeur, Chemistry Institute - Federal University of Rio de Janeiro/UFRJ - Brazil.

M. Mohammed Nawfal Ghazzal, Professeur, Université Paris Saclay – France.

Mme Almudena Marti Morant, Professeur, Université de Lorraine – France.

Directeur de thèse: M. Ivaldo Itabaiana Junior, Professeur, Chemistry school - Federal University of Rio de Janeiro/UFRJ - Brazil

Co-Directeurs de thèse : M. Rodrigo Octavio Mendonça Alves de Souza, Professeur, Chemistry Institute - Federal University of Rio de Janeiro/UFRJ – Brazil.

M. Robert Wojcieszak, Researcher at Centre National de la Recherche Scientifique – France.

Thèse préparée dans le Laboratoire UCCS et BOSSGroup/IQ-UFRJ.

Ecole Doctorale SMRE 104 (UCCS) et Graduate Program in Chemistry (PGQu/IQ-UFRJ).

ACKNOWLEDGMENTS

To start, I'd like to extend my appreciation to myself for my persistence and refusal to give up.

I want to express my gratitude to the God for granting me the fortitude to progress, despite the numerous challenges that emerged along this path. My heartfelt appreciation goes out to my mother, Arilda Avelar, for her unwavering belief in me and her relentless dedication to nurturing my aspirations, fully aware of the formidable challenges we would face.

I extend my heartfelt gratitude to my siblings, Rodolfo, Priscila, Paloma, Patrícia, and Damião, as well as all my friends, for their unwavering trust in my abilities and their consistent messages of encouragement. I would like to give a special acknowledgment to my dear friend Elessandra de Paula for her continuous words of support and her steadfast belief in my potential.

I want to express my gratitude to my colleagues and fellow researchers at the residential village (UFRJ). I extend my thanks to my friends and colleagues at BossGroup, including Raquel, Viviane, Anderson, Renata, Marcelo Tavares, Júlio, Alexandre, Marco, Larissa, Wallace, Fernanda Sagrillo, Fernanda Lima, Caio, Sara, Bernardo and Giulia, for the friendship, the delicious meals (especially cakes), shared laughter and, of course, countless cups of coffee.

I would like to express my sincere thanks to my friends at Centrale Lille, including Sara Navarro, Zaher Raad, Jing Yu and Mohamad. To my Brazilian/European friends Deizi Peron, Simon David, Raphaela, Leticia, and Elise. A special mention goes to Clara Vweikert and Mateus Freitas for their invaluable psychological support and the wonderful moments we shared while living on the other side of the ocean. Being with you made the process easier.

I wish to convey my heartfelt appreciation to my advisor, Rodrigo Octavio Mendonça Alves de Souza, for his support, and his guidance in paving the way forward. I'd also like to extend my gratitude to my advisor, Ivaldo Itabaiana Junior, for his wholehearted support, belief in my potential, dedication, meticulous guidance, encouragement during moments of despair, assistance with experiments, and, most importantly, for the invaluable knowledge that contributed

significantly to my research. A special thank you to Dr Robert Wojcieszak for accepting me at Centrale Lille and providing all the support during this journey. Thank you immensely.

I would also like to extend my gratitude to my course friends, Quelli, Tereza, Paulo, Thais and Regiane, for their unwavering support, infectious enthusiasm, friendship, companionship, and for being there to assist me through the toughest moments. Our shared laughter in the university corridors has been a source of joy and strength.

I deeply thank my remarkable research partner and forever friend, Mauro Roger Batista Pousada Gomez, for all countless incredible moments together, marked by unwavering companionship and profound reflections that have enriched my journey. I cherish our friendship immensely, and I believe this is just the beginning of many more remarkable experiences to come. Thank you for your wonderful presence in my life. I LOVE.

The Federal University of Rio de Janeiro and Centrale Lille, its faculty, management and administration that provided the opportunity for the window that today I see a higher horizon, filled with the kindled confidence in the merit and ethics present here, and to everyone who directly or indirectly was part of my training, my thank you very much.

RÉSUMÉ

Chaque année, des milliards de tonnes de biomasse lignocellulosique (LB) sont générées, et seule une petite partie est réutilisée, couramment utilisée comme fourrage ou à des fins énergétiques et matérielles. Par conséquent, de nouvelles stratégies sont nécessaires pour valoriser ces *commodités* car la biomasse est une importante matière première alternative pour obtenir des produits chimiques d'intérêt à partir de ressources renouvelables. Dans cette tendance, une autre alternative prometteuse est l'application d'enzymes associées à la chimie synthétique pour explorer de nouveaux produits d'intérêt industriel. Parmi les produits de la pyrolyse rapide, on trouve le bio-oil, un mélange visqueux résultant de l'oxydation des polymères de biomasse, dont le principal composant est la lévoglucosane (1,6-anhydroglucopyranose), un sucre anhydre utilisé comme bloc de construction pour divers composés industriels d'intérêt. Par exemple, il peut être hydrolysé en glucose et utilisé dans des processus de fermentation pour obtenir une large gamme de produits. Cependant, cette molécule offre d'autres possibilités chimiques en raison de ses groupes hydroxyles libres et de sa partie hydrophobe relative. Ce glucide anhydre peut être acylé pour obtenir des esters de glucides et d'acides gras (CFAEs) présentant un équilibre hydrophile-lipophile hautement apprécié comme tensioactifs. Dans cette étude, la lévoglucosane commerciale (LGCom) et celle obtenue à partir de la pyrolyse de la cellulose (BoE) ont été acylées par transestérification/estérification en utilisant différents donneurs d'acyl dans des systèmes continus et en lots. Les réactions ont été catalysées par des lipases libres et immobilisées en présence de différents solvants organiques. De plus, nous avons démontré, pour la première fois, l'acylation directe de BoE et l'influence de l'acétonitrile (ACN) et du cyrène (CYE) sur la stabilité des lipases *Candida Rugosa* (CR) et *Candida antarctica* B (CalB) en utilisant la fluorimétrie de balayage différentiel (NanoDSF) à des concentrations de substrat de 20 à 300 mM. Nous avons également étudié l'effet de la chaîne alkyle pour la synthèse des CFAEs. Dans la réaction en lots utilisant LGCom comme substrat, des conversions et des

sélectivités optimales ont été obtenues avec différents donneurs d'acyl, tels que le laurate d'éthyle (C12), le palmitate d'éthyle (C16), le stéarate d'éthyle (C18) et l'oléate d'éthyle (C18*), préparés in situ en utilisant une stratégie intégrée médiée par les lipases commerciales Novozym®435 (N435), PSIM, et le biocatalyseur maison CaLB_epoxy. En conséquence, tous les biocatalyseurs ont principalement généré des CFAEs, N435 étant plus sélectif pour produire des esters lauriques (MONLAU) (99% à 50°C) et PSIM pour produire des esters oléiques (MONOLE) (97% à 55°C), tandis que CaLB_epoxy a montré une plus grande sélectivité pour produire des MONOLE (83% à 55°C). Dans la réaction en lots utilisant BoE, les meilleurs résultats ont été obtenus avec N435 en ACN, le donneur d'acyl éthyl octanoate (C8) atteignant une conversion de 74%. En général, il a été observé que l'augmentation de l'hydrophobicité du donneur d'acyl a contribué à une plus grande régiosélectivité pour le groupe hydroxyle lié au carbone 4, atteignant jusqu'à 99 % pour C18* en ACN sur Calb_epoxy en utilisant LGCom à 55 °C. Les profils de stabilité thermique de CalB et CR suggèrent une plus grande stabilité en CYE, avec des valeurs de points de fusion des protéines (T_m) de 61°C pour CalB et de 53°C pour CR. Grâce aux paramètres cinétiques obtenus à partir des constantes de Michaelis-Menten générées par le tracé doublement réciproque, une inhibition par le substrat LGCom a été indiquée. De plus, les données sur l'efficacité catalytique suggèrent une plus grande affinité enzyme-substrat en présence de CYE. Dans le système en flux continu, il a été possible d'optimiser les conditions de réaction, la température et le temps de résidence, atteignant une conversion maximale à 61°C en 77 minutes. De plus, il y a eu un gain de productivité de plus de 100 fois par rapport au système en lots dans toutes les comparaisons. Enfin, les CFAEs ont été testés pour leur tension interfaciale et leur activité biologique. Pour un mélange de 4-O' et de 2-O-Lauryl-1,6-anhydroglucopyranose (MONLAU), la tension interfaciale minimale (IFT^{\min}) obtenue était de 9.6 mNm^{-1} à une concentration micellaire critique (CMC) de 50 mM. Des valeurs similaires ont été obtenues pour un mélange de 4 et de 2-O-Palmitoyl-1,6-anhydroglucopyranose (MONPAL), jamais rapporté auparavant dans la littérature, avec une IFT^{\min} de 8.8 mNm^{-1} à 50 mM. Pour un mélange de 4 et de 2-O-Stearoyl-1,6-

anhydroglucopyranose (MONEST) et un mélange de 4 et de 2-O-Oleoyl-1,6-anhydroglucopyranose (MONOLE), la CMC était supérieure à 60 mM, et les valeurs d'IFT^{min} étaient respectivement de 14.1 mNm⁻¹ et de 10.2 mNm⁻¹. Dans ces études, il n'a pas été possible d'obtenir des diesters ou des triesters de LG (levoglucosane) avec de longues chaînes à partir du donneur d'acyle (>C12). Cependant, la formation de monoesters aux positions C2 et C4 a été observée dans toutes les conditions testées. Grâce au système à flux continu, il a été possible de maximiser la synthèse de CFAE par rapport au système discontinu. En outre, le recyclage des biocatalyseurs immobilisés a démontré la stabilité robuste du système. En outre, des données prometteuses ont été obtenues pour la concentration minimale inhibitrice (CMI) et la concentration minimale bactéricide (CMB) de MONLAU contre des souches de *Staphylococcus aureus* à 0,25 mM.

Mots-clefs: Lipase, Transestérification, Glucides et Biomasse.

ABSTRACT

Every year, billions of tons of lignocellulosic biomass are generated, and only a small portion is reused, commonly used as food and/or for energy and material purposes. Therefore, new strategies are needed to valorize these raw materials, as biomass is an excellent alternative feedstock for obtaining chemicals of interest from renewable resources. In this trend, another promising alternative is the application of enzymes in conjunction with synthetic chemistry to explore new products of industrial interest. Among the products of fast pyrolysis is bio-oil, whose main component is levoglucosane (1,6 anhydroglucopyranose), an anhydrous sugar used as a base for various industrially relevant compounds. This anhydrous carbohydrate can be acylated to obtain carbohydrate fatty acid esters (CFAEs) with a highly appreciated hydrophilic-lipophilic balance as surfactants. In this study, commercial levoglucosane (LGCom) and levoglucosane obtained from cellulose pyrolysis (BoE) were acylated by transesterification/esterification using various acyl donors in continuous and batch systems catalyzed by free and immobilized lipases in the presence of different organic solvents. As a result, all biocatalysts mainly produced carbohydrate fatty acid esters (CFAEs) with different selectivities. In the batch reaction using BoE, the best results were obtained with N435 in ACN, with the acyl donor ethyl octanoate (C8) achieving a conversion of 74%. The thermal stability profiles of CalB and CR suggested increased stability in CYE, with protein melting point (T_m) values of 61°C for CalB and 53°C for CR. From the kinetic parameters obtained from the Michaelis-Menten constants, substrate inhibition by LG was indicated. In the continuous system, a productivity increase of over 100 times was achieved compared to the batch system in all comparisons. Finally, CFAEs were tested for interfacial tension and biological activity. Promising data were obtained for the minimum inhibitory concentration (MIC) and minimum bactericidal concentration (MBC) of MONLAU against *Staphylococcus aureus* strains at 0.25 mM.

Key words: Lipase, Transesterification, Carbohydrate and Biomass.

SUMMARY

ACKNOWLEDGMENTS.....	2
RÉSUMÉ	4
ABSTRACT.....	7
SUMMARY	8
LIST OF FIGURES	11
LIST OF TABLES.....	17
ABBREVIATIONS AND ACRONYMS	18
1 – Introduction	20
2. Literature Review	26
2.1. What's lignocellulosic biomass?	26
2.1.1. Lignin	27
2.1.2. Hemicellulose.....	29
2.1.3. Cellulose	31
2.2. Application of pyrolysis in the valorisation of lignocellulosic biomass.....	34
2.2.1. Pyrolysis reactor.....	36
2.3. Levoglucosan as a platform to obtain molecules with high added-value.....	39
2.3.1. Enzymatic approach.....	51
2.3.1.1. Lipases.....	54
2.3.1.1.1. Hydrolysis Mechanism.....	54
2.3.1.1.2. Catalytic Promiscuity of lipases	56
2.3.1.1.2.1. Synthesis of sugar esters	59
2.3.1.2. Strategy for enzyme immobilization	62
2.3.1.2.1. Covalent binding	64
2.3.1.2.2. Adsorption.....	66
2.3.1.3. Biocatalysis under continuous flow conditions	67
2.3.1.3.1. Lipases applied in continuous flow	68
2.3.1.3.1.1. Esterification reaction	68
2.3.1.3.1.2. Transesterification reaction	70
3. Objective.....	73
3.1. Specific objectives.....	73
4. Materials and Methods.....	74
4.1. Materials	74

4.2. Methods	74
4.2.1. Immobilization of lipase CalB	74
4.2.2. Hydrolytic activity assay	75
4.2.2.1. Triacylglycerol hydrolysis	75
4.2.2.2. Hydrolysis of 4-Nitrophenyl dodecanoate to p-nitrophenol.....	75
4.2.3. Levoglucosan derivatization	76
4.2.3.1. Silylation with BSTFA and MSTFA	76
4.2.3.2. Silylation with tert-butyl dimethyl silane chloride	76
4.2.4. Lipase-catalysed acylation of levoglucosan in batch	77
4.2.4.1. Esterification of long-chain fatty acids	77
4.2.4.2. Transesterification of levoglucosan	77
4.2.4.2.1. Initial screening	77
4.2.4.2.2. Directly in bio-oil enriched with levoglucosan (BoE).....	82
4.2.4.2.3. Determination of kinetic parameters	83
4.2.5. Nano differential scanning fluorimetry (NanoDSF).....	84
4.2.6. Lipase-catalysed acylation of levoglucosan in continuous flow.....	84
4.2.6.1. Experimental setup.....	84
4.2.6.2. Design of experiments (DoE)	85
4.2.6.2.1. Transesterification of levoglucosan	87
4.2.6.2.2. Determination of productivity	88
4.2.7. Determination of surface activity	88
4.2.8. Antibacterial Assays	90
4.2.9. Minimal inhibitory concentration (MIC)	90
4.2.10. Minimal bactericidal concentration (MBC)	90
5. Results and Discussions	91
5.1. Lipase-catalysed acylation of levoglucosan in batch	91
5.1.1. Initial Screening.....	91
5.1.2. Directly in bio-oil enriched with levoglucosan (BoE)	100
5.1.2.1. Screening of lipase from different sources applied in LGCom and BoE	101
5.1.2.2. Nano differential scanning fluorimetry (NanoDSF).....	104
5.1.2.3. Effect of alkyl chain on the synthesis of levoglucosan esters from BoE	109
5.1.2.4. Effect of substrate ratio	112
5.2. Kinetic studies	113
5.3. Lipase-catalysed acylation of levoglucosan in continuous flow.....	120
5.3.1. Optimization using DoE in a model reaction	120

5.3.2. Synthesis of long-chain CFAEs	124
5.3.3. Evaluation of interfacial tension between oil/water in different concentrations of CFAEs	128
5.3.4. Antibacterial assays	131
Conclusion	133
Future perspectives	134
REFERENCE.....	135
ANNEX A.....	159
ANNEX B.....	161
ANNEX C.....	189
ANNEX D.....	192
ANNEX E.....	195

LIST OF FIGURES

Figure 1: Annual global production lignocellulosic biomass and reused by agricultural (Dahmen et al., 2019).....	21
Figure 2: General representation for highly valued products obtained by chemical and biochemical. CFAEs: Carbohydrate fatty acid esters (Adapted (DO NASCIMENTO et al., 2022)).	22
Figure 3: General structure of the main compounds presents in the lignocellulosic biomass (Adapted: Itabaiana Junior et al., 2020).	26
Figure 4: Lignin precursor alcohols and β -O-4'/ β - β' bonds formed (Xu et al., 2017b).	28
Figure 5: Redox neutral and cleavages under reductive conditions of the β -O-4'-ether linkage in 2-aryloxy-1-arylethanols to generate acetophenone (X. Wang & Rinaldi, 2013).....	28
Figure 6: Photochemical C–O Bond Fragmentation in Flow (Magallanes et al., 2019).	29
Figure 7: Representative structure of xylan, a type of hemicellulose (X. Yang et al., 2020).	30
Figure 8: Principal pathways to cellulose formation (Klemm et al., 2005).	31
Figure 9: Platform chemicals from cellulosic biorefinery (Reshmy et al., 2022).....	33
Figure 10: Representation of an experimental test equipment (Pandey et al., 2019).	36
Figure 11: Proposed cellulose biorefinery using fast pyrolysis, hydrolysis, and fermentation (Buendia-Kandia et al., 2020).....	39
Figure 12: Some examples of exceptionally prized products obtained through chemical and biochemical transformations by LG (Adapted from: (Itabaiana Junior et al., 2020; Bassut et al., 2022).	41
Figure 13: Schematic representation of primary and secondary reactions in cellulose pyrolysis (Adapted from (Itabaiana Junior et al., 2020).	42
Figure 14: Simplified mechanism of cellulose pyrolysis highlighting the main degradation pathways and key volatile markers. Adapted from (Le Brech et al., 2016a).....	44

Figure 15: Proposed of methodology for the production and purification of LG from lignocellulosic biomass. Adapted from (ITABAIANA JUNIOR et al., 2020).	49
Figure 16: Eukaryotic enzymatic cleavage and phosphorylation through the action LGK to produce G6P (M. Yang et al., 2022).	53
Figure 17: Hydrolysis reaction of triacylglycerols catalysed by lipases. Adapted from (BENITO-GALLO et al., 2015).	54
Figure 18: Crystallographic structure representative of the CalB lipase. The catalytic triad at the active site is displayed: Ser105, His224 and Asp187 (PDB code: 1TCA).	55
Figure 19: General simplified mechanism of lipase-catalysed amidation (Lima et al., 2019).	56
Figure 20: Use of CalB in the amidation of acid ends of amino acid chains as a key step in the synthesis of short peptides (Lima et al., 2019).	57
Figure 21: Selective aminolysis of 1-tert-butyl-2-ethyl-2,3-dihydro-1-H-pyrrole-1,2-dicarboxylate to obtain a precursor of Saxagliptin (Active ingredient for the treatment of diabetes) (Lima et al., 2019).	58
Figure 22: Lipase-catalyzed Knoevenogel condensations (de María et al., 2019).	58
Figure 23: Regioselective enzymatic transesterification of lobucavir catalysed by <i>Pseudomonas cepacia</i> lipase.	59
Figure 24: Possible conformational structures for LG in the axial position.	61
Figure 25: Diagram illustrating major enzyme immobilization methods. Reversible methods include adsorption, ionic bonding, and affinity. Irreversible methods include covalent bonding, entrapment, and cross-linking (Adapted from T.sriwong & Matsuda, 2022).	63
Figure 26: Continuous flow basics and equipment. (a) The continuous flow legend. (b) Continuous flow reactors (c) An example of a continuous flow system scheme, different pumps, and reactors.	68
Figure 27: Esterification reaction between racemic 1,2-isopropylidene glycerol and stearic acid catalyzed by RMIM under continuous flow conditions (Junior et al., 2012).	70

Figure 28: Glycerol carbonate synthesis by applying a combination of the immobilized biocatalysts PPL and CalB (Do Nascimento et al., 2019).71

Figure 29: General procedure for lipase-catalyzed transesterification reaction of levoglucosan 1. Conditions: 2 ethyl esters of a: laurate, b: palmitate, c: stearate, and d: oleate (2.0 mmol), 3 levoglucosan monoesters aliphatic chains, and 4 ethanol.78

Figure 30: General procedure for lipase-catalysed transesterification reaction of LG 1 (40 mM) with acyl donor 2 (1:2 equivalents), biocatalyst (12U), 300 rpm, 120h at 55 °C. Conditions: 2 ethyl esters of a: acetate (C2), b: hexanoate (C6), c: octanoate (C8), d: laurate (C12), e: palmitate (C16), f: stearate (C18) and g oleate (C18*), 3-4I-II-IIIa and 5a levoglucosan esters, aliphatic chains, and ethanol.83

The thermal stability of free lipase was investigated via NanoDSF (Magnusson et al., 2019) using the Prometheus NT.Plex. (NanoTemper® Technologies) (Figure 31). Protein samples were prepared at a concentration of 1.0 mg/mL in sodium phosphate buffer pH 7.0 (100 mM). After that, different solutions containing 20 µL the protein and organic solvent (CYE and ACN), respectively, were prepared and analysed.84

Figure 32: Representation and equipment used in the continuous flow system. Esterification reaction of levoglucosan with different vinyl esters. *Reactor volume: 7.854mL. a: vinyl laurate, b: vinyl palmitate, c: vinyl stearate and d: vinyl oleate. Immobilized Enzyme: N435 = Novozym 435 (Candida antarctica lipase B), immobilized in resin Lewatit VP OC 1600; CaLB_Epoxy = Candida antarctica lipase B immobilized on epoxy support by our research group.85

Figure 33: Esterification reaction of levoglucosan with lauric acid. *Reactor volume packed with N435: 7.854mL.86

Figure 34: Esterification reaction of levoglucosan with different vinyl esters. * Reactor volume: 7,854 mL. a: vinyl laurate, b: vinyl palmitate, c: vinyl stearate and d: vinyl oleate.87

Figure 35: Regioselectivity in the enzymatic acetylation of levoglucosan in CH ₃ CN with ethyl aliphatic esters. Analyses were performed in a gas chromatograph equipped with a mass spectrometry detector (GC-MS) (DO NASCIMENTO et al., 2019).....	95
Figure 36: Regioselectivity in the enzymatic acetylation of levoglucosan (1 mmol, 163 mg) in CH ₃ CN (5.0 mL) with ethyl oleate (2 mmol, 619 mg) were introduced into a vial containing the supported enzyme (40 mg, 0.8% (v/v)). The mixture was stirred at 55°C for about five days and the course of the reaction was monitored by means of GC-MS (DO NASCIMENTO et al., 2019).	96
Figure 37: ¹ H-NMR Spectrum for 2-O-Oleoyl-1,6-anhydroglucopyranose.....	98
Figure 38: Nuclear effect of the Overhauser difference spectra for irradiation in the H-4 compound 1 at 3.61 ppm (H-4).	99
Figure 39: HMBC for 2-O-Estearyl-1,6-anhydroglucopyranose (CDCl ₃).....	99
Figure 40: Transesterification reaction between levoglucosan and ethyl acetate with different biocatalysts in acetonitrile and cyrene as solvent. Conditions: a) Commercial LG (LGCom) and b) Bio oil enriched with LG (BoE).	102
Figure 41: Representative chromatogram of BoE dissolved in acetonitrile and analysed on GC-FID.....	104
Figure 42: Representations of NanoDSF thermograms showing the ratio between the fluorescence signals at 350 and 330 nm and the first derivative of this ratio for analyzing the T _{Onset} and T _m values. Conditions: 1 mg/mL of protein in 100 mM sodium phosphate buffer pH 7.0 in a) Lipase B of <i>Candida antarctica</i> (CaLB) and b) <i>Candida Rugosa</i> (CR).....	106
Figure 43: Representations of NanoDSF thermograms showing the ratio between the fluorescence signals at 350/330 nm and the first derivative of this ratio for analysing the T _{Onset} and T _m values. Conditions: 1 mg/mL of free enzyme in 100 mM sodium phosphate buffer pH 7.0 in different organic solvents; CaLB in a) acetonitrile (ACN) and b) cyrene (CYE); and CR in c) ACN and d) CYE.	108

Figure 44: Representations of NanoDSF thermograms showing the ratio between fluorescence signals at 350 and 330 nm and the first derivative of this ratio for analysis of refolding values. Conditions: 1 mg/mL lipase in 100 mM sodium phosphate buffer pH 7.0 in different organic solvents. **CaIB** in **a)** ACN and **b)** CYE; and **CR** in **c)** ACN and **d)** CYE. 109

Figure 45: Results for transesterification reaction between different acyl donors with BoE in ACN and CYE. Conditions: ethyl esters: acetate (**C2**); hexanoate (**C6**); octanoate (**C8**); laurate (**C12**); palmitate (**C16**); stearate (**C18**) and oleate (**C18***). BoE (40 mM) and acyl donors (1:2) in two organic solvents: acetonitrile (ACN) and cyrene (CYE) at 55°C, 120h and 300 rpm..... 110

Figure 46: Results for transesterification reaction between ethyl acetate and BoE in CYE for different concentrations of ethyl acetate (40-100-150 and 200 mM) in function of the different concentrations of BoE 50-80 and 130 mM in total reaction time at 80h. 113

Figure 47: Lineweaver–Burk plot of the reversed initial velocity of transesterification of levoglucosan (20-300 mM) with ethyl acetate (50-300 mM) in function of reversed concentration levoglucosan: **a)** acetonitrile (ACN) and **b)** cyrene (CYE)..... 114

Figure 48: Dixon plot of initial rate reciprocal plot of LGCom transesterification with ethyl acetate (50-300 mM) in function of LGCom concentration (20-300 mM) in: **a)** acetonitrile (ACN); **b)** cyrene (CYE)..... 115

Figure 49: Lineweaver–Burk plot of initial rate of LGCom transesterification (20-300 mM) in function of ethyl acetate concentration (50-300 mM) in: **a)** acetonitrile (ACN); **b)** cyrene (CYE). 116

Figure 50: Secondary plot of slope $1/[\text{ethyl acetate}]$ versus reciprocal concentration of $1/[\text{LGCom}]$ in two solvents: **a)** acetonitrile and **b)** cyrene. 117

Figure 51: Secondary plot of intercept $1/[\text{ethyl acetate}]$ versus reciprocal concentration of $1/[\text{LGCom}]$ in two solvents: **a)** acetonitrile and **b)** cyrene. 118

Figure 52: Esterification reaction of levoglucosan with lauric acid. *Reactor volume packed with N435: 7.854mL. 121

Figure 53: a) Response surface and b) level curve of the conversion in the model reaction of esterification of levoglucosan with lauric acid relating temperature and time.121

Figure 54: Acylation of levoglucosan with different acyl donors in 61 °C and residence time 77 min using **N435** as biocatalyst. Selectivity **3I-a**: 4-O-Lauryl-1,6-anhydroglucopyranose; Selectivity **3II-a**: 3-OLauryl-1,6-anhydroglucopyranose and Selectivity **3III-a**: 2-O-Lauryl-1,6-anhydroglucopyranose. Analyses were performed in a gas chromatograph equipped with a mass spectrometry detector (GC-MS).123

Figure 55: Relationship between the concentration of CFAs and interfacial tension.129

LIST OF TABLES

Table 1: Levels used in central composite planning for two variables.	86
Table 2: Acylation of levoglucosan in CH ₃ CN.	92
Table 3 : ¹³ C and ¹ H chemical shifts (ν, ppm) in CDCl ₃ as solvent for compounds 1 and 2. J _{HH} coupling constants are represented in parenthesis.	97
Table 4: Regioselectivity in the transesterification reaction between different alkyl esters and BoE in the presence of ACN and CYE with N435.	111
Table 5: Kinetic parameters obtained for the transesterification of different acyl donors in the presence of LGCom in ACN and CYE.....	119
Table 6: Regioselectivity in the enzymatic acetylation of levoglucosan in CH ₃ CN with vinyl aliphatic esters in continuous flow. Analyses were performed in a GC-MS.....	125
Table 7: Comparative between the values of conversion and productivity for batch and continuous flow systems	126
Table 8: Recycling of biocatalysts applied in the transesterification reaction.....	128
Table 9: Interface active properties of CFAs.	129
Table 10: Minimal inhibitory concentration (MIC) and minimal bactericidal concentration (MBC) of products and substrates against Staphylococcus aureus strains.....	132

ABBREVIATIONS AND ACRONYMS

(LB) Lignocellulosic biomass

(RLB) Residual lignocellulosic biomass

(CFAEs) Carbohydrate fatty acid esters

(LGCom) Commercial levoglucosan

(BoE) Levoglucosan obtained from cellulose pyrolysis

(ACN) Acetonitrile

(CYE) Cyrene

(CR) Lipase from *Candida Rugosa*

(CalB) Lipase from *Candida antarctica* B

(NanoDSF) Differential scanning fluorimetry

(C2) Levoglucosan monoester: acetate

(C6) Levoglucosan monoester: hexanoate

(C8) Levoglucosan monoester: octanoate

(C12) Levoglucosan monoester: laurate

(C16) Levoglucosan monoester: palmitate

(C18) Levoglucosan monoester: stearate

(C18*) Levoglucosan monoester: oleate

(N435) Novozyme® 435 is a commercially available immobilized lipase produced by Novozyme®.

It is based on immobilization via interfacial activation of lipase B from *Candida antarctica* on a resin, Lewatit VP OC 1600.

(PSIM) *Pseudomonas Cepacea* immobilized on a commercially available microporous polypropylene support.

(Calb_epoxy) CalB immobilized by hydrophobic adsorption.

(MONLAU) Mixture of 4 and 2-O-lauryl-1,6-anhydroglucopyranose

(MONPAL) Mixture of 4 and 2-O-Palmitoyl-1,6-anhydroglucopyranose

(MONEST) Mixture of 4 and 2-O-Stearoyl-1,6-anhydroglucopyranose

(MONOLE) Mixture of 4 and 2-O-Oleoyl-1,6-anhydroglucopyranose

(T_m) Melting point of a protein

(IFT^{min}) Minimum interfacial tension

(CMC) Critical micelle concentration

(MIC) Minimum inhibitory concentration

(MBC) Minimum bactericidal concentration

(LG) Levoglucosan

(HLB) Hydrophobic-lipophilic balance

(DoE) Design of Experiments

(SWs) Solid waste

(%C) Percent carbon

(DP) Degree of polymerization

(TG) Triglycerides

(DG) Diacylglycerols

(MG) Monoglycerides

(Ser) L-Serine (amino acid residues)

(Asp) L-Aspartate (amino acid residues)

(His) L-Histidine (amino acid residues)

(pI) Isoelectric point

(CaIA) Lipase from *Candida antarctica* A

(PPL) *Porcine pancreatic* Lipase

(CPR) Centrifugal partition reactor

(RMIM) Commercial immobilized lipase from *Rhizomucor miehei*

(SSB) Sweet sorghum bagasse

(BC) Biochar

(LRGP) Reaction and Process Engineering Laboratory

1 – Introduction

The global economy faces the dual challenge of providing support for an ever-expanding global population while improving living standards. However, this endeavor faces constraints imposed by the limits set by our planet (Johan Rockstrom et al., 2009). The utilization of bio-based resources, often denoted as the "bioeconomy," emerges as a promising prospect capable of serving as a catalyst for the shift towards a sustainable economic and lifestyle paradigm (European Commission (EC), 2012). The effectiveness of current production and consumption models can be heightened by transitioning from a fossil fuel-driven economy to a bioeconomy centered around products derived from biological sources, recycling, and renewable energy sources (Lokko et al., 2018).

The bioeconomy, as defined by the European Commission, entails the knowledge-driven production of renewable biological resources and the conversion of these resources and waste into valuable products, including food for human consumption, feed, biologically sourced products, and bioenergy (European Commission (EC), 2012)). Numerous countries and organizations have implemented strategies to showcase their commitment to this concept, with a notable example being the European Union's Horizon 2020 Research and Innovation Framework Programme, where the bioeconomy features prominently as one of the six primary societal challenges. In this context, the availability of cheap raw materials and renewable energy is the foundation for global sustainability, where strategies for the development of clean technologies for chemical processes aim to balance economic and environmental aspects (Tang et al., 2005).

Residual lignocellulosic biomass is a highly abundant and carbon neutral renewable resource that does not compete with the food production cycle. Its composition ranges from 40% to 50% cellulose, 20% to 30% hemicellulose, 20% to 25% lignin, and 1.5% to 3% ash (López Ortiz et al., 2013; Wong Sak Hoi & Martincigh, 2013; H. Yang et al., 2007). Therefore, the development of new strategies is important to add value to these commodities (Octave & Thomas, 2009).

Different methods can be applied to convert this material into high value-added products. However, it is estimated that every year 182 billion tons of this waste material is generated. Out of these, 4.6 billion tonnes of lignocellulosic biomass residues are produced as agricultural by-products with only approximately 25% being utilized intensively (Figure 1) (Dahmen et al., 2019). For instance, the sugarcane industry has a high utilization of lignocellulosic biomass to produce biofuels, such as first-generation ethanol, in addition to limited reutilization of the bagasse to produce second and third-generation ethanol. Hence, the development of new strategies combined with different technologies can be an alternative to improve the use of these natural resources (DAHMEN et al., 2019; OKOLIEA et al., 2022).

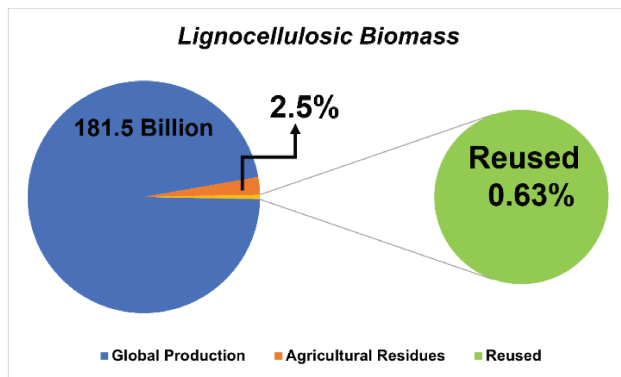


Figure 1: Annual global production lignocellulosic biomass and reused by agricultural (Dahmen et al., 2019).

In this context, the fractions of lignocellulosic material can be separated through different fractionation processes (Solange I. Mussatto, 2016) and used as a platform in diverse technologies (Banu J et al., 2021; Buendia-Kandia et al., 2020). For example, through the fast pyrolysis of cellulose, various organic compounds could be generated in short intervals of time. This process mainly produces a bio-oil, a viscous mixture resulting from the oxidation of biomass polymers, of which their main component is levoglucosan (1,6-anhydro- β -D- glucopyranose) (LG) (Itabaiana Junior et al., 2020; Rocha et al., 2013), an anhydrous sugar that can be converted into various value-added chemicals (Figure 2) (Itabaiana Junior et al., 2020).

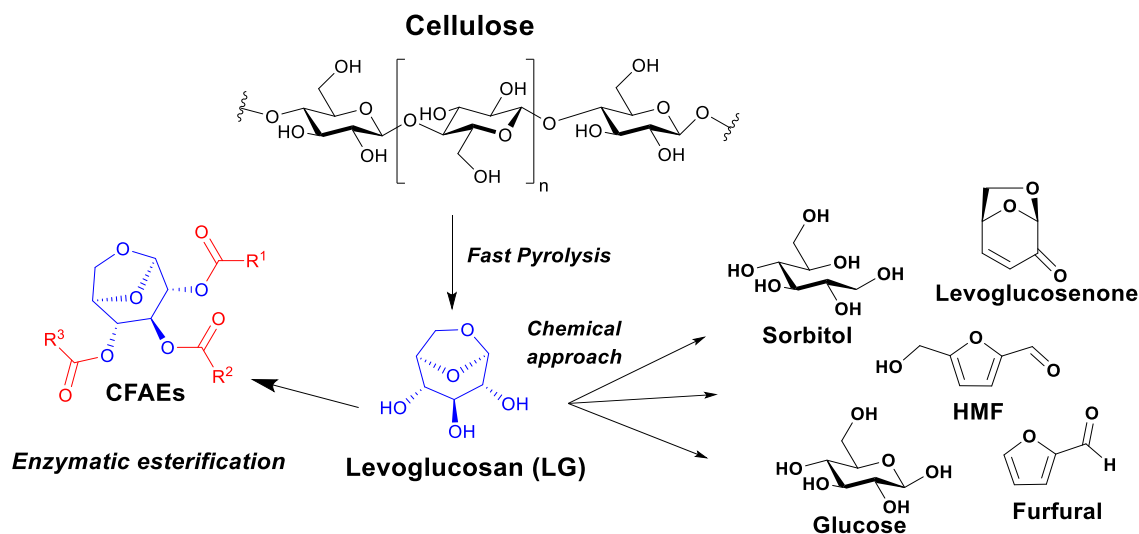


Figure 2: General representation for highly valued products obtained by chemical and biochemical. **CFAEs:** Carbohydrate fatty acid esters (Adapted (DO NASCIMENTO et al., 2022)).

LG can be hydrolyzed into glucose and is used in fermentative processes to produce various products. However, this carbohydrate offers other chemical possibilities; its free hydroxyl groups can be esterified through chemical or enzymatic reactions under batch or continuous flow conditions using different acyl donors to access various mono-, di-, and triesters. These compounds can exhibit highly appreciated properties and potentially useful activities, such as antitumor, antimicrobial, and surface activities, respectively (DO NASCIMENTO et al., 2022; ITABAIANA JUNIOR et al., 2020; PARK; WALSH, 2021).

In this scenario, LG can be a promising chemical platform for the synthesis of carbohydrate fatty acid esters, known as CFAEs. Additionally, it is an excellent alternative to produce various products, such as 5-hydroxymethylfurfural (HMF), furfural, sorbitol, levoglucosenone (Figure 2) (Itabaiana Junior et al., 2020).

The structure-activity relationship of CFAEs depends on the degree of substitution of hydroxyl groups, as well as the size and amount of unsaturation in the alkyl chains, which can lead to compounds with a hydrophilic-lipophilic balance (HLB) of great industrial interest (EL-

LAITHY; SHOUKRY; MAHRAN, 2011; PARK; WALSH, 2021; ANDRÉS et al., 2020; CHANG; SHAW, 2009; PETKOVA, 2021).

Amphiphilic esters are currently produced through alkaline glycerolysis of natural oils and fats at high temperatures and pressures. In addition to the high energy consumption, the conditions used lead to low productivity and the formation of polymerization by-products, resulting in dark spots and low product quality, which requires further purification steps (Kennedy et al., 2006).

By enzymatic routes, the use of lipases (triacylglycerol ester hydrolases E.C.3.1.1.3) (DO NASCIMENTO et al., 2019) has been prominent in industrial production of high value-added esters due to various advantages. Notably, lipases possess the capability of exhibiting both hydrolysis and esterification activities, eliminating the need for cofactors, and displaying high regioselectivity, enantioselectivity, and chemo-selectivity in reactions (Mendes et al., 2023).

The transformations catalyzed by lipases play a crucial role in organic synthesis to meet the increasing demand for enantiomerically pure compounds, such as pharmaceuticals, agrochemicals, and natural products. This is mainly due to their ability to catalyze various reactions, including asymmetric esterification, asymmetric transesterification, and asymmetric hydrolysis, without the need for cofactors (Mendes et al., 2023).

One challenging task in the chemical synthesis of CFAEs is achieving regioselectivity of a single secondary OH function during acylation, as it is notoriously difficult to predict. Consequently, several protections and deprotection steps are necessary to selectively incorporate a single ester function onto the carbohydrate hydroxyl, consuming a significant amount of energy and/or reagents, contrary to the principles defined in "Green Chemistry." Green Chemistry calls for the development of technologies with lower environmental impact and the synthesis of pure products with minimal formation of side compounds (Gamayurova et al., 2021).

An increasingly prominent alternative is the use of enzymatic processes, where lipases are the most suitable class of enzymes for such reactions. As well as demonstrated in numerous

studies (DO NASCIMENTO et al., 2019a; GALLETTI et al., 2007) high yields and regioselectivity can be achieved using milder operating conditions with enzymatic processes, resulting in greater purity of the final product (Otto et al., 1998). However, a recurrent barrier that persists is the lack of enzyme stability at high temperatures, inhibition by solvents and/or reagents and products. These factors may hinder the application of enzymatic processes on an industrial scale (Chapman et al., 2018). However, a way around these problems is the application of immobilized enzymes. Thus, studies on enzyme immobilization have been widely reported by several research groups, which have described greater robustness and stability of these biocatalysts, making them suitable for these applications.

Enzyme immobilization can be an effective method to improve the performance of its free forms. Compared to free enzymes, immobilized enzymes with long-term operational stability can be easily recovered and reused, thereby reducing the costs of catalytic processes (Cipolatti et al., 2016; Datta et al., 2013; Homaei et al., 2013; Romero-Fernández & Paradisi, 2020). The activity of immobilized lipases depends on certain parameters, such as the types of enzymes and supports used, as well as the immobilization protocols. Different supports or various protocols on the same support allow the development of systems with different stabilities and specificities, depending on the material employed, the intensity of enzyme-support interaction, and the orientation of the enzyme on the support surface. Additionally, the active center can be partially blocked due to the immobilization process (de Souza et al., 2017), and it can also lead to substrate diffusion issues. These problems can have a distinct impact on enzyme activity, depending on the different immobilization strategies used.

Here, we performed the application of free and immobilized lipases in the synthesis of CFAEs through esterification/transesterification reactions of commercial levoglucosan (LGCom) and obtained from cellulose pyrolysis (BoE) with different acyl donors. We demonstrated that the CFAEs synthesized in batch reactions were readily translated into a continuous flow system, where temperature and residence time conditions were optimized with the aid of the statistical

DoE (Design of Experiments) approach. Additionally, the thermal stability profile of the free lipases *Candida antarctica* B (CalB) and *Candida Rugosa* (CR) was studied in different solvents, and the kinetic parameters were determined using the Michaelis-Menten constants obtained from the double-reciprocal plot.

Finally, the obtained CFAEs from a mixture of 4 and 2: O-Lauryl-1,6-anhydroglucopyranose (MONLAU), O-Palmitoyl-1,6-anhydroglucopyranose (MONPAL), O-Stearoyl-1,6-anhydroglucopyranose (MONEST), and O-Oleoyl-1,6-anhydroglucopyranose (MONOLE), respectively, were applied in tests for biological and surface activity, yielding promising results.

2. Literature Review

The term "biomass" encompasses all biologically generated organic materials that can function as a renewable energy source (Solange I. Mussatto, 2016). Biomass can be sourced from various origins, including plants, agricultural residues, forestry waste, food scraps, and even microorganisms. Within this organic matter lies stored energy, typically in the form of organic compounds like cellulose, hemicellulose, starch, and others (Haq et al., 2021).

2.1. What's lignocellulosic biomass?

Plant cell walls are a rich source of biopolymers, sugars, chemicals, and a sustainable alternative to petrochemicals. Its woody parts that give them rigidity are made up mainly of three main types of carbon-based polymers. Which are cellulose (40-60%), hemicellulose (20-40%), and lignin (10-25%) depending on both biomass form and maturity, along with other minor components, such as acetyl, minerals, and phenolic groups, which are collectively called lignocellulosic biomass (LB) (Sanderson, 2011), organized in a complex, non-uniform and three-dimensional spatial structure (Figure 3) (Zoghلامي & Paës, 2019).

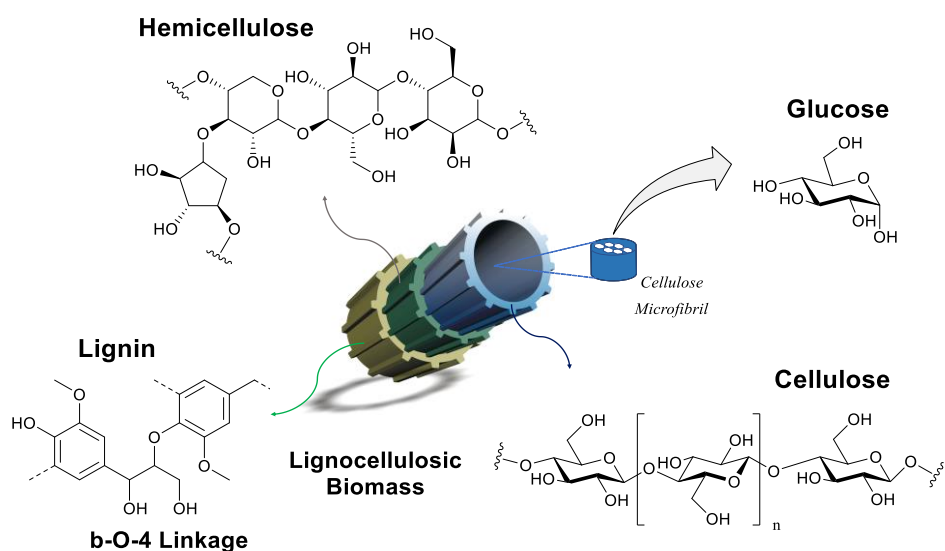


Figure 3: General structure of the main compounds presents in the lignocellulosic biomass (Adapted: Itabaiana Junior et al., 2020).

The first step in valorisation of LB is pretreatment, which helps isolate the cellulose, hemicellulose, and lignin components. By altering the supra-molecular framework of the lignin-hemicellulose–cellulose matrix, pretreatment processes modulate the binding properties of lignocellulosic biomass.

2.1.1. Lignin

Lignin is a renewable and ubiquitous natural polymer being a rich source of high-quality carbon, its structure is composed of aromatic rings with various functional groups, such as methoxy, phenylpropane, non-carbohydrate polyphenolic substances and some groups of terminal aldehydes in the side chain that can be used as an ideal carbon precursor due to its low cost, renewability and abundance totalling approximately 15-35% by weight of LB (Scelsi et al., 2021). The largest lignin generator is the pulp and paper industries that obtain this polymeric residue through the Kraft pulping process which with the advancement of the continuous development of biorefineries should increase substantially (Sharma et al., 2022).

In addition, it's the only biopolymer that contains the phenylpropanoid monomers (Zakzeski et al., 2010). These compounds can be used as building blocks for polymers, bisphenols, polyesters, polyurethane, and resins, among others. It's estimated that 50 million tons of lignin are produced annually, mainly by cellulose industries, where only 2% is commercially exploited to obtain products with high aggregate value and the rest is burned as fuel (Xu et al., 2017a). It has a heterogeneous structure formed through the radical polymerization of monolignols units of the alcohols *p*-coumaryl (*p*-hydroxyphenyl), coniferyl (guaiacyl) and sinapyl (syringyl); linked to each other by different links, such as β -O-4', α -O-4', 5-5', β - β' , β -5' and β -1' differentiating with respect to the number of methoxide groups (OCH₃) linked to the aromatic ring (Figure 4).

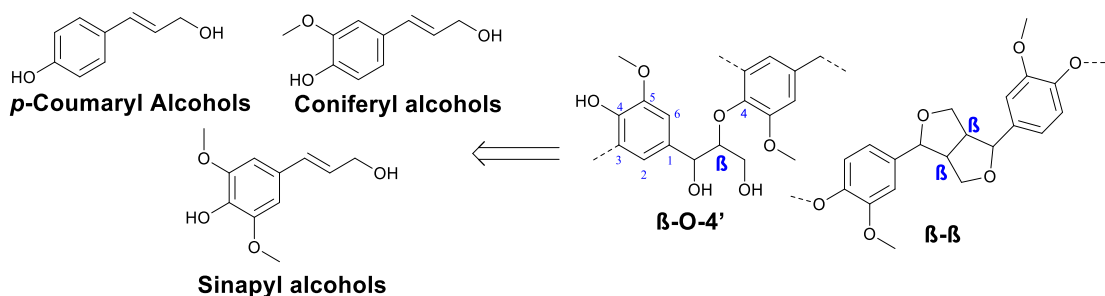


Figure 4: Lignin precursor alcohols and β -O-4'/ β - β' bonds formed (Xu et al., 2017b).

Its structure, composed of aromatic monomers, constitutes an attractive raw material to produce high value compounds and, therefore, would complement products derived from cellulose processing. However, the events of non-uniform polymerization that form it create a variety of functional groups and stereochemical configurations that reflect on its low solubility in a variety of organic compounds and non-trivial challenges for the selective depolymerization of this biopolymer. The transformation of lignin into useful chemicals can be carried out through a variety of thermochemical processes, including pyrolysis, hydrolysis, hydrogenolysis, oxidation, among others.

Several strategies have been reported to overcome these challenges (MAGALLANES et al., 2019; ROTH; SPIESS, 2015; ZHANG et al., 2018). For example, Sameni *et al.* (Sameni et al., 2017) reported a study of the solubility parameters of acetylated and non-acetylated lignin in different organic solvents. As a result, lignin solubility was better in the absence of hydroxyl groups. Wang and Rinaldi (X. Wang & Rinaldi, 2013) reported the use of Raney Nickel for the reductive cleavage of lignin, using isopropyl alcohol as a hydrogen donor (Figure 5).

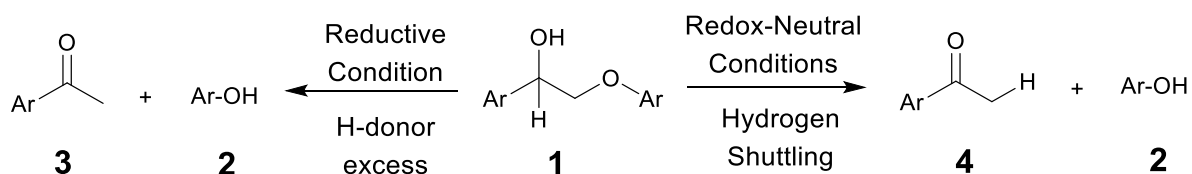


Figure 5: Redox neutral and cleavages under reductive conditions of the β -O-4'-ether linkage in 2-aryloxy-1-arylethanol to generate acetophenone (X. Wang & Rinaldi, 2013).

The relative abundance (45-60 %) of the C-O bond in β -O-4' of lignin, has been used as an important factor for its selective depolymerization (LARSSON; MIKSCHE, 1971; NIMZ, 1974). Thus, Magallanes *et al.* (Magallanes *et al.*, 2019) proposed a two-stage and operationally simple degradation approach involving aerobic oxidation catalyzed by palladium (Pd) and photocatalytic reductive cleavage of the β -O-4' bond in a variety of lignin model systems, in batch and continuous flow, releasing (β -hydroxy) ketones and phenols as products of the reaction (Figure 6).

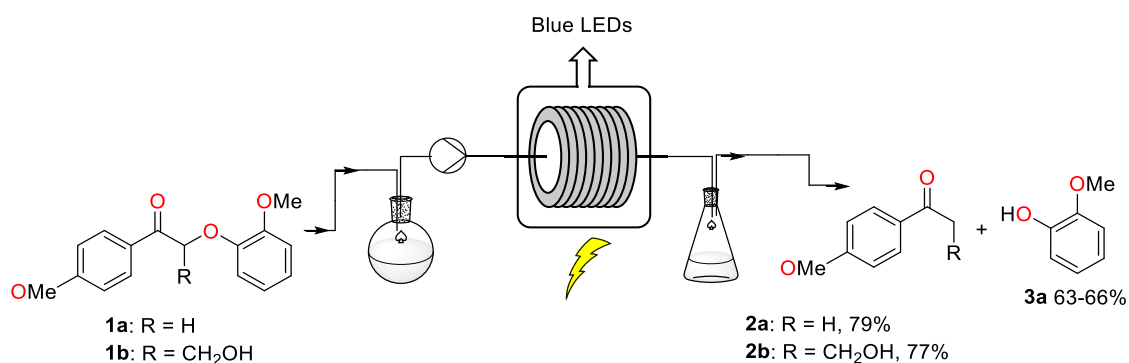


Figure 6: Photochemical C–O Bond Fragmentation in Flow (Magallanes *et al.*, 2019).

The application of continuous flow reactors in photocatalysis has received special attention, because it usually allows for short reaction times, better heat and mass transfer, light transfer rates and reduced safety risks, compared to conventional batch processing.

The complex polymeric structure of lignin, requires the combined and critical use of several methods with complementary performances, highlighting the optimization of the lignocellulosic biomass fractionation process, which can significantly affect its native structure (Shuai & Luterbacher, 2016) and the development of efficient catalytic methods for its selective depolymerization, performing a central role in the valorization of lignin.

2.1.2. Hemicellulose

Hemicellulose is made up of simple polysaccharides linked together by β -(1,3)- and β -(1,4)-glycosidic bonds that are easily be degradable into monosaccharides. It is the second most

abundant branched hetero biopolymers that it is among the constituents of lignocellulosic biomass present in plant cell walls. The various bonds along with lignin and cellulose, such as, hydrogen and covalent contribute to provide structured strength and to make difficult its isolation (Speight, 2020). However, the short lateral chain of non-crystalline structure commonly called amorphous contains a lower degree of polymerization. Therefore, it can be harnessed to produce energy, polymeric food, and medicine (Luo et al., 2019). Its structure consists mostly of pentoses, such as xylose and arabinose, and hexoses, presenting several environmental aspects positive to their subsequent use, including thermoelectricity, hydrophobicity, water-solubility, biological functionality, and good conductivity (Figure 7) (X. Yang et al., 2020).

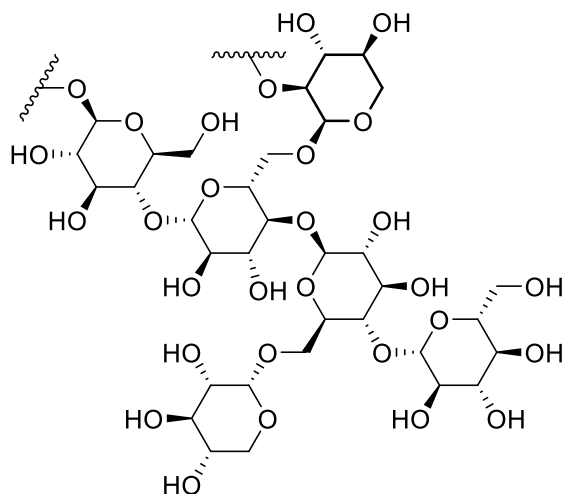


Figure 7: Representative structure of xylan, a type of hemicellulose (X. Yang et al., 2020).

From the biomass, the hemicellulose can be basically obtained through two steps: separation, the components can be precipitated by organic solvent, and extraction, by dilute alkali. For example, Zhang *et al.* claimed that hot alkali extraction became the efficient extraction method (Ang Zhang et al., 2018). However, this method causes a complicated separation of lignin that is obtained in high concentration together with hemicellulose. Other authors proposed the utilization of organic acid. For instance, Li *et al.* utilized acetic acid during separation step and obtained yield

from 82.30% to 100%, but it resulted in a highly low extraction yield which was 16% approximately. Consequently, it has been a challenge to acquire high purity of hemicellulose (J. Li et al., 2021).

2.1.3. Cellulose

The most abundant renewable polymer on earth presents in the cell walls of higher plants, in marine organism and even created by microbial biosynthesis (bacteria, fungi, algae) (H. Du Le et al., 2020). Its chemical structure is composed of the same polymer chain which is connected by D-glucopyranosyl units through β -1,4-glycosidic bonds and extensive hydrogen bonding which makes its breakdown to monomers difficult. Possessing microscopic properties which have important effects on their microscopic energy, such as rheology, colloidal stability, etc. Each unit of glucose has hydroxyl groups in C2, C3 and C6, which can form hydrogen bonds between them. The length of the polymer chain depends on the cellulose source and is related to the number of glucose units or degree of polymerization of LB (Figure 8) (Klemm et al., 2005).

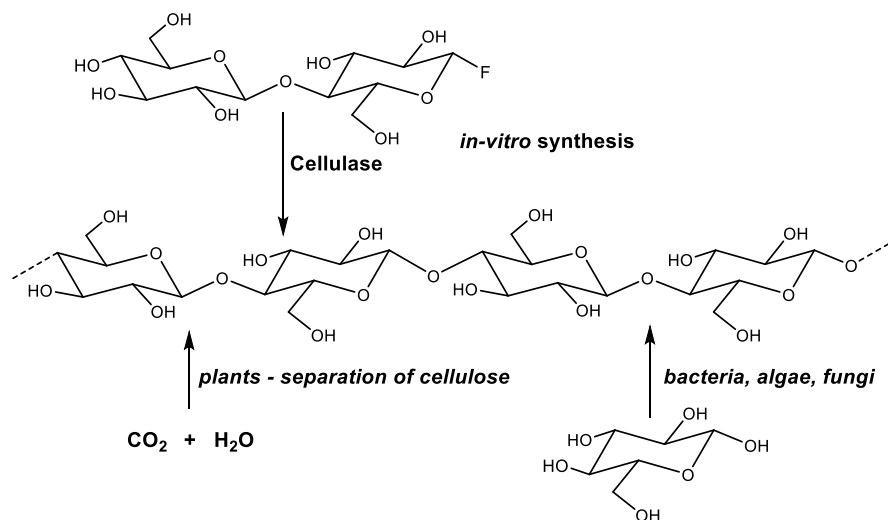


Figure 8: Principal pathways to cellulose formation (Klemm et al., 2005).

The molecular structure reveals cellulose its characteristic properties such as hydrophilicity, degradability, biocompatibility, stereo regularity, chirality, and broad chemical

variability that is related to the high reactivity of the OH groups. Thereby, the properties of cellulose are therefore determined by a defined hierarchical order in supramolecular structure and organization (Klemm et al., 2005).

Several pathways can be used to obtain cellulose, such as those highlighted in figure 8 (Klemm et al., 2005; Nakatsubo et al., 1996; Nobles et al., 2001). However, the dominant pathway for its production is from plants that are isolated by large-scale chemical pulping, separation, and purification processes. Thus, cellulose is commonly derived from wood source and isolated under harsh alkaline or acidic conditions (Frederick et al., 2008).

Different methods more eco-friendly are proposed to obtain cellulose. Van Spronsen *et al.* proposed the separation of the different fractions of the lignocellulosic material using ionic liquids and acetic acid as a co-solvent. These authors reported that the previous hydrolysis of the biomass in acid catalysis by addition of acetic acid favours the solubilization of its different fractions in the ionic liquid and later they can be separated by precipitation with solvents such as ethanol and water (Van Spronsen et al., 2011). Lara-Serrano *et al.* proposed the use of inorganic salt hydrates ($ZnCl_2 \cdot 4H_2O$) for total fractionation of biomass through dissolution/precipitation method (Lara-Serrano et al., 2023). The cellulose can be carried purified out biologically and/or chemically. The biological method is an eco-friendly, however, it has low productivity and depends on microbial enzymes. On the other hand, the chemical methods are non-ecofriendly, but it has high productivity and many types of equipment and steps (Hasanin et al., 2018).

In the current world context, cellulose has characteristics that give it clear advantages over synthetic fibers, having an enormous potential for replacing materials of fossil origin, polluting and harmful to ecosystems. Thus, attractors for pulp applications include packaging, healthcare, electronics, and printing (Aziz et al., 2022). Due to the presence of an activated hydroxyl group, cellulose and its derivatives have the advantage that they can be easily modified with other related functional groups, such as oxidation, esterification, etherification, graft copolymerization, cross-linking reactions, etc (Aziz et al., 2022).

The conversion of cellulose biomass to renewable and valuable chemicals has become the topic of intense research mostly driven by growing concerns about the depletion of petroleum oil reserves and the need to build sustainable societies (Guleria et al., 2019). In this context, biochemical fermentation is major method adopted for the bioconversion of cellulose to platform chemicals. It involves three steps including pre-treatment, saccharification and fermentation (Reshmy et al., 2022). During this process the cellulose hydrolyzed produced monomeric sugars that can be converted by a variety of microorganisms and/or chemical process in several biomaterials and platform chemicals such as levulinic acid, succinic acid, lactic acid, sorbitol, hydroxymethyl furfural, polyethylene, polylactic acid, polytrimethylene terephthalate, polyhydroxyalkalones, etc (Figure 9) (Reshmy et al., 2022).

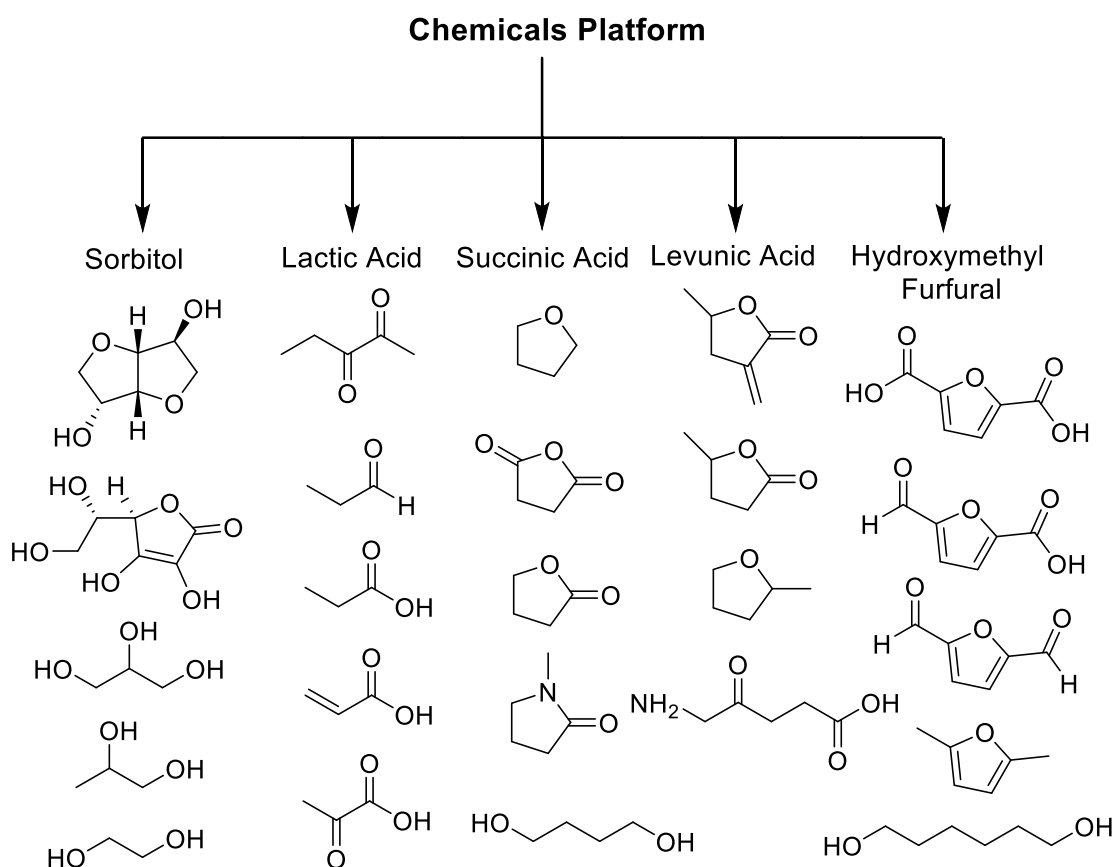


Figure 9: Platform chemicals from cellulosic biorefinery (Reshmy et al., 2022).

The valorization of LB offers significant environmental advantages compared to fossil fuels; they produce less environmental pollution, less carbon dioxide emissions and can ease global energy shortages (X. Zhang et al., 2013).

In general, two process can be applied to convert cellulose into high added-value products: catalytic or biological process. According to Desvaux *et al.*, its direct fermentation undergoes long reaction times, taking several days. In addition to the low yield of the final product (Desvaux et al., 2001). On the other hand, it is possible to carry out its depolymerization through acid hydrolysis which produces a maximum yield of glucose of about 70% by weight with reaction times of about 2 hours. However, this process requires an expensive corrosion-resistant reactor operated at high pressures and temperatures which represents a high operating cost related to acid recovery and high dilution of sugars in water (Rinaldi & Schüth, 2009; Shu-Lai Mok et al., 1992). Another option that has been commonly used is enzymatic hydrolysis. However, the high cost of the process makes it difficult to apply it on an industrial scale for this purpose. For this reason, several approaches are being proposed to its depolymerization, in highlighted the *fast* pyrolysis (Buendia-Kandia et al., 2020; Carvalheiro et al., 2008; Chandel et al., 2018; Fang & Riisager, 2021; Frederick et al., 2008; Lara-Serrano et al., 2023; J. Li et al., 2021).

2.2. Application of pyrolysis in the valorisation of lignocellulosic biomass

Pyrolysis is the most usually utilized thermochemical conversion process that can convert biomass feedstock into bio-oil yields (liquid), non-condensable gases, and biochar (BC) (a solid residue), depending on the type of method and operating parameters (Q. Wang et al., 2020); it can be classified into two types based on the heating time ($t_{heating}$) and the pyrolysis reaction time (t_r). Where slow pyrolysis ($t_{heating} \gg t_r$) and fast pyrolysis ($t_{heating} \ll t_r$) (Saravanan et al., 2019).

This high flexibility has caused the pyrolysis process to produce a wide range of valuable materials with different yields by changing operating parameters, including residence time, heating rate, and temperature (Kwon et al., 2018). In biomass pyrolysis the process has been taking place in the temperature range of 300–650°C differently compared to 800-1000°C for gassing and 200-300 °C for roasting (Saravanan et al., 2019). The characterized pyrolysis methods and their products are as follows:

✓ Torrefaction: It is a thermochemical process that involves the heating of biomass in the absence of oxygen at temperatures typically ranging from 200 to 300 degrees Celsius. This process results in the production of torrefied biomass.

✓ Carbonization: It is a high-temperature process that involves the conversion of organic materials, such as wood or biomass, into charcoal through the removal of volatile components, leaving behind carbon-rich residue.

✓ Fast pyrolysis: It is a thermochemical conversion process used to convert biomass into bio-oil or pyrolysis oil. It involves rapidly heating biomass in the absence of oxygen at high temperatures (typically between 350 and 600 degrees Celsius) for a short duration. This process yields several valuable products, with the primary one being bio-oil.

✓ Flash pyrolysis: It is a rapid and high-temperature thermochemical process used to convert biomass into a range of valuable products, including chemicals, gases, and bio-oil. Unlike slow pyrolysis, which typically yields more biochar and less bio-oil, flash pyrolysis is designed to maximize the production of these valuable products.

✓ Ultrarapid pyrolysis: It is an advanced thermochemical process that involves the extremely fast heating of biomass to ultra-high temperatures, typically in the range of 1000 to 1400 degrees Celsius, in a matter of milliseconds. This rapid heating leads to the production of primarily chemicals and gases, and it is designed to minimize the formation of biochar and bio-oil.

✓ Vacuum pyrolysis: It is a specialized pyrolysis process that is conducted under reduced pressure or vacuum conditions, typically below atmospheric pressure. This unique approach to

pyrolysis is often employed in the context of solid waste biorefineries to convert various organic solid wastes, including biomass and municipal solid waste, into bio-oil and other valuable products.

✓ Hydro pyrolysis: It is a thermochemical conversion process that combines pyrolysis with the use of hydrogen gas (H_2) to convert biomass into bio-oil and other valuable products. This method has gained attention due to its potential for improving the quality of bio-oil and reducing the production of undesirable byproducts.

✓ Methane pyrolysis: It is also known as methane cracking, is a chemical process that involves the thermal decomposition of methane (CH_4) into its constituent elements, primarily hydrogen (H_2) and solid carbon. This process is carried out at elevated temperatures and is used to produce hydrogen gas for various industrial applications, particularly in the chemical and petrochemical industries.

2.2.1. Pyrolysis reactor

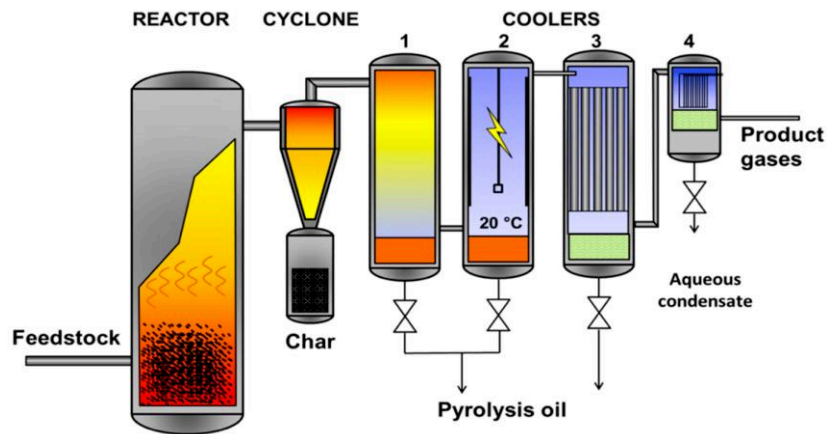


Figure 10: Representation of an experimental test equipment (Pandey et al., 2019).

The design of the pyrolysis reactor (Figure 10) is a crucial factor in the pyrolysis process as it plays a significant role in determining the qualitative and quantitative distribution of the

products (J.-S. Kim & Choi, 2018). Extensive research has been conducted on a reactor with the aim of enhancing two critical factors that contribute to achieving higher product yields: heating rate and residence time (Buendia-Kandia et al., 2020; Campuzano et al., 2019; Vo et al., 2022). The primary features of pyrolysis reactors include the generation of a high heat exchange rate, maintaining a controlled and moderate temperature, and ensuring rapid cooling or quenching of the pyrolysis reactor vapours. These aspects are crucial for the efficient operation of the reactors (Saravanan et al., 2019).

There are several commonly used reactor types for the pyrolysis of solid waste (SWs). Each reactor differs in terms of its working principle, advantages, and experimental setup (Saravanan et al., 2019). The following are some of the reactors used in this process:

- ✓ **Fixed Bed Reactor:** This reactor consists of a stationary bed of solid waste material through which heat is applied. It offers good control over the pyrolysis process and allows for the collection of valuable by-products.
- ✓ **Fluidized Bed Reactor:** In this type of reactor, solid waste particles are suspended and fluidized by a gas stream. It provides efficient heat transfer and allows for uniform heating and mixing of the material.
- ✓ **Rotary Kiln Reactor:** This reactor involves the rotation of a cylindrical vessel to facilitate the pyrolysis process. It offers continuous operation and allows for better control over heat and mass transfer.
- ✓ **Vacuum Pyrolysis Reactor:** This reactor operates under reduced pressure, which lowers the boiling points of volatile components. It enables the pyrolysis of materials at lower temperatures and reduces the risk of thermal degradation.
- ✓ **Auger Reactor:** An auger reactor employs a screw mechanism to move solid waste material through a heated chamber. It provides good mixing and heat transfer while allowing for continuous processing.

These reactor types represent a diverse range of approaches for pyrolysis, each with its own advantages and considerations depending on the specific requirements of the process.

Biomass pyrolysis has gained recognition as a highly efficient thermochemical conversion process, primarily because it allows for the extraction of both chemical compounds and calorific value from LB. This process enables the conversion of biomass into valuable products such as biofuels, biochar, and various chemicals, contributing to sustainable energy production and resource utilization (Enaime et al., 2020).

Sahoo *et al.* reported that this conversion technique can give bio-oil yields of up to 70–95% of the original biomass's weight (Sahoo et al., 2019). Zaini *et al.* proposed a process simulations of biomass pyrolysis coupled with steam reforming and water-gas-shift to produce of bio-oil that presented yield value of 46.0 wt.% dry biomass (Zaini et al., 2021). Chen *et al.* suggested the torrefaction is an efficient pretreatment method to improve the quality of biomass feedstock and resulting bio-oil. In this study, the sweet sorghum bagasse (SSB) was first pre-treated by torrefaction at different temperatures (230, 260, and 290 °C) resulting torrefied SSB was subsequently pyrolyzed at 500 °C to produce bio-oil (Chen et al., 2022).

The pyrolysis technology can be directly applied to biomass or its various fractions. Additionally, it can be effectively coupled with other processes, including biological processes, which holds great promise to produce chemicals in future integrated biorefineries. By integrating pyrolysis with biological processes, such as fermentation or enzymatic conversion, the overall value and versatility of the biomass feedstock can be enhanced. This integrated approach offers a promising pathway to maximize the utilization of biomass resources and generate valuable chemicals, further promoting the development of sustainable and economically viable biorefinery systems.

Thus, Buendia-Kandia *et al.* proposed the production of acetone and butanol through the cellulose pyrolysis, and later, fermentation by bacteria (*Clostridium acetobutylicum*). In this process, pyrolysis of cellulose was performed in a continuous fluidized bed reactor equipped with

a staged condensation system, including a warm electrostatic precipitator that separate pyrolytic vapours according to their condensation point (Buendia-Kandia et al., 2020). The different fractions obtained are rich in Levoglucosan (LG), a 1,6-anhydro derivative of beta-d-glucopyranose, which is mainly formed by cellulose or starch pyrolysis, and it can't be fermentable by *Clostridium acetobutylicum* (Figure 11) (Buendia-Kandia et al., 2020).

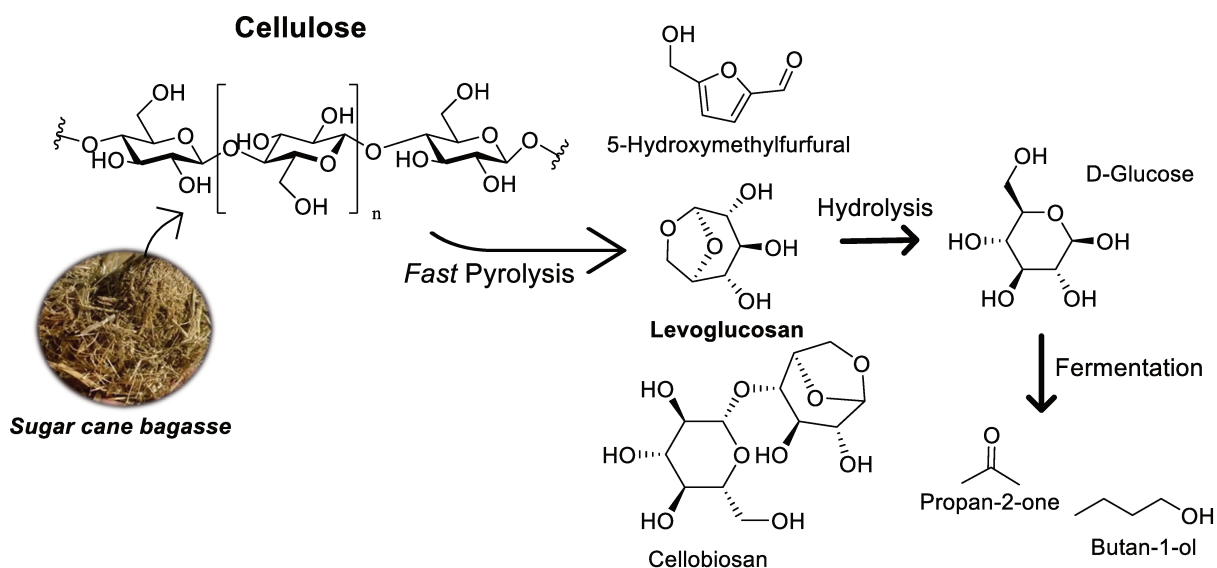


Figure 11: Proposed cellulose biorefinery using fast pyrolysis, hydrolysis, and fermentation (Buendia-Kandia et al., 2020).

2.3. Levoglucosan as a platform to obtain molecules with high added-value

LG is a bicyclic anhydride derivative of β-D-glucopyranose. It is primarily produced through the pyrolysis of cellulose or starch. Cellulose is often preferred over starch in this context due to its availability and the fact that it does not compete with the food supply (Itabaiana Junior et al., 2020a). By utilizing cellulose as a feedstock for pyrolysis, the production of LG can be achieved in a sustainable manner, supporting the development of renewable and environmentally friendly processes.

Due to its distinctive presence in biomass burning emissions, LG has been widely used as a molecular marker for identifying and quantifying biomass burning events. It serves as a

valuable tool for assessing air quality, particularly in areas where biomass burning is prevalent. LG can be measured in atmospheric samples and used to monitor and analyse the impact of biomass burning on local and regional air pollution (Y. Li et al., 2021). Additionally, the presence of LG has been utilized to reconstruct past fire histories, known as paleo-fire records. By analysing LG concentrations in snow and ice samples from glaciers, scientists can gain insights into historical biomass burning events and fire activity over long time scales (You & Xu, 2017). This information helps in understanding past climate dynamics and ecosystem changes.

One of the products obtained through fast pyrolysis of biomass is bio-oil. Bio-oil is a viscous mixture that arises from the oxidation of biomass polymers. Its composition includes various components, with LG being a prominent constituent (Figure 12) (Rocha et al., 2013), this anhydrous sugar can be converted to different high added-value chemicals such as glucose, 5-hydroxymethylfurfural (HMF), furfural, sorbitol, levoglucosenone, and as highlighted in this work, carbohydrate fatty acid esters, denoted as CFAEs (Figure 12) (Itabaiana Junior et al., 2020; Bassut et al., 2022).

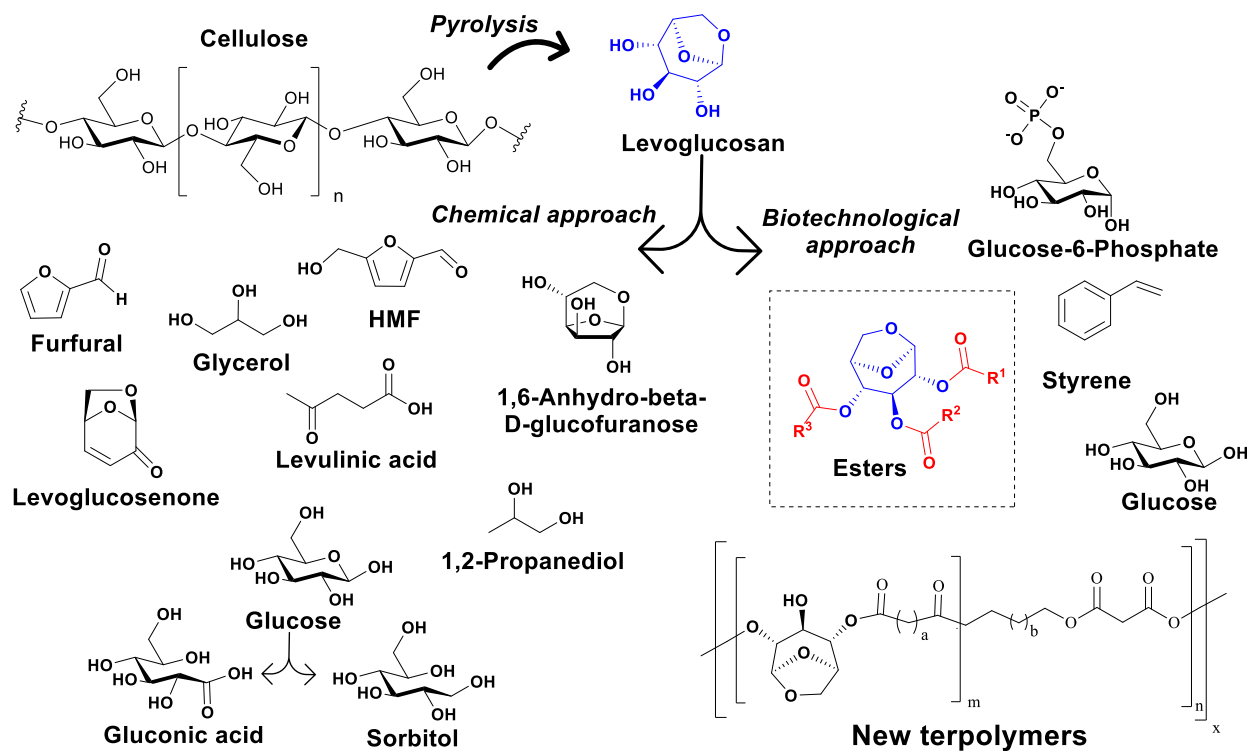


Figure 12: Some examples of exceptionally prized products obtained through chemical and biochemical transformations by LG (Adapted from: (Itabaiana Junior et al., 2020;.Bassut et al., 2022).

LG is indeed a significant product of cellulose pyrolysis. Extensive research has been conducted on cellulose pyrolysis, and its production of LG has been thoroughly reviewed in previous studies (KAMIŃSKA et al., 2018; LE ÂDE; BLANCHARD; BOUTIN, 2002; WANG et al., 2017). The yields of LG obtained through pyrolysis can vary significantly, ranging from 5 to 80 percent carbon (%C). These variations depend on various factors, including the experimental conditions employed, the type of reactor utilized, and the specific characteristics of the lignocellulosic substrate being pyrolyzed, as reviewed by (Maduskar et al., 2018).

The complex interplay between heat transfer, phase changes, chemical reactions, and mass transfer in cellulose pyrolysis contributes to the wide range of LG yields observed. Understanding these fundamental mechanisms and their interactions is crucial for optimizing pyrolysis conditions and enhancing the yield of LG and other desired products from cellulose (Dufour et al., 2011; Westerhof et al., 2016). Overall, the heating of cellulose particles during

pyrolysis leads to depolymerization reactions, phase changes, and subsequent secondary reactions in the liquid and gas phases. The resulting products are then transferred from the cellulose particles to the surrounding gas, contributing to the overall composition and yield of the pyrolysis products (Figure 13) (ITABAIANA JUNIOR et al., 2020; SUUBERG; MILOSAVLJEVIC; OJA, 1996a).

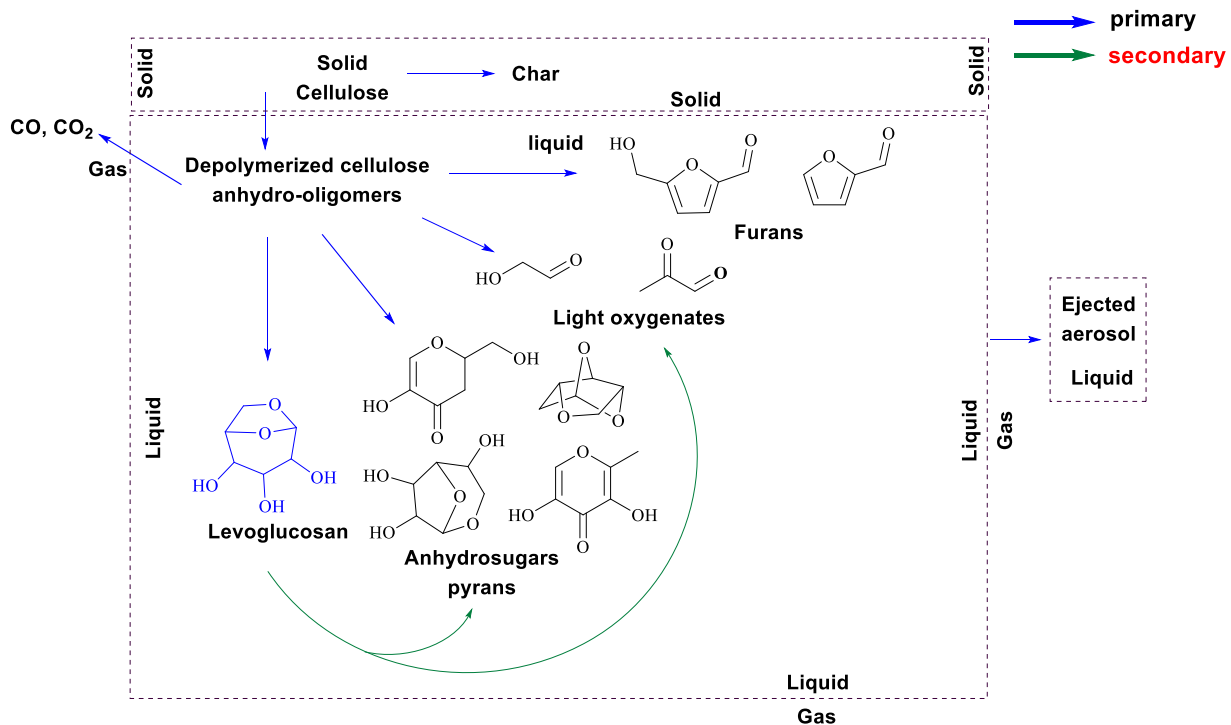


Figure 13: Schematic representation of primary and secondary reactions in cellulose pyrolysis (Adapted from (Itabaiana Junior et al., 2020).

Regardless of the specific heat transfer mechanism employed, it is essential for the pyrolysis reactor to provide a high heat flux density (measured in watts per square meter, W/m^2) to the surfaces of the cellulose particles for a fluidized bed reactor the LG formation is around $450\text{--}500\text{ }^\circ\text{C}$ (Rover, Johnston, Whitmer, et al., 2014). This high heat flux density ensures that the particles receive sufficient heat energy, promoting the pyrolysis reactions and facilitating the formation of LG (Boutin et al., 1998; De Jenga et al., 1982).

The initial stage of depolymerization involves an endothermic process, meaning that it absorbs heat. Similarly, the evaporation of intermediate liquids during this process is also characterized by an endothermic nature. On the other hand, the crosslinking reactions that give rise to the formation of char, a solid substance rich in carbon, are exothermic, indicating that they release heat (S-I Mok & Antal, 1983; Suuberg et al., 1996b).

Secondly, when cellulose is subjected to heating, it undergoes several chemical reactions. The mechanisms of cellulose pyrolysis have been under investigation since the early twentieth century (Lédé, 2012). The primary conversion of cellulose predominantly occurs within the temperature range of 300 °C to 450 °C. These mechanisms can be influenced by the operating conditions, such as the temperature of the heat source and heat flux density, as well as the presence of inorganic substances. Cellulose can be converted through three main pathways: i) Transglycosylation; ii) Dehydration or iii) Open ring/fragmentation (Figure 14).

The combination of various mechanisms results in the formation of compounds derived from cellulose, such as furans and methylglyoxal. Specifically, furans are generated through open-ring reactions and dehydration, which facilitate the transformation of the glucopyranose structure into furan rings. Transglycosylation reactions are responsible for the formation of LG. In this context recent significant advancements in theoretical chemistry, utilizing methods like ab initio calculation and density functional theory (DFT) models, have unveiled crucial insights into the fundamental reactions involved. Due to the considerable computational expenses associated with DFT modeling, the reactants used in the models are typically smaller surrogates of cellulose, such as glucose, cellobiose, or celotriose (Lu et al., 2018).

Maduskar *et al.* proposed a catalytic mechanism wherein vicinal hydroxyl groups present in neighbouring cellulose sheets play a crucial role in facilitating the transglycosidic C-O bond activation and subsequent formation of LG (Maduskar et al., 2018). This catalytic promotion of LG formation occurs through the involvement of reactive hydroxyl groups, particularly in mass-

transport limited experiments where the intermediate liquids generated during cellulose fast pyrolysis hold significant importance (Maduskar et al., 2018).

The formation of LG is influenced by the degree of polymerization (DP), crystallinity, and allomorph type of cellulose. Wang *et al.* conducted a study revealing that within the temperature range of 350 to 450 °C, cellulose samples with higher crystallinity exhibited higher yields of mono-anhydrosugars, specifically levoglucosan and levoglucosenone, during fast pyrolysis. This finding was determined using pyrolysis-gas chromatography/mass spectrometry (Py-GC/MS) analysis (Figure 14) (Z. Wang et al., 2013).

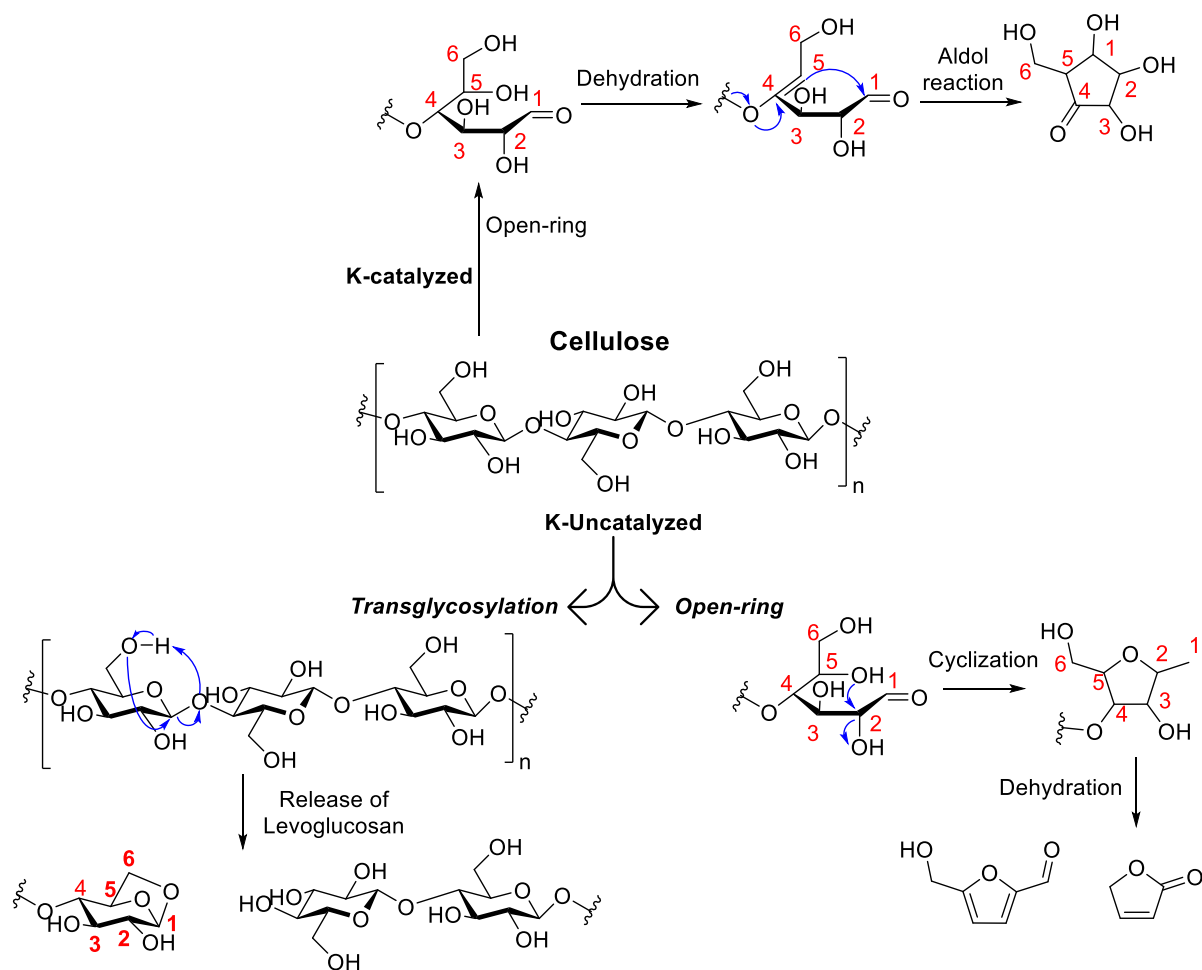


Figure 14: Simplified mechanism of cellulose pyrolysis highlighting the main degradation pathways and key volatile markers. Adapted from (Le Brech et al., 2016a).

In contrast, Shanks *et al.* conducted a study demonstrating that the crystallinity index, DP, and feedstock type had a negligible influence on the distribution of resulting products (J. Zhang *et al.*, 2014). These findings suggest that hydrogen bonding and van der Waals forces do not significantly impact the primary reactions involved in the thermal decomposition of cellulose under fast pyrolysis conditions. Therefore, there is currently no consensus regarding the effect of DP and crystallinity of cellulose on LG yields. However, there is a consensus regarding the significant impact of minerals on LG formation. Minerals present in the LB have been found to hinder the formation of LG through transglycosylation reactions, while simultaneously promoting the generation of cyclopentenones via rearrangement (aldol reaction) and carbohydrate dehydration processes (Le Brech *et al.*, 2016b). Due to this effect, a proposal has been made to demineralize LB to enhance LG yield (Oudenhoven *et al.*, 2013). By removing or reducing the mineral content, it is believed that the inhibitory impact on LG formation can be mitigated, potentially leading to increased LG production.

Indeed, several review articles have been published on the topic of removing minerals from biomass and its subsequent influence on cellulose pyrolysis (Lachos-Perez *et al.*, 2023; Molton & Demmitt, 1977). While a comprehensive overview of these articles is beyond the scope of this response can provide a brief example. One such example involves leaching pinewood with an acid-rich bio-oil fraction prior to biomass pyrolysis, which has been shown to effectively eliminate the alkali ions initially present in the biomass (Oudenhoven *et al.*, 2013). This approach aims to reduce the mineral content and its potential inhibitory effects, thereby potentially improving the pyrolysis process and increasing the yield of desired products such as LG.

During the washing step, no significant consumption of acetic acid was observed. However, rinsing the biomass after acid washing was necessary to achieve maximal LG production. This rinsing step aimed to remove the washing liquid containing the dissolved minerals. Oudenhoven *et al.* implemented this method and successfully achieved a LG yield of

17 wt% (based on anhydrous wood mass) following the demineralization of pine wood using the acid-rich fraction of the bio-oil (Oudenhoven et al., 2013).

To summarize, based on fundamental knowledge of cellulose pyrolysis, the following factors can optimize LG yield:

- ✓ Use of small particles: Utilizing small particle sizes promotes both intra-particle heat and mass transfers, facilitating efficient pyrolysis.
- ✓ Demineralization of woody biomass: Acid leaching or similar methods can help remove minerals from the biomass, reducing their inhibitory effects on LG formation.
- ✓ Fast heating rate: Employing a fast-heating rate, such as in a fluidized bed reactor, ensures rapid pyrolysis and enhances the production of LG.
- ✓ Moderate reactor temperature: A moderate reactor temperature of around 500 °C is considered optimal for LG yield.
- ✓ Low residence time: Maintaining a low residence time of vapors, approximately 1 second at 500 °C, allows for efficient conversion and prevents excessive degradation of LG.

By considering these factors, it is possible to enhance the production of LG during cellulose pyrolysis.

Despite the considerable research conducted on the fundamental aspects of LG formation, there remains a scarcity of studies focused on achieving significant LG yields in larger-scale and continuous reactors (Liaw et al., 2013; Patwardhan et al., 2011; Westerhof et al., 2016). However, some notable achievements have been reported.

For instance, Piskorz *et al.* were able to produce up to 38 wt% of LG (based on the mass of anhydrous cellulose) in a continuous pilot-scale fluidized bed reactor. They employed Avicel cellulose treated with 5 mass% sulfuric acid at 90 °C for 5.5 hours, operating the reactor at a gas residence time of 0.5 seconds and a sand temperature of 500 °C (Piskorz et al., 1989).

Additionally, Patwardhan *et al.* reported a LG yield of 42 wt% (based on cellulose) in a fluidized bed reactor operating at 500 °C and a gas residence time of 1.3 seconds (Patwardhan *et al.*, 2011).

These studies highlight promising results in achieving higher LG yields in continuous reactors, providing valuable insights for scaling up the production of LG through optimized process parameters and reactor configurations.

In the purification process, the initial stage involves the staged condensation of vapors at the outlet of the pyrolysis reactor. This condensation system serves to selectively separate and recover compounds present in the vapor phase based on their boiling points. The objective is to obtain a heavy oil fraction enriched with LG, while separating the light oil fraction containing compounds such as aldehydes, alcohols, and carboxylic acids (Pollard *et al.*, 2012b).

The separated light fractions, which consist of these various compounds, can be utilized for other purposes. For example, they can be employed in the pre-treatment of biomass for demineralization. By valorizing the light fractions for pre-treatment, they contribute to enhancing the overall efficiency and yield of LG production (Westerhof *et al.*, 2016).

In the study conducted by Pollard *et al.* (Pollard *et al.*, 2012a) obtained various fractions with distinct chemical and physical properties through staged condensation. The sugar fractions, including LG, were recovered alongside phenolic compounds, referred to as "heavy ends."

Further purification of the condensed bio-oil containing the LG-rich fraction is necessary for subsequent chemical or biological conversion processes. To enhance the fermentation of the LG fraction by fungi and yeasts, purification methods have been employed on LG-rich bio-oils derived from wood pyrolysis. These purification methods include:

- ✓ Aqueous extraction: This process involves removing lignin from the bio-oil, leaving behind the LG fraction in an aqueous extract.
- ✓ Activated charcoal treatment: In this method, both lignin and aromatics are removed from the bio-oil using activated charcoal, resulting in a purified LG fraction.

✓ Acid hydrolysis: This approach removes lignin and aromatics while converting LG into glucose through hydrolysis. The resulting bio-oil contains purified glucose, and the LG fraction is transformed.

The detoxification of bio-oils through these purification methods enables yeast and fungi to effectively utilize the LG present in the wood pyrolysate liquor, thereby facilitating downstream processes and applications (Pollard et al., 2012a).

By leveraging the disparity in water solubility between sugars (such as LG) and phenolic compounds derived from lignin, it becomes possible to selectively extract and recover the desired sugar-rich fraction from the pyrolysis products. This extraction method provides an effective means of separating and obtaining the sugar components for further processing or utilization. In this context, Rover's study demonstrated the efficient extraction of sugars, predominantly LG, using a water-based extraction process. Through two water washes, the sugars were extracted at a remarkable yield of over 93 wt% (Rover, Johnston, Jin, et al., 2014).

The recent study conducted by Rover *et al.* represents the first investigation on the production of purified LG crystals using a combination of liquid/liquid extraction, adsorption, and crystallization techniques (Rover et al., 2019). The methodology employed in this study is schematically represented in Figure 15, illustrating the sequential steps involved in the purification process. This innovative approach offers a promising means of obtaining highly purified LG crystals, potentially enhancing their applications and facilitating further research in this field.

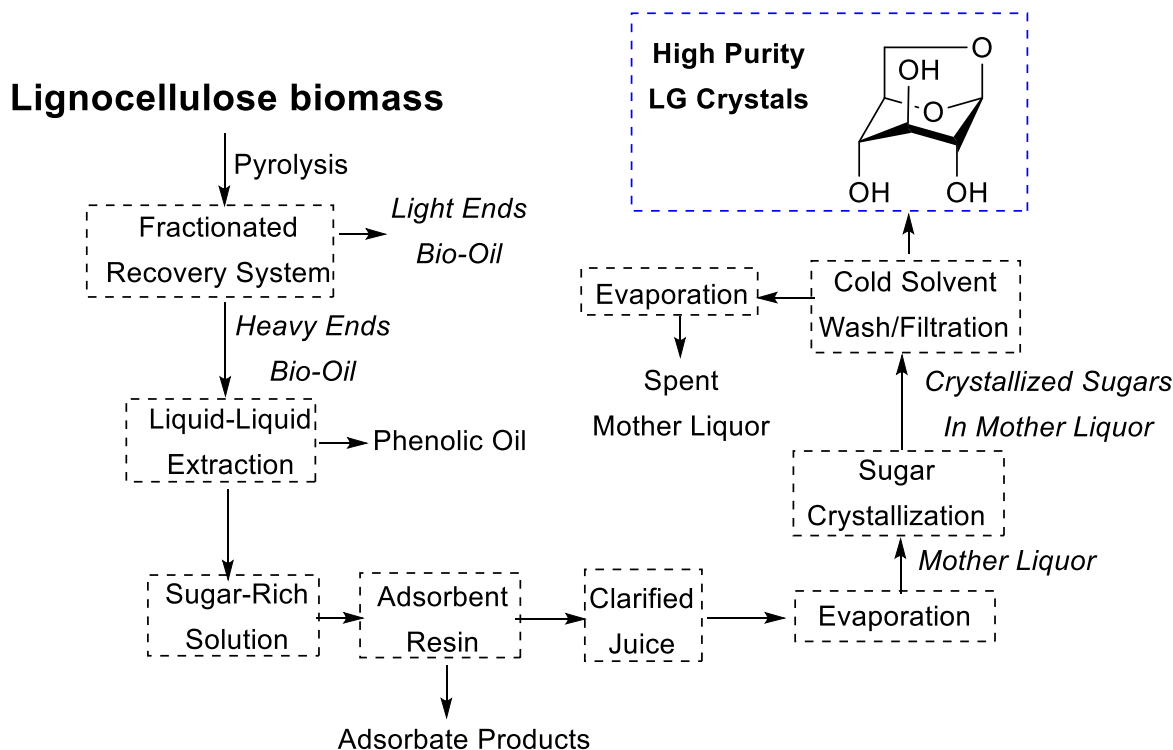


Figure 15: Proposed methodology for the production and purification of LG from lignocellulosic biomass. Adapted from (ITABAIANA JUNIOR et al., 2020).

In the study by Rover *et al.*, a combination of bio-oil fractionation, liquid-liquid extraction, and filtration using acid resins was employed to achieve a high yield of total sugars. The process resulted in the recovery of 81.2 wt% of total sugars, with the levoglucosan (LG) portion accounting for 44.7 wt%. Successful removal of the phenolic fraction was accomplished through filtration using Sepabeads SP207 resins. Following solvent evaporation, crystallization was performed, resulting in a LG recovery of 24.7% from the mother liquor. The crystals obtained exhibited a high purity level of 102.5% ($\pm 3.109\%$ at the 99% confidence level), indicating a successful purification process. Furthermore, the authors conducted a techno-economic analysis, which revealed that the production of high-purity LG crystals could be achieved at a cost of \$1333 per metric ton (MT). This cost was significantly lower than the current market price for comparable LG crystals with similar purity levels. These findings highlight the feasibility and economic viability of producing purified LG crystals using the proposed methodology (Rover et al., 2019).

Indeed, the reduction of inhibitory compounds and the efficient separation of LG from other components have been significant challenges in the valorisation of bio-oil. As mentioned previously, various pretreatment methods applied to biomass can result in the formation of inhibitory compounds that can impede the desired conversion processes. Their presence can hinder the efficient production and separation of LG or other valuable compounds from the bio-oil.

Addressing this challenge requires the development of effective pretreatment strategies and separation techniques to minimize the formation and impact of inhibitory compounds. By optimizing pretreatment methods and implementing suitable purification and separation processes, researchers aim to enhance the yield and purity of LG while mitigating the inhibitory effects of other compounds, enabling more efficient bio-oil valorization (K. Zhang et al., 2016).

Nowadays, there has been a notable increase in industrial interest in the production of LG and other anhydro sugars (Rover et al., 2019). This growing interest can be attributed to several factors. Firstly, LG holds significant potential in the chemical industry, as it can be utilized in the manufacturing of various products as already mentioned, in highlighted sorbitol. Its versatile properties and wide range of potential applications make it an attractive option for industrial utilization.

Another advantage lies in the synthesis process of LG itself, which involves pyrolysis. Pyrolysis is a thermal decomposition process that does not require the use of solvents or enzymes to depolymerize cellulose. This feature simplifies the production process and makes it easily scalable, thereby facilitating its commercial applications. The absence of solvents and enzymes reduces the complexity and costs associated with the production of LG (Venderbosch & Prins, 2010).

These combined factors make LG an attractive candidate for industrial applications, offering a sustainable and commercially viable alternative to traditional materials and processes

in various sectors. As a result, the industrial interest and investment in LG production have witnessed a significant upsurge.

In this scenario, LG might be a promising chemical platform for the synthesis of several compounds. LG can be transformed into derived esters with a hydrophobic/hydrophilic balance that is of great value as surfactants, emulsifiers, or even lubricants, showing great potential of application in the most diverse industrial sectors.

Currently, several studies have turned their attention to the application of pure LG in different approaches to produce high added value compounds. In fact, the use of LG in the absence of pyrolysis inhibitors and by-products may provide new biotechnological possibilities. However, the molecule also imposes barriers. LG is not highly hydrophilic, its dissolution in organic solvents usually applied in the organic synthesis can be limited (Mochida & Kawamura, 2004). In addition, it is already known that LG has instability in some organic solvents, leading to the formation of side products, decreasing the efficiency of some catalytic systems. Hu *et al.* analysed the effect and the influence of several solvents on the stability of LG during acid catalysis at 70 °C using Amberlyst 70 and demonstrated that the nature of the solvent strongly impacts the product distribution and polymer formation in acid-catalysed conversions (Hu et al., 2012). Alcohols could inhibit the growth of soluble polymers, different from water. Chloroform is not a suitable solvent, although acetone reacted with LG, resulting in polymerization. DMSO catalysed the conversion of a complex series of derivatives of LG (Figure 12) including HMF and 2,5-furandicarboxaldehyde. According to Climent et al. LG serves as a versatile platform molecule to produce value-added chemicals. It offers a wide range of possibilities as multiple chemo or enzymatic pathways can be utilized to obtain these valuable products (Climent et al., 2011).

2.3.1. Enzymatic approach

The LG present in bio-oil can be directly utilized through fermentative processes, where microorganisms are used to assimilate LG as an organic carbon source (D. Chang et al., 2022). To ensure efficient metabolism of LG by microorganisms, the presence of LG kinase (LGK) and LG dehydrogenase (LGDH) enzymes are essential (Bacik et al., 2011). These enzymes play fundamental roles in the conversion and utilization of LG by microorganisms. In certain cases, these enzymes can be naturally found in filamentous fungi, yeasts, and wild-type bacteria, which facilitates the direct assimilation of LG (Bacik et al., 2011; D. Chang et al., 2022). When these enzymes are naturally present in the microorganisms used, it eliminates the need for additional genetic modifications or engineering to introduce these specific enzymes. The microorganisms can readily utilize LG as a carbon source, thanks to the presence of LGK and LGDH enzymes. This natural occurrence simplifies the process of LG assimilation and enhances the efficiency of the overall fermentation process. However, in situations where LGK and LGDH enzymes are not naturally present in the microbial strains used, it is possible to obtain these enzymes through protein engineering tools. This involves modifying or introducing genes into microbial cells, resulting in the production of the necessary enzymes for LG metabolism.

Initially, LG undergoes phosphorylation into glucose-6-phosphate by either levoglucosan kinase (LGK) or 1,6-anhydro-N-acetylmuramic acid kinase (AnmK). Subsequently, glucose-6-phosphate is metabolized through the glycolysis pathway. Alternatively, levoglucosan can undergo sequential metabolism involving oxidation, β -elimination, hydration, and reduction (Figure 16) (M. Yang et al., 2022).

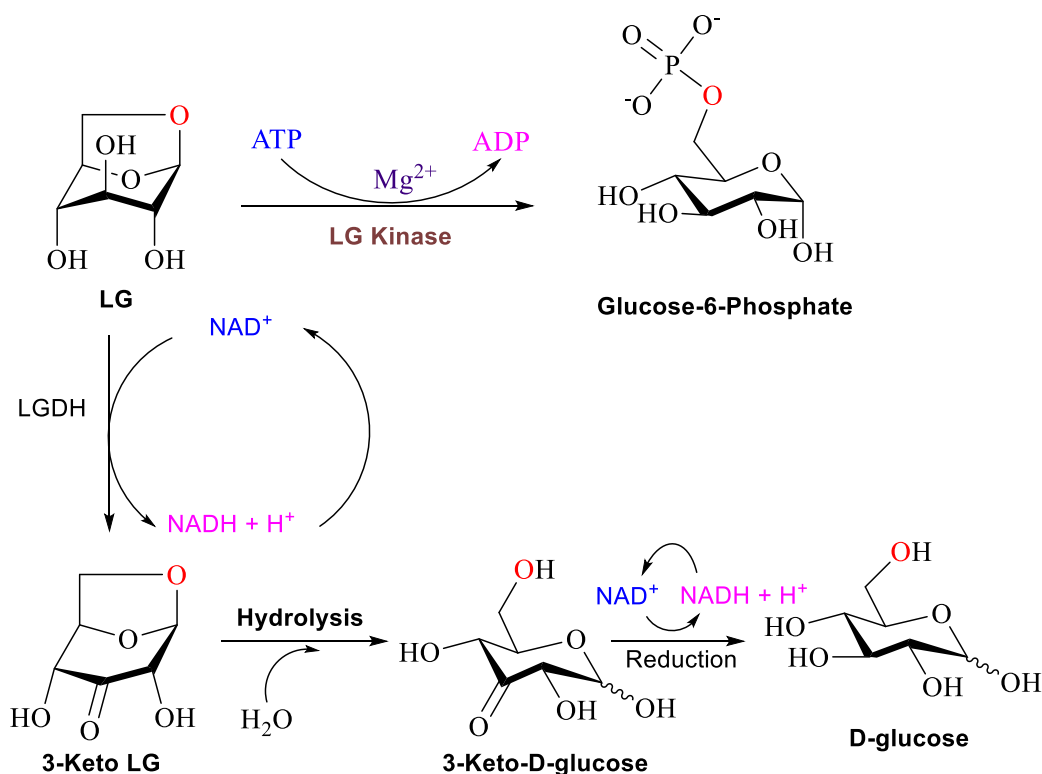


Figure 16: Eukaryotic enzymatic cleavage and phosphorylation through the action LGK to produce G6P (M. Yang et al., 2022).

Another approach is the hydrolysis of LG to glucose can be performed chemically by using specific catalysts or enzymatically using enzymes such as glucosidases or cellulases (Linger et al., 2016). Both methods break down the LG molecule, releasing glucose as a product. Glucose, being a commonly metabolized sugar, can be readily consumed by different microbial strains as a carbon source for their metabolic processes. Furthermore, bio-oil, derived from biomass pyrolysis, can contain various compounds that may act as inhibitors to microbial growth and metabolism. These inhibitors can include phenolic compounds, organic acids, furans, and other by-products of pyrolysis. If not effectively removed or mitigated, these inhibitors can have detrimental effects on the activity and productivity of the microorganisms involved in the fermentation process (Bacik et al., 2011; D. Chang et al., 2022; Itabaiana Junior et al., 2020a; Linger et al., 2016).

On the other hand, enzymatic catalysis offers a more selective and environmentally friendly approach. Enzymes can be employed directly outside cells to catalyse specific reactions and convert LG into desired compounds with high efficiency and selectivity. For example, lipases can be utilized to perform various transformations on LG, unlocking its potential to produce bioactive molecules, pharmaceuticals, fine chemicals, or specialty products.

2.3.1.1. Lipases

Lipases, classified as triglycerides (TG) acyl hydrolases (E.C. 3.1.1.3), exhibit the ability to hydrolyse TG within aqueous emulsions. This hydrolysis process results in the release of fatty acids, diacylglycerols (DG), monoglycerides (MG), and glycerol esters (Figure 17). These compounds possess diverse structures of acyl groups and alkyl chains (Chandra et al., 2020). Besides hydrolysis activity they display interesterification, esterification, aminolysis and alcoholysis activity which are contributed to wide range industries (Aguillón et al., 2019; do Nascimento et al., 2019; Do Nascimento et al., 2019; do Nascimento et al., 2023; Do Nascimento, Vargas, Rodrigues, Leão, De Moura, Leal, Bassut, De Souza, Wojcieszak, & Itabaiana, 2022). They do not require any cofactor and belongs to the class of serine hydrolases.

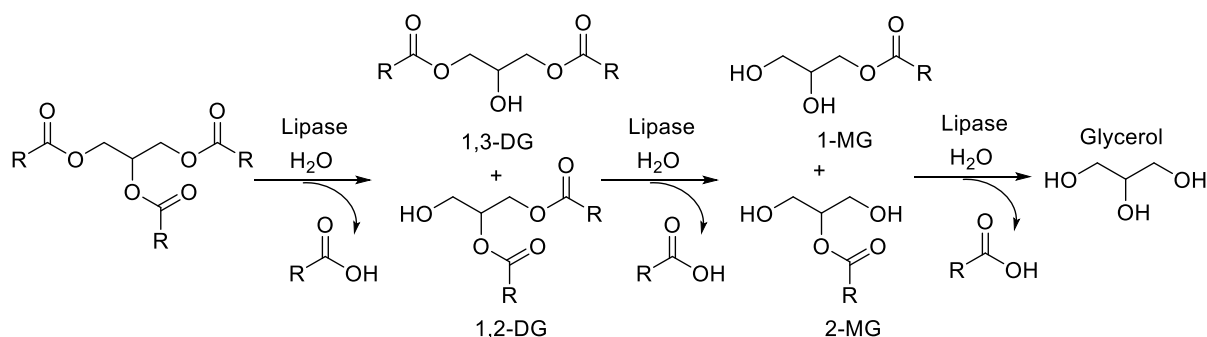


Figure 17: Hydrolysis reaction of triacylglycerols catalysed by lipases. Adapted from (BENITO-GALLO et al., 2015).

2.3.1.1.1. Hydrolysis Mechanism

Lipases exhibit a distinctive tertiary structure known as α/β -hydrolase folding, characterized by a hydrophobic β central leaf composed of eight different β chains connected to six α -helices. This structural arrangement is also observed in lipase B from *Candida antarctica* (CalB), showcasing the α/β -hydrolase folds (Figure 18).

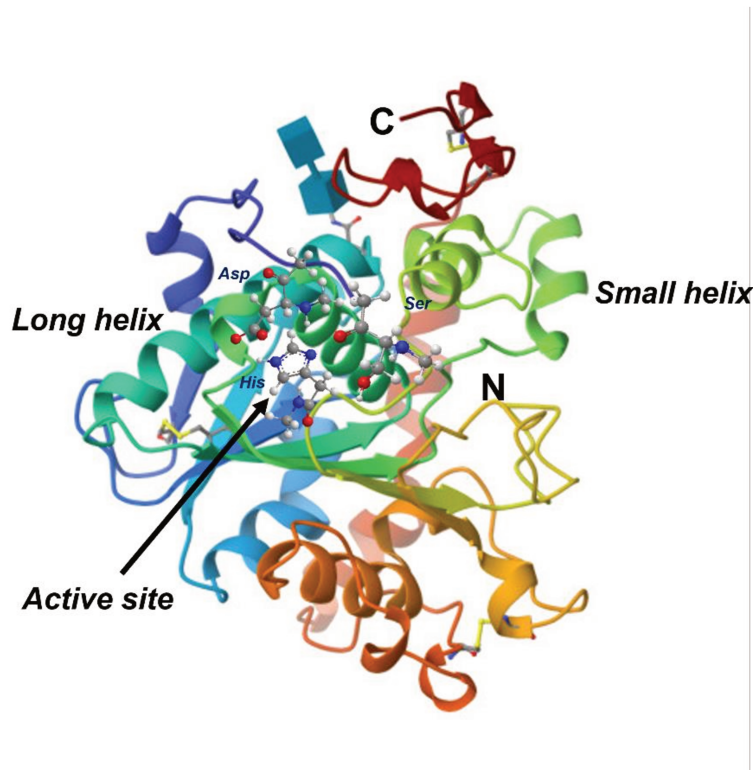


Figure 18: Crystallographic structure representative of the CalB lipase. The catalytic triad at the active site is displayed: Ser105, His224 and Asp187 (PDB code: 1TCA).

Lipases function according to the classical catalytic triad mechanism that are composed of amino acid residues L-serine (Ser), L-aspartate (Asp) (or glutamate), and L-histidine (His), an oxyanion hole, and typically a hydrophobic "cap" formed by an α -helix that covers the active enzyme site (Cen et al., 2019).

The lipase CalB is composed of 317 amino acids and has a molecular weight of 33 kDa. It has an isoelectric point (pI) of 6.0. CalB adopts an open-closed conformation, which is highly influenced by factors such as pH, temperature, solvent, and substrate conditions. Unlike CalA, CalB does not possess a lid or interfacial activation mechanism (Martinelle et al., 1995).

The mechanism of the lipase reaction is commonly known as "bi-bi ping pong" and entails the serine residue reacting with the carboxylic acid or ester group present in the substrate, leading to the formation of an acyl-enzyme intermediate. Upon formation of the acyl-enzyme and facilitated by hydrogen bonding with neighbouring amino acid residues, a nucleophilic attack occurs, leading to the generation of the product and subsequent regeneration of the biocatalyst (Figure 18) (Lima et al., 2019).

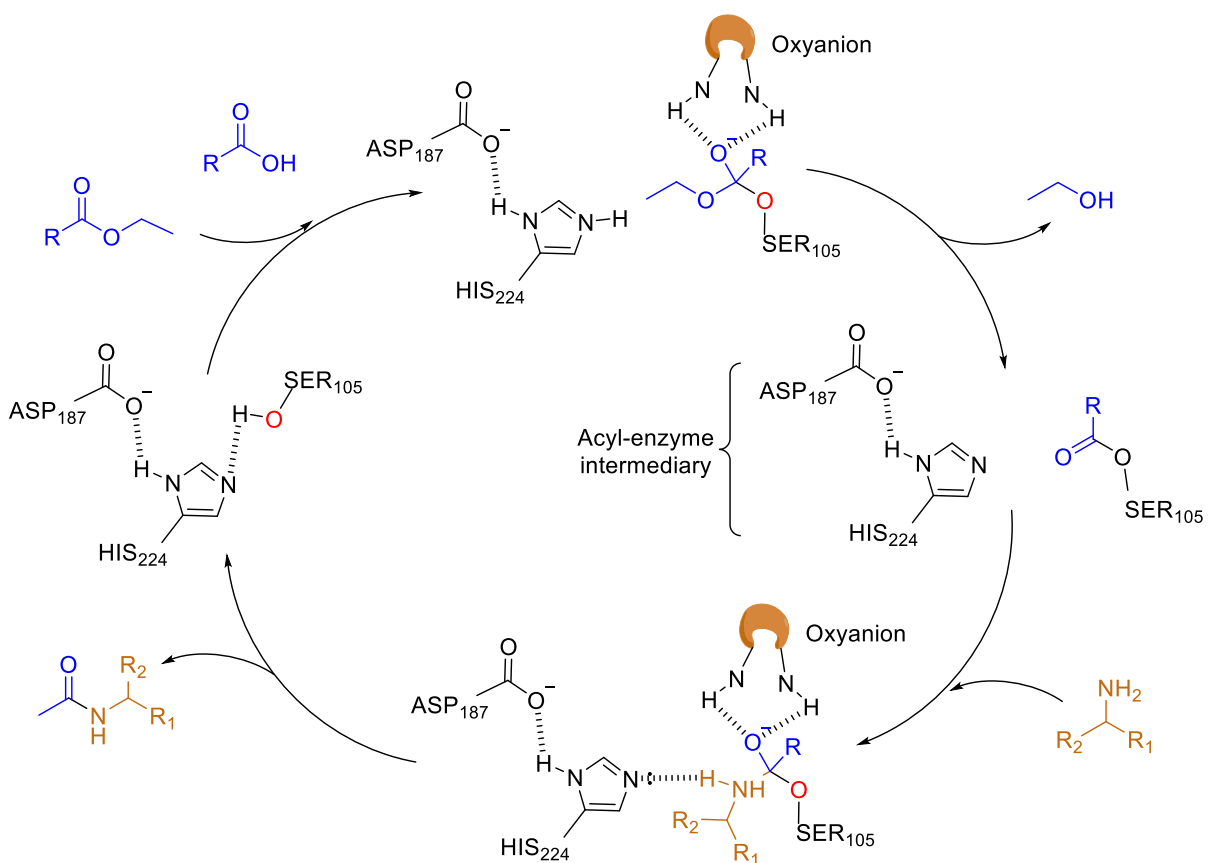


Figure 19: General simplified mechanism of lipase-catalysed amidation (Lima et al., 2019).

2.3.1.1.2. Catalytic Promiscuity of lipases

Enzymes exhibit high levels of chemo-, regio-, and enantioselectivity. They are environmentally friendly, operate under mild conditions, and display substrate promiscuity, thereby holding tremendous potential for applications in chemical transformations. Enzymes offer

numerous advantages over traditional catalysts (Angajala et al., 2016; Gamayurova et al., 2021; Gotor-Fernández et al., 2006; Miranda et al., 2015).

In this context, lipases exhibit the ability to hydrolyse various ester and amide substrates through an acyl-enzyme intermediate when the reaction is carried out in the presence of water. However, when the reaction takes place in an organic solvent and in the presence of other nucleophilic species, different products can be obtained (Gotor-Fernández et al., 2006). These products may arise from transesterification reactions (in the case of esters), aminolysis or ammonolysis reactions (in the case of amides), esterification, epoxidations, aldol reactions, Michael addition, and kinetic resolution of alcohols and amine (Lima et al., 2019). There are several examples of lipases applied in organic synthesis.

The widespread use of lipases as promiscuous catalysts takes advantage of their substrate promiscuity, such as in selective reactions involving the generation or cleavage of amide bonds. Two outstanding examples are proposed by Lima *et al.*: i. amidification of amino acids and peptides using CalB, as shown in Figure 20, and ii. selective transamidation to obtain a precursor of Saxagliptin (an active ingredient in some diabetes drugs), as illustrated in Figure 21 (Lima et al., 2019).

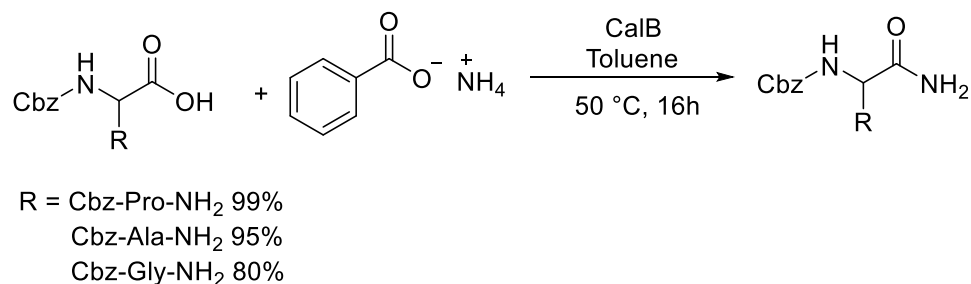


Figure 20: Use of CalB in the amidation of acid ends of amino acid chains as a key step in the synthesis of short peptides (Lima et al., 2019).

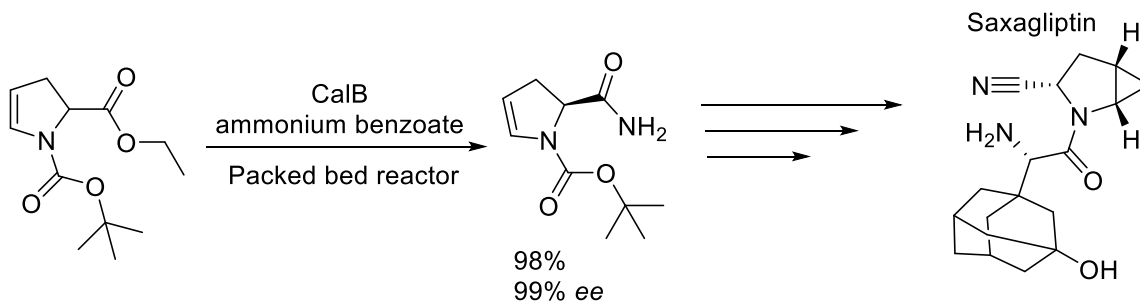


Figure 21: Selective aminolysis of 1-tert-butyl-2-ethyl-2,3-dihydro-1H-pyrrole-1,2-dicarboxylate to obtain a precursor of Saxagliptin (Active ingredient for the treatment of diabetes) (Lima et al., 2019).

In a patent from Nanjing Tech University granted in 2018 (de María et al., 2019), various lipases were employed as catalysts for the Knoevenagel reaction, which involves the reaction between indolin-2-one and different aromatic aldehydes, resulting in the synthesis of the corresponding 3-arylidene derivatives. These compounds find broad applications as therapeutic agents, exhibiting antibacterial, antitumor, or anti-inflammatory properties. Among the catalysts tested, porcine pancreatic lipase (PPL) demonstrated remarkable effectiveness in a water/dimethyl sulfoxide (DMSO) mixture (1/4 v/v) at a temperature of 45°C (Figure 22).

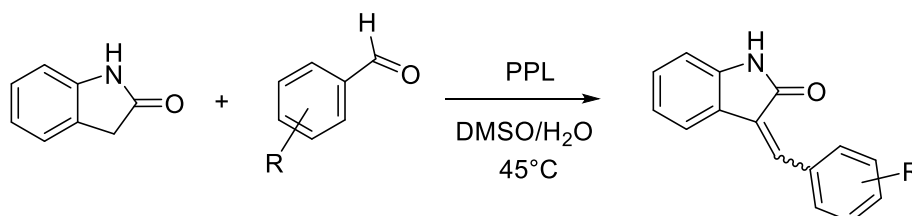


Figure 22: Lipase-catalyzed Knoevenagel condensations (de María et al., 2019).

The recognition of various organic substrate types and their successful performance in organic solvents are examples of catalytic promiscuity. An interesting example is the transesterification of Lobucavir with the protected amino acid Cbz-L-valine to synthesize the prodrug Lobucavir L-valine, an antiviral agent used in the treatment of herpes and hepatitis B viruses. The reaction, catalyzed by *Pseudomonas cepacia* lipase, exhibited selectivity and yielded

the Cbz-protected intermediate of Lobucavir L-valine with a yield of 87% (Figure 23) (Cossy, 2012).

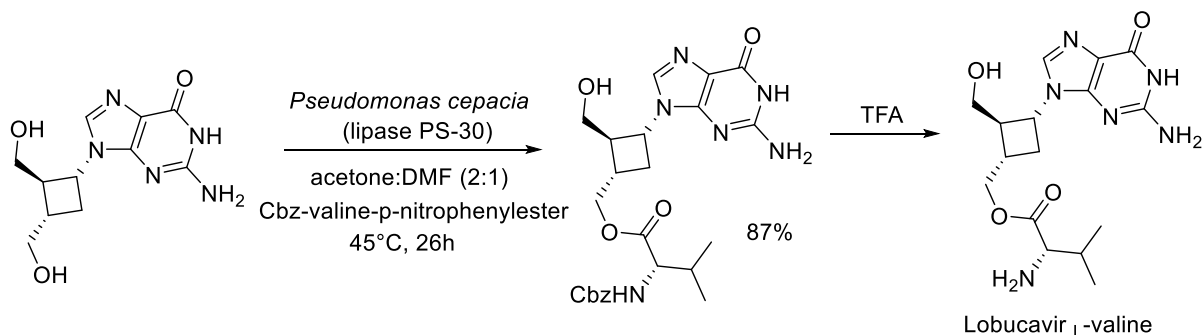


Figure 23: Regiospecific enzymatic transesterification of lobucavir catalysed by *Pseudomonas cepacia* lipase.

In general, lipases are the most suitable class of enzymes applied in the ester production. Among some advantages, lipases show activity in organic solvents and do not need co-factors (Do Nascimento et al., 2019). In addition, because they recognize a high range of substrates, they can be modelled through immobilization or metabolic engineering tools to adapt to reaction conditions.

2.3.1.1.2.1. Synthesis of sugar esters

Sugar esters are widely recognized for their excellent properties as effective biosurfactants, biolubricant, and biological activity, finding diverse applications in the industrial sector. Both chemical and enzymatic approaches have been employed in the esterification of various sugars (Suttili et al., 2013), which consist of a carbohydrate as the hydrophilic group and a fatty acid as the lipophilic group. Their properties as surfactants are influenced by the length of the alkyl chain and degree of saturation and/or unsaturation.

Sun *et al.* conducted a study on the surface properties of monoacyl trehaloses with varying acyl chains and degrees of unsaturation. The results revealed that the critical micellar concentration (CMC) of unsaturated monoacyl trehalose was influenced by both the degree of

unsaturation and the length of the acyl chain. Importantly, the impact of the chain length on the CMC value was significantly stronger compared to that of the degree of unsaturation (Y. E. Sun et al., 2009). Furthermore, Puterka *et al.* showcased that modifying either the sugar or fatty acid constituent of sugar ester compounds can modify the insecticidal efficacy of the compound (Puterka et al., 2003).

El-Baz *et al.* investigated the potential application of glucose fatty acid esters derived from polyunsaturated fatty acids in biological activity tests. In this study, the glucose fatty acid esters that were synthesized demonstrated noteworthy biological activities against significant human pathogenic microorganisms, *Aedes Aegyptus* larvae, and the SKOV-3 ovarian cancer cell line. These activities are attributed to the fatty acids present in the esters (El-Baz et al., 2021).

The first study on the esterification of LG was published in 1973. Among various sugars, LG was esterified with different acid chlorides or acid anhydrides in pyridine. The results revealed that LG adopts different conformations in the reaction medium, leading to the formation of intramolecular hydrogen bonds. This results in varying reactivities of the hydroxyl groups, leading to the formation of different products depending on the acid chloride used (Macleod & R Schroeder, 1973).

The same principles were observed in the study conducted by Ward and Shafizadeh (Waziu & Sharzadeh, 1982a). However, unlike the previous study, linear chain acyl donors (such as octanoyl and hexadecanoyl chloride) were utilized as reagents. As a result, there was reduced steric hindrance between the reagents, leading to the formation of mixtures of mono- and diesters, along with regioisomers.

Due to these characteristics, the enzymatic acylation of LG has been the subject of limited research. In LG, the acetyl groups are found at positions 1 and 6, while the remaining secondary hydroxyl groups are in the axial position. Accordingly, LG demonstrates significantly lower reactivity compared to glucose and other sugars, both chemically and enzymatically. This distinct attribute poses a significant challenge in achieving selective acylation of a single secondary

hydroxyl group, as the presence of three hydroxyl groups in its structure allows for the formation of monoesters, diesters and triesters at positions C2, C3, and C4 (HUNTER; HALL; SANDERS, 1983).

The pyranose ring of LG exhibits two possible conformations: inverted chair and boat type (Galletti et al., 2007). In the chair conformation, intramolecular hydrogen bonding takes place between the hydroxyl group at C3 in the axial position and the oxygen at C6, also in the axial position. This hydrogen bonding interaction contributes to a higher stability of the molecule, resulting in an increased population of this conformation. However, it also decreases the reactivity of LG as a nucleophile (Uriarte et al., 2018). Furthermore, similar hydrogen donor-acceptor interactions can occur with the hydroxyl groups at C2 and C4, as depicted in Figure 24 A1-A3.

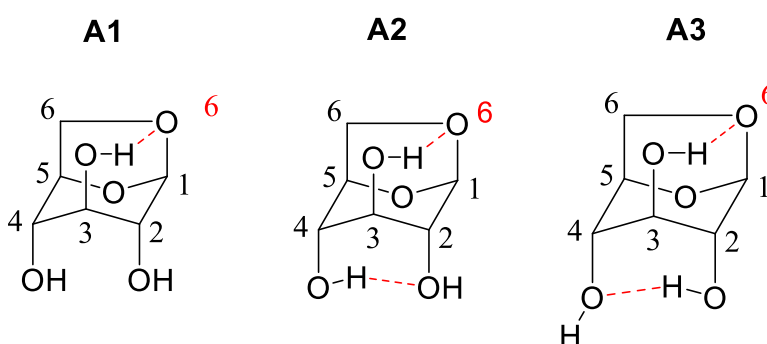


Figure 24: Possible conformational structures for LG in the axial position.

In this context, Pulido and Gotor (Pulido & Gotor, 1994) observed the regioselective monoacylation of the secondary hydroxyl, 4-O-, of carbohydrates with ester oximes in 1,4-dioxane. Galletti *et al.* (Galletti et al., 2007) proposed the acetylation of LG in the presence of short-medium chain acyl donors using acetonitrile and ionic liquids as solvent. The esterification occurred mainly in the 4-O-hydroxyl. Holmstrøm and Pedersen (Holmstrøm & Pedersen, 2020) obtained high degrees of regioselectivity in the acetylation of functionalized glycosides.

Currently, amphiphilic esters are mainly produced from alkaline glycerolizations of natural oils and fats at elevated temperatures and pressures. Besides the high energy consumption, the

conditions used result in low yields and the formation of polymerization by-products, resulting in dark spots and poor product quality, which requires expensive further purification steps. Thus, the use of enzymatic processes can overcome these problems and lead to a more environmentally friendly approach.

As shown in several studies, high yields and regioselectivity can be obtained under milder operating conditions alongside high purity of the final product. However, a recurrent barrier persists, *i.e.*, instability of the enzyme at high temperatures, inhibition by solvent and/or reagents and products, or under turbulent flow conditions, making application difficult for application on an industrial scale. Nevertheless, studies on enzymatic immobilization have been widely disseminated by several research group that report better robustness and stability of these biocatalysts, what are suitable for these applications.

2.3.1.2. Strategy for enzyme immobilization

Immobilization is an effective method that can be used to improve the performance of free enzymes, transforming them from a homogeneous to a heterogeneous catalyst (Zahirinejad et al., 2021). In contrast to free enzymes, immobilized enzymes may exhibit activity retention, which means they demonstrate enhanced biochemical and physicochemical characteristics and long-term operational stability. This enables their application at elevated temperatures, across a broad pH spectrum, with high substrate concentrations, and even in non-aqueous solvents. Furthermore, they can be easily recovered and reused, thereby reducing the costs associated with catalytic processes (Lahiji et al., 2021).

The activity of immobilized enzymes is influenced by various parameters, including the types of enzymes and supports used, as well as the specific protocols employed for immobilization (Sirisha et al., 2016). Immobilizing enzymes on different supports and/or utilizing different protocols on the same support enables the creation of systems with diverse stabilities

and specificities (Radt, 2018). This variability is dependent on factors such as the nature of the support material, the strength of the interaction between the enzyme and support, and the orientation of the enzyme molecule on the surface of the support.

The immobilization methods encompass reversible and irreversible techniques, which can enhance the physicochemical properties. Reversible immobilization methods include adsorption, metal binding, and ionic binding, where enzymes can adhere to a surface through weak interactions (Bilal et al., 2018). On the other hand, irreversible immobilization methods involve entrapment, where enzymes are physically trapped within a matrix, and covalent binding, where enzymes are chemically linked to a support material, ensuring their long-term stability and reusability. These diverse immobilization techniques provide flexibility in the application of enzymes in various batch and continuous flow industrial processes (Figure 25) (T. SRIWONG; MATSUDA, 2022).

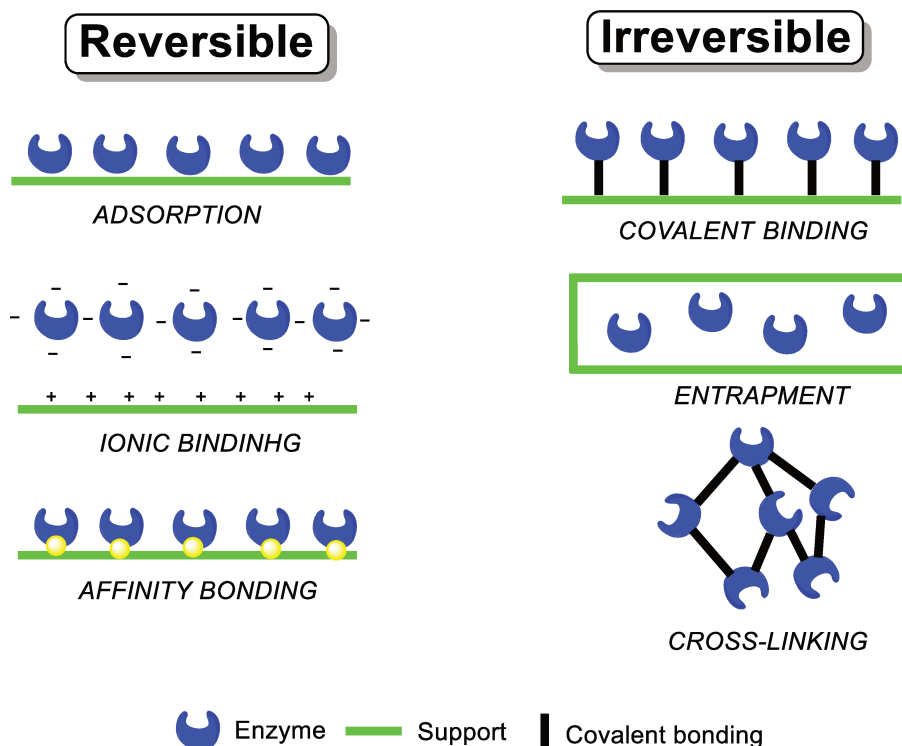


Figure 25: Diagram illustrating major enzyme immobilization methods. Reversible methods include adsorption, ionic binding, and affinity. Irreversible methods include covalent binding, entrapment, and cross-linking (Adapted from T.sriwong & Matsuda, 2022).

When selecting a support material, several characteristics must be taken into consideration. It should demonstrate excellent stability, possess significant pore structures, and provide a large surface area to maximize the efficiency of immobilization. Additionally, the support material should be easily modifiable to facilitate the process of enzyme immobilization. Moreover, it is highly desirable for the support material to be cost-effective, readily available, and environmentally friendly (D. M. Liu & Dong, 2020a). Featured in this work covalent bonding and adsorption.

2.3.1.2.1. Covalent binding

Covalent binding is a well-established and effective technique used for immobilizing enzymes by creating strong and stable linkages between the enzymes and support materials. This method securely connects the enzymes to the support matrix, enhancing their stability and enabling their reusability. The formation of covalent bonds ensures a long-lasting attachment of the enzymes to the support material, even under challenging reaction conditions (W. Wang et al., 2015).

The utilization of this method for enzyme immobilization offers numerous advantages, including decreased enzyme leaching, prolonged enzyme lifespan, and enhanced control over enzyme loading and distribution within the support matrix. It is recognized as a reliable and robust approach for a wide range of applications in biocatalysis and other processes reliant on enzymes (Trevan, 1988). By undergoing covalent binding, enzymes experience an elevation in their stereospecificity, resulting in improved stability. A notable example is the covalent bonding of lipases to glyoxyl agarose, which exhibited a remarkable 3-fold increase in enantioselectivity (Fernández-Lorente et al., 2001). The utilization of this method significantly reduces the risk of enzyme leakage, even when exposed to high substrate concentrations or strong buffer solutions,

which are often associated with denaturation reactions (Bayne et al., 2013). In this strategy, covalent binding is achieved by activating the support through the addition of reactive molecules, which in turn modify the polymer's backbone to activate the entire matrix. Hydrophilic polysaccharide polymers are commonly utilized as the primary supports in this approach (Besharati Vineh et al., 2018; D. M. Liu & Dong, 2020b). Additionally, electrophilic groups are utilized and created on the support material at the initial stage of the reaction. These groups establish strong interactions with the nucleophiles of the proteins, further enhancing the binding and stability of the immobilized enzymes. In this approach, several functional groups of amino acids are also suitable for utilization. Examples include the carboxylic group of aspartic acid, hydroxyl group of threonine, amino group of arginine, sulfhydryl group of thiols, as well as imidazole and indole groups. Furthermore, carriers containing an epoxy group are employed, as they readily react with amino groups under mild conditions, resulting in the formation of stable bonds (Do Nascimento et al., 2019; Ortiz, Ferreira, Barbosa, dos Santos, et al., 2019; Trevan, 1988). However, the application of covalent binding does come with some limitations. For instance, this strategy often involves several steps and requires longer incubation durations to ensure effective immobilization (Marrazza, 2014). In certain cases, it may be necessary to make additional modifications to the enzyme's structure to expose suitable functionalities for covalent binding. However, these alterations in the reaction media can carry the risk of enzyme denaturation (dos Santos et al., 2022; Meryam Sardar, 2015). Moreover, the typical binding capacity of immobilized enzymes to carriers is relatively low, with approximately 0.02 g of enzyme per gram of carrier. This limited binding capacity poses challenges for widespread industrial applications (Marrazza, 2014). Additionally, the immobilization of enzymes on carriers can impose constraints on their mobility, which may limit the occurrence of conformational changes required for efficient catalysis. As a result, enzyme activity can be reduced (Shen et al., 2011). Nonetheless, despite the limitations, the advantages of this immobilization strategy outweigh the

drawbacks. It offers increased enzyme stability and allows for efficient recovery and reuse of the enzymes.

2.3.1.2.2. Adsorption

Enzyme immobilization through adsorption is a technique that involves attaching enzymes to a support material through physical adsorption interactions. This process entails the enzymes being adsorbed onto the surface of the support, enabling reversible immobilization. Various materials, including ion-exchange resins, alumina, activated carbon, and others, can be utilized as supports. This approach offers multiple benefits, such as enzyme reutilization, extended stability, and the ability to perform continuous or batch operations. Enzyme immobilization via adsorption is widely employed in various industrial applications and biotechnological processes (Brady & Jordaan, 2009; Jesionowski et al., 2014).

Based on the protein arrangement and matrix charges, it is possible to achieve a strongly adsorbed and undistorted enzyme. However, it is important to note that not all enzymes can be immobilized on any carrier material. The successful adsorption relies on specific conditions being met, such as the affinity between the enzyme and the carrier material. Therefore, while various carrier materials can be employed, the compatibility between the enzyme and the carrier is crucial for appropriate adsorption to occur (Maghraby et al., 2023).

The presence of specific active groups on the carrier material ensures successful adsorption by facilitating interactions between the enzymes and carriers. However, if these active groups are not present, the interactions can be modified by adding carrier modifiers that enable connections between the enzymes and carriers. These modifiers help establish the necessary interactions and enhance the adsorption process. By introducing appropriate carrier modifiers, it becomes possible to facilitate the desired connections between enzymes and carriers, even in the absence of naturally occurring active groups (Jesionowski et al., 2014).

The advantages of enzyme immobilization by adsorption include the minimal requirement for activation steps, the use of few reagents, and its cost-effectiveness, making it an easily implemented method.

2.3.1.3. Biocatalysis under continuous flow conditions

Biocatalytic transformations have been traditionally carried out in batch reactors. However, performing those transformations in a continuous flow fashion has been shown to be a more efficient method capable of producing the desired product in higher yield and over shorter periods of time. Process security and integration of downstream processes such as in-line liquid–liquid extraction, solid adsorption, quenching, membrane separation, and solvent evaporation have also been important differentials from the traditional batch reaction (Fitzpatrick & Ley, 2016).

Several recent reviews have highlighted significant advancements in the field of biocatalytic transformations conducted under continuous flow conditions. Turner and colleagues conducted a comprehensive review that showcased numerous examples of fine chemical synthesis through biotransformation in flow (Thompson et al., 2019). Weiss and Tamborini contributed extensively to the field with their studies on new technologies, as well as the introduction of appropriate terminology and metrics for biocatalytic reactions in flow (Figure 26) (Britton et al., 2018; Tamborini et al., 2018). Additionally, Woodley and Lindeque developed a systematic approach for selecting the most suitable reactor for continuous pharmaceutical production (Lindeque & Woodley, 2019).

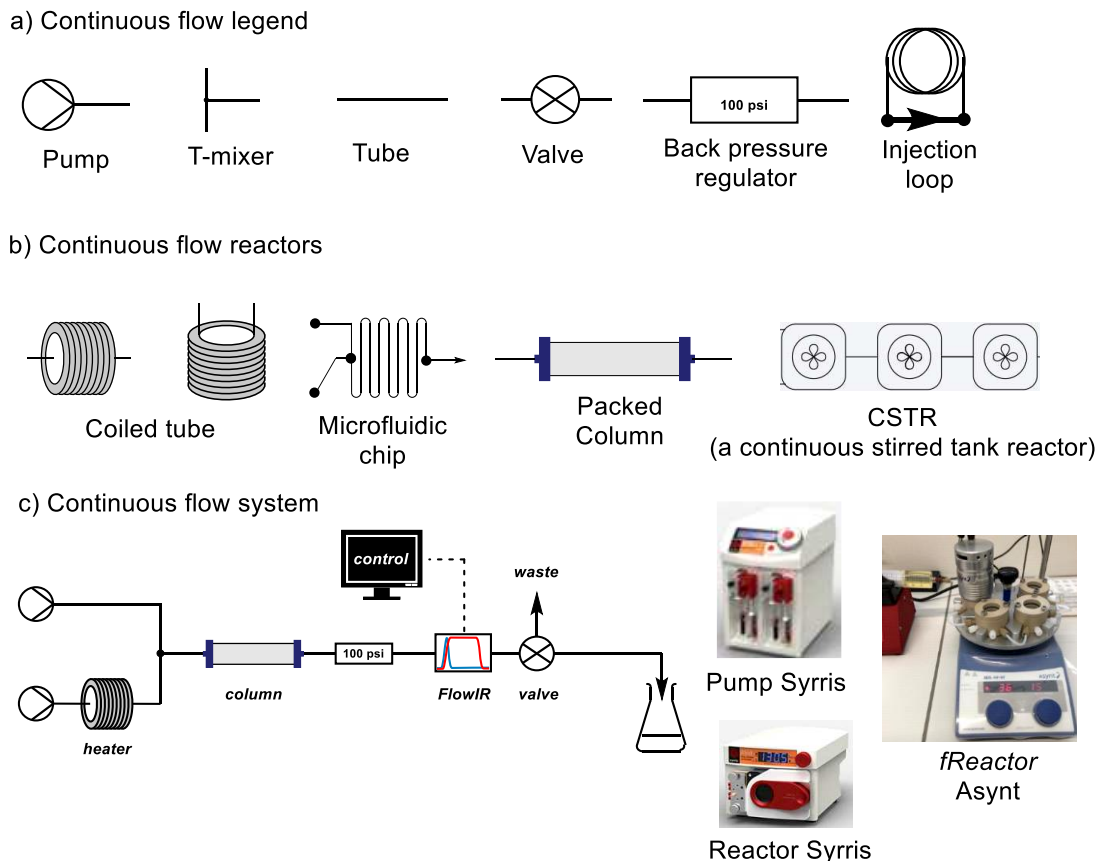


Figure 26: Continuous flow basics and equipment. (a) The continuous flow legend. (b) Continuous flow reactors (c) An example of a continuous flow system scheme, different pumps, and reactors.

In this context, transesterification and esterification are a specific class of reactions that have been successfully applied in biocatalytic continuous flow setups.

2.3.1.3.1. Lipases applied in continuous flow

2.3.1.3.1.1. Esterification reaction

Among the commercially available enzymes, Novozym® 435 (N435) (immobilization via interfacial activation of lipase B from *Candida antarctica* on a resin, Lewatit VP OC 1600) is the most applied in esterification reactions because of its advanced properties, such as a wide range of operating temperature 20–110 °C, good recyclability, and high activity (Britton et al., 2018). In 2008, Woodcock *et al.* applied N435 to the synthesis of alkyl esters using

fatty acids as substrates in a continuous flow packed bed system and compared the results with batch mode operation. Using the butyl hexanoate as a model reaction, they achieved after 10 minutes in the batch reaction only 3.3% ester conversion, compared to 92.7% in the continuous setup. Although comparable productivity has been obtained, the continuous flow system presented better stability, easier product recovery, and a potentially easier scale up (Woodcock et al., 2008).

Different ways to intensify the processes by applying different types of reactors have been recently studied. Besides the most used plug flow reactors, some papers have described promising results performing esterification reactions in microfluid devices and in different systems configuration (Bolivar et al., 2011; Ezeji et al., 2007). Condoret *et al.* performed the esterification of oleic acid with n-butanol in a biphasic enzymatic system in continuous mode using a centrifugal partition reactor (CPR). They were able to achieve higher productivity than a conventional batch reactor with the additional benefit of working in a system with integrated separation of free catalyst, reducing separation steps (Nioi et al., 2019).

Another key factor in the design of biocatalytic systems is to make a wise choice of the solvent. Some challenging esterification reactions involve substrates with different polarities and choosing the right medium can potentially improve the results. It also important to select solvents that comply with green chemistry postulates, biocatalyst compatible, cost-effective, with low viscosity, and reusable. One example of esterification that involves substrates with different polarities is the esterification of glycerol and benzoic acid to afford α -monobenzoate glycerol (α -MBG). In a recent work, Domínguez de María *et al.* performed this reaction in continuous flow using N435 in a packed bed reactor. To overcome solubility problems, they used deep eutectic solvents (DES) and phosphate buffer 100 mM pH 7.0 as a cosolvent (10% v/v), achieving a system with lower viscosity, efficient substrate solubility, high enzyme compatibility, and conversions 59% higher compared to the batch bioreactors (Guajardo et al., 2019).

Using the commercial immobilized lipase from *Rhizomucor miehei* (RM IM), de Souza *et al.* synthesized the monostearin from natural oil and fats. In this work, authors utilized a X-Cube (ThalesNano) system that is composed of a packed bed reactor that was filled with RM IM, a temperature controller, and a continuous pump. The best conversion was obtained by heating the reactor at 60 °C with a flow rate of 0.6 mL·min⁻¹ (residence time of three minutes). Under these conditions, 87% of conversion was achieved (Figure 27) (Junior *et al.*, 2012).

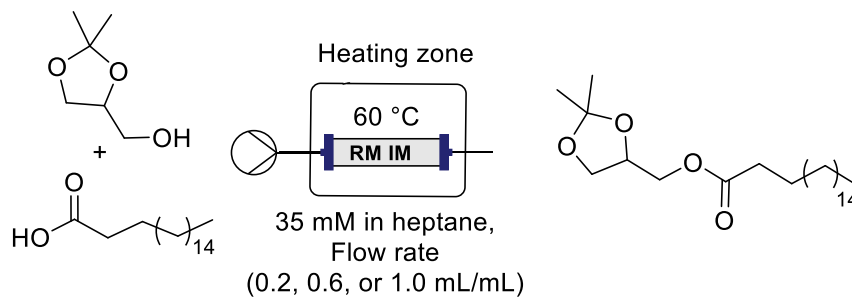


Figure 27: Esterification reaction between racemic 1,2-isopropylidene glycerol and stearic acid catalyzed by RMIM under continuous flow conditions (Junior *et al.*, 2012).

2.3.1.3.1.2. Transesterification reaction

Besides the esterification of carboxylic acids, there is also the possibility to synthesize esters by transesterification reactions. In this type of reaction, it happens in the chemical reaction between an ester and an alcohol, resulting in a new ester and a new alcohol. Like esterification, transesterifications are also performed mainly by lipases, but instead of a carboxylic acid, an ester is used as substrate. Compared to the chemical route, that is performed at severe conditions and can present low selectivity, the transesterification performed by lipases can be conducted at milder conditions and are in general highly selectivity.

Because of its wide range of applications, lipases can be used in cascade processes. One example is the synthesis of glycerol carbonate under continuous flow conditions. De Souza *et al.* proposed a glycerol carbonate production from vegetable oils by a cascade triacylglycerol hydrolysis, biodiesel synthesis, and esterification of the remaining glycerol with dimethyl

carbonate toward. This reaction was performed in a packed bed reactor using N435 as a biocatalyst and achieved 85% conversion and high selectivity (Leão et al., 2016). This protocol was further optimized by applying a handmade catalyst with the co-immobilization of lipases from Porcine pancreas (PPL) and CalB on epoxy resins, leading to a total conversion of vegetable oil with >99% selectivity (Figure 28) (DO NASCIMENTO et al., 2019).

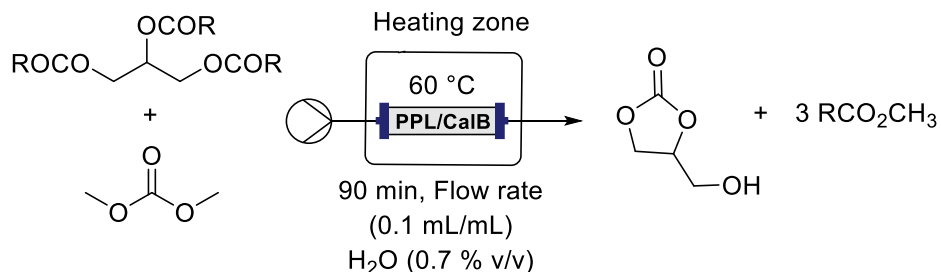


Figure 28: Glycerol carbonate synthesis by applying a combination of the immobilized biocatalysts PPL and CalB (Do Nascimento et al., 2019).

Transesterification in continuous flow can also be a strategy to synthesize active pharmaceutical ingredient (APIs). A recent work from Wang *et al.* reported the synthesis of 1-caffeoylglycerol from methyl caffeate and glycerin with the DES choline chloride urea as a cosolvent in a packed reactor containing N435. In this setting, they were able to increase the yield to 97% and reduce the reaction time by 75% besides guarantee the reusability for until 20 times (X. Liu et al., 2019).

Continuous flow technology is still in its early stages when it comes to realizing its full potential in biotechnology and biocatalysis. However, significant progress in this research field can only be achieved if we are willing to shift our approach to bioprocess design. It requires a departure from conventional batch processing methods and a shift towards embracing the advantages and unique opportunities presented by continuous flow systems. By embracing this change and adopting innovative strategies, we can unlock the full potential of continuous flow technology.

Based on the literature review outlined, the main objective of this study is to investigate the regioselectivity involved in the synthesis of levoglucosan esters obtained commercially and from cellulose pyrolysis. The synthesis will be catalyzed by lipases free and immobilized in continuous and batch systems. Subsequently, the synthesized esters will be evaluated for their biological activity and potential usefulness as surfactants.

3. Objective

This project proposed an integrated methodology with different technologies to obtain esters from commercial levoglucosan and obtained from the pyrolysis of residual cellulose from lignocellulosic biomass. These esters were synthesized through an enzymatic process using free and immobilized lipases in batch and continuous flow reactors. Additionally, the synthesized esters were subjected to biological activity tests and evaluated for their potential properties as biosurfactants.

3.1. Specific objectives

- ❖ Immobilize commercial *Candida antarctica* lipase B by covalent bonding on epoxide support.
- ❖ Apply pure commercial levoglucosan and crude bio-oil obtained by pyrolysis in esterification/transesterification reactions with different acyl donors catalysed by commercially immobilized lipases and by our research group.
- ❖ Compare conversions and productivity in batch and continuous flow reactors.
- ❖ Separate and characterize the products formed in terms of regioselectivity for hydroxyls linked to carbon 2 (C2), carbon 3 (C3) and carbon 4 (C4).
- ❖ Monitor the recyclability of biocatalysts.
- ❖ Optimize the continuous flow reaction using DoE (Design of Experiments).
- ❖ Statistically analyse DoE results and generate empirical models for an experimental dataset.
- ❖ Apply levoglucosan monoesters in amphiphilicity test for surfactants, relative percentage of hydrophilic groups to lipophilic groups (HBL-hydrophilic-lipophilic balance) and, in addition, biological assays.
- ❖ Activity test for all used biocatalysts.

4. Materials and Methods

4.1. Materials

The commercial immobilized (Novozym[®]40086 and Novozym[®]435) and free lipases (Lipase B *Candida antarctica*, recombinant from *Aspergillus oryzae* (CalB) and *Candida rugosa* (CR)) were purchased from Novozymes[®] (Bagsvaerd, Denmark). Lipase from *Pseudomonas Cepacia* was purchased from Sigma-Aldrich. 1,6-anhydroglucopyranose (commercial levoglucosan (LGCom)) was purchased from Start BioScience. Bio-oil enriched with levoglucosan (BoE) was obtained in collaboration by Reactions and Process Engineering Laboratory (LRGP) (Buendia-Kandia et al., 2020). Epoxy resin Purolite[®]ECR8205F was purchased from Purolite[®] International Limited. Aliphatic esters, Aliphatic carboxylic acids, N-Methyl-N-(trimethylsilyl) trifluoroacetamide (MSTFA), NO-Bis (trimethylsilyl) trifluoroacetamide (BSTFA), and tert-butyltrimethylsilyl chloride (TBDMSCl) were purchased from Sigma-Aldrich. All other reagents that were used were of analytical grade.

4.2. Methods

4.2.1. Immobilization of lipase CalB

Epoxy resin Purolite[®]ECR8205F polymer was applied as support for CalB immobilization by hydrophobic adsorption (CalB_epoxy). For this purpose, 1 mL of the enzyme solution (0.62 U/mL of specific activity of both lipases) was diluted in 20 mL of phosphate buffer (25 mM and pH 7.0) and added to the appropriate support (3.0 g). The mixture was stirred for 4 h at 20 °C at 180 rpm, 8 followed by vacuum filtration. At the end, the supernatant was collected and stored for protein quantification. The solid material was gravity filtered and dried at 25 °C (DO NASCIMENTO et al., 2019).

4.2.2. Hydrolytic activity assay

4.2.2.1. Triacylglycerol hydrolysis

The activities of free and immobilized lipases were determined as follows: 1 mL of extract or 10 mg of each supported enzyme were added to 19 mL of an emulsion that was prepared with olive oil (5% v/v) and arabic gum (10% v/v) in sodium phosphate buffer (100 mM, pH 7.0). The reactions were carried out under stirring (200 rpm) at 35°C for 30 min. The reactions were then stopped by the addition of 20 mL of acetone–ethanol mixture (1:1 v/v) and the fatty acids that were produced were extracted under agitation (200 rpm) for 10 min and titrated until end-point (pH 11.0) with NaOH solution (0.04 N). The blank assays were performed by adding the extract just after the addition of the acetone–ethanol solution to the flask. One unit of lipase activity (U) was defined as the amount of enzyme that catalyses the release of 1 μmol of fatty acids per minute under the assay conditions. All samples were compared with the commercial preparation N435 (see ANNEX-A: A1-Table A1).

4.2.2.2. Hydrolysis of 4-Nitrophenyl dodecanoate to p-nitrophenol

The lipase activity was determined using a spectrophotometric methodology as according to the method describe by Barros (de Barros et al., 2009) with modifications (Aljawish et al., 2019). The method is based on monitoring the hydrolysis of 4-Nitrophenyl dodecanoate (pNP-dodecanoate) to p-nitrophenol (p-NP), a yellow compound quantified by the absorbance at 400 nm. Substrate solution (1.0 mL) is composed of 4-Nitrophenyl dodecanoate (50 mM) in sodium phosphate buffer (100 mM, pH 7). The reaction was started by adding 10 mg of immobilized enzyme or 5 mg of free enzyme and kept under agitation at 300 rpm at 37 °C during 15 min. The blank reaction was prepared without 4-Nitrophenyl dodecanoate (Eq. 1).

$$Activity (U.mg^{-1}) = \frac{\Delta A_{400\text{ nm}}^{Test} - \Delta A_{400\text{ nm}}^{Blank}}{\epsilon * m} \times Df \quad \text{Equation 1}$$

Where A_{400} is the absorbance of p-NP at 400 nm; t is the reaction time (min); m is the total weight of the biocatalyst (mg); ϵ micromolar extinction coefficient of p-nitrophenol at 400 nm (0.0148) and D_f dilution factor. U corresponds to the enzyme activity, and one unit of lipase activity is defined as the amount of enzyme required to release 1 nmol (10^{-9} mol) of p-nitrophenyl per minute at pH 7 and 37 °C using p-nitrophenyl dodecanoate as substrate. The enzymatic activity of each enzyme using the spectrophotometric method based on monitoring the hydrolysis of pNP-dodecanoate to p-nitrophenol (p-NP) was shown in Table A2 (see ANNEX-A: A2-Table A2).

4.2.3. Levoglucosan derivatization

To obtain the best resolution in the analysis of the acylation products of levoglucosan by gas chromatograph equipped with a mass spectrometry detector (GC-MS) as well as to determine the selectivity of the lipases on the position of the hydroxyl groups, we investigated silylation with BSTFA, MSTFA, and tert-butyldimethylsilane chloride (see ANNEX-B: B1.1-Figure 1-3).

4.2.3.1. Silylation with BSTFA and MSTFA

For the derivation of OH-levoglucosan, 20 μ L of the sample were transferred to gas chromatography (GC) auto-sampling flasks containing 50 μ L of pyridine and 50 μ L of the derivatizing agent. The flasks were purged with argon gas (Ar), sealed, and coated with Teflon. The derivative conditions were determined after the investigation of various experimental parameters including the reaction time and the temperature on the analytical responses of the compounds, TLC (Thin Layer Chromatography) monitoring.

4.2.3.2. Silylation with tert-butyl dimethyl silane chloride

Triethylamine (5.54 mL, 39.80 mmol) at ambient temperature under argon was added to a solution of the levoglucosan compound (992.00 mg, 6.12 mmol) in dichloromethane (75 mL). The mixture was cooled to 0 °C and tert-butyldimethylsilane chloride (5.40 mL, 30.6 mmol) was slowly added in the reaction medium. The ice bath was removed, and the reaction was kept under stirring at room temperature for 3 h and 30 min, TLC monitoring. The mixture was evaporated under reduced pressure, the residue was diluted with hexane (20 mL), and the salt was filtered followed by washing with hexane.

4.2.4. Lipase-catalysed acylation of levoglucosan in batch

4.2.4.1. Esterification of long-chain fatty acids

A stock solution containing the appropriate amount of fatty acid lauric, palmitic, stearic, or oleic and ethanol (1:1—7.50 mmol, 150 mM) in hexane was prepared and added to a 50 mL flask with the biocatalyst N435 (200 mg). The reactions were performed at 40 °C during 2 h and 200 rpm of stirring on a shaker. At the end, the samples were collected and derivatized with 10 µL of MSTFA and diluted to 1.0 mL of ethyl acetate and subsequently analysed on a gas chromatograph equipped with a mass spectrometry detector (GC-MS).

4.2.4.2. Transesterification of levoglucosan

4.2.4.2.1. Initial screening

Esterification of commercial levoglucosan was performed following the methodology previously described by Galletti *et al.* (Galletti et al., 2007) with adaptations: the first step consisted of the production of the acyl donors. All transesterification reactions were performed having acyl donors as the ethyl esters of lauric, palmitic, stearic, and oleic acids (see procedure 4.2.4.1). For transesterification experiments (Figure 29), levoglucosan (1 mmol, 163 mg), and the appropriate

acyl donor (2 mmol) were introduced into a vial containing 5 mL of CH₃CN and the supported enzyme (40 mg, 0.8 % (m/v)).

The mixture was stirred at 50–65 °C for about five days, and the reaction progress was monitored by TLC and GC–MS. To stop the reaction, the biocatalysts were filtered, and the products were separated by flash chromatography. The monoesters were easily separated, which were obtained as a mixture. The final products were carefully identified by NMR: ¹H, ¹³C, HMBC (Heteronuclear Multiple Bond Correlation), HSQC (Heteronuclear Single Quantum Coherence), ¹H,¹H-COSY (“Correlation Spectroscopy”) and NOEdiff (NOE “difference spectroscopy”) spectra, FTIR spectrum ν (cm⁻¹, KBr), HRMS (High-Resolution Mass Spectrometry) for further details, see ANNEX B – B2-4), and GC–MS analysis (see ANNEX B – B1- figure 1-3).

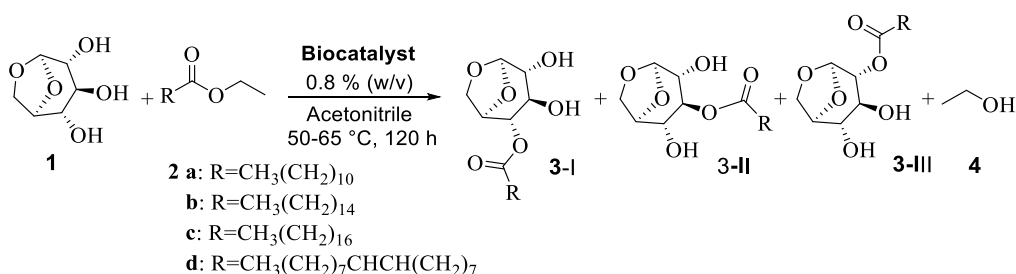
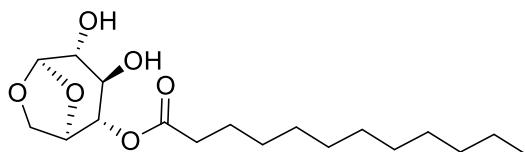


Figure 29: General procedure for lipase-catalyzed transesterification reaction of levoglucosan 1. Conditions: 2 ethyl esters of a: laurate, b: palmitate, c: stearate, and d: oleate (2.0 mmol), 3 levoglucosan monoesters aliphatic chains, and 4 ethanol.

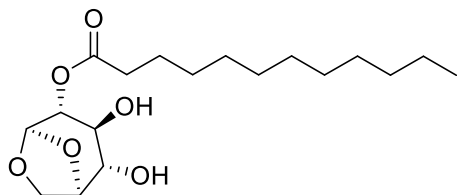
4-O-Lauryl-1,6-anhydroglucopyranose



¹H-NMR (500 MHz, DMSO) δ 5.26 (d, J = 4.7 Hz, 1H, OH), 5.18 (s, 1H), 5.13 (d, J = 5.1 Hz, 1H, OH), 4.43 (m, 1H, H4), 4.41 (m, 1H, H5), 3.90 (dd, J = 6.7 Hz, 1H, H6 endo), 3.52 (dd, J = 7.1 and 5.4, 1H, H6 exo), 3.37 (m, 1H, H3), 3.22 (d, J = 4.2 Hz, 1H, H2), 2.32 (t, J = 7.4 Hz, 2H, CH₂CH₂COO), 1.54 (dt, J = 14.4, 7.3 Hz, 2H, CH₂CH₂COO), 1.24 (m, 16H, CH₃(CH₂)₈), 0.85 (t, J = 6.9 Hz, 3H, CH₃CH₂). ¹³C NMR (500 MHz, DMSO-d₆) δ 172.28, 102.03, 76.57, 74.88, 69.47,

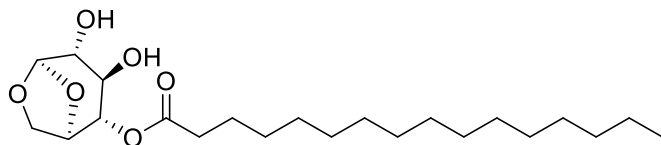
69.33, 65.29, 34.17, 33.98, 31.75, 29.44, 29.33, 29.16, 28.87, 28.83, 24.86, 22.55, 14.42. HRMS calculated for (M+Na)⁺ C₁₈H₃₂O₆: 367.2091, found: 367.2114. Rf: 0.29 (Eluent: Hexane/Ethyl acetate 1:1 - Developer: Sulfuric acid/Ethanol).

2-O-Lauryl-1,6-anhydroglucopyranose



¹H-NMR (400 MHz, DMSO- d₆) δ 5.21 (s, 1H, H-1), 5.18 (d, J = 6.6 Hz, 1H, OH), 5.11 (d, J = 7.0 Hz, 1H, OH), 4.57 (m, 1H, H-2), 4.40 (td, J = 6.0, 1.0 Hz, 1H, H-5), 3.83 (dd, J = 7.4 Hz, 0.9 Hz, 1H, H-6 endo), 3.56 (dd, J = 7.3 Hz, 5.8 Hz, 1H, H-6 exo), 3.35 (m, 1H, H-4), 3.16 (m, 1H, H-3), 2.29 (t, J = 11.7 Hz, 2H, CH₂CH₂COO), 1.51 (m, 2H, CH₂CH₂COO), 1.24 (m, 16H, CH₃(CH₂)₈), 0.85 (t, J = 6.8 Hz, 3H, CH₃CH₂). ¹³C NMR (500 MHz, DMSO-d₆) δ 172.28, 102.05, 76.58, 74.89, 69.49, 69.34, 65.29, 34.17, 33.98, 31.75, 29.44, 29.33, 29.15, 28.88, 28.83, 24.86, 22.55, 14.41. HRMS calculated for (M+Na)⁺ C₁₈H₃₂O₆: 367.2091, found: 367.2114. Rf: 0.21 (Eluent: Hexane/Ethyl acetate 1:1 - Developer: Sulfuric acid/Ethanol).

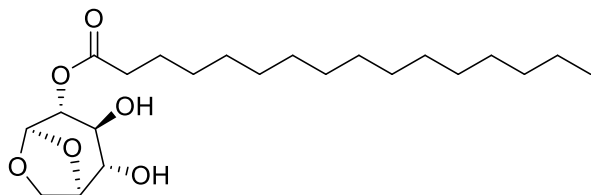
4-O-Palmitoyl-1,6-anhydroglucopyranose



¹H-NMR (500 MHz, CDCl₃) δ 5.51 (s, 1H), 4.75 (m, 1H, H4), 4.59 (d, J = 6.0 Hz, 1H, H5), 4.24 (d, J = 7.1 Hz, 1H, H6 endo), 3.81 (dd, J = 7.9, 5.5 Hz, 1H, H6 exo), 3.78 (m, 1H, H3), 3.56 (m, 1H, H2), 2.39 (m, 2H, CH₂CH₂COO), 1.65 (m, 2H, CH₂CH₂COO), 1.28 (m, 24H, CH₃(CH₂)₁₂), 0.88 (t, J = 7.0 Hz, 3H, CH₃CH₂). ¹³C NMR (400 MHz, CDCl₃) δ 173.68, 102.21, 74.30, 72.43, 71.20,

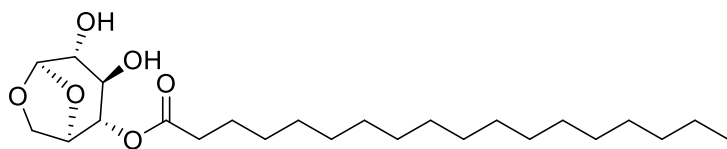
69.58, 65.73, 34.13, 31.71, 29.64, 29.58, 29.54, 29.44, 29.39, 29.25, 29.21, 29.17, 29.10, 29.06, 24.72, 22.15, 13.96. HRMS calculated for (M+Na)⁺ C₂₂H₄₀O₆: 423.2717, found: 423.2717. Rf: 0.29 (Eluent: Hexane/Ethyl acetate 1:1 - Developer: Sulfuric acid/Ethanol).

2-O-Palmitoyl-1,6-anhydroglucopyranose



¹H-NMR (400 MHz, CDCl₃) δ 5.44 (s, 1H, H1), 4.76 (m, 1H, H2), 4.58 (d, J = 5.3 Hz, 1H, H5), 4.06 (dd, J = 7.5, 0.4 Hz, 1H, H6 endo), 3.81 (dd, J = 7.5, 5.8 Hz, 1H, H6 exo), 3.63 (m, 1H, H4), 3.56 (m, 1H, H3), 2.34 (t, J = 7.5, 1.9 Hz, 2H, CH₂CH₂COO), 1.60 (m, 2H, CH₂CH₂COO), 1.28 (m, 24H, CH₃(CH₂)₁₂), 0.88 (t, J = 6.8 Hz, 3H, CH₃CH₂). ¹³C NMR (400 MHz, CDCl₃) δ 173.15, 101.46, 76.15, 73.75, 69.07, 68.20, 65.11, 34.50, 32.07, 29.84, 29.81, 29.74, 29.66, 29.59, 29.55, 29.51, 29.37, 29.30, 29.22, 24.99, 22.84, 14.25. HRMS calculated for (M+Na)⁺ C₂₂H₄₀O₆: 423.2717, found: 423.2898. Rf: 0.21 (Eluent: Hexane/Ethyl acetate 1:1 - Developer: Sulfuric acid/Ethanol).

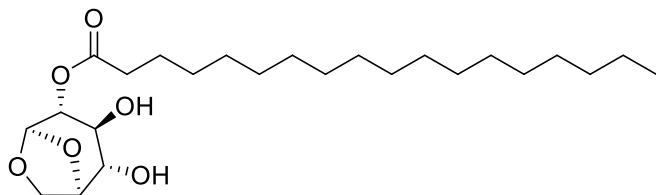
4-O-Estearyl-1,6-anhydroglucopyranose



¹H-NMR (500 MHz, CDCl₃) δ 5.50 (s, 1H, H1), 4.73 (d, J = 0.6 Hz, 1H, H4), 4.58 (d, J = 5.1 Hz, 1H, H5), 4.24 (d, J = 7.8 Hz, 1H, H6 endo), 3.80 (dd, J = 7.7, 5.5 Hz, 1H, H6 exo), 3.76 (m, 1H, H3), 3.56 (d, J = 1.3 Hz, 1H, H2), 2.39 (t, J = 7.6 Hz, 2H, CH₂CH₂COO), 1.66 (m, 2H, CH₂CH₂COO), 1.29 (m, 28H, CH₃(CH₂)₁₄), 0.88 (t, J = 6.9 Hz, 3H, CH₃CH₂). ¹³C NMR (500 MHz, CDCl₃) δ 172.96, 102.24, 74.52, 72.68, 71.48, 70.15, 65.90, 34.41, 32.07, 29.84-29.78, 29.73, 29.66, 29.59, 29.50,

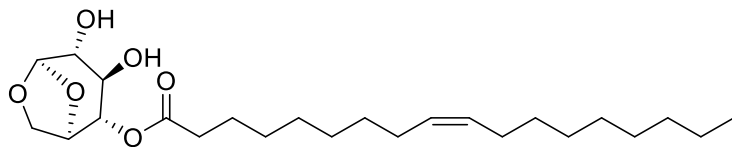
29.37, 29.22, 27.37, 27.34, 25.04, 22.83, 14.26. HRMS calculated for (M+Na)⁺ C₂₄H₄₄O₆: 451.3030, found: 451.2897. Rf: 0.30 (Eluent: Hexane/Ethyl acetate 1:1 - Developer: Sulfuric acid/Ethanol).

2-O-Estearyl-1,6-anhydroglucopyranose



¹H-NMR (400 MHz, CDCl₃) δ 5.44 (s, 1H, H1), 4.75 (m, 1H, H2), 4.59 (d, J = 1.5 Hz, 1H, H5), 4.06 (d, J = 7.4 Hz, 1H, H6 endo), 3.80 (dd, J = 7.6, 5.8 Hz, 1H, H6 exo), 3.61 (m, 1H, H4), 3.55 (m, 1H, H3), 2.34 (t, J = 7.4 Hz, 2H, CH₂CH₂COO), 1.62 (m, 2H, CH₂CH₂COO), 1.29 (m, 28H, CH₃(CH₂)₁₄), 0.88 (t, J = 6.8 Hz, 3H, CH₃CH₂). ¹³C NMR (400 MHz, CDCl₃) δ 173.05, 102.26, 76.12, 73.75, 69.01, 68.10, 65.09, 34.41, 32.07, 29.92, 29.83, 29.80, 29.74, 29.67, 29.59, 29.50, 29.48, 29.37, 29.28, 29.22, 27.34, 24.99, 22.83, 14.25. HRMS calculated for (M+Na)⁺ C₂₄H₄₄O₆: 451.3030, found: 451.2978. Rf: 0.22 (Eluent: Hexane/Ethyl acetate 1:1 - Developer: Sulfuric acid/Ethanol)

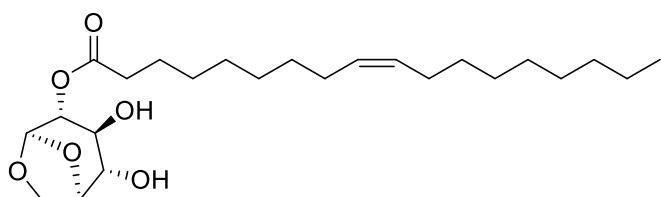
4-O-Oleoyl-1,6-anhydroglucopyranose



¹H-NMR (500 MHz, CDCl₃) δ 5.50 (s, 1H, H1), 5.34 (m, 2H, H9' and H10'), 4.74 (m, 1H, H4), 4.58 (d, J = 4.9 Hz, 1H, H5), 4.24 (d, J = 7.7 Hz, 1H, H6 endo), 4.12 (dd, , 1H, OH), 3.81 (dd, J = 7.6, 5.7 Hz, 1H, H6 exo), 3.78 (m, 1H, H3), 3.57 (m, 1H, H2), 2.63 (m, 1H, OH), 2.39 (t, J = 7.6 Hz, 2H, CH₂CH₂COO), 2.05 (m, 4H, H8' and H11'), 1.64 (m, 2H, CH₂CH₂COO), 1.29 (m, 20H, H4'-H7')

and H12'-H17'), 0.88 (t, J = 6.6 Hz, 3H, CH_3CH_2). ^{13}C NMR (500 MHz, CDCl_3) δ 172.88, 130.21, 129.86, 102.27, 74.54, 72.70, 71.53, 70.17, 65.91, 34.40, 32.05, 29.92, 29.83, 29.67, 29.47, 29.46, 29.28, 29.23, 29.19, 27.35(2C), 25.04, 22.82, 14.24. HRMS calculated for $(\text{M}+\text{Na})^+$ $\text{C}_{24}\text{H}_{42}\text{O}_6$: 449.2833, found: 449.3098. Rf: 0.30 (Eluent: Hexane/Ethyl acetate 1:1 - Developer: Sulfuric acid/Ethanol).

2-O-Oleoyl-1,6-anhydroglucopyranose



^1H -NMR (500 MHz, CDCl_3) δ 5.44 (s, 1H, H1), 5.34 (m, 2H, H9'-H10'), 4.76 (m, 1H, H2), 4.58 (d, J = 5.4 Hz, 1H, H5), 4.06 (d, J = 7.0 Hz, 1H, H6 endo), 3.81 (dd, J = 7.4, 5.9 Hz, 1H, H6 exo), 3.61 (s, 1H, H4), 3.54 (d, J = 1.0 Hz, 1H, H3), 2.34 (t, J = 7.5 Hz, 2H, $\text{CH}_2\text{CH}_2\text{COO}$), 2.00 (m, 4H, H8' and H11'), 1.64 (m, 2H, $\text{CH}_2\text{CH}_2\text{COO}$), 1.29 (m, 20H, H4'-H7' and H12'-H17'), 0.87 (t, J = 6.9 Hz, 3H, CH_3CH_2). ^{13}C NMR (500 MHz, CDCl_3) δ 173.09, 130.21, 129.82, 101.44, 76.09, 73.72, 69.02, 68.11, 65.08, 34.50, 32.04, 29.90, 29.82, 29.73, 29.66, 29.46, 29.27, 29.22, 29.18, 27.37 (2C), 24.96, 22.82, 14.25. HRM calculated for $(\text{M}+\text{Na})^+$ $\text{C}_{24}\text{H}_{42}\text{O}_6$: 449.2833, found: 449.2852. Rf: 0.22 (Eluent: Hexane/Ethyl acetate 1:1 - Developer: Sulfuric acid/Ethanol).

4.2.4.2.2. Directly in bio-oil enriched with levoglucosan (BoE)

The solubility of BoE was investigated in three organic solvents: acetonitrile (ACN), cyclopentyl methyl ether (CPME) and cyrene (CYE). A stock solution containing LG (40 mM) and ethyl acetate (1:2) in the appropriate solvent was prepared and added to a 2.0 mL flask containing the biocatalyst (12 U). For the BoE, a calibration curve was used to equalize the amount of LG between LGCom and BoE (See ANNEX A – A3).

The reactions were carried out at 55 °C for 120 h and 300 rpm in a carousel reactor (Radleys®). At the end, the samples were collected and diluted to 0.5 mL of acetonitrile and subsequently analyzed. After screening, other longer chain ethyl esters were applied as acyl donors: hexanoate, octanoate, laurate, palmitate, stearate and oleate respectively, keeping the same experimental conditions (Figure 30).

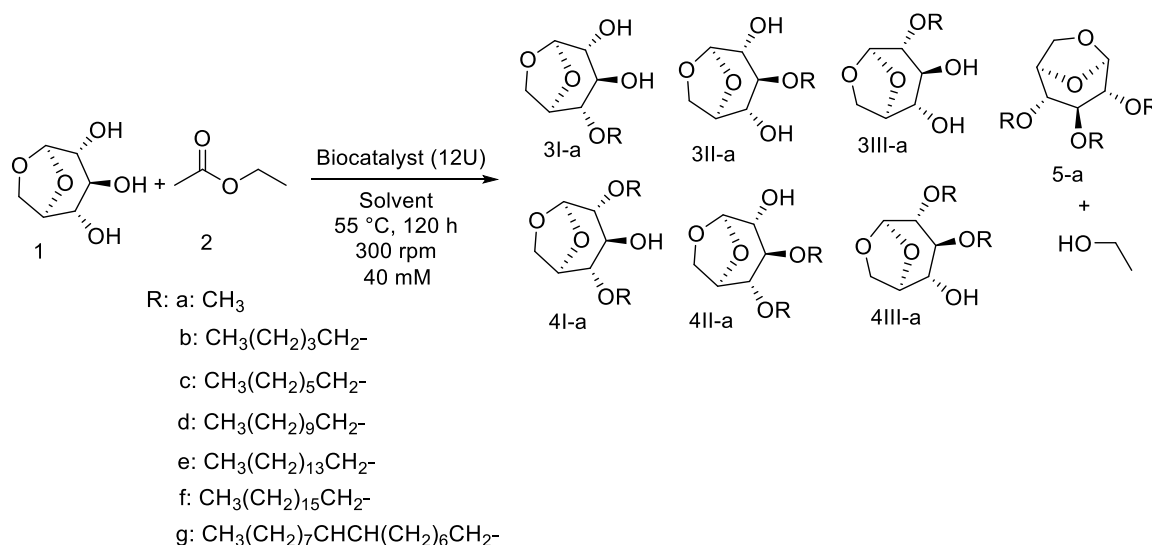


Figure 30: General procedure for lipase-catalysed transesterification reaction of LG **1** (40 mM) with acyl donor **2** (1:2 equivalents), biocatalyst (12U), 300 rpm, 120h at 55 °C. Conditions: **2** ethyl esters of **a**: acetate (C2), **b**: hexanoate (C6), **c**: octanoate (C8), **d**: laurate (C12), **e**: palmitate (C16), **f**: stearate (C18) and **g** oleate (C18*), **3-4I-II-IIIa** and **5a** levoglucosan esters, aliphatic chains, and **ethanol**.

4.2.4.2.3. Determination of kinetic parameters

The enzyme kinetics was monitored in terms of kinetic parameters including the Michaelis–Menten constant (K_m), maximum reaction velocity (V_{max}), dissociation constant of EB complex (K_i) and for A (K_{iA}). These kinetic parameters were derived from the Lineweaver–Burk plots and the Michaelis–Menten kinetic model (LINEWEAVER et al., 1934). For that, different concentrations from 20 to 300 mM of levoglucosan were esterified with two acyl donors (ethyl acetate and ethyl oleate) in two solvents (acetonitrile and cyrene) by Novozymes 435® (2 % w/v) at 55 °C during 24h and 400 rpm.

4.2.5. Nano differential scanning fluorimetry (NanoDSF)

The thermal stability of free lipase was investigated via NanoDSF (Magnusson et al., 2019) using the Prometheus NT.Plex. (NanoTemper® Technologies) (Figure 31). Protein samples were prepared at a concentration of 1.0 mg/mL in sodium phosphate buffer pH 7.0 (100 mM). After that, different solutions containing 20 μ L the protein and organic solvent (CYE and ACN), respectively, were prepared and analysed.



Figure 31: Prometheus NT.Plex. (NanoTemper® Technologies).

The capillaries were filled with 10 μ L samples and placed on the sample holder. A temperature gradient of 0.5 $^{\circ}$ C/min from 20 to 75 $^{\circ}$ C with excitation 10% and the intrinsic protein fluorescence at 330 and 350 nm was recorded with a total analysis time of 2 h and 20 min.

4.2.6. Lipase-catalysed acylation of levoglucosan in continuous flow

4.2.6.1. Experimental setup

In order to run the experiment as described, it is recommended to have the following equipment: reactor (Omnifit BenchMark® Microbore boron silicate glass column) of 15 mm in internal diameter and 100 mm in length and variable bed height, PTFE tubing (0.5 mm internal diameter), tubing fittings, one syringe pumps (Asia, Syrris), or equivalent, one stirrer-hotplates to

initial solution (Figure 32). In a flask, the solution containing the starting materials was prepared and immersed in a shaking bath. Syrris® syringe pumps were used to transport the solution containing the reagents into the fixed bed reactor at different flow rates, according to the previously defined residence time. Solubility tests were performed (See ANNEX C – C1).

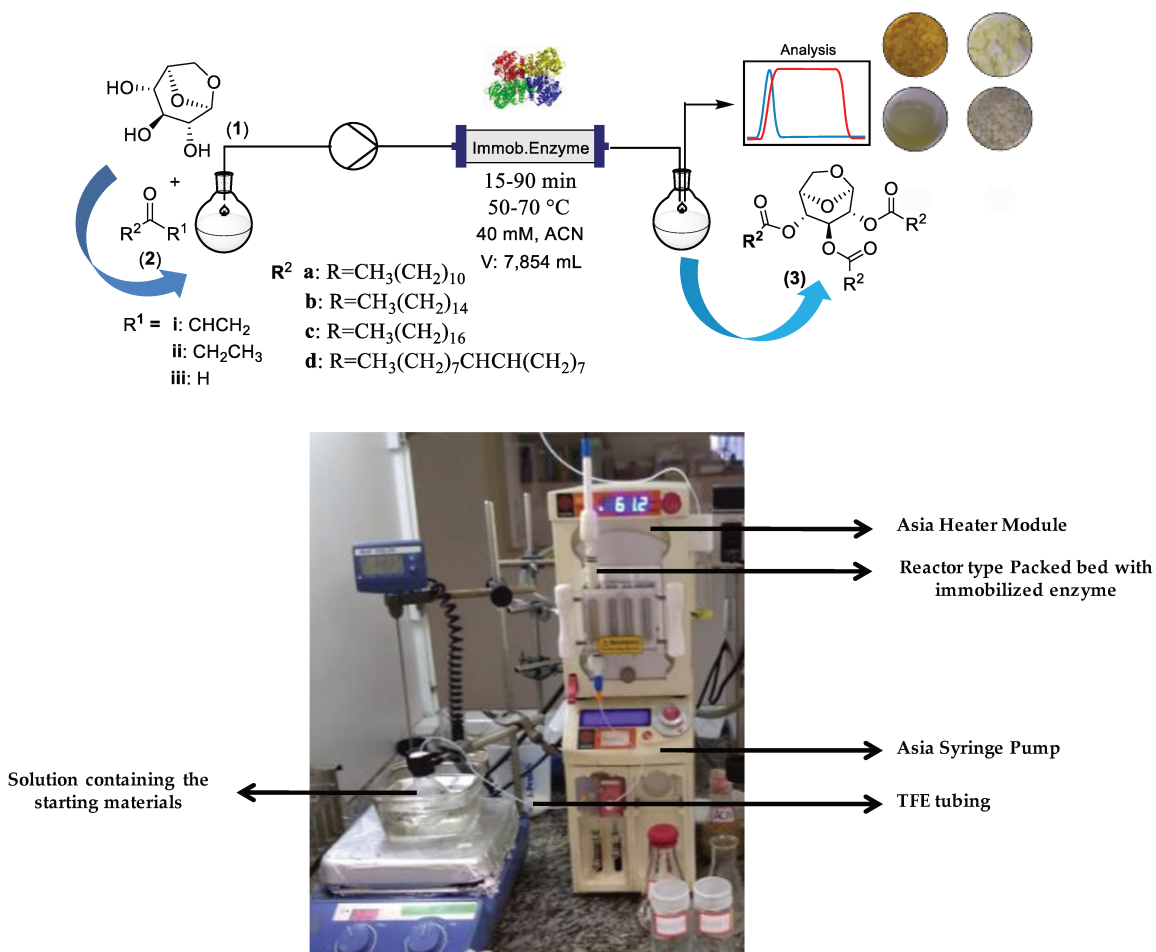


Figure 32: Representation and equipment used in the continuous flow system. Esterification reaction of levoglucosan with different vinyl esters. *Reactor volume: 7.854mL. a: vinyl laurate, b: vinyl palmitate, c: vinyl stearate and d: vinyl oleate. Immobilized Enzyme: N435 = Novozym 435 (Candida antarctica lipase B), immobilized in resin Lewatit VP OC 1600; CaLB_Epoxy = Candida antarctica lipase B immobilized on epoxy support by our research group.

4.2.6.2. Design of experiments (DoE)

To find the optimal experimental conditions of the variables (temperature and residence time) in the synthesis of levoglucosan esters in continuous flow, the experimental design approach was used. The DoE main objective was to increase the conversion in the esterification reaction of levoglucosan with lauric acid, according to the figure 33.

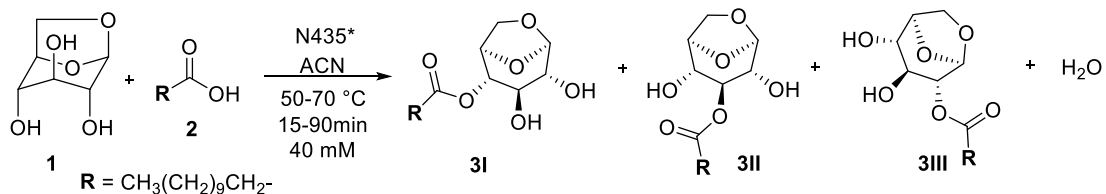


Figure 33: Esterification reaction of levoglucosan with lauric acid. *Reactor volume packed with N435: 7.854mL.

It is important to point out that the significant experimental variables that interfere in the system were selected according to the screening performed for the model reaction in a batch system (DO NASCIMENTO et al., 2019). After the selection of the significant variables, the optimization step was performed using the Central Composite Design (CCD). At this stage, the previously selected variables were studied with five levels, which allowed establishing the best working conditions in the synthesis of levoglucosan esters in continuous flow.

The CCD makes it possible to carry out the response surface methodology because the variables used are worked on at five levels. These levels: $(-\alpha, -1, 0, +1, +\alpha)$, are coded by convention and correspond to the five levels studied for the two variables (X1 and X2), where $(-\alpha)$ is the lowest level, $(+\alpha)$ is the top level and 0 is the center point). Table 1 shows the coded levels and the experimental values studied for the two variables Temperature and Residence time in the CCD (see ANNEX C – C2).

Table 1: Levels used in central composite planning for two variables.

variable	Code	Level				
		(-1,414)	(-)	0	(+)	(+1,414)
(X1) Temperature (°C)	T	50	53	60	67	70
(X2) Residence time (min)	tr	15	26	52,5	79	90

These levels have been defined to ensure that all areas of the parameter space can be explored, regardless of the range of factors (see ANNEX C – C2).

A stock solution containing levoglucosan and lauric acid (1:1, 40 mM) in acetonitrile was prepared and added to a 50 mL flask and kept under agitation at 300 rpm at 55 °C. Then, was pumped into the fixed bed reactor packed with N435, 2.0 g, to a total volume of 7.854mL. Flow rates of 87-524 $\mu\text{L}\cdot\text{min}^{-1}$ was used, and, in addition, different temperatures were evaluated, ranging from 50 to 70 °C. It is known that in a continuous flow, the reaction time is determined by the ratio between the reactor volume and the flow used in the system. A triplicate was performed for the best experimental condition found. After optimizing the temperature and residence time, the influence of the acyl donor on the LG esterification or transesterification reaction was analysed.

4.2.6.2.1. Transesterification of levoglucosan

After the screening step where the influence of temperature, residence time and acyl donor were investigated in the levoglucosan acetylation reaction, the best results were applied for the synthesis of levoglucosan esters containing alkyl chains of variable length, with up to 18 saturated carbons and unsaturated, biocatalyzed by N435 and CalB_Epoxy (CalB immobilized in epoxy resin by our research group) (Do Nascimento et al., 2019) according to the figure 34.

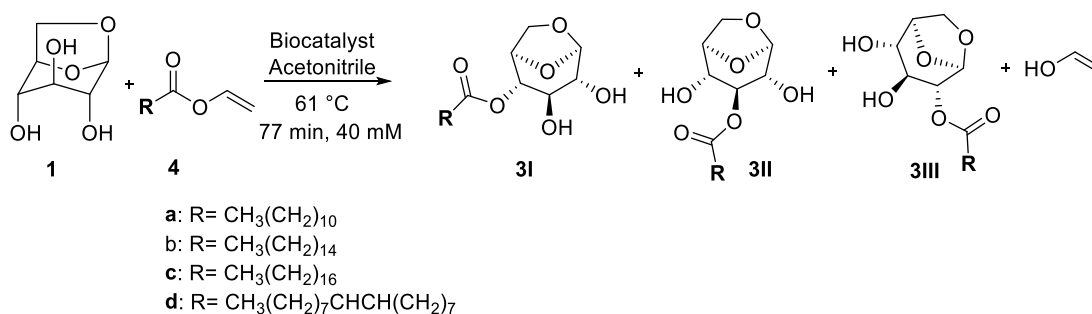


Figure 34: Esterification reaction of levoglucosan with different vinyl esters. * Reactor volume: 7,854 mL. **a:** vinyl laurate, **b:** vinyl palmitate, **c:** vinyl stearate and **d:** vinyl oleate.

The reaction progress was monitored by TLC. After stopping the reaction, CFAEs were separated by flash chromatography (Eluent: Ethyl acetate/Hexane 1:1—Developer: Sulfuric acid/Ethanol). To determine the selectivity of the lipases in the position of the hydroxyl groups, the final product, obtained as a mixture of 4-O' and 2-O' levoglucosan monoesters (MONLAU, MONPAL, MONEST and MONOLE) were silylated with BSTFA and analyzed by gas chromatography with a mass spectrometry detector (GC-MS) (see Appendix B).

4.2.6.2.2. Determination of productivity

In batch

$$\text{Productivity (P)}: \frac{V * C_r * f_r * \left(\frac{P_{MPROD}}{P_{MREAG}}\right) * conv * sel}{100 * S_A * T} \quad (\text{Equation 2})$$

In flow

$$\text{Productivity (P)}: \frac{F * C_r * f_r * \left(\frac{P_{MPROD}}{P_{MREAG}}\right) * conv * sel}{100 * S_A} \quad (\text{Equation 3})$$

Where, **V** is the reaction volume (mL), **F** is the flow rate (mL.min⁻¹), **T** is the reaction time, **C_r** is the concentration (mg.mL⁻¹), **f_r** is the purity LG (%), **P_{MPROD}** and **P_{MREAG}** are molecular weight of product and reagent (g.mol⁻¹), respectively, **conv** is the conversion (%), **sel** is the selectivity for CFAEs (%), **S_A** is the specific activity.

4.2.7. Determination of surface activity

The HLB value has been estimated by the ^1H NMR spectrum through the integration of the proton signals from the lipophilic and hydrophilic parts of the molecule. These values represent an empirical numerical correlation of the emulsifying and solubilizing properties of different surface-active agents (DAVIES, 1957). The term I_{gph} denotes the integration amplitude of the hydrophilic groups and I_{tot} refers to the total integration amplitude of the protons in the molecule. The ratio H describes the relative hydrophilic part of the molecule and can be used to estimate HLB value applying the equation described of Rabaron and coworkers (Rabaron et al., 1993) (equation 4).

$$H = \frac{I_{\text{gph}}}{I_{\text{tot}}} \ll \text{HLB} = \frac{60H}{H+2} \quad (\text{Equation 4})$$

The HLB scale ranges from 0 to 20. In the range of 3.5 to 6.0, surfactants are more suitable for use in W/O emulsions. Surfactants with HLB values in the 8 to 18 range are most used in O/W emulsions (PAUL BECHER, 1988). For the interface tension (IFT) measurements, a two-step process was used. First, compounds were dissolved in olive oil and pendant drop of organic solutions were formed in aqueous environments. To achieve this, the CFAs solutions were loaded into a syringe connected to a U-shape needle. Then, the needle was placed at the bottom of a quartz cell containing distilled water (dispersion medium), and by moving the plunger downward, a drop of volume 15 μL was formed at the tip of the needle. The so-formed drop is illuminated by means of a light source, and a high-resolution CCD camera was used to capture the drop profile (see ANNEX D). The determination of the interfacial tension was calculated according to the Young-Laplace equation defined for the pendant drop (PD) method. A Goniometer OCA25 (DataPhysic Instruments, Germany) was used at room temperature and 1.0 atm pressure, and the droplet profiles were captured every 1 s for a total period of 20s. CMC values were determined by plotting the interfacial tension vs. the concentration (in mM).

4.2.8. Antibacterial Assays

For the antibacterial activity assessment *Staphylococcus aureus* species were used, one clinical and three strains from American Type Culture Collection (ATCC). All information about the bacterial species, correspondent codes, isolation source, and susceptibility 18 profile is described in Table D2 (see ANNEX D). The clinical strain was isolated from patients of Clementino Fraga Filho University Hospital (HUCFF), UFRJ, RJ, Brazil (Leal et al., 2010).

4.2.9. Minimal inhibitory concentration (MIC)

The MIC of the compounds (MONLAU, MONPAL, MONOLE, MONEST, lauric acid and levoglucosan) was determined by the broth microdilution technique in 96-microtiter plates (CLSI, 2015), using a bacterial solution equivalent to a 0.5 McFarland scale (108 CFU/mL) subsequently diluted 1 :10 (107 CFU/mL). The samples were prepared at final concentrations of 1.0, 0.5, 0.250, 0.125, 0.0625 and 0.03125 mM. The bacterial growth was evaluated using resazurin. After 24 h, 20 µL of aqueous resazurin solution (0.85%) was added in each well, and then the microplate was incubated again for 4 h at 37°C.

4.2.10. Minimal bactericidal concentration (MBC)

The MBC assay of MONLAU was determined according to Isenberg (Isenberg, 1988). To perform this assay three concentrations of active samples were used at concentrations 0.250 mM (MIC), 0.5 (2x-MIC), 1.0 mM (4x-MIC).

5. Results and Discussions

5.1. Lipase-catalysed acylation of levoglucosan in batch

5.1.1. Initial Screening

We started this work investigating the influence of the main reaction parameters in order to find the best conditions to produce mono and diesters of levoglucosan from acyl donors with long carboxylic acid chain (>12C) both by lipase-catalysed esterification and transesterification. The selectivity of commercial and home-made biocatalysts was also evaluated. Initially, the esterification of commercial LG was evaluated by applying long chain fatty acids with acetonitrile as a solvent, as described in the experimental section. As expected, none of the biocatalysts demonstrated satisfactory ester conversion ($\leq 30\%$ —data not shown) under the conditions investigated, where lauric acid showed the best result (30% of conversion and poor selectivity). Galletti *et al.* (Galletti et al., 2007) applied the lipase PS (*Pseudomonas cepacia*) on acylation of levoglucosan with several acyl donors, such as vinyl esters (acetate and laurate) and carboxylic acids (acetic and lauric) in alternative green solvents, where CH_3CN and the ionic liquid [MOEMIm] [dca] were the most suitable. As a result, carboxylic acids could effectively substitute vinyl esters as acylating agents when ionic liquids were the solvent of choice. The reaction times were quite long (more than 5 days) with poor selectivity to monoesters. Chemical strategies for the synthesis of levoglucosan esters with acyl chlorides have already been described in the 1990s (Waziu & Sharzadeh, 1982b). In addition, just a few papers have explored the enzymatic esterification of this anhydrous sugar. However, in levoglucosan, the carbons C1 and C6 present an acetalic function and the remaining secondary hydroxyl groups are in the axial position. Therefore, levoglucosan is much less reactive than glucose or other sugars, both to chemical and enzymatic attack. This peculiar feature can be extended to the regioselective acylation of a single

secondary OH function that represents a very challenging task. The second strategy was to evaluate the performance of previously mentioned biocatalysts on the transesterification of levoglucosan using several acyl donors at different temperatures, aiming to investigate the selectivity for mono- and diesters. Results are shown in Table 2.

Table 2: Acylation of levoglucosan in CH₃CN.

1 **2 a:** R=CH₃(CH₂)₁₀
b: R=CH₃(CH₂)₁₄
c: R=CH₃(CH₂)₁₆
d: R=CH₃(CH₂)₇CHCH(CH₂)₇

Entry	Biocatalyst *	Acyl Donor **	Conversion (%) (3-I + 3-II + 3-III)		
			50 °C	55 °C	65 °C
1	N435	a	46	92	68
2		b	97	90	62
3		c	58	84	31
4		d	48	86	49
5	CaLB_epoxy	a	49	29	68
6		b	76	70	64
7		c	0	61	16
8		d	12	93	77
9	PSIM	a	51	52	12
10		b	49	74	51
11		c	47	70	0
12		d	8	72	67

*N435=Novozym 435 (*Candida antarctica* lipase B), immobilized on macroporous acrylic type ion exchange resin; CaLB_epoxy = *Candida antarctica* lipase B immobilized on epoxy support by our research group and PSIM=lipase from *Pseudomonas cepacea* immobilized on ceramic particles.**2 equivalent, **a:** ethyl laurate, **b:** ethyl palmitate, **c:** ethyl stearate, and **d:** ethyl oleate.

Analysis by TLC analysis ($R_f=0.30$ and $R_f=0.21$) and subsequent GC-MS confirmation demonstrated that monoesters could be obtained as major products in all reactions together with traces of diesters (<1% relative intensity could be noted after separation and analysis by high resolution mass spectrometry). According to Table 2, better conversions could be achieved by N435 using ethyl laurate and ethyl palmitate as acyl donors at 55 °C and 50 °C, respectively (Entry

1 and 2). Comparing these results for those obtained by CaLB_epoxy, a change in substrate preference was observed, leading to average conversions in levoglucosan palmitate at 50 °C and 55 °C. Surprisingly, high conversions in levoglucosan oleate ester was also obtained (93%, Entry 8), which until now, is a result that has not been reported. The lipase CaLB presents a very reduced hydrophobic lid and, therefore, does not require interfacial activation to perform hydrolysis and esterification reactions. N435 is a commercial preparation containing CaLB immobilized in cationic resin by ionic adsorption, with hydrolysis activity of 256 U/g. The home-made CaLB_epoxy biocatalyst contains CaLB immobilized by hydrophobic adsorption on epoxides in Purolite® ECR 82057, with hydrolysis activity of 419 U/g. Previous work of our group (Aguillón et al., 2019; Do Nascimento et al., 2019; S. Souza, R. Almeida, G. Garcia, R. Leão, J. Bassut, 2017) demonstrated that this derivative also showed higher esterification potential than N435 with a protein load of 11 mg/g of support against 15 mg/g of support presented by N435. In addition, the immobilization method that was applied in the new biocatalyst may have been responsible for a conformational modification of the enzyme as a product of protein-support hydrophobic interactions, making the catalytic site more suitable to receive the ethyl oleate acyl donor selectively (Figure 35). The use of epoxy-functionalized resins as enzyme support is advantageous because they have been considered as dual resins since they are versatile and can generate different interactions with the enzymes to be immobilized according to changing the pH and the ionic force that is applied in the immobilization environment. These supports are very stable at a neutral pH, even under humid conditions, and can be stored for a long period. In addition, these supports can stabilize the enzyme by multipoint covalent binding, resulting in high stabilization to the derivatives (Babaki et al., 2015; Schummer et al., 2009; Zdráhal et al., 2002). The epoxy groups undergo nucleophilic attack of different groups on the surface of the enzyme such as amino, thiol, and hydroxyl, allowing intense interactions between the enzyme and the support. Epoxy groups are weakly reactive under mild conditions such as neutral pH and low ionic strength. Thus, the immobilization using this type of support must be performed in two steps: in

the first, the enzyme is adsorbed onto the surface of the support (Mateo et al., 2003). High ionic strength is required at this stage to force the hydrophobic adsorption of the proteins on the support. After a long incubation time of the enzyme adsorbed at pH 7.0, the derivative is incubated at alkaline pH (around 10.0) to effect multi-interactions between the enzyme and the support through covalent bonding promoted by epoxy groups on the susceptible amino acids of the enzyme, giving greater stiffness to the derivative and thus, obtaining derivatives with high thermal stability. High conversions were also observed for lipase PSIM, mainly at 55 °C, where similar conversions to palmitate, stearate, and oleate were demonstrated. In addition, the values were also higher than PSIM (8750.0 U/g), despite having high hydrolysis activity, and showed conversions below 75% for all the conditions that were analysed.

The study of levoglucosan conformation is important to understand the obtained results since the presence of three hydroxyls in the structure allows the formation of monoesters and diesters at positions C2, C3, and C4. Under the studied conditions, it was not possible to find significant diester formation. However, studies were done to evaluate lipase regioselectivity towards levoglucosan monoesters. The pyranose ring of levoglucosan can adopt two conformations: inverted chair and boat type (Boissière-Junot et al., 1998; Mateo et al., 2003). In the chair conformation, the intramolecular interactions, due to hydrogen bonding occurring between the hydroxyl of C3 in the axial position and the oxygen in C6, also in the axial position, contribute to a greater stabilization of the molecule, increasing its population, but decreasing its reactivity as a nucleophile (Rotticci, 2000; Rotticci, 2000). The same interaction, hydrogen donor-acceptor, can occur with the hydroxyls in C2 and C4, according to figure 24.

Comparing the obtained values, it is possible to observe that the regioselectivity of N435 is slightly influenced by the temperature and size of the alkyl chain, exhibiting a similar tendency for OH at C4 and C2 in all conditions that were explored, except for ethyl laurate (Figure 35-N435, I-a- 50 °C), where it is possible to observe a loss of regioselectivity at higher temperatures. Different values were obtained for CalB_epoxy and PSIM where the preference occurred for OH-

C4, as can be observed for ethyl oleate (Figure 35-**CalB_epoxy,3-Id**) and ethyl laurate (Figure 32-**PSIM,3-Ia**), respectively (for more information see ANNEX C – C4).

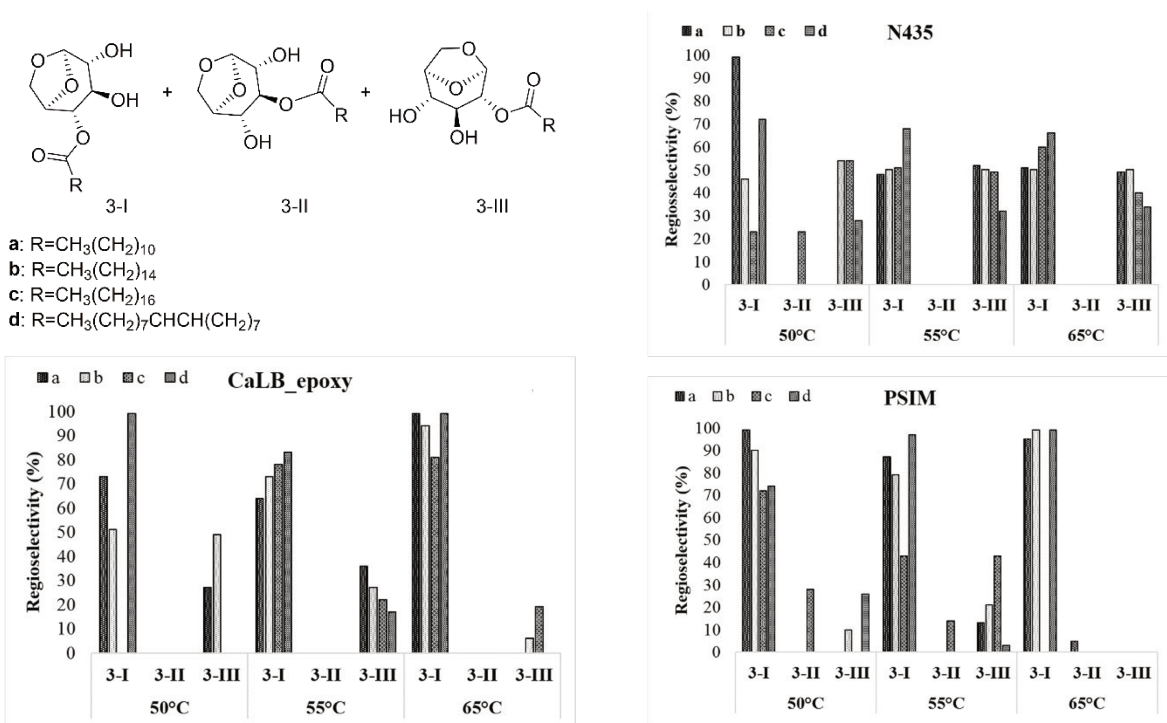


Figure 35: Regioselectivity in the enzymatic acetylation of levoglucosan in CH_3CN with ethyl aliphatic esters. Analyses were performed in a gas chromatograph equipped with a mass spectrometry detector (GC-MS) (DO NASCIMENTO et al., 2019).

The acyl moiety of the acyl-donor is covalently bound to the active site of the enzyme during the two transition states in the catalytic triad (Hunter et al., 1983; Uriarte et al., 2018). Moreover, the alcohol and the acyl binding sites are close to each other. Hence, the acyl moiety is likely to influence the regioselectivity of lipase towards the alcohol and the length and shape of the acyl part of the acyl donor indeed influence the regioselectivity of the reaction. It was observed that regioselectivity increased with longer acyl groups for CalB_epoxy and PSIM, as presented in Figure 35. Figure 36 shows the representative chromatograms of the reaction of levoglucosan with ethyl oleate mediated by N435, CalB_epoxy, and PSIM at 55 °C in acetonitrile, where the peaks corresponding to the retention times 48.52 and 48.76 min correspond to the regioisomers obtained during the reaction. To verify the regioselectivity of the reaction studied, regioisomers

were isolated and characterized by HRMS, $^1\text{H-NMR}$, $^{13}\text{C-NMR}$, NOEDIFF, and Infrared (FTIR) techniques (see ANNEX B).

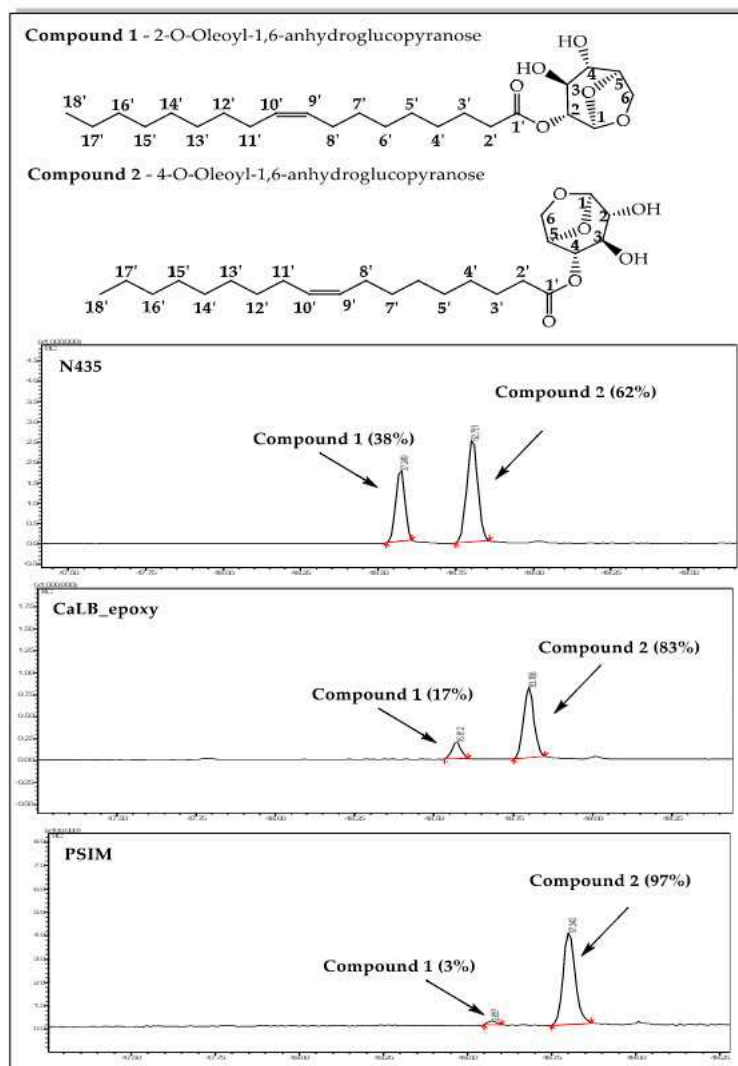


Figure 36: Regioselectivity in the enzymatic acetylation of levoglucosan (1 mmol, 163 mg) in CH_3CN (5.0 mL) with ethyl oleate (2 mmol, 619 mg) were introduced into a vial containing the supported enzyme (40 mg, 0.8% (v/v)). The mixture was stirred at 55°C for about five days and the course of the reaction was monitored by means of GC-MS (DO NASCIMENTO et al., 2019).

To unequivocally determine the structure of compounds 1 and 2, 2D NMR (HMBC and HSQC) experiments were carried out. Once the structure of compounds 1 and 2 is determined, it can be established what compound is formed in the transesterification reaction. Table 3 shows

the ^1H -NMR chemical shifts (ν , ppm) and coupling constants (J_{HH} , Hz), and ^{13}C chemical shifts (ν , ppm) for compounds 1 and 2.

Table 3 : ^{13}C and ^1H chemical shifts (ν , ppm) in CDCl_3 as solvent for compounds 1 and 2. J_{HH} coupling constants are represented in parenthesis.

Carbon/Hydrogen	1		2	
	^{13}C	^1H	^{13}C	^1H
1	101.25	5.44 s	102.27	5.51 s
2	73.54	4.76 m	70.17	3.57 m
3	67.91	3.54 d (1.0 Hz)	71.53	3.78 m
4	68.86	3.61 s	72.50	4.74 m
5	76.01	4.58 d (5.4 Hz)	74.54	4.58 d (4.9 Hz)
6	64.88	4.06 d (H6 endo, 7.0 Hz) 3.81 dd (H6 exo, 7.4 and 5.9 Hz)	65.91	4.24 d (H6 endo, 7.7 Hz) 3.81 dd (H6 exo, 7.6 and 5.7 Hz)
2'	34.38	2.34 t (7.5 Hz)	34.4	2.39 t (7.6 Hz)
3'	24.77	1.64 m	25.04	1.64 m
4'-7 and 12'-17'	29.18–29.90	1.28 m	29.19–29.92	1.29 m
8' and 11'	27.16 and 27.23	2.0 m	27.31 and 27.38	2.02 m
9' and 10'	129.82–130.21	5.34 m	130.2–129.86	5.34 m
18'	14.25	0.87 t (6.9 Hz)	14.24	0.88 t (6.6 Hz)

The signs CH and CH_2 of compounds 1 and 2 can be more easily identified by comparing the ^1H -NMR, ^{13}C -DEPT135, and HSQC spectra, allowing the distinction between the methinics and methylenics carbon signals, and by ^1H - ^1H -COSY, it was possible to obtain the correlations between the hydrogens that are coupled by $^{2-3}J_{\text{H,H}}$ (geminal and vicinal couplings, measurable in the 1D spectrum) and, thus, discern the multiplicity of signals observed in the ^1H -NMR spectrum. The signal of the methinics carbons CH-2, CH-3, and CH-4 of the levoglucosan pyranose ring is relatively more difficult, however it has been monitored by careful consideration of spectrum correlations with coupling interaction at one and three C-H carbons (Rotticci, 2000).

The results showed that the chemical displacement of CH-4 at compound 1 appears around $\delta\text{H} = 3.61$ ppm lower than in compound 2 ($\delta\text{H} = 4.74$ ppm) (See annex B.4). Different displacements were also observed for ring CH-2, and it was not possible to observe significant differences for others. The values of the chemical displacements of the methinics carbons CH-2 and CH-4 reveal modification dependent on the substituent groups that are present in the gem-hydroxyls in C2 and C4 (Figure 37).

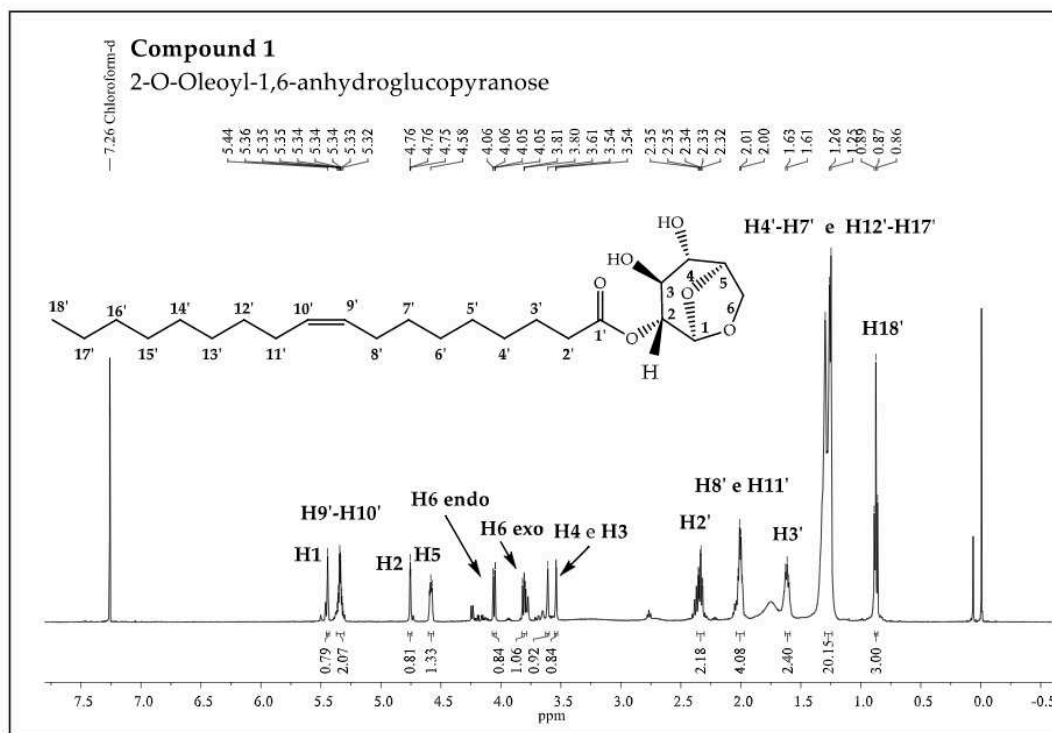


Figure 37: $^1\text{H-NMR}$ Spectrum for 2-O-Oleoyl-1,6-anhydroglucopyranose.

In this context, NOEdiff experiments can be used to confirm previous assignments, as well as to distinguish between levoglucosan monoester. When irradiating H2 (compound 1) at 4.76 ppm, there is an increase in the signal intensity related to hydrogens of the aliphatic ester chain by 1.35 ppm due to the Overhauser effect. When irradiating at 3.61 ppm (H4), it was not possible to observe an n.O.e (Figure 38) and HMBC for 2-O-Estearyl-1,6-anhydroglucopyranose was also used to confirm the structure (Figure 39).

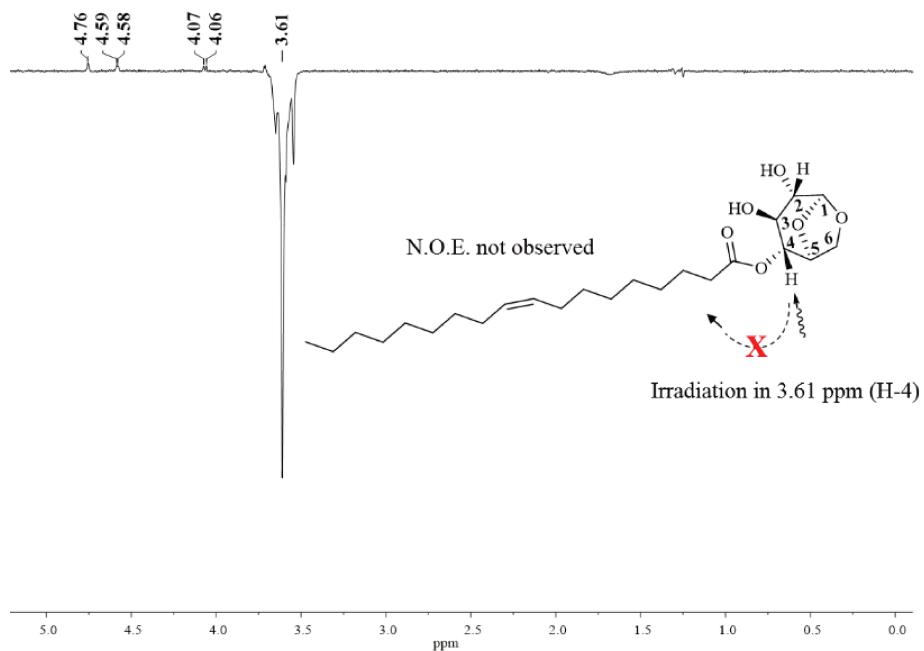


Figure 38: Nuclear effect of the Overhauser difference spectra for irradiation in the H-4 compound 1 at 3.61 ppm (H-4).

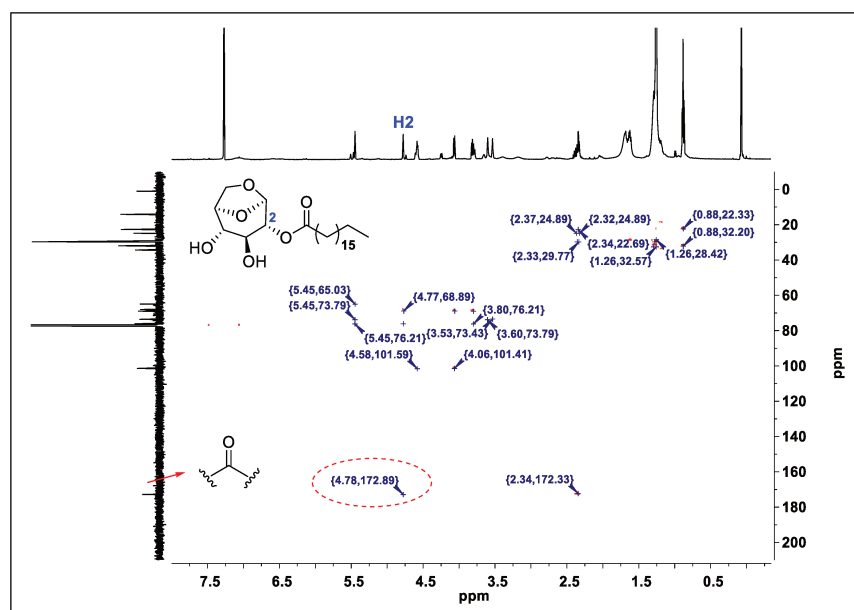


Figure 39: HMBC for 2-O-Esteryl-1,6-anhydroglucopyranose (CDCl_3).

These experiments clearly showed that there are marked differences between reactivities on C2 and C4 hydroxyl groups and also that the type of binding and support chosen for enzyme

immobilization can influence the selectivity of the enzyme so that the hydroxyl groups can be selectively transesterified, since CalB_epoxy and N435 have the same enzyme CalB, but immobilized on different supports, generating different interactions between enzyme and support and consequently, different spatial conformations, revealing different preferences in the reaction under study. Without detailed knowledge of the chemistry of the N435 support, it is not yet possible to attribute these observed differences to electronic, steric, or directed factors. To the best of our knowledge, this is the only example of this type of selective transesterification in the levoglucosan group in the presence of saturated and unsaturated long chain ($\geq C16$) aliphatic esters using the enzymatic process.

5.1.2. Directly in bio-oil enriched with levoglucosan (BoE)

We started this work with a simple test of the solubility of levoglucosan obtained from cellulose pyrolysis (BoE) in different organic solvents used for transesterification reactions. According to the results obtained (see ANNEX B), BoE is partially soluble in ACN and CYE at 55°C and insoluble at temperatures lower or equal to 50 °C. For CPME, the solubilization was not observed in these conditions, only for higher temperatures (> 60 °C).

Among the proposed solvents, ACN has already been used in several reactions for transesterification of the LG biocatalyzed by lipases showing good results (do Nascimento et al., 2019; Do Nascimento, Vargas, Rodrigues, Leão, De Moura, Leal, Bassut, De Souza, Wojcieszak, Itabaiana, et al., 2022; Galletti et al., 2007). However, studies carried out by Capelo *et al.* (Capello et al., 2007), showed that this solvent has a low net calorific value and therefore low environmental credits for incineration and waste treatment, presenting a relatively high environmental impact in its manufacture. CPME could be the ideal emerging green solvent alternative, but its low solubility in BoE at 55 °C and its use in LG transesterification showed low conversions to form the products of interest (Gasparetto et al., 2022). A possible alternative is cyrene (dihydrolevoglucosenone

(CYE)), a dipolar aprotic solvent, which is synthesized from residual cellulose (Comba et al., 2018), and it has demonstrated good conversions and solubility under reaction conditions for the synthesis of CFAEs and, in addition, it can be produced from the hydrogenation of levoglucosenone (LGO) generated from dehydration of LG.

Based on these results and our expertise in the synthesis of CFAEs using lipases (DO NASCIMENTO et al., 2019, 2022), it was proposed for this study to replace ACN with a more environmentally friendly solvent for these biocatalyzed reactions, CYE.

5.1.2.1. Screening of lipase from different sources applied in LGCom and BoE

Initially, four commercial lipases, including two immobilized N435 and N40086, and two free lipases CalB and CR were evaluated in the transesterification of ethyl acetate with LGCom and BoE. Considering the success already reported for the transesterification of LG with long-chain esters using N435 and its wide application in the production of esters, we used this biocatalyst such as reference and, the acyl donor chosen was the one with the smallest alkyl chain, where it was possible to observe the esterification in the three hydroxyl groups of LG.

For N435, Figure 40a-b show conversion values between 51% and 49% using LGCom such as substrate and 43–42% for BoE in ACN and CYE, respectively. Values close to those found by Galletti *et al.* (59%) (Galletti et al., 2007), who investigated the use of vinyl acetate in the esterification of LGCom in ACN. For N40086 it was notable that conversions to CFAEs were significantly lower compared to N435, about a 42% decrease in conversion to LGCom in ACN and 34% for BoE in CYE. Furthermore, low conversions for free enzymes in both conditions (Figure 40a-b) were observed.

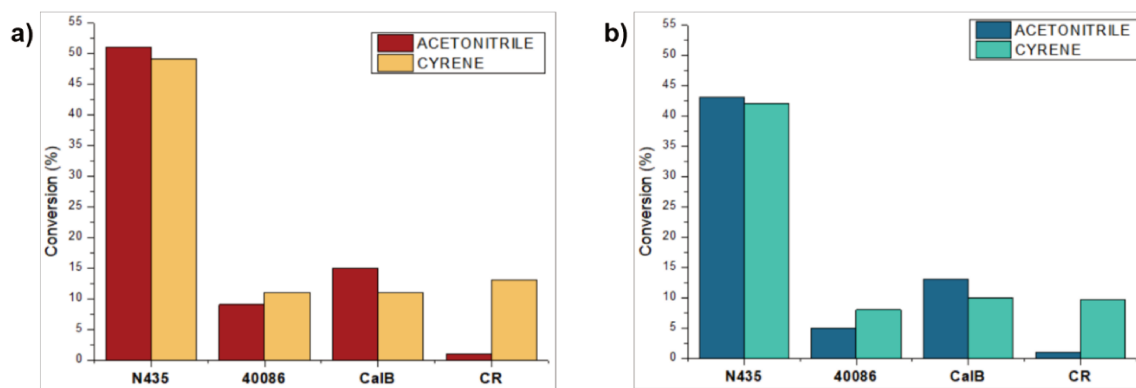


Figure 40: Transesterification reaction between levoglucosan and ethyl acetate with different biocatalysts in acetonitrile and cyrene as solvent. Conditions: **a)** Commercial LG (LGCom) and **b)** Bio oil enriched with LG (BoE).

In general, the behaviour between the two LG sources did not show significant differences. However, it was possible to observe a lower conversion with BoE, which may be related to the presence of impurities that were not removed during the pyrolysis process. Data obtained by gas chromatography with a flame ionization detector suggests that there are approximately 9% of impurities in BoE (Figure 41).

The impurities found in BoE may have been formed through the ring opening during the pyrolysis of cellulose (LE BRECH et al., 2016), these compounds can cause a negative contribution to the formation of LG esters due to the possible interactions with the active site of the enzyme. Furthermore, among the impurities are lactones that can undergo enzymatic polymerization and, consequently, compete with the substrates of interest for the catalytic site of the lipase (Veld et al., 2009).

Studies by Shang Sun and Liya Tian (S. Sun & Tian, 2018) for the synthesis of benzyl cinnamate using N40086 in different solvents demonstrated a relationship between yield and solvent polarity. These authors reported an increase in the esterification activity of cinnamic acid with benzyl alcohol in non-polar solvents. Based on log P values, it was observed that the solvent isooctane (Log P, 4.5) presented higher yield values compared to polar chloroform (log P, 2.0). According to the authors, the low yield may be related to the fact that the essential water on the

surface of the immobilized enzyme was deprived by the increase in solvent polarity. He *et al.* (He *et al.*, 2022) also studied the influence of the polarity of organic solvents in biocatalyzed reactions and observed that for the transesterification reaction of 1-(4-methoxyphenyl) ethanol with different acyl donors using ACN as solvent, N40086 is completely inactivated. The low conversions found in our studies using N40086, a lipase derived from *Rhizomucor miehei* immobilized on acrylic resin granules (S. Sun & Tian, 2018), may be related to its greater sensitivity to the increase in polarity of the solvents ACN (Log P – 0.33) and CYE (Log P, – 1,52), the reason is the ease in removing water that is essential to maintain the conformation of the active enzyme. Thus, complete removal of water would drastically distort this conformation and inactivate the enzyme (Gorman & Dordick, 1992). It is worth noting that not only log P alone, but the cumulative effect of several other parameters such as dipole moment, dielectric constant, hydrogen bonding and polarizability can alter the esterification activity of N40086 (Khmelnitsky *et al.*, 1988).

These results agree with the specificity of the lipases present in these supports, *Rhizomucor miehei* (N40086) and *Candida antarctica* B (N435) with the chain length of acyl donors during LG acylation. CalB has greater activity in the presence of short and medium chain fatty acids with a decrease in its activity for long alkyl chains. While *Rhizomucor miehei* has relatively low activity for short chain fatty acids, but activity increased for longer fatty acids (Rgen Pleiss *et al.*, 1998). More details on the influence of chain size for N435 will be discussed later in this study.

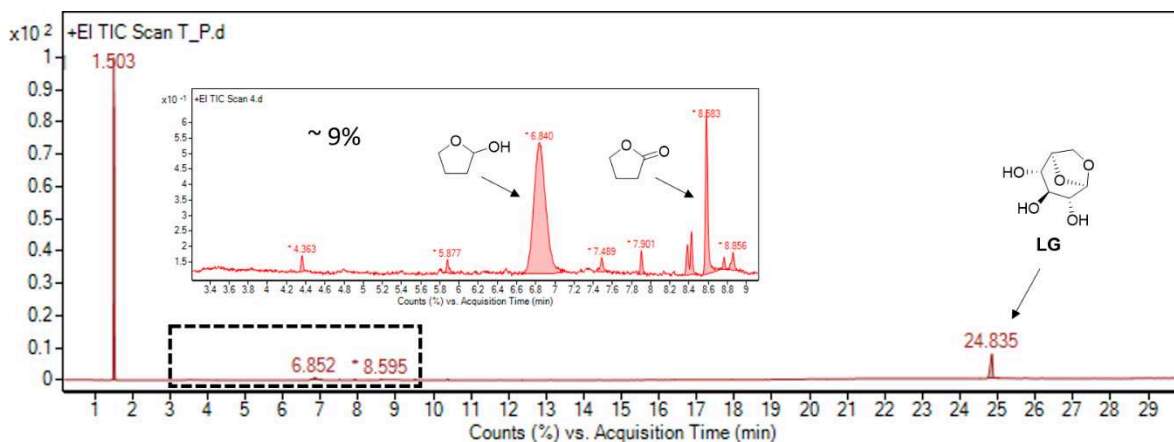


Figure 41: Representative chromatogram of BoE dissolved in acetonitrile and analysed on GC-FID.

For free enzymes, maximum of conversion values was observed for CalB: 15% using LGCom, 36% lower compared to N435 and 13% conversion for BoE in ACN. For CR, the change of solvent significantly affected the reaction with conversion values below 1% for both substrates in ACN (Fig. 37a-b). These results suggest that the catalytic potential of the free lipase was affected by the greater instability of the protein under more extreme temperature and/or solvent conditions compared to the immobilized enzyme. The higher thermal stability of enzymes can be correlated with their stability in different organic solvents. Therefore, thermostability studies were performed for free lipases in both solvents using differential nano scanning fluorimetry (nanoDSF) technology with Prometheus NT.48. Flex® (NanoTemper Technologies, Munich, Germany).

5.1.2.2. Nano differential scanning fluorimetry (NanoDSF)

In our study, nanoDSF technology was used to evaluate the thermal stability of two free commercial lipases, CalB and CR, in sodium phosphate buffer 100 mM at pH 7.0 (Figure 42a-b). The thermodynamic (or conformational) stability of the enzyme is given by the difference in Gibbs free energy (ΔG) between the folded and unfolded states and can be obtained instantaneously by measuring the melting temperature of the protein (T_m). Under environmental conditions, the

folded state, corresponding to the catalytically active form, is favoured. However, the increase in temperature may favour the shift of the enzyme's conformational equilibrium to the unfolded, catalytically inactive form, being experimentally observable as a characteristic curve of the sigmoidal property from which the T_m is derived as an inflection point (Samra & He, 2012). Therefore, heat-stable proteins are more tolerable to the presence of destabilizing agents and, moreover are preferred as early candidates for protein engineering by rational design or directed evolution, as activity and specificity are often obtained at the expense of stability (Bershtein et al., 2006; Bloom et al., 2006). Thereby, evaluating thermal stability is an excellent choice for screening of the best experimental conditions. Temperature is an easy-to-control parameter that is widely used to increase the rate of a biocatalyzed reaction. However, there is an optimal condition to be reached to avoid its thermal inactivation (P. Zhang et al., 2019). Several techniques have been developed to facilitate the study of the thermal stability of proteins, highlighted in this work, the technique that uses the nanoDSF technology that determines T_m measuring the intrinsic change of double UV fluorescence in tryptophan and tyrosine residues in proteins with emission wave lengths of 330 and 350 nm exposed after the protein unfolding induced by the increase in temperature (Chattopadhyay & Varadarajan, 2019; Kotov et al., 2021; Lobo et al., 2021). Thus, thermal denaturation curves of the proteins were obtained by nanoDSF (Figure 42).

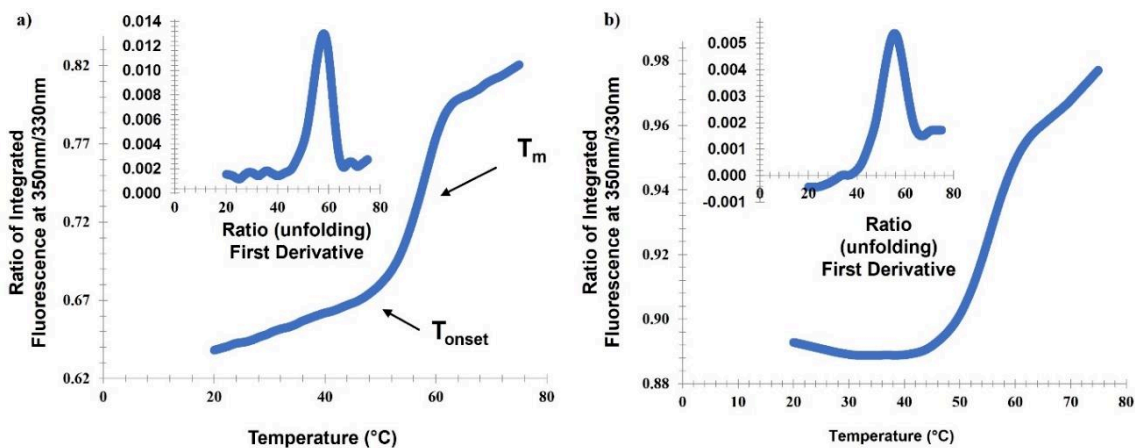


Figure 42: Representations of NanoDSF thermograms showing the ratio between the fluorescence signals at 350 and 330 nm and the first derivative of this ratio for analyzing the T_{onset} and T_m values. Conditions: 1 mg/mL of protein in 100 mM sodium phosphate buffer pH 7.0 in **a)** Lipase B of *Candida antarctica* (CalB) and **b)** *Candida Rugosa* (CR).

Thermograms were evaluated to monitor the detectable temperature at which a protein begins to unfold (T_{onset}) and the midpoint(s) of the unfolding transition temperature (T_m) (S. H. Kim et al., 2022). As shown in Figure 42a-b, this instrument can simultaneously determine the parameter of conformational stability, based on protein unfolding transitions. Thus, between the temperature range 20–75 °C, the values obtained for CalB in phosphate buffer pH 7.0 were $T_{\text{onset}} = 46.7$ °C and $T_m = 58$ °C (Figure 39a), values close to those found by Le *et al.* (Q. A. T. Le et al., 2012). for wild-type CalB with $T_m = 54.8$ °C that was measured by differential scanning fluorimetry (DSF) through CFX96™ Real-Time PCR Detection System (Bio-Rad, Hercules, CA). For CR the values obtained were slightly lower, with $T_{\text{onset}} = 43.5$ °C and $T_m = 55$ °C. According to Li *et al.* (G. Li et al., 2018) CR has low thermal, with initial inactivation temperature starting at 45 °C, values close to those found in this study (Figure 42b).

In this context, the influence of ACN and CYE solvents on lipase stability was also evaluated. Figure 43a-b shows a different unfolding profile for CalB in the presence of both solvents. In ACN (Figure 43a), CalB has a $T_m = 46$ °C, while for CYE this value corresponds to 61 °C (Figure 43b), demonstrating that there is a greater thermal stability for CalB in CYE.

However, T_{onset} in ACN was higher compared to CYE (30 and 20 °C, respectively), suggesting that there is a greater kinetic instability for CalB in the presence of CYE compared to ACN when the initial temperature is low. Moreover, when the temperature increases, the unfolding process appears to be slower for CalB in CYE. The modification of T_m is probably due to the alternation of the hydration layer around the protein, which may be related to the higher polarity of the solvents. In addition, CYE interacts chemically and reversibly with water, forming its geminal diol (De Bruyn et al., 2019) and, therefore, greater ability to capture water molecules around the catalytic site of the enzyme when the temperature is low, until that the equilibrium condition is reached. Furthermore, the thermostability for CR in the different solvents was also analysed. Figure 40c-d show that in ACN the protein has a lower stability compared to CYE. T_{onset} data obtained in both solvents indicate that denaturation starts from the first temperature of the analysis (20 °C) reaching 50% unfolding at $T_m = 38$ °C for ACN and at $T_m = 53$ °C for CYE. The low thermal stability for CR has been reported in the literature by several authors (S. W. Chang et al., 2006; De Bruyn et al., 2019; G. Li et al., 2018), that highlight a half-life of less than 1 h at 50 °C with a total loss of catalytic activity at 60 °C (Pereira et al., 2001).

After reaching the maximum temperature of 75 °C, the measurement continued during the cooling process to the temperature of 20 °C, with the aim of investigating the reversibility of the denaturation events observed during the heating process for the free lipases CalB and CR in both solvents. The curves associated with the refolding process are given in Figure 44.

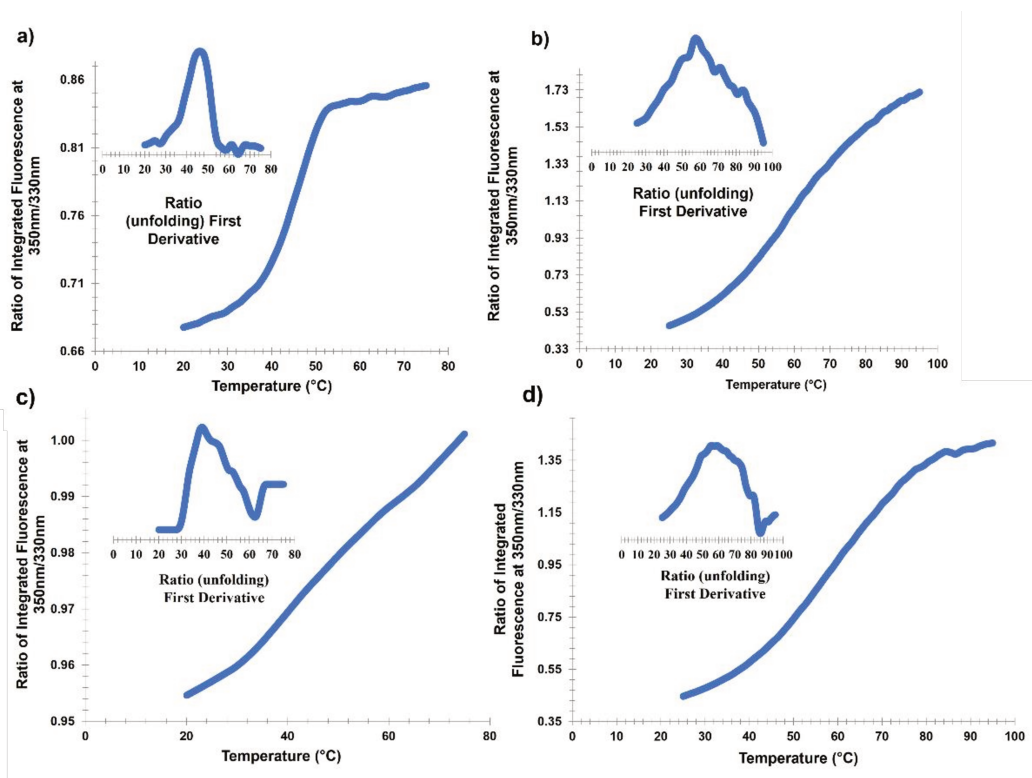


Figure 43: Representations of NanoDSF thermograms showing the ratio between the fluorescence signals at 350/330 nm and the first derivative of this ratio for analysing the T_{Onset} and T_m values. Conditions: 1 mg/mL of free enzyme in 100 mM sodium phosphate buffer pH 7.0 in different organic solvents; CalB in **a)** acetonitrile (ACN) and **b)** cyrene (CYE); and CR in **c)** ACN and **d)** CYE.

During the cooling step, we determined the first derivative of the fluorescence ratio at 350/330 nm and at different temperatures from those associated with denaturation. Furthermore, it can be observed for CR in ACN that when the temperature was below 38 °C an increase in fluorescence ratio was observed, indicating the potential movement of aromatic amino acid residues within the structure of the protein (Figure 44c). This result could suggest a very limited renaturation, probably due to the aggregation process occurring after the denaturation during the heating step, as already observed by Ronzetti *et al.* (RONZETTI *et al.*, 2022) when they analysed the thermal denaturation of HtrA-family bacterial protease using differential scanning fluorimetry (DSF). Therefore, the behaviour of free lipases exposed to different solvents and temperatures explains the low conversions obtained for the synthesis of CFAEs. Noteworthy for CR in ACN that

showed conversion lower than 1% for both conditions (Figure 40). Its low T_m value suggests that for the reaction temperature practically all the proteins are in the unfolded form and therefore without catalytic potential.

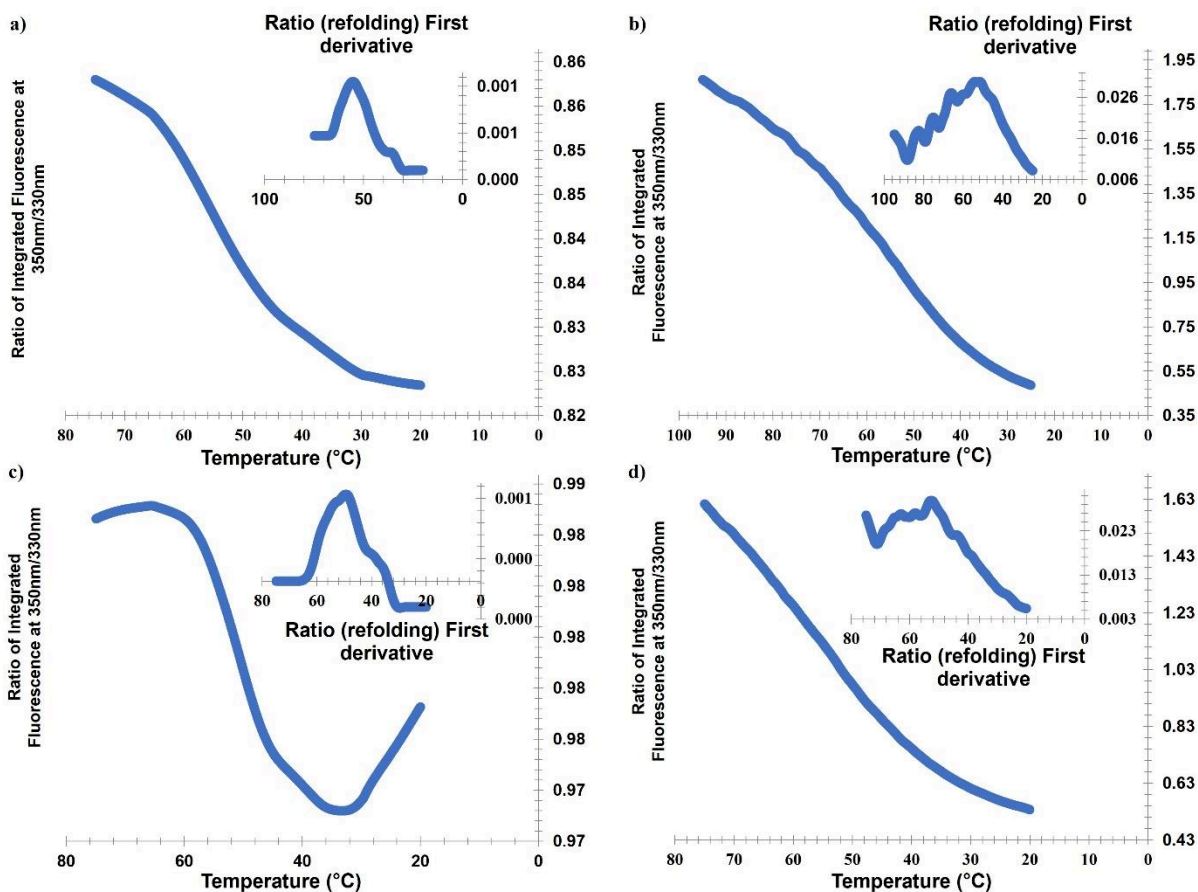


Figure 44: Representations of NanoDSF thermograms showing the ratio between fluorescence signals at 350 and 330 nm and the first derivative of this ratio for analysis of refolding values. Conditions: 1 mg/mL lipase in 100 mM sodium phosphate buffer pH 7.0 in different organic solvents. **CalB** in **a)** ACN and **b)** CYE; and **CR** in **c)** ACN and **d)** CYE.

5.1.2.3. Effect of alkyl chain on the synthesis of levoglucosan esters from BoE

Based on initial tests, N435 was selected as the ideal biocatalyst to explore the effect of alkyl chain size on CFAEs formation through BoE. Figure 45 shows that the increase in the alkyl chain of the acyl donor contributes positively to the synthesis of CFAEs for both solvents. For

CYE, this increase occurs gradually until carbon C16 and with a tendency to decrease from there. For ACN, on the other hand, this increase occurs until C8 and then assumes a non-gradual behaviour with the increase of the alkyl chain (Torres-Gavilán et al., 2006; P. Y. Wang et al., 2008). This behaviour for C12–18 long-chain acyl donors has already been reported (DO NASCIMENTO et al., 2019), however, using a LGCom.

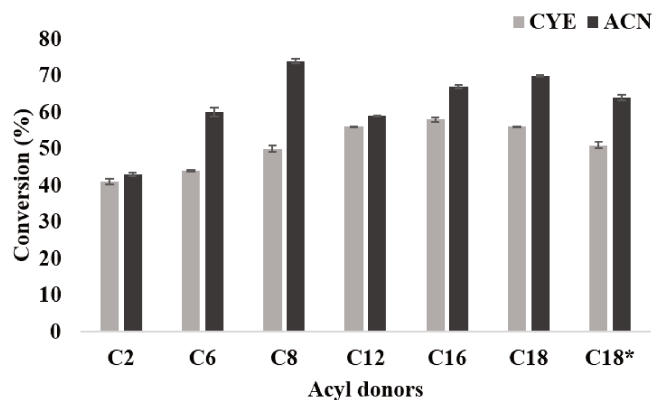


Figure 45: Results for transesterification reaction between different acyl donors with BoE in ACN and CYE. Conditions: ethyl esters: acetate (C2); hexanoate (C6); octanoate (C8); laurate (C12); palmitate (C16); stearate (C18) and oleate (C18*). BoE (40 mM) and acyl donors (1:2) in two organic solvents: acetonitrile (ACN) and cyrene (CYE) at 55°C, 120h and 300 rpm.

These results are consistent with those published by Arcens *et al.* (Arcens et al., 2020) who observed better conversions to long-chain acyl donors during the synthesis of sugar esters of fatty acids biocatalyzed by N435. So, the substrate specificity of the lipase seems to be related to the length and shape of the alkyl chain, with a weak specific interaction in the short chain and strong steric hindrance in the long chain (P. Zhang et al., 2019). In addition, the results are not very unexpected, since the increase in the alkyl chain can provide a greater interaction with the hydrophobic pocket of CalB. Nonetheless, its fatty acids cleavage binding site is relatively short and has a small hydrophobic area located an elliptical, steep funnel of $9.5 \times 4.5 \text{ \AA}$ (Rgen Pleiss et al., 1998), which may limit its activity for very long-chain acyl donors and, consequently, decreased the conversion between C16 and C18.

Moreover, the presence of three hydroxyl groups in the LG structure and the different experimental conditions allow the formation of a mixture of mono-, di- or tri-acylated compounds. Table 4 shows the regioselectivity through the two solvents, cyrene (CYE) and acetonitrile (ACN), in different sizes of the alkyl chain and in the presence of BoE.

Table 4: Regioselectivity in the transesterification reaction between different alkyl esters and BoE in the presence of ACN and CYE with N435.

Acyl donors	Solvent	Conversion (%)	Regioselectivity (%)						
			3I-a	3II-a	3III-a	4I-a	4II-a	4III-a	5a
<i>Ethyl Acetate</i>	CYE	27	50	0	44	0	0	0	6
	ACN	56	55	0	37	4	0	0	4
<i>Ethyl Hexanoate</i>	CYE	43	53	0	47	0	0	0	0
	ACN	60	48	0	42	7	0	0	3
<i>Ethyl Octanoate</i>	CYE	50	55	0	45	0	0	0	0
	ACN	74	50	0	43	4	0	0	3
<i>Ethyl Laurate</i>	CYE	56	72	0	28	0	0	0	0
	ACN	59	58	0	42	0	0	0	0
<i>Ethyl Palmitate</i>	CYE	58	69	0	31	0	0	0	0
	ACN	67	87	0	13	0	0	0	0
<i>Ethyl Stearate</i>	CYE	56	75	0	25	0	0	0	0
	ACN	70	70	0	30	0	0	0	0
<i>Ethyl Oleate</i>	CYE	51	67	0	33	0	0	0	0
	ACN	64	62	0	38	0	0	0	0

For short-chain acyl donors (C2–8), a mixture of monoacylated compounds (3I-a and 3III-a) can be observed on the hydroxyl groups attached to carbons 2 and 4. Furthermore, a low

selectivity can be observed for the di- and tri-acylated compounds. When increasing the length of the alkyl chain, a preference for the hydroxyl bonded to carbon 4 is observed for both the solvents.

Regarding regioselectivity, these results agree with those obtained by Galletti and Nascimento *et al.* (DO NASCIMENTO *et al.*, 2019; GALLETTI *et al.*, 2007). Although, the conversion values were lower compared to the reactions performed by our research group with the LGCom source, with conversions above 90%. The decrease in conversion may be related to the type of reactor used. In a first study, our research group produced the CFAEs in a Biovera® orbital shaker type reactor. However, for this study, due to the low solubility of BoE under the conditions used, a carousel type reactor (Radleys®) was used, as mentioned in Section 4.2.4.2.2. The magnetic stirring used in this type of reactor destroyed the N435 support (Ortiz, Ferreira, Barbosa, Dos Santos, *et al.*, 2019) resulting in a fine powder that, in addition to hindering its separation from the reaction medium, can alter the catalytic activity due to enzyme leaching. Therefore, attention must be taken when considering the use of N435 in mechanically stirred batch reactors, for example in limiting the stirring speed or in using other less aggressive configurations (Ortiz, Ferreira, Barbosa, Dos Santos, *et al.*, 2019).

5.1.2.4. Effect of substrate ratio

Different concentrations of both substrates, ethyl acetate (40, 100, 150 and 200 mM) and BoE (50, 80 and 130 mM) were used. The conversion increased from 24% to 41% when the acyl donor concentration was increased by a factor of 5 times (40–200 mM) in 80 h to 50 mM of BoE (Figure 46). However, at higher concentrations of BoE, the conversion decreased from 41% (50 mM) to 23% (130 mM) for a fixed concentration of the acyl donor (200 mM) and from 24% to 11% in 40 mM (Figure 46). This decrease in the conversion to higher concentrations of BoE suggests an inhibition by levoglucosan or by the impurities present in the BoE that was attributed the formation of more dead-end enzyme-LG complex with increasing BoE concentration. These

indicated that at high concentration of BoE, the inhibition of N435 by BoE was significant. Therefore, kinetic studies were performed with LGCom in an orbital shaker reactor for a better understanding of the results.

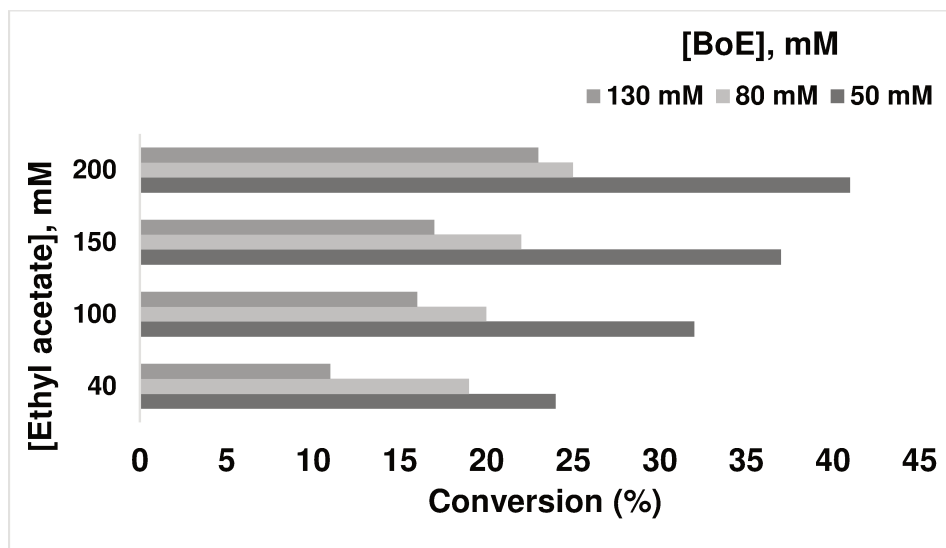


Figure 46: Results for transesterification reaction between ethyl acetate and BoE in CYE for different concentrations of ethyl acetate (40-100-150 and 200 mM) in function of the different concentrations of BoE 50-80 and 130 mM in total reaction time at 80h.

5.2. Kinetic studies

A kinetic study was carried out with N435 to understand the reaction mechanism. The effect of solvent and concentration of both reagents (LGCom and acyl donors ethyl acetate and ethyl oleate) were investigated. We determined the initial rate (V_0) from reactions realized at different fixed concentrations of LGCom (20–300 mM) and at different concentrations of acyl donors (50–300 mM) (see ANNEX D3). The increasing the concentration of ethyl acetate does not significantly alter the initial rate of the reaction. However, for LGCom it was observed that the increase in the molar concentration contributed to an increase in the initial rate of the reaction.

For both solvents, there is a sharp increase in the initial rate for the range of initial concentration of LGCom (20–80 mM), which was expected since high-affinity sites are occupied

in this range (Bisswanger, 2017). In higher concentrations of substrates, high-affinity sites are saturated, and the occupation of low-affinity sites are preferred. Due to the superposition of different saturation functions, a slow increase in reaction rate can be observed when increasing the LGCom concentration until it reaches a saturation limit above 200 mM (Bisswanger, 2017). The K_m and V_{max} values were determined from the Lineweaver-Burk graphs derived from Figure 47a-b, in which the transesterification reaction of ethyl acetate is presented as a function of the LGCom concentration.

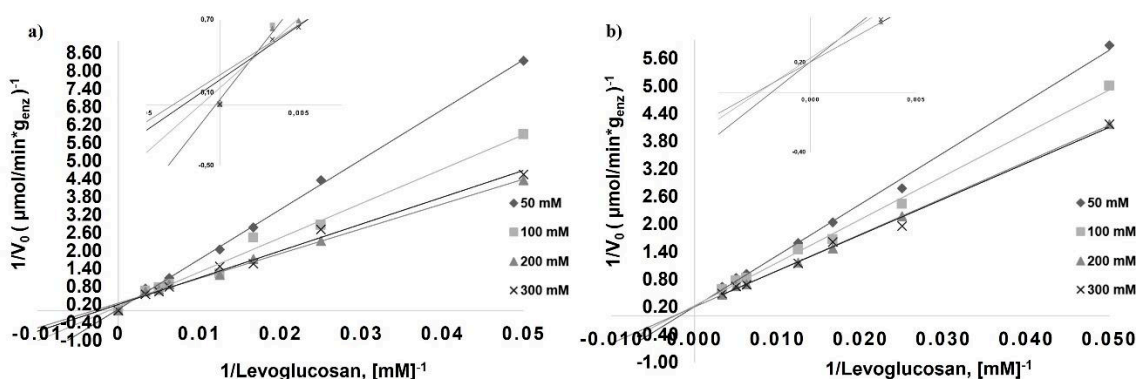


Figure 47: Lineweaver–Burk plot of the reversed initial velocity of transesterification of levoglucosan (20–300 mM) with ethyl acetate (50–300 mM) in function of reversed concentration levoglucosan: **a)** acetonitrile (ACN) and **b)** cyrene (CYE).

The results suggest that the reaction rate mainly depends on the LGCom concentration. Furthermore, decreasing acyl donor concentration increases the slope and decreases the intercept on the $1/V_0$ axis up to the $1/V_{max}$ limit, where a mixture of non-parallel and intersecting narrow lines can be observed. The specific shape of the slope of these lines is influenced by the concentration of fixed substrate. The same was observed when we increased the size of the acyl donor alkyl chain through ethyl oleate (see ANNEX D).

These results indicate a mechanism that requires the association of the second substrate to the enzyme-substrate complex before formation of the product. This suggests that the slope and intercepts were affected by LGCom in a partially uncompetitive inhibition (Bisswanger, 2017), for both solvents. This is confirmed by Dixon plot (Bisswanger, 2017), through reciprocal plot of

initial rate in function of the concentration of possible inhibitor (LGCom), showing nonlinear curves characteristic of this type of inhibitor (Figure 48) (Bisswanger, 2017).

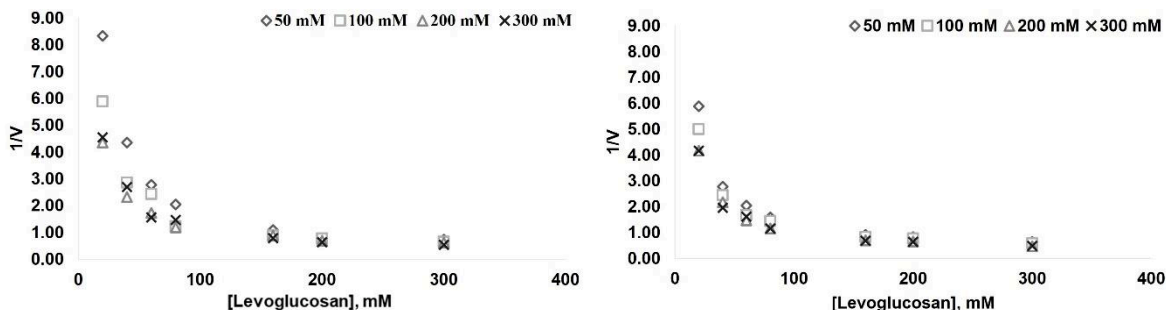


Figure 48: Dixon plot of initial rate reciprocal plot of LGCom transesterification with ethyl acetate (50-300 mM) in function of LGCom concentration (20-300 mM) in: **a)** acetonitrile (ACN); **b)** cyrene (CYE).

In most cases, induced substrate inhibitions are not complete because the inhibitor escapes from the EB complex at a reduced and finite rate (Punekar, 2018). In this context, some authors have reported enzymatic inhibition by both the acyl donor and alcohol (Hari Krishna & Karanth, 2002; Lopresto et al., 2014; Zaidi et al., 2002), on the contrary other authors established enzymatic inhibition only by acid (Bisswanger, 2017; Ortiz, Ferreira, Barbosa, Dos Santos, et al., 2019) or alcohol (Garcia et al., 1999; Yadav & Lathi, 2003).

When the ethyl acetate concentration varied, for fixed LGCom concentration, the reaction rates increase with increasing LGCom concentration and the lines do not cross the same point above the horizontal and vertical axes for both solvents, indicating that the inhibition is stronger at low concentrations of LGCom, as can be seen in the shape of the curve for 20 mM and a negative cooperativity for concentrations greater than 200 mM (Figure 49). The plots obtained for ethyl oleate were like the short-chain acyl donor, suggesting that chain size does not change the reaction profile (see ANNEX D).

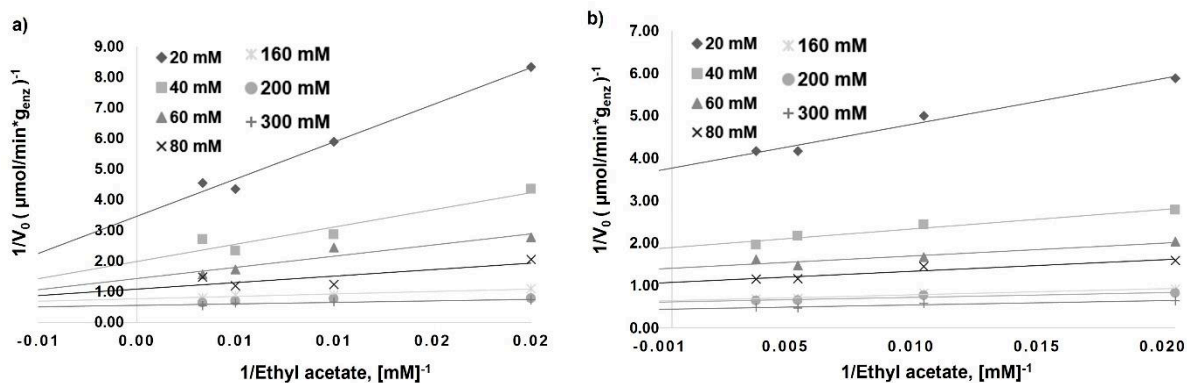


Figure 49: Lineweaver–Burk plot of initial rate of LGCom transesterification (20-300 mM) in function of ethyl acetate concentration (50-300 mM) in: **a)** acetonitrile (ACN); **b)** cyrene (CYE).

According to the results, an ordered bi-bi sequential mechanism with dead-end inhibition is suggested (Segel, 2013), where a reaction with two substrates forms two products – being widely accepted to describe the general kinetics of lipase-mediated esterification reactions, following the kinetics of Michaelis-Menten. In this reaction the substrate A first binds with the free enzyme E and forms an enzyme-A complex AE. The second reactant B then combines with AE to form a ternary complex AEB or it may react with free enzyme to yield a dead-end complex (EB). This ternary complex then transfers to another ternary complex P1EP2, which releases the first product (P1), and then the second product P2 and the free enzyme (Papamichael et al., 2019). The general kinetics equation is expressed considering the possibility of inhibition by both substrates that form dead-end complexes with the enzyme (alcohol) or with the intermediate acyl complex (Sousa et al., 2021; Wallace Cleland, 1989). In an ordered bi-bi system the two substrates lead to two products, where the initial velocity in the absence of products is given by the Eq. 5:

$$V = \frac{V_{max}[A][B]}{K_{ia}K_{mb} + K_{mb}[A] + K_{ma}[B] + [A][B]} \quad \text{Equation 5}$$

Those terms in the denominator representing free **E** are multiplied by $(1 + \frac{[B]}{K_i})$ (Itabaiana et al., 2013). Therefore, the equation 6 becomes:

$$V = \frac{V_{max}[A][B]}{(K_{ia}K_{mb}(1 + \frac{[B]}{K_i})) + K_{mb}[A] + (K_{ma}(1 + \frac{[B]}{K_i})) + [A][B]} \quad \text{Equation 6}$$

Where V_{max} is the maximum velocity; v is the initial rate of reaction; $[A]$ and $[B]$ are the initial concentrations of acyl donor and levoglucosan, respectively; K_{ma} is Michaelis constant for acyl donor; K_{mb} is Michaelis constant for levoglucosan; K_i is the dissociation constant for EB and K_{ia} is the dissociation constant for $[A]$.

The Lineweaver-Burk plots obtained for different fixed concentrations of the substrates can be used to find the kinetic parameters through the apparent value of the slopes and the intercept. Whereby, Figure 50 was plotted again using the slope of the line corresponding to each fixed concentration of levoglucosan and ethyl acetate. The data obtained showed good linearity for both solvents. Furthermore, Figure 51 was obtained by plotting the intercept of each line corresponding to the fixed LGCom concentration. The data showed good linearity which agrees with what is expected for dead-end substrate inhibition in an ordered bi-bi sequential mechanism.

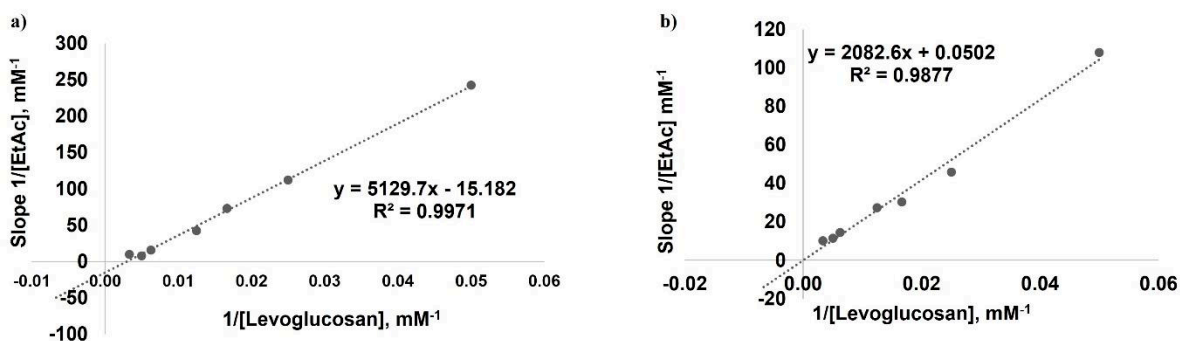


Figure 50: Secondary plot of slope 1/[ethyl acetate] versus reciprocal concentration of 1/[LGCom] in two solvents: **a)** acetonitrile and **b)** cyrene.

The Michaelis-Menten kinetic parameters determined from the Lineweaver-Burk plot are summarized in Table 5. The magnitude of the differences in K_m and the K_i values express,

respectively, the differences in the affinity of the biocatalyst for the substrates and the inhibitory effects of the substrate on the enzymes. These parameters are essential for expansion studies and reactor design (CLELAND, 1963).

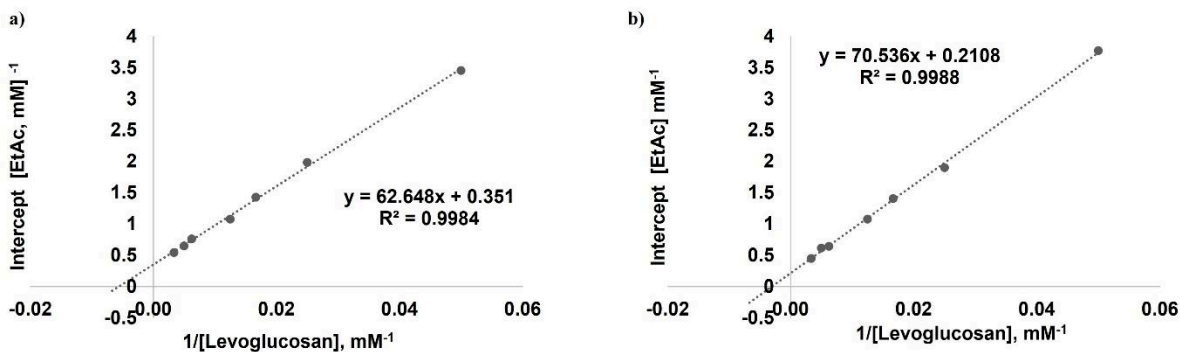


Figure 51: Secondary plot of intercept $1/[\text{ethyl acetate}]$ versus reciprocal concentration of $1/[\text{LGCom}]$ in two solvents: **a)** acetonitrile and **b)** cyrene.

The results showed that the constant K_m of the transesterification reaction of ethyl acetate in CYE ($K_{mA} = 25 \text{ mM}$) was lower than that of the reaction with ACN ($K_{mA} = 82 \text{ mM}$) while the maximum reaction rate in CYE ($V_{\max} = 4,60 \mu\text{mol}/\text{min} \cdot G_{\text{enz}}$) showed values close to the reaction in ACN ($V_{\max} = 4.10 \mu\text{mol}/\text{min} \cdot G_{\text{enz}}$). Consequently, the catalytic efficiency (V_{\max}/K_m) (Da Silva et al., 2020) for the reaction in CYE (0.184) is four times greater than in ACN (0.05) due to a better affinity with the enzyme. In ACN, the size of the alkyl chain of the acyl donor did not affect the reaction rate. However, there was a $> 50\%$ decrease in the V_{\max}/K_{mA} ratio due to an increase in K_{mA} . Different results for CYE showed a small increase of approximately 13% for ethyl oleate. Although, K_{iA} is lower for both acyl donors, which means a greater inhibitory effect on CYE than on ACN. K_m values for ethyl acetate and oleate indicated that N435 has a higher affinity for both acyl donors and a low affinity for LG. In other works, the authors also reported a higher affinity for the acyl donor using lipases. Pawar e Yadav (Pawar & Yadav, 2015) observed a 27-fold higher affinity for vinyl acetate during regioselective monoacylation of 3-aryloxy-1, 2-propanediol. Zhang et al. (C. Zhang et al., 2021) when studying the enzymatic kinetics of the esterification of

acetic acid with ethanol, observed that the acyl donor presented a $K_m = 137$ mM while for the alcohol $K_m = 689$ mM. On the contrary, I. Itabaiana Jr. *et al.* (Itabaiana *et al.*, 2013) observed a higher affinity for alcohol ($K_m = 43.4$ mM) during esterification of solketal with stearic acid biocatalyzed by CalB. Furthermore, the V_{max} calculated in this work is close to that presented by Yadav and Lathi (Yadav & Lathi, 2003) for the synthesis of butyl isobutyrate using N435 ($V_{max} = 0,02$ mmol/min*Genz) and also, close values were found by Shang Sun and Bingxue Hu (S. Sun & Hu, 2017) that reported greater affinities for the acyl donor with $K_m = 86$ mM for the transesterification of ethyl caffeate with glycerol catalysed by N435. Thus, despite favourable kinetic results and thermostability for the cyrene better conversion results were obtained for acetonitrile. According to Pérez-Venegas *et al.* (Pérez-Venegas *et al.*, 2020) Calb in N435 is more stable than in its free form. Thereby, it is suggested that its acquired during immobilization stability favoured the application of CalB in ACN. On the contrary, the high viscosity of CYE may have generated a negative result due to the increase in diffusion effects present in the immobilized CalB which can be circumvented by increasing the temperature of the reaction medium in future studies.

Table 5: Kinetic parameters obtained for the transesterification of different acyl donors in the presence of LGCom in ACN and CYE.

Solvent	Acyl donor	Parameter / Values					
		V_{max} , ($\mu\text{mol}/\text{min} \cdot \text{Genz}$)	K_{mA} , (mM)	K_{mB} , (mM)	K_{ia} , (mM)	K_i , (mM)	V_{max}/K_{mA}
Acetonitrile	EthAct	4,10	82	179	155	4	0,050
	EthOle	4,17	196	452	136	2	0,021
Cyrene	EthAct	4,60	25	272	35	15	0,184
	EthOle	4,46	19	106	24	28	0,235

Note: Ethyl acetate (EthAct) and Ethyl oleate (EthOle); Maximum velocity (V_{max}); Michaelis constant for acyl donor (K_{mA}) and for levoglucosan (K_{mb}); Dissociation constant for EB (K_{ia}); Dissociation constant for acyl donor (K_i) and catalytic efficiency (V_{max}/K_{mA}).

5.3. Lipase-catalysed acylation of levoglucosan in continuous flow

One of the biggest obstacles in continuous flow chemistry is the handling of solids that can form during the chemical reaction or in the piping that precedes the entry of reagents into the reactor, usually leading to clogging of the channels. Furthermore, the low solubility of the starting materials can make flow-through synthesis a challenging task (Bloemendal et al., 2020; Guidi et al., 2020). Thus, and in order to obtain the best reaction conditions, the reagents were prepared at a concentration of 40 and 100 mM, respectively, and submitted to solubility tests at different temperatures (See ANNEX C).

According to the results obtained, it is possible to observe the insolubility of levoglucosan in acetonitrile at temperatures less than or equal to 50 °C. For the acyl donors: lauric acid, vinyl palmitate and vinyl oleate were soluble in all conditions analyzed, whereas laurate and vinyl stearate were soluble at temperatures greater than or equal to 50 °C. In addition, for the molar concentrations analyzed, the solubility profile remained constant, varying only with the temperature change. Therefore, due to the low solubility of levoglucosan at temperature below 50°C and for the experimental conditions available in the laboratory, it was necessary to heat the starting material before pumping it into the fixed bed reactor.

5.3.1. Optimization using DoE in a model reaction

The model reaction used was the esterification of levoglucosan with lauric acid (Figure 52). In the application of the experimental planning, the input variables used were temperature (X1) and residence time (X2). And as response variable (Y) the conversion (%). In the CCD, 11 experiments were performed at random and the matrix of experiments with the obtained conversion (%) responses are shown in table S1 (See ANNEX C). After the execution of all experiments, a second-order equation was obtained:

$$Y = b_0 + b_1T + b_2t + b_1T^2 + b_1t^2 + b_1Tt \quad (\text{Equation 7})$$

Where,

Y = conversion response (%); b_i = coefficients of the generated model for T (temperature) and tr (residence time).

The model equation coefficients were obtained using Equation 8 (BARROS NETO; et al., 2016; VICENTINI et al., 2011) below:

$$b = (X^t X)^{-1} (X^t Y) \text{ (Equation 8)}$$

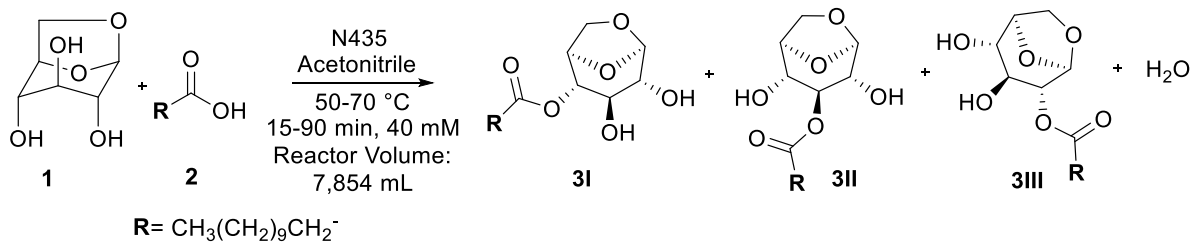


Figure 52: Esterification reaction of levoglucosan with lauric acid. *Reactor volume packed with N435: 7.854mL.

From the generated model it was possible to build the response surface and the level curve (Figure 53a-b).

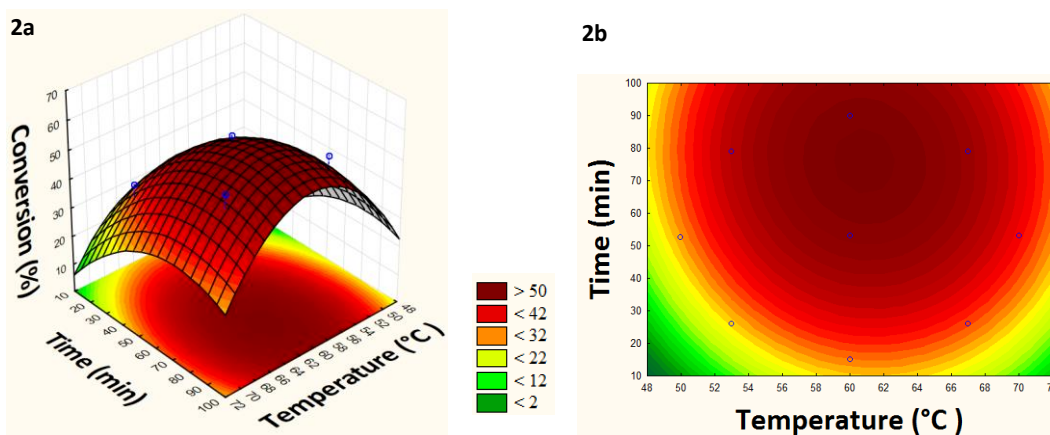


Figure 53: a) Response surface and b) level curve of the conversion in the model reaction of esterification of levoglucosan with lauric acid relating temperature and time.

Based on response surface and levels curve analysis (Figure 53a-b) can verify that at temperatures below 54 °C and short residence times (10–25 min) the conversion remained below 20%, increasing linearly with the increase of these two parameters, until reaching a maximum conversion (55%) at 61 °C and 77 min. It was also observed that for temperatures above 69 °C and residence times less than 30 min, the conversion tends to remain below 22%, indicating that there is dependence between these two factors. Besides, there is an ideal working range between 60–62 °C and 70–80 min for maximizing conversion.

In the esterification reaction using carboxylic acid, one of the products formed is water, a strong nucleophile in deacylation of the acyl enzyme, shifting the balance in the opposite direction, *i.e.*, hydrolysis of the product (this is a thermodynamically controlled synthesis) (Chulalaksananukul et al., 1990; Rhee et al., 2003) and, consequently, decreasing the reaction yield. To shift the balance towards the products and increase yield, it is common to use in excess of one of the reagents or remove one of the products, usually water (Bornscheuer & Kazlauskas, 2005).

Alternatively, it is possible to obtain the products desired by changing the leaving group of the acylating agent, avoiding, for example, formation of water in the reaction medium and, furthermore, improve the solubility of the starting materials. Thus, after optimizing the temperature and residence time, the best conditions obtained were applied in the model reaction by varying the acyl donor output group (Figure 54).

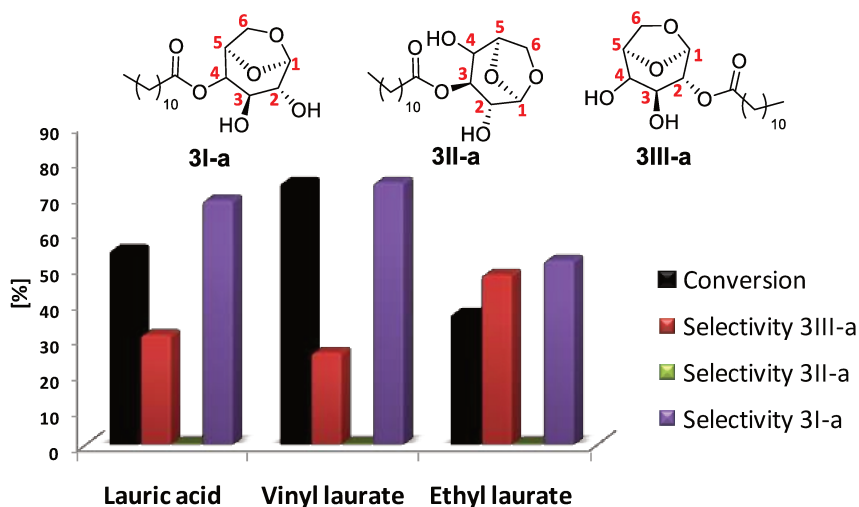


Figure 54: Acylation of levoglucosan with different acyl donors in 61 °C and residence time 77 min using **N435** as biocatalyst. Selectivity **3I-a**: 4-O-Lauryl-1,6-anhydroglucopyranose; Selectivity **3II-a**: 3-O-Lauryl-1,6-anhydroglucopyranose and Selectivity **3III-a**: 2-O-Lauryl-1,6 anhydroglucopyranose. Analyses were performed in a gas chromatograph equipped with a mass spectrometry detector (GC-MS).

Better results were obtained using vinyl laurate as acylating agent, with conversion 74%, selectivity 3I-a of 75% and 3III-a of 25%. The formation of 3-O-lauryl-1,6-anhydro-glucopyranose (selectivity 3II-a) was not observed. According to Boissière-Junot *et al.* (Boissière-Junot *et al.*, 1998) the orientation of the hydroxyls (axial or equatorial) or neighbouring substituent governs the regioselectivity of acetylation catalysed by lipase. When the C3-OH is axial a high regioselectivity is observed for the adjacent axial C4- or C2-OH (Boissière-Junot *et al.*, 1998). Moreover, studies carried out by Uriarte *et al.* (Uriarte *et al.*, 2018) suggest that in chair conformation, interactions by intramolecular hydrogen bonds that occur between C3-OH and oxygen in C6, both in the axial position, stabilize the molecule, decreasing its reactivity as a nucleophile. As a result, a preference for 3I-a or 3III-a must be observed (Boissière-Junot *et al.*, 1998).

The low conversion and loss of selectivity obtained using ethyl laurate 40% may be related to its partial solubility under applied experimental conditions. Contrary to that, the reaction in the presence of completely soluble lauric acid showed a conversion 55%, 19% lower compared to

the vinyl donor, however, better than the values reported by Galletti *et al.* (Galletti et al., 2007) 40% conversion using lauric acid for the batch reaction for about five days.

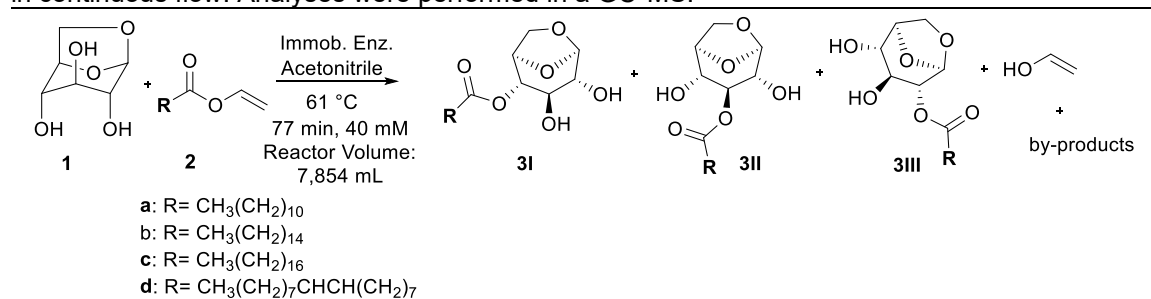
Another point to be highlighted is the vinyl alcohol formed that tautomerizes to acetaldehyde irreversibly, a more stable compound that also contributes to shifting the chemical balance in the direct direction of the reaction, thereby increasing the yield of the desired ester (Yadav & Trivedi, 2003). The results suggest the great potential of vinyl acyl donors for the synthesis of levoglucosan esters in continuous flow, not only for their solubility, but also for the best conversions and selectivities obtained.

5.3.2. Synthesis of long-chain CFAEs

Finally, after screening, the promising results obtained in the acylation of levoglucosan with vinyl donor motivated us to evaluate a complementary in flow approach regarding the regioselectivity presented by CalB_Epoxy, applied to obtain CFAEs of levoglucosan in the batch condition (do Nascimento et al., 2019).

The transesterification reaction was carried out in the presence of a series of vinyl esters containing alkyl chains of variable length (C12–C18), as well as in the presence of biocatalyst N435 used as reference. The results are shown in Table 6.

Table 6: Regioselectivity in the enzymatic acetylation of levoglucosan in CH₃CN with vinyl aliphatic esters in continuous flow. Analyses were performed in a GC-MS.



Entry	Immobilized Enzyme *	Acyl Donor**	Regioselectivity (%)			
			3I	3II	3III	By-products
1	N435	a	75	-	25	-
2		b	76	-	24	-
3		c	73	-	27	-
4		d	75	-	25	-
5	CalB_Epoxy	a	33	-	10	57
6		b	50	-	15	35
7		c	43	-	17	40
8		d	45	-	14	41

*N435 = Novozym 435 (*Candida antarctica* lipase B), immobilized on macroporous acrylic type ion exchange resin; CalB_Epoxy = *Candida antarctica* lipase B immobilized on epoxy support by our research group and **2 equivalents, **a** = vinyl laurate, **b** = vinyl palmitate, **c** = vinyl stearate and **d** = vinyl oleate.

As a result, the formation of by-products using N435 was not observed. In contrast, there was the formation of by-products in the presence of CalB_Epoxy, respectively (Table 6).

Regarding regioselectivity, N435 showed similar values between 23% for 3IIIa–d, and 77% for 3Ia–d for all acyl donors used, *i.e.*, there was a preference for the hydroxyl linked to C4 for the acylation of levoglucosan. However, there was the formation of by-products using CalB_Epoxy, reducing the selectivity for the desired products (Table 6 – entries 5–8). In contrast to observed by Do Nascimento *et al.* (do Nascimento *et al.*, 2019) for the batch reaction, with N435 being more selective to produce lauric esters (99% at 50 °C) while CalB_Epoxy was more selective to produce oleic esters (83% at 55 °C) of LG, respectively.

Compared to the batch system (do Nascimento et al., 2019) the productivity values obtained for the continuous flow reaction were higher in all samples, even with the loss of selectivity for CFAEs using CalB_Epoxy (Table 7). Calculations obtained for specific activity showed that CalB_Epoxy presented 41.33 U mg⁻¹ of protein, a value approximately 2.5 times higher than that obtained for N435 of 16.53 U mg⁻¹ of protein. These results suggest that the high specific activity for CalB_Epoxy may have contributed to significant gains for productivity, although the selectivity values for CFAEs are lower than for N435.

Table 7: Comparative between the values of conversion and productivity for batch and continuous flow systems

Entry	Immobilized Enz.*	Acyl donor**	Conversion (%)	Productivity***	
				Batch	Continuous Flow
1	N435	a	74	0.030	3.660
2		b	76	0.034	4.370
3		c	57	0.034	3.511
4		d	85	0.035	5.211
5	CalB_Epoxy	a	59	0.003	0.511
6		b	99	0.010	1.500
7		c	99	0.009	1.481
8		d	97	0.014	1.420

*N435 = Novozym 435 (*Candida antarctica* lipase B), immobilized on macroporous acrylic type ion exchange resin; *CaLB_Epoxy = *Candida antarctica* lipase B immobilized on epoxy support by our research group **2 equivalent, a: vinyl laurate, b: vinyl palmitate, c: vinyl stearate and d: vinyl oleate. ***Productivity = mg of product.h⁻¹.S_A⁻¹ of biocatalyst.

For a better understanding of the results, it is important to highlight the differences between the N435 and CalB_Epoxy biocatalysts. According to Ortiz *et al.* (Ortiz, Ferreira, Barbosa, Dos Santos, et al., 2019) N435 is a CalB immobilized by hydrophobic adsorption *via* interfacial activation on a Lewatit VP OC 1600 resin used as a support. The same protocol was applied by Do Nascimento *et al.* (Do Nascimento et al., 2019) in the immobilization

of CalB, but in epoxy acrylate resin ECR 8205 (Purolite®), denominated CalB_Epoxy. Therefore, the difference between the two biocatalysts lies in the support used for their immobilization and, consequently, in the way these enzymes attach themselves to the solid material, which reflects on their specific chemical, biochemical, mechanical and kinetic properties (Ortiz, Ferreira, Barbosa, Dos Santos, et al., 2019).

As mentioned, in both biocatalysts the lipase was adsorbed on the hydrophobic surface of the support *via* an interfacial activation protocol (Do Nascimento et al., 2019). This method of immobilization has some advantages, for example, they can almost completely retain their activity (Manoel et al., 2015). Moreover, it is less sensitive to variation in experimental conditions because there is no conformational equilibrium to be changed (Bastida et al., 1998; Fernandez-Lafuente et al., 1998; Hirata et al., 2016; Palomo et al., 2003). However, as it is a reversible immobilization and based on hydrophobic interactions, enzymes can detach from the support and go to the reaction medium, resulting in a loss of enzymatic charge with a subsequent decrease in its activity.

For biocatalysts N435 and CalB_Epoxy, leaching of the enzyme was not observed after the passage of pure solvent through the fixed bed reactor. However, the reagents, as well as the products formed during the reaction can lead to the desorption of the lipase molecules into to reaction medium as well as the polymeric components of the support, contaminating the product, as reported by Hirata *et al.* (Hirata et al., 2016) where free fatty acids and di or monoglycerides, which have recognized detergent properties, favoured enzyme desorption. Furthermore, bimolecular aggregates may have been formed in the immobilization and/or leaching during the reaction with subsequent interaction between two open forms of the lipase (Palomo et al., 2003). When this occurs, the effect can be quite negative because these dimers will be immobilized along with the monomeric enzyme molecules. This phenomenon may have occurred with CalB_Epoxy, changing its properties (Palomo et al., 2003, 2004).

Finally, the results for the recycling of biocatalysts suggested a low conversion loss in the five applications, reinforcing the stability of the proposed system.

Table 8: Recycling of biocatalysts applied in the transesterification reaction.

Entry	Immob. Enz.*	Acyl donor**	Conversion (%)				
			I	II	III	IV	V
1	N435	a	71	66	64	58	49
2		b	69	65	62	55	51
3		c	54	51	45	39	33
4		d	79	74	69	66	59
5	CaLB_Epoxy	a	53	49	47	43	38
6		b	91	87	84	81	77
7		c	95	92	88	83	79
8		d	93	89	84	79	72

*N435 = Novozym 435 (*Candida antarctica* lipase B), immobilized on macroporous acrylic type ion exchange resin;

*CaLB_Epoxy = *Candida antarctica* lipase B immobilized on epoxy support by our research group **2 equivalent, a:

vinyl laurate, b: vinyl palmitate, c: vinyl stearate and d: vinyl oleate.

5.3.3. Evaluation of interfacial tension between oil/water in different concentrations of CFAEs

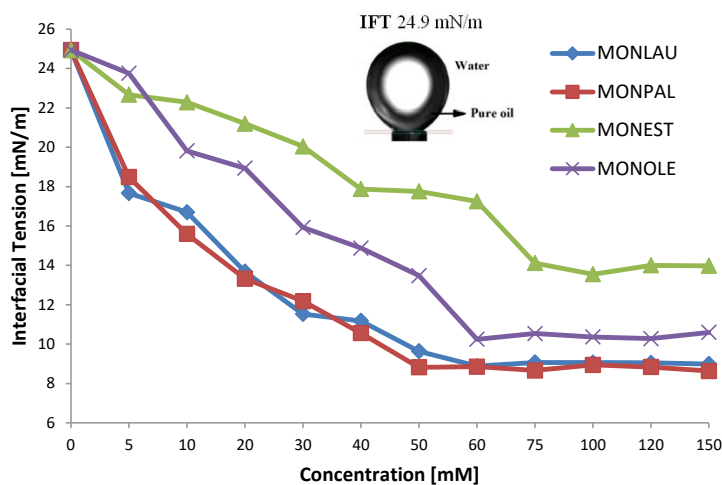
Table 9 shows the theoretical values of HLB calculated for CFAs using the Becher equation (equation (1)) (PAUL BECHER, 1988). These values between 4.42 and 5.91 and the low solubility in water, especially for compounds from 2-4, suggest an application as a wetting agent or as oil-soluble hydrophobic (w/o) emulsifiers (DAVIES, 1957).

Table 9: Interface active properties of CFAs.

Entry	Compound*	Oil solubility (mg.mL ⁻¹)	HLB value	IFT ^{min} (mN.m ⁻¹)	CMC (mM)
1	MONLAU	>100	5.91	8.98	53
2	MONPAL	>100	4.80	8.63	50
3	MONEST	>100	4.42	13.97	76
4	MONOLE	>100	4.61	10.59	62

*Mixture of 4- and 2-: O-Lauryl-1,6-anhydroglucopyranose (MONLAU), O-Palmitoyl-1,6-anhydroglucopyranose (MONPAL), O-Estearyl-1,6-anhydroglucopyranose (MONEST) and O-Oleoyl-1,6-anhydroglucopyranose (MONOLE).

In this context, the behavioural trend values of CFAEs were measured through experimental studies by the pendant drop method (Arashiro & Demarquette, 1999), of the minimum interfacial tension (IFT^{min}) in function of the concentration of CFAEs in oil-water (Figure 55).

**Figure 55:** Relationship between the concentration of CFAs and interfacial tension.

The IFT^{min} is one of the key parameters that govern the compatibility between the components of the blend (Wu, 1987). It results from the difference in energy between molecules at a fluid interface when compared to their bulk counterparts (Berry et al., 2015). Compounds with

properties such as surfactants tend to distribute themselves at interfaces between phases with different degrees of polarity, forming a molecular film that reduces interfacial and surface tension.

In this context, a drop in the voltage value at the water–oil interface was observed with the increase of the molar concentration of CFAEs in the oil and it remained practically constant after 50 mM, thus revealing a state in which the surfaces of the tested samples are saturated with the CFAEs molecules. From this specific concentration, called critical micelle concentration (CMC), thermodynamically stable molecular aggregates begin to form. The structure of the surfactant and the experimental condition define how these molecules are submerged within the fluid (Könnecker et al., 2011).

Also, it is possible to note that compounds 1-2 (MONLAU and MONPAL) showed a similar behavior, with a considerable decrease in IFT^{\min} below CMC, in the range of 24.8 mNm^{-1} and 86 mNm^{-1} , and with non-significant variations for high concentrations of CFAEs, above the CMC. Thus, it is suggested a greater affinity of these molecules with the aqueous medium, compared to compounds 3 and 4, so that these compounds were able to spread, and reduce the tension at the interface with the aqueous medium more effective, at 50 mM. In contrast, MONEST and MONOLE the CMC was greater than 60 mM and IFT^{\min} in the range of $13.7\text{-}10.5 \text{ mNm}^{-1}$.

Preliminary evaluation of the active properties of the MONLAU product were reported by Galletti *et al.*, which obtained an HLB value of 5.9 and 45 mNm^{-1} at 0.019 ng mm^2 (Galletti et al., 2007). Furthermore, Kootery *et al.* suggest that monoacylated levoglucosan esters can be considered as representative renewable surfactants (Parambath Kootery et al., 2014).

These results corroborate those obtained in this work of the 9.2 mNm^{-1} at 53 mM for MONLAU. Moreover, similar results were obtained for MONPAL e MONOLE, without description in the literature, with 8.8 mNm^{-1} at 53 mM and 10.25 mNm^{-1} at 60 mM, which indicates lipophilic water in oil emulsifier.

5.3.4. Antibacterial assays

Staphylococcus aureus is a bacterium that is frequently encountered on the skin and mucous membranes of both humans and animals. It is a pathogenic microorganism notorious for its capacity to induce a diverse array of infections in humans (Howden et al., 2023). These infections span from common skin ailments and abscesses to more severe conditions like pneumonia, sepsis, and endocarditis (Malanovic & Lohner, 2016). Notably, certain strains of *Staphylococcus aureus* exhibit resistance to antibiotics, with methicillin-resistant *Staphylococcus aureus* (MRSA) being a prominent example. Treating MRSA infections can be particularly challenging due to their resistance to conventional antibiotics (Howden et al., 2023; J. Kim et al., 2023; Malanovic & Lohner, 2016).

The results referring the minimal inhibitory concentration and minimal bactericidal concentration, of esterified compounds against *Staphylococcus aureus* strains, are shown in Table 10. The alkyl chain length of CFAEs significantly influenced the antibacterial activity. Among the tested substances MONEST and LG were not able to inhibit the growth of the selected strains at concentration ≤ 1 mM. Concerning the esterified products, MONLAU and MONOLE showed higher activity, highlighting MONLAU which presented MIC values lower than that of the lauric acid substrate. MONLAU was able to inhibit the growth of all MSSA and MRSA strains at 0.25 mM. Since, MRSA presents a multidrug-resistant pattern for variable antimicrobial classes, such macrolides, fluoroquinolones, aminoglycosides, tetracyclines, and lincosamides (Algammal et al., 2020), this is a promising result, once the World Health Organization (WHO) considers methicillin-resistant and vancomycin intermediate, and resistant, *Staphylococcus aureus* to be a high priority pathogen.

In Gram-positive bacteria such as *Staphylococcus aureus*, the lipid bilayer is predominantly made up of phosphatidylglycerol, which contains branched fatty acids, notably with

a significant proportion of anteiso C15:0 and C17:0 chains (Malanovic & Lohner, 2016). Regarding CFAEs, a C12:0 alkyl chain length appears to be the most effective for intercalating into Gram-positive bacterial membranes, thereby maximizing their antibacterial properties. However, an increased in the alkyl chain length of CFAEs, diminished their affinity for bacterial cell membranes, resulting in a loss of antibacterial efficacy.

Table 10: Minimal inhibitory concentration (MIC) and minimal bactericidal concentration (MBC) of products and substrates against *Staphylococcus aureus* strains.

Compound	ATCC 25923	ATCC 29213	ATCC 33591	517
	MSSA	MSSA	MRSA	MRSA
MONLAU	0.25 mM	0.25 mM	0.25 mM	0.25 mM
	0.25 mM ^a	0.25 mM ^a	0.25 mM ^a	0.25 mM ^a
MONEST	> 1.0 mM	> 1.0 mM	> 1.0 mM	> 1.0 mM
MONPAL	> 1.0 mM	> 1.0 mM	1.0 mM	> 1.0 mM
MONOLE	1.0 mM	0.5 mM	0.25 mM	1.0 mM
Lauric Acid	0.5 mM	0.5 mM	0.5 mM	0.5 mM
Levoglucosan	> 1.0 mM	> 1.0 mM	> 1.0 mM	> 1.0 mM
Methicillin	0.5 µg.mL ⁻¹	0.25 µg.mL ⁻¹	4.0µg.mL ⁻¹	4.0 µg.mL ⁻¹

^aminimal bactericidal concentration (MBC). MSSA: methicillin-sensitive *Staphylococcus aureus*. MRSA: methicillin-resistant *Staphylococcus aureus*.

Due to this promising result, bactericidal and bacteriostatic modes of action of MONLAU were evaluated, and the MBC assay indicated the bactericidal effect of MONLAU against all strains (MIC = MBC), including for methicillin-resistant *Staphylococcus aureus*. This was the first report on the antibacterial activity of levoglucosan fatty acid esters. MONLAU, against *S. aureus*, showed higher activities compared to other CFAEs reported in literature, such sucrose monolaurate (MIC = MBC = 0.4 mM) (K. M. Park et al., 2018), methyl α -D-glucopyranoside monolaurate (MIC = 188 µg.mL⁻¹) (X. Zhang et al., 2015) and sucrose monocaprato (MIC > 400 µg.mL⁻¹) (J.D. Monk et al., 1996).

Conclusion

In these studies, the integration of alkyl ester production with the transesterification of commercial levoglucosan (LGCom) and levoglucosan obtained from cellulose pyrolysis (BoE) was successfully achieved. Various lipases, both in free and immobilized forms, were employed as catalysts in these reactions. Furthermore, NanoDSF technology revealed that the solvent used could influence the thermostability of lipases.

The regioselectivity of the reactions was fully confirmed through a range of analytical techniques, including NMR (^1H , ^{13}C , HMBC, HSQC, ^1H , ^1H -COSY, NOEdiff), FTIR spectroscopy (ν , cm^{-1} , KBr), HRMS (High-Resolution Mass Spectrometry), and GC–MS analysis. These methods confirmed the formation of monoesters and the accurate esterification positions, which were reported for the first time in levoglucosan esters.

The continuous flow synthesis of CFAEs was successfully optimized using Design of Experiments (DoE), leading to substantial improvements in both productivity and regioselectivity, particularly in the case of C4-OH, when compared to the batch process. Additionally, the recycling of immobilized biocatalysts showcased the system's robust stability.

A preliminary analysis the variability in the alkyl chain length of CFAEs suggest a significant impact on both their interfacial and antibacterial properties. Out of the CFAEs tested with differing alkyl chain lengths, MONLAU (C12) exhibited the highest antibacterial activity and MONPAL (C16) presented favourable surfactant properties at various monoester concentrations, not previously documented in the literature. This research will aid in the structured investigation of how the hydrophobic segment influences the functional characteristics of amphiphilic compounds.

Future perspectives

- ✚ To separate levoglucosan monoesters from positions C2 and C4, followed by their application in tests to evaluate surfactant properties and biological activity.
- ✚ To synthesize the short-chain levoglucosan esters in a continuous flow system and subsequently apply them in biological activity assessments.
- ✚ To investigate regioselectivity in the synthesis of short-chain levoglucosan esters in continuous flow.
- ✚ To carry out the production of levoglucosan esters in the presence of Cyrene as a solvent in a continuous flow system.

REFERENCE

- Aguillón, A. R., Avelar, M. N., Gotardo, L. E., de Souza, S. P., Leão, R. A. C., Itabaiana, I., Miranda, L. S. M., & de Souza, R. O. M. A. (2019). Immobilized lipase screening towards continuous-flow kinetic resolution of (\pm)-1,2-propanediol. *Molecular Catalysis*, *467*(January), 128–134. <https://doi.org/10.1016/j.mcat.2019.01.034>
- Algammal, A. M., Hetta, H. F., Elkelish, A., Alkhalifah, D. H. H., Hozzein, W. N., Batiha, G. E. S., Nahhas, N. El, & Mabrok, M. A. (2020). Methicillin-resistant staphylococcus aureus (MRSA): One health perspective approach to the bacterium epidemiology, virulence factors, antibiotic-resistance, and zoonotic impact. *Infection and Drug Resistance*, *13*, 3255–3265. <https://doi.org/10.2147/IDR.S272733>
- Aljawish, A., Heuson, E., Bigan, M., & Froidevaux, R. (2019). Lipase catalyzed esterification of formic acid in solvent and solvent-free systems. *Biocatalysis and Agricultural Biotechnology*, *20*(June). <https://doi.org/10.1016/j.bcab.2019.101221>
- Andrés, J., Vargas, M., Orduña, J., Bernardo, M., Metzker, G., Gomes, E., Boscolo, M., Paulo, S., Sciences, E., & Jose, S. (2020). A new synthetic methodology for pyridinic sucrose esters and their antibacterial effects against Gram -positive and Gram -negative strains. *Carbohydrate Research*, *489*(September 2019), 107957. <https://doi.org/10.1016/j.carres.2020.107957>
- Ang Zhang, L., Urbano, A., Clermont, G., Swigon, D., Banerjee, I., & Parker, R. S. (2018). APT-MCMC, a C++/Python implementation of Markov Chain Monte Carlo for parameter identification HHS Public Access. *Comput Chem Eng*, *110*, 1–12. <https://doi.org/10.1016/j.jcompchemeng>
- Angajala, G., Pavan, P., & Subashini, R. (2016). Lipases: An overview of its current challenges and prospectives in the revolution of biocatalysis. In *Biocatalysis and Agricultural Biotechnology* (Vol. 7). <https://doi.org/10.1016/j.bcab.2016.07.001>
- Arashiro, E. Y., & Demarquette, N. R. (1999). Use of the pendant drop method to measure interfacial tension between molten polymers. *Materials Research*, *2*(1), 23–32. <https://doi.org/10.1590/S1516-14391999000100005>
- Arcens, D., Grau, E., Grelier, S., Cramail, H., & Peruch, F. (2020). Impact of Fatty Acid Structure on CALB-Catalyzed Esterification of Glucose. *European Journal of Lipid Science and Technology*, *122*(4), 1900294. <https://doi.org/10.1002/ejlt.201900294>
- Aziz, T., Farid, A., Haq, F., Kiran, M., Ullah, A., Zhang, K., Li, C., Ghazanfar, S., Sun, H., Ullah, R., Ali, A., Muzammal, M., Shah, M., Akhtar, N., Selim, S., Hagagy, N., Samy, M., & Al Jaouni, S. K. (2022). A Review on the Modification of Cellulose and Its Applications. In *Polymers* (Vol. 14, Issue 15). MDPI. <https://doi.org/10.3390/polym14153206>
- Babaki, M., Yousefi, M., Habibi, Z., Brask, J., & Mohammadi, M. (2015). Preparation of highly reusable biocatalysts by immobilization of lipases on epoxy-functionalized silica for production of biodiesel from canola oil. *Biochemical Engineering Journal*, *101*, 23–31. <https://doi.org/10.1016/j.bej.2015.04.020>

- Bacik, J. P., Whitworth, G. E., Stubbs, K. A., Yadav, A. K., Martin, D. R., Bailey-Elkin, B. A., Vocadlo, D. J., & Mark, B. L. (2011). Molecular basis of 1,6-anhydro bond cleavage and phosphoryl transfer by *Pseudomonas aeruginosa* 1,6-anhydro-N-acetylmuramic acid kinase. *Journal of Biological Chemistry*, 286(14), 12283–12291. <https://doi.org/10.1074/jbc.M110.198317>
- Banu J, R., Sugitha, S., Kavitha, S., Kannah R, Y., Merrylin, J., & Kumar, G. (2021). Lignocellulosic Biomass Pretreatment for Enhanced Bioenergy Recovery: Effect of Lignocelluloses Recalcitrance and Enhancement Strategies. *Frontiers in Energy Research*, 9(November), 1–17. <https://doi.org/10.3389/fenrg.2021.646057>
- BARROS NETO, B., SCARMINIO, I. S., & BRUNS, R. E. (2010). *Como Fazer Experimentos - 4.ed.: Pesquisa e Desenvolvimento na Ciência e na Indústria. 2010.* (2010 Grupo A - Bookman, Ed.).
- Bassut, J., Nasr, K., Stoclet, G., Bria, M., Raquez, J. M., Favrelle-Huret, A., Wojcieszak, R., Zinck, P., & Itabaiana, I. (2022). Lipase-Catalyzed Synthesis of Biobased Polyesters Containing Levoglucosan Units. *ACS Sustainable Chemistry and Engineering*, 10(50), 16845–16852. <https://doi.org/10.1021/acssuschemeng.2c05258>
- Bastida, A., Sabuquillo, P., Armisen, P., Fernández-Lafuente, R., Huguet, J., & Guisán, J. M. (1998). A single step purification, immobilization, and hyperactivation of lipases via interfacial adsorption on strongly hydrophobic supports. *Biotechnology and Bioengineering*, 58(5), 486–493. [https://doi.org/10.1002/\(SICI\)1097-0290\(19980605\)58:5<486::AID-BIT4>3.0.CO;2-9](https://doi.org/10.1002/(SICI)1097-0290(19980605)58:5<486::AID-BIT4>3.0.CO;2-9)
- Bayne, L., Ulijn, R. V., & Halling, P. J. (2013). Effect of pore size on the performance of immobilised enzymes. In *Chemical Society Reviews* (Vol. 42, Issue 23, pp. 9000–9010). Royal Society of Chemistry. <https://doi.org/10.1039/c3cs60270b>
- Berry, J. D., Neeson, M. J., Dagastine, R. R., Chan, D. Y. C., & Tabor, R. F. (2015). Measurement of surface and interfacial tension using pendant drop tensiometry Joseph. *JOURNAL OF COLLOID AND INTERFACE SCIENCE*, 454, 226–237. <https://doi.org/10.1016/j.jcis.2015.05.012>
- Bershtein, S., Segal, M., Bekerman, R., Tokuriki, N., & Tawfik, D. S. (2006). Robustness-epistasis link shapes the fitness landscape of a randomly drifting protein. *Nature*, 444(7121), 929–932. <https://doi.org/10.1038/nature05385>
- Besharati Vineh, M., Saboury, A. A., Poostchi, A. A., Rashidi, A. M., & Parivar, K. (2018). Stability and activity improvement of horseradish peroxidase by covalent immobilization on functionalized reduced graphene oxide and biodegradation of high phenol concentration. *International Journal of Biological Macromolecules*, 106, 1314–1322. <https://doi.org/10.1016/j.ijbiomac.2017.08.133>
- Bilal, M., Zhao, Y., Rasheed, T., & Iqbal, H. M. N. (2018). Magnetic nanoparticles as versatile carriers for enzymes immobilization: A review. *International Journal of Biological Macromolecules*, 120, 2530–2544. <https://doi.org/10.1016/j.ijbiomac.2018.09.025>
- Bisswanger, H. (2017). *Enzyme Kinetics* (WILEY-VCH, Ed.; Third, enl).

- Bloemendal, V. R. L. J., Janssen, M. A. C. H., Van Hest, J. C. M., & Rutjes, F. P. J. T. (2020). Continuous one-flow multi-step synthesis of active pharmaceutical ingredients. *Reaction Chemistry and Engineering*, 5(7), 1186–1197. <https://doi.org/10.1039/d0re00087f>
- Bloom, J. D., Labthavikul, S. T., Otey, C. R., & Arnold, F. H. (2006). Protein stability promotes evolvability. *Proceedings of the National Academy of Sciences*, 103(15), 5869–5874. <https://doi.org/10.1073/pnas.0510098103>
- Boissière-Junot, N., Tellier, C., & Rabiller, C. (1998). On the Regioselective Acylation of 1,6-Anhydro- β -d- and l-Hexopyranoses Catalysed by Lipases: Structural Basis and Synthetic Applications. *Journal of Carbohydrate Chemistry*, 17(1), 99–115. <https://doi.org/10.1080/07328309808005771>
- Bolivar, J. M., Wiesbauer, J., & Nidetzky, B. (2011). Biotransformations in microstructured reactors: More than flowing with the stream? *Trends in Biotechnology*, 29(7), 333–342. <https://doi.org/10.1016/j.tibtech.2011.03.005>
- Bornscheuer, U. T., & Kazlauskas, R. J. (2005). Hydrolases in Organic Synthesis. In *Hydrolases in Organic Synthesis: Regio- and Stereoselective Biotransformations: Second Edition*. Wiley. <https://doi.org/10.1002/3527607544>
- Boutin, O., Ferrer, M., & Lédé, J. (1998). Radiant flash pyrolysis of cellulose—Evidence for the formation of short life time intermediate liquid species. *Journal of Analytical and Applied Pyrolysis*, 47(1), 13–31. [https://doi.org/10.1016/S0165-2370\(98\)00088-6](https://doi.org/10.1016/S0165-2370(98)00088-6)
- Brady, D., & Jordaan, J. (2009). Advances in enzyme immobilisation. In *Biotechnology Letters* (Vol. 31, Issue 11, pp. 1639–1650). <https://doi.org/10.1007/s10529-009-0076-4>
- Britton, J., Majumdar, S., & Weiss, G. A. (2018). Continuous flow biocatalysis. *Chemical Society Reviews*, 47(15), 5891–5918. <https://doi.org/10.1039/c7cs00906b>
- Buendia-Kandia, F., Greenhalf, C., Barbiero, C., Guedon, E., Briens, C., Berruti, F., & Dufour, A. (2020). Fermentation of cellulose pyrolysis oil by a Clostridial bacterium. *Biomass and Bioenergy*, 143, 105884. <https://doi.org/10.1016/j.biombioe.2020.105884>
- Campuzano, F., Brown, R. C., & Martínez, J. D. (2019). Auger reactors for pyrolysis of biomass and wastes. *Renewable and Sustainable Energy Reviews*, 102(December 2018), 372–409. <https://doi.org/10.1016/j.rser.2018.12.014>
- Capello, C., Fischer, U., & Hungerbühler, K. (2007). What is a green solvent? A comprehensive framework for the environmental assessment of solvents. *Green Chemistry*, 9(9), 927–993. <https://doi.org/10.1039/b617536h>
- Carvalho, F., Duarte, L. C., & Gírio, F. M. (2008). Hemicellulose biorefineries: a review on biomass pretreatments. In *Journal of Scientific & Industrial Research* (Vol. 67). <https://repositorio.ineg.pt/handle/10400.9/791>
- Cen, Y., Singh, W., Arkin, M., Moody, T. S., Huang, M., Zhou, J., Wu, Q., & Reetz, M. T. (2019). Artificial cysteine-lipases with high activity and altered catalytic mechanism created by laboratory evolution. *Nature Communications*, 10(1). <https://doi.org/10.1038/s41467-019-11155-3>

- Chandel, A. K., Garlapati, V. K., Singh, A. K., Antunes, F. A. F., & da Silva, S. S. (2018). The path forward for lignocellulose biorefineries: Bottlenecks, solutions, and perspective on commercialization. In *Bioresource Technology* (Vol. 264, pp. 370–381). Elsevier Ltd. <https://doi.org/10.1016/j.biortech.2018.06.004>
- Chandra, P., Enespa, Singh, R., & Arora, P. K. (2020). Microbial lipases and their industrial applications: A comprehensive review. In *Microbial Cell Factories* (Vol. 19, Issue 1). BioMed Central Ltd. <https://doi.org/10.1186/s12934-020-01428-8>
- Chang, D., Wang, C., Ul Islam, Z., & Yu, Z. (2022). Omics analysis coupled with gene editing revealed potential transporters and regulators related to levoglucosan metabolism efficiency of the engineered *Escherichia coli*. *Biotechnology for Biofuels and Bioproducts*, 15(1). <https://doi.org/10.1186/s13068-022-02102-4>
- Chang, S. W., Lee, G. C., & Shaw, J. F. (2006). Codon optimization of *Candida rugosa* lip1 gene for improving expression in *Pichia pastoris* and biochemical characterization of the purified recombinant LIP1 lipase. *Journal of Agricultural and Food Chemistry*, 54(3), 815–822. <https://doi.org/10.1175/JAS3661.1>
- Chang, S. W., & Shaw, J. F. (2009). Biocatalysis for the production of carbohydrate esters. *New Biotechnology*, 26(3–4), 109–116. <https://doi.org/10.1016/j.nbt.2009.07.003>
- Chapman, M. R., Cosgrove, S. C., Turner, N. J., Kapur, N., & Blacker, A. J. (2018). Highly Productive Oxidative Biocatalysis in Continuous Flow by Enhancing the Aqueous Equilibrium Solubility of Oxygen. *Angewandte Chemie - International Edition*, 57(33), 10535–10539. <https://doi.org/10.1002/anie.201803675>
- Chattopadhyay, G., & Varadarajan, R. (2019). Facile measurement of protein stability and folding kinetics using a nano differential scanning fluorimeter. *Protein Science*, 28(6), 1127–1134. <https://doi.org/10.1002/pro.3622>
- Chen, D., Li, J., Zhang, T., Li, S., Wang, J., Niu, W., Liu, Y., Zheng, A., & Zhao, Z. (2022). Advancing biomass pyrolysis by torrefaction pretreatment: Linking the productions of bio-oil and oxygenated chemicals to torrefaction severity. *Fuel*, 330. <https://doi.org/10.1016/j.fuel.2022.125514>
- Chulalaksananukul, W., Condoret, J. S., Delorme, P., & Willemot, R. M. (1990). Kinetic study of esterification by immobilized lipase in n-hexane. *FEBS Letters*, 276(1–2), 181–184. [https://doi.org/10.1016/0014-5793\(90\)80537-S](https://doi.org/10.1016/0014-5793(90)80537-S)
- Cipolatti, E. P., Valério, A., Henriques, R. O., Moritz, D. E., Ninow, J. L., Freire, D. M. G., Manoel, E. A., Fernandez-Lafuente, R., & De Oliveira, D. (2016). Nanomaterials for biocatalyst immobilization-state of the art and future trends. *RSC Advances*, 6(106), 104675–104692. <https://doi.org/10.1039/c6ra22047a>
- Cleland, W. W. (n.d.). *THE KINETICS OF ENZYME-CATALYZED REACTIONS WITH TWO OR MORE SUBSTRATES OR PRODUCTS II. INHIBITION: NOMENCLATURE AND THEORY*.
- Climent, M. J., Corma, A., & Iborra, S. (2011). Converting carbohydrates to bulk chemicals and fine chemicals over heterogeneous catalysts. *Green Chemistry*, 13(3), 520–540. <https://doi.org/10.1039/c0gc00639d>

- CLSI. (2015). Performance Standards for Antimicrobial Susceptibility Testing; Twenty-Second Informational Supplement Clinical and Laboratory Standards Institute. In *CLSI document M100-S16CLSI, Wayne, PA* (Vol. 32, Issue 1).
- Comba, M. B., Tsai, Y. H., Sarotti, A. M., Mangione, M. I., Suárez, A. G., & Spanevello, R. A. (2018). Levoglucosenone and Its New Applications: Valorization of Cellulose Residues. In *European Journal of Organic Chemistry* (Vol. 2018, Issue 5, pp. 590–604). Wiley-VCH Verlag. <https://doi.org/10.1002/ejoc.201701227>
- Cossy, J. R. (2012). 1.1 Introduction: The Importance of Chirality in Drugs and Agrochemicals. In *Comprehensive Chirality* (Vol. 1, pp. 1–7). Elsevier Ltd. <https://doi.org/10.1016/B978-0-08-095167-6.00101-4>
- Da Silva, A. P. T., Bredda, E. H., de Castro, H. F., & Da Rós, P. C. M. (2020). Enzymatic catalysis: An environmentally friendly method to enhance the transesterification of microalgal oil with fusel oil for production of fatty acid esters with potential application as biolubricants. *Fuel*, 273. <https://doi.org/10.1016/j.fuel.2020.117786>
- Dahmen, N., Lewandowski, I., Zibek, S., & Weidtmann, A. (2019). Integrated lignocellulosic value chains in a growing bioeconomy: Status quo and perspectives. *GCB Bioenergy*, 11(1), 107–117. <https://doi.org/10.1111/gcbb.12586>
- Datta, S., Christena, L. R., & Rajaram, Y. R. S. (2013). Enzyme immobilization: an overview on techniques and support materials. *3 Biotech*, 3(1), 1–9. <https://doi.org/10.1007/s13205-012-0071-7>
- DAVIES, J. T. (1957). A Quantitative kinetic theory of emulsion type I. Physical chemistry of the emulsifying agent. In 1957. London: Butterworths (Ed.), *Proceedings of the Second International Congress of Surface Activity* (pp. 426–438).
- de Barros, D. P. C., Fonseca, L. P., Fernandes, P., Cabral, J. M. S., & Mojovic, L. (2009). Biosynthesis of ethyl caproate and other short ethyl esters catalyzed by cutinase in organic solvent. *Journal of Molecular Catalysis B: Enzymatic*, 60(3–4), 178–185. <https://doi.org/10.1016/j.molcatb.2009.05.004>
- De Bruyn, M., Budarin, V. L., Misefari, A., Shimizu, S., Fish, H., Cockett, M., Hunt, A. J., Hofstetter, H., Weckhuysen, B. M., Clark, J. H., & Macquarrie, D. J. (2019). Geminal Diol of Dihydrolevoglucosenone as a Switchable Hydrotrope: A Continuum of Green Nanostructured Solvents. *ACS Sustainable Chemistry and Engineering*, 7(8), 7878–7883. <https://doi.org/10.1021/acssuschemeng.9b00470>
- De Jenga, C. I., Antal, M. J., & Jones, M. (1982). Yields and composition of sirups resulting from the flash pyrolysis of cellulosic materials using radiant energy. *Journal of Applied Polymer Science*, 27(11), 4313–4322. <https://doi.org/10.1002/app.1982.070271121>
- de María, P. D., de Gonzalo, G., & Alcántara, A. R. (2019). Biocatalysis as useful tool in asymmetric synthesis: An assessment of recently granted patents(2014-2019). In *Catalysts* (Vol. 9, Issue 10). MDPI. <https://doi.org/10.3390/catal9100802>
- de Souza, S. P., de Almeida, R. A. D., Garcia, G. G., Leão, R. A. C., Bassut, J., de Souza, R. O. M. A., Itabaiana, I., Souza, S. P. de Almeida, R. A. D. de Garcia, G. G., Leão, R. A. C., Bassut, J., Souza, R. O. M. A. de, & Jr, and I. I. (2017). Immobilization of lipase B from

- Candida antarctica* on epoxy-functionalized silica: Characterization and improving biocatalytic parameters. *Journal of Chemical Technology and Biotechnology*, 93(January), 105–111. <https://doi.org/10.1002/jctb.5327>
- Desvaux, M., Guedon, E., & Petitdemange, H. (2001). Kinetics and Metabolism of Cellulose Degradation at High Substrate Concentrations in Steady-State Continuous Cultures of *Clostridium cellulolyticum* on a Chemically Defined Medium. *Applied and Environmental Microbiology*, 67(9), 3837–3845. <https://doi.org/10.1128/AEM.67.9.3837-3845.2001>
- do Nascimento, M. A., Gotardo, L. E., Bastos, E. M., Almeida, F. C. L., Leão, R. A. C., de Souza, R. O. M. A., Wojcieszak, R., & Itabaiana, I. (2019). Regioselective acylation of levoglucosan Catalyzed by *Candida Antarctica* (CaLB) lipase immobilized on epoxy resin. *Sustainability (Switzerland)*, 11(21), 1–15. <https://doi.org/10.3390/su11216044>
- Do Nascimento, M. A., Gotardo, L. E., Leão, R. A. C., De Castro, A. M., De Souza, R. O. M. A., & Itabaiana, I. (2019). Enhanced Productivity in Glycerol Carbonate Synthesis under Continuous Flow Conditions: Combination of Immobilized Lipases from Porcine Pancreas and *Candida antarctica* (CALB) on Epoxy Resins. *ACS Omega*, 4(1), 860–869. <https://doi.org/10.1021/acsomega.8b02420>
- do Nascimento, M. A., Leão, R. A. C., Froidevaux, R., Wojcieszak, R., de Souza, R. O. M. A., & Itabaiana, I. (2023). A new approach for the direct acylation of bio-oil enriched with levoglucosan: Kinetic study and lipase thermostability. *Biochemical Engineering Journal*, 195. <https://doi.org/10.1016/j.bej.2023.108915>
- Do Nascimento, M. A., Vargas, J. P. C., Rodrigues, J. G. A., Leão, R. A. C., De Moura, P. H. B., Leal, I. C. R., Bassut, J., De Souza, R. O. M. A., Wojcieszak, R., & Itabaiana, I. (2022). Lipase-catalyzed acylation of levoglucosan in continuous flow: Antibacterial and biosurfactant studies. *RSC Advances*, 12(5), 3027–3035. <https://doi.org/10.1039/d1ra08111j>
- Do Nascimento, M. A., Vargas, J. P. C., Rodrigues, J. G. A., Leão, R. A. C., De Moura, P. H. B., Leal, I. C. R., Bassut, J., De Souza, R. O. M. A., Wojcieszak, R., Itabaiana, I., Nascimento, M. A. do, Vargas, J. P. C., Rodrigues, J. G. A., Leão, R. A. C., Moura, P. H. B. de, Leal, I. C. R., Bassut, J., Souza, R. O. M. A., Wojcieszake, R., ... E. (2022). Lipase-catalyzed acylation of levoglucosan in continuous flow: Antibacterial and biosurfactant studies. *RSC Advances*, 12(5), 3027–3035. <https://doi.org/10.1039/d1ra08111j>
- dos Santos, P. M., Baruque, J. R., de Souza Lira, R. K., Leite, S. G. F., do Nascimento, R. P., Borges, C. P., Wojcieszak, R., & Itabaiana, I. (2022). Corn Cob as a Green Support for Laccase Immobilization—Application on Decolorization of Remazol Brilliant Blue R. *International Journal of Molecular Sciences*, 23(16). <https://doi.org/10.3390/ijms23169363>
- Du Le, H., Loveday, S. M., Singh, H., & Sarkar, A. (2020). Pickering emulsions stabilised by hydrophobically modified cellulose nanocrystals: Responsiveness to pH and ionic strength. *Food Hydrocolloids*, 99. <https://doi.org/10.1016/j.foodhyd.2019.105344>
- Dufour, A., Quartassi, B., Bounaceur, R., & Zoulalian, A. (2011). Modelling intra-particle phenomena of biomass pyrolysis. *Chemical Engineering Research and Design*, 89(10), 2136–2146. <https://doi.org/10.1016/j.cherd.2011.01.005>

- El-Baz, H. A., Elazzazy, A. M., Saleh, T. S., Dourou, M., Mahyoub, J. A., Baeshen, M. N., Madian, H. R., & Aggelis, G. (2021). Enzymatic synthesis of glucose fatty acid esters using scos as acyl group-donors and their biological activities. *Applied Sciences (Switzerland)*, *11*(6). <https://doi.org/10.3390/app11062700>
- El-laithy, H. M., Shoukry, O., & Mahran, L. G. (2011). Novel sugar esters proniosomes for transdermal delivery of vinpocetine: Preclinical and clinical studies. *European Journal of Pharmaceutics and Biopharmaceutics*, *77*(1), 43–55. <https://doi.org/10.1016/j.ejpb.2010.10.011>
- Enaime, G., Baçaoui, A., Yaacoubi, A., & Lübken, M. (2020). Biochar for wastewater treatment-conversion technologies and applications. In *Applied Sciences (Switzerland)* (Vol. 10, Issue 10). MDPI AG. <https://doi.org/10.3390/app10103492>
- Ezeji, T., Qureshi, N., & Blaschek, H. P. (2007). Comparison of Two-Phase Lipase-Catalyzed Esterification on Micro and Bench Scale. *Bioresource and Bioengineering*, *97*(6), 1460–1469. <https://doi.org/10.1002/bit>
- Fang, W., & Riisager, A. (2021). Recent advances in heterogeneous catalytic transfer hydrogenation/hydrogenolysis for valorization of biomass-derived furanic compounds. *Green Chemistry*, *23*(2), 670–688. <https://doi.org/10.1039/d0gc03931d>
- Felipe, B.-K., Greenhalf, C., Barbiero, C., Guédon, E., Briens, C., Dufour, A., Berruti, F., Fer-, al, Buendia-Kandia, F., Greenhalf, C., Barbiero, C., Guedon, E., Briens, C., Berruti, F., & Dufour, A. (n.d.). *Fermentation of cellulose pyrolysis oil by a Clostridial bacterium*. <https://doi.org/10.1016/j.biombioe.2020.105884i>
- Fernandez-Lafuente, R., Armisén, P., Sabuquillo, P., Fernández-Lorente, G., & Guisán, J. M. (1998). Immobilization of lipases by selective adsorption on hydrophobic supports. *Chemistry and Physics of Lipids*, *93*(1–2), 185–197. [https://doi.org/10.1016/S0009-3084\(98\)00042-5](https://doi.org/10.1016/S0009-3084(98)00042-5)
- Fernández-Lorente, G., Terreni, M., Mateo, C., Bastida, A., Fernández-Lafuente, R., Dalmases, P., Huguet, J., & Guisán, J. M. (2001). Modulation of lipase properties in macro-aqueous systems by controlled enzyme immobilization: enantioselective hydrolysis of a chiral ester by immobilized Pseudomonas lipase. *Enzyme and Microbial Technology*, *28*(4–5), 389–396. [https://doi.org/10.1016/S0141-0229\(00\)00324-0](https://doi.org/10.1016/S0141-0229(00)00324-0)
- Fitzpatrick, D. E., & Ley, S. V. (2016). Engineering chemistry: Integrating batch and flow reactions on a single, automated reactor platform. *Reaction Chemistry and Engineering*, *1*(6), 629–635. <https://doi.org/10.1039/c6re00160b>
- Frederick, W. J., Lien, S. J., Courchene, C. E., DeMartini, N. A., Ragauskas, A. J., & lisa, K. (2008). Co-production of ethanol and cellulose fiber from Southern Pine: A technical and economic assessment. *Biomass and Bioenergy*, *32*(12), 1293–1302. <https://doi.org/10.1016/j.biombioe.2008.03.010>
- Galletti, P., Moretti, F., Samori, C., & Tagliavini, E. (2007). Enzymatic acylation of levoglucosan in acetonitrile and ionic liquids. *Green Chemistry*, *9*(9), 987–991. <https://doi.org/10.1039/b702031g>

- Gamayurova, V. S., Zinov'eva, M. E., Shnaider, K. L., & Davletshina, G. A. (2021). Lipases in Esterification Reactions: A Review. *Catalysis in Industry*, 13(1), 58–72. <https://doi.org/10.1134/S2070050421010025>
- Garcia, T., Sanchez, N., Martinez, M., & Aracil, J. (1999). Enzymatic synthesis of fatty esters. *Enzyme and Microbial Technology*, 25(7), 591–597. [https://doi.org/10.1016/S0141-0229\(99\)00083-6](https://doi.org/10.1016/S0141-0229(99)00083-6)
- Gasparetto, H., de Castilhos, F., & Paula Gonçalves Salau, N. (2022). Recent advances in green soybean oil extraction: A review. In *Journal of Molecular Liquids* (Vol. 361). Elsevier B.V. <https://doi.org/10.1016/j.molliq.2022.119684>
- Gorman, L. A. S., & Dordick, J. S. (1992). Organic solvents strip water off enzymes. *Biotechnology and Bioengineering*, 39(4), 392–397. <https://doi.org/10.1002/bit.260390405>
- Gotor-Fernández, V., Brieva, R., & Gotor, V. (2006). Lipases: Useful biocatalysts for the preparation of pharmaceuticals. *Journal of Molecular Catalysis B: Enzymatic*, 40(3–4), 111–120. <https://doi.org/10.1016/j.molcatb.2006.02.010>
- Guajardo, N., Schrebler, R. A., & Domínguez de María, P. (2019). From batch to fed-batch and to continuous packed-bed reactors: Lipase-catalyzed esterifications in low viscous deep-eutectic-solvents with buffer as cosolvent. *Bioresource Technology*, 320–325. <https://doi.org/10.1016/j.biortech.2018.11.026>
- Guidi, M., Seeberger, P. H., & Gilmore, K. (2020). How to approach flow chemistry. *Chemical Society Reviews*, 49(24), 8910–8932. <https://doi.org/10.1039/c9cs00832b>
- Guleria, A., Kumari, G., & Saravanamurugan, S. (2019). Cellulose valorization to potential platform chemicals. In *Biomass, Biofuels, Biochemicals: Recent Advances in Development of Platform Chemicals* (pp. 433–457). Elsevier Inc. <https://doi.org/10.1016/B978-0-444-64307-0.00017-2>
- Haq, I., Qaisar, K., Nawaz, A., Akram, F., Mukhtar, H., Zohu, X., Xu, Y., Mumtaz, M. W., Rashid, U., Azlina, W., Ab, W., Ghani, K., Shean, T., & Choong, Y. (2021). *Advances in Valorization of Lignocellulosic Biomass towards Energy Generation*. 1–25.
- Hari Krishna, S., & Karanth, N. G. (2002). Lipases and lipase-catalyzed esterification reactions in nonaqueous media. In *Catalysis Reviews - Science and Engineering* (Vol. 44, Issue 4, pp. 499–591). <https://doi.org/10.1081/CR-120015481>
- Hasanin, M. S., Mostafa, A. M., Mwafy, E. A., & Darwesh, O. M. (2018). Eco-friendly cellulose nano fibers via first reported Egyptian *Humicola fuscoatra* Egyptia X4: Isolation and characterization. *Environmental Nanotechnology, Monitoring and Management*, 10, 409–418. <https://doi.org/10.1016/j.enmm.2018.10.004>
- He, B., Tang, F., Sun, C., Su, J., Wu, B., Chen, Y., Xiao, Y., Zhang, P., & Tang, K. (2022). Resolution of (R,S)-1-(4-methoxyphenyl)ethanol by lipase-catalyzed stereoselective transesterification and the process optimization. *Chirality*, 34(2), 438–445. <https://doi.org/10.1002/chir.23402>
- Hirata, D. B., Albuquerque, T. L., Rueda, N., Virgen-Ortíz, J. J., Tacias-Pascacio, V. G., & Fernandez-Lafuente, R. (2016). Evaluation of different immobilized lipases in

- transesterification reactions using tributyrin: Advantages of the heterofunctional octyl agarose beads. *Journal of Molecular Catalysis B: Enzymatic*, 133, 117–123. <https://doi.org/10.1016/j.molcatb.2016.08.008>
- Holmstrøm, T., & Pedersen, C. M. (2020). Enzyme-Catalyzed Regioselective Acetylation of Functionalized Glycosides. *European Journal of Organic Chemistry*, 2020(29), 4612–4615. <https://doi.org/10.1002/ejoc.202000696>
- Homaei, A. A., Sariri, R., Vianello, F., & Stevanato, R. (2013). Enzyme immobilization: An update. *Journal of Chemical Biology*, 6(4), 185–205. <https://doi.org/10.1007/s12154-013-0102-9>
- Howden, B. P., Giulieri, S. G., Wong Fok Lung, T., Baines, S. L., Sharkey, L. K., Lee, J. Y. H., Hachani, A., Monk, I. R., & Stinear, T. P. (2023). Staphylococcus aureus host interactions and adaptation. In *Nature Reviews Microbiology* (Vol. 21, Issue 6, pp. 380–395). Nature Research. <https://doi.org/10.1038/s41579-023-00852-y>
- Hu, X., Wu, L., Wang, Y., Mourant, D., Lievens, C., Gunawan, R., & Li, C. Z. (2012). Mediating acid-catalyzed conversion of levoglucosan into platform chemicals with various solvents. *Green Chemistry*, 14(11), 3087–3098. <https://doi.org/10.1039/c2gc35961h>
- Hunter, B. K., Hall, L. D., & Sanders, J. K. M. (n.d.). *The Conformation of Vinblastine in Solution as Determined by N.O.E. Difference Spectroscopy*.
- Hunter, B. K., Hall, L. D., & Sanders, J. K. M. (1983). The conformation of vinblastine in solution as determined by n.o.e. difference spectroscopy. *Journal of the Chemical Society, Perkin Transactions 1*, 657. <https://doi.org/10.1039/p19830000657>
- Innovating for A Bioeconomy for Europe Sustainable Growth*. (n.d.).
- Isenberg, H. D. (1988). Antimicrobial susceptibility testing: A critical evaluation. *Journal of Antimicrobial Chemotherapy*, 22(SUPPL. A), 73–86. https://doi.org/10.1093/jac/22.supplement_a.73
- Itabaiana, I., Gonçalves, K. M., Cordeiro, Y. M. L., Zoumpantioti, M., Leal, I. C. R., Miranda, L. S. M., De Souza, R. O. M. A., & Xenakis, A. (2013). Kinetics and mechanism of lipase catalyzed monoacylglycerols synthesis. *Journal of Molecular Catalysis B: Enzymatic*, 96, 34–39. <https://doi.org/10.1016/j.molcatb.2013.06.008>
- Itabaiana Junior, I., Avelar Do Nascimento, M., De Souza, R. O. M. A., Dufour, A., & Wojcieszak, R. (2020a). Levoglucosan: A promising platform molecule? In *Green Chemistry* (Vol. 22, Issue 18, pp. 5859–5880). Royal Society of Chemistry. <https://doi.org/10.1039/d0gc01490g>
- Itabaiana Junior, I., Avelar Do Nascimento, M., De Souza, R. O. M. A., Dufour, A., & Wojcieszak, R. (2020b). Levoglucosan: A promising platform molecule? *Green Chemistry*, 22(18), 5859–5880. <https://doi.org/10.1039/d0gc01490g>
- J.D. Monk, Hathcox, A. K., & Beuchat, L. R. (1996). Inhibitory effects of sucrose monolaurate, alone and in combination with organic acids, on *Listeria monocytogenes* and *Staphylococcus aureus*. *Food Microbiology*, 13(3), 213–225. <https://doi.org/10.1111/j.1365-2672.1996.tb03276.x>

- Jesionowski, T., Zdarta, J., & Krajewska, B. (2014). Enzyme immobilization by adsorption: A review. In *Adsorption* (Vol. 20, Issues 5–6, pp. 801–821). Kluwer Academic Publishers. <https://doi.org/10.1007/s10450-014-9623-y>
- Johan Rockström and colleagues. (2009). A safe operating space for humanity. *Nature*, *461*, 472–475. <https://www.nature.com/articles/461472a>
- Jude A. Okoliea; Emmanuel I., & Meshach E. Tabatc, Uzezi Orivrid, Andrew Nosakhare Amenaghawone, Patrick U. Okoyef, Burcu Gunesg,*uel I. Epelleb, Meshach E. Tabatc, Uzezi Orivrid, Andrew Nosakhare Amenaghawone, Patrick U. Okoye, *. (2022). Waste biomass valorization for the production of biofuels and value- added products: A comprehensive review of thermochemical, biological and integrated processes. *Process Safety and Environmental Protection*, *159*, 323–344. <https://doi.org/10.1016/j.psep.2021.12.049>
- Junior, I. I., Flores, M. C., Sutili, F. K., Leite, S. G. F., Leandro, L. S., Leal, I. C. R., & De Souza, R. O. M. A. (2012). Lipase-catalyzed monostearin synthesis under continuous flow conditions. *Organic Process Research and Development*, *16*(5), 1098–1101. <https://doi.org/10.1021/op200132y>
- Kamińska, E., Madejczyk, O., Tarnacka, M., Jurkiewicz, K., Wolnica, K., Śmiszek-Lindert, W. E., Kamiński, K., & Paluch, M. (2018). Anhydrosaccharides - A new class of the fragile plastic crystals. *Journal of Chemical Physics*, *148*(7). <https://doi.org/10.1063/1.5011672>
- Kennedy, J. F., Kumar, H., Panesar, P. S., Marwaha, S. S., Goyal, R., Parmar, A., & Kaur, S. (2006). Enzyme-catalyzed regioselective synthesis of sugar esters and related compounds. In *Journal of Chemical Technology and Biotechnology* (Vol. 81, Issue 6, pp. 866–876). <https://doi.org/10.1002/jctb.1473>
- Khmelnitsky, Yu. L., Levashov, A. V., Klyachko, N. L., & Martinek, K. (1988). Engineering biocatalytic systems in organic media with low water content. *Enzyme and Microbial Technology*, *10*(12), 710–724. [https://doi.org/10.1016/0141-0229\(88\)90115-9](https://doi.org/10.1016/0141-0229(88)90115-9)
- Kim, J., Yu, H., Yang, E., Choi, Y., & Chang, P. S. (2023). Effects of alkyl chain length on the interfacial, antibacterial, and antioxidative properties of erythorbyl fatty acid esters. *LWT*, *174*. <https://doi.org/10.1016/j.lwt.2022.114421>
- Kim, J.-S., & Choi, G.-G. (2018). Pyrolysis of Lignocellulosic Biomass for Biochemical Production. In *Waste Biorefinery*. Elsevier B.V. <https://doi.org/10.1016/b978-0-444-63992-9.00011-2>
- Kim, S. H., Yoo, H. J., Park, E. J., & Na, D. H. (2022). Nano differential scanning fluorimetry-based thermal stability screening and optimal buffer selection for immunoglobulin G. *Pharmaceuticals*, *15*(1). <https://doi.org/10.3390/ph15010029>
- Klemm, D., Heublein, B., Fink, H. P., & Bohn, A. (2005). Cellulose: Fascinating biopolymer and sustainable raw material. In *Angewandte Chemie - International Edition* (Vol. 44, Issue 22, pp. 3358–3393). <https://doi.org/10.1002/anie.200460587>
- Könnecker, G., Regelman, J., Belanger, S., Gamon, K., & Sedlak, R. (2011). Environmental properties and aquatic hazard assessment of anionic surfactants: Physico-chemical,

- environmental fate and ecotoxicity properties. *Ecotoxicology and Environmental Safety*, 74(6), 1445–1460. <https://doi.org/10.1016/j.ecoenv.2011.04.015>
- Kotov, V., Mlynek, G., Vesper, O., Pletzer, M., Wald, J., Teixeira-Duarte, C. M., Celia, H., Garcia-Alai, M., Nussberger, S., Buchanan, S. K., Morais-Cabral, J. H., Loew, C., Djinic-Carugo, K., & Marlovits, T. C. (2021). In-depth interrogation of protein thermal unfolding data with MoltenProt. *Protein Science*, 30(1), 201–217. <https://doi.org/10.1002/pro.3986>
- Kwon, E. E., Lee, T., Ok, Y. S., Tsang, D. C. W., Park, C., & Lee, J. (2018). Effects of calcium carbonate on pyrolysis of sewage sludge. *Energy*, 153, 726–731. <https://doi.org/10.1016/j.energy.2018.04.100>
- Lachos-Perez, D., Martins-Vieira, J. C., Missau, J., Anshu, K., Siakpebru, O. K., Thengane, S. K., Morais, A. R. C., Tanabe, E. H., & Bertuol, D. A. (2023). Review on Biomass Pyrolysis with a Focus on Bio-Oil Upgrading Techniques. *Analytica*, 4(2), 182–205. <https://doi.org/10.3390/analytica4020015>
- Lahiji, S., Hemmati, R., Homaei, A., Saffar, B., & Ghorbani, M. (2021). Improved thermal stability of phytase from *Yersinia intermedia* by physical adsorption immobilization on amino-multiwalled carbon nanotubes. *Bioprocess and Biosystems Engineering*, 44(10), 2217–2228. <https://doi.org/10.1007/s00449-021-02598-4>
- Lara-Serrano, M., Sboiu, D. M., Morales-de-la-Rosa, S., & Campos-Martin, J. M. (2023). Selective Fragmentation of Lignocellulosic Biomass with ZnCl₂·4H₂O Using a Dissolution/Precipitation Method. *Applied Sciences (Switzerland)*, 13(5). <https://doi.org/10.3390/app13052953>
- Larsson, S., & Miksche, G. E. (1971). *Gaschromatographische Analyse von Ligninoxidationsprodukten* (pp. 647–662).
- Le Âde, J., Blanchard, F., & Boutin, O. (n.d.). *Radiant ash pyrolysis of cellulose pellets: products and mechanisms involved in transient and steady state conditions q*. <http://www.fuel>
- Le Brech, Y., Jia, L., Cissé, S., Mauviel, G., Brosse, N., & Dufour, A. (2016a). Mechanisms of biomass pyrolysis studied by combining a fixed bed reactor with advanced gas analysis. *Journal of Analytical and Applied Pyrolysis*, 117, 334–346. <https://doi.org/10.1016/j.jaap.2015.10.013>
- Le Brech, Y., Jia, L., Cissé, S., Mauviel, G., Brosse, N., & Dufour, A. (2016b). Mechanisms of biomass pyrolysis studied by combining a fixed bed reactor with advanced gas analysis. *Journal of Analytical and Applied Pyrolysis*, 117, 334–346. <https://doi.org/10.1016/j.jaap.2015.10.013>
- Le Brech, Y., Jia, L., Cissé, S., Mauviel, G., Brosse, N., & Dufour, A. (2016c). Mechanisms of biomass pyrolysis studied by combining a fixed bed reactor with advanced gas analysis. *Journal of Analytical and Applied Pyrolysis*, 117, 334–346. <https://doi.org/10.1016/j.jaap.2015.10.013>
- Le, Q. A. T., Joo, J. C., Yoo, Y. J., & Kim, Y. H. (2012). Development of thermostable *Candida antarctica* lipase B through novel in silico design of disulfide bridge. *Biotechnology and Bioengineering*, 109(4), 867–876. <https://doi.org/10.1002/bit.24371>

- Leal, I. C. R., Dos Santos, K. R. N., Júnior, I. I., Antunes, O. A. C., Porzel, A., Wessjohann, L., & Kuster, R. M. H. (2010). Ceanothane and lupane type triterpenes from zizyphus joazeiro an anti-staphylococcal evaluation. *Planta Medica*, 76(1), 47–52. <https://doi.org/10.1055/s-0029-1185947>
- Leão, R. A. C., De Souza, S. P., Nogueira, D. O., Silva, G. M. A., Silva, M. V. M., Gutarra, M. L. E., Miranda, L. S. M., Castro, A. M., Junior, I. I., & De Souza, R. O. M. A. (2016). Consecutive lipase immobilization and glycerol carbonate production under continuous-flow conditions. *Catalysis Science and Technology*, 6(13), 4743–4748. <https://doi.org/10.1039/c6cy00295a>
- Lédé, J. (2012). Cellulose pyrolysis kinetics: An historical review on the existence and role of intermediate active cellulose. In *Journal of Analytical and Applied Pyrolysis* (Vol. 94, pp. 17–32). Elsevier B.V. <https://doi.org/10.1016/j.jaap.2011.12.019>
- Li, G., Chen, Y., Fang, X., Su, F., Xu, L., & Yan, Y. (2018). Identification of a hot-spot to enhance: *Candida rugosa* lipase thermostability by rational design methods. *RSC Advances*, 8(4), 1948–1957. <https://doi.org/10.1039/c7ra11679a>
- Li, J., Liu, Z., Feng, C., Liu, X., Qin, F., Liang, C., Bian, H., Qin, C., & Yao, S. (2021). Green, efficient extraction of bamboo hemicellulose using freeze-thaw assisted alkali treatment. *Bioresource Technology*, 333. <https://doi.org/10.1016/j.biortech.2021.125107>
- Li, Y., Fu, T. M., Yu, J. Z., Feng, X., Zhang, L., Chen, J., Boreddy, S. K. R., Kawamura, K., Fu, P., Yang, X., Zhu, L., & Zeng, Z. (2021). Impacts of Chemical Degradation on the Global Budget of Atmospheric Levoglucosan and Its Use As a Biomass Burning Tracer. *Environmental Science and Technology*, 55(8), 5525–5536. <https://doi.org/10.1021/acs.est.0c07313>
- Liaw, S. S., Zhou, S., Wu, H., & Garcia-Perez, M. (2013). Effect of pretreatment temperature on the yield and properties of bio-oils obtained from the auger pyrolysis of Douglas fir wood. *Fuel*, 103, 672–682. <https://doi.org/10.1016/j.fuel.2012.08.016>
- Lima, R. N., dos Anjos, C. S., Orozco, E. V. M., & Porto, A. L. M. (2019). Versatility of *Candida antarctica* lipase in the amide bond formation applied in organic synthesis and biotechnological processes. In *Molecular Catalysis* (Vol. 466, pp. 75–105). Elsevier B.V. <https://doi.org/10.1016/j.mcat.2019.01.007>
- Lindeque, R. M., & Woodley, J. M. (2019). Reactor Selection for Effective Continuous Biocatalytic Production of Pharmaceuticals. *Catalysts*, 9(3), 262. <https://doi.org/10.3390/catal9030262>
- Lineweaver, H., & Burk, D. (1934). The Determination of Enzyme Dissociation Constants. *Journal of the American Chemical Society*, 56(3), 658–666. <https://doi.org/10.1021/ja01318a036>
- Linger, J. G., Hobdey, S. E., Franden, M. A., Fulk, E. M., & Beckham, G. T. (2016). Conversion of levoglucosan and cellobiosan by *Pseudomonas putida* KT2440. *Metabolic Engineering Communications*, 3, 24–29. <https://doi.org/10.1016/j.meteno.2016.01.005>
- Liu, D. M., & Dong, C. (2020a). Recent advances in nano-carrier immobilized enzymes and their applications. In *Process Biochemistry* (Vol. 92, pp. 464–475). Elsevier Ltd. <https://doi.org/10.1016/j.procbio.2020.02.005>

- Liu, D. M., & Dong, C. (2020b). Recent advances in nano-carrier immobilized enzymes and their applications. In *Process Biochemistry* (Vol. 92, pp. 464–475). Elsevier Ltd. <https://doi.org/10.1016/j.procbio.2020.02.005>
- Liu, X., Meng, X. Y., Xu, Y., Dong, T., Zhang, D. Y., Guan, H. X., Zhuang, Y., & Wang, J. (2019). Enzymatic synthesis of 1-caffeoylglycerol with deep eutectic solvent under continuous microflow conditions. *Biochemical Engineering Journal*, 142(July 2018), 41–49. <https://doi.org/10.1016/j.bej.2018.11.007>
- Lobo, S. A., Bączyk, P., Wyss, B., Widmer, J. C., Jesus, L. P., Gomes, J., Batista, A. P., Hartmann, S., & Wassmann, P. (2021). Stability liabilities of biotherapeutic proteins: Early assessment as mitigation strategy. *Journal of Pharmaceutical and Biomedical Analysis*, 192(20). <https://doi.org/10.1016/j.jpba.2020.113650>
- Lokko, Y., Heijde, M., Schebesta, K., Scholtès, P., Van Montagu, M., & Giacca, M. (2018). Biotechnology and the bioeconomy—Towards inclusive and sustainable industrial development. In *New Biotechnology* (Vol. 40, pp. 5–10). Elsevier B.V. <https://doi.org/10.1016/j.nbt.2017.06.005>
- López Ortiz, A., Neri Segura, F. J., Sandoval Jabalera, R., Marques Da Silva Paula, M., Arias Del Campo, E., Salinas Gutiérrez, J., Escobedo Bretado, M. A., & Collins-Martínez, V. (2013). Low temperature sugar cane bagasse pyrolysis for the production of high purity hydrogen through steam reforming and CO₂ capture. *International Journal of Hydrogen Energy*, 38(28), 12580–12588. <https://doi.org/10.1016/j.ijhydene.2013.06.059>
- Lopresto, C. G., Calabrò, V., Woodley, J. M., & Tufvesson, P. (2014). Kinetic study on the enzymatic esterification of octanoic acid and hexanol by immobilized *Candida antarctica* lipase B. *Journal of Molecular Catalysis B: Enzymatic*, 110, 64–71. <https://doi.org/10.1016/j.molcatb.2014.09.011>
- Lu, Q., Hu, B., Zhang, Z. xi, Wu, Y. ting, Cui, M. shu, Liu, D. jia, Dong, C. qing, & Yang, Y. ping. (2018). Mechanism of cellulose fast pyrolysis: The role of characteristic chain ends and dehydrated units. *Combustion and Flame*, 198, 267–277. <https://doi.org/10.1016/j.combustflame.2018.09.025>
- Luo, Y., Li, Z., Li, X., Liu, X., Fan, J., Clark, J. H., & Hu, C. (2019). The production of furfural directly from hemicellulose in lignocellulosic biomass: A review. *Catalysis Today*, 319, 14–24. <https://doi.org/10.1016/j.cattod.2018.06.042>
- Macleod, J. M., & Rschroeder, L. (1973). SELECTIVE ESTERIFICATION OF 1,6-ANHYDROHEXOPYRANOSSES: THE POSSIBLE ROLE OF INTRAMOLECULAR HYDROGEN-BONDING. In *Curb&y&ate Research* (Vol. 30).
- Maduskar, S., Maliekkal, V., Neurock, M., & Dauenhauer, P. J. (2018). On the Yield of Levoglucosan from Cellulose Pyrolysis. *ACS Sustainable Chemistry and Engineering*, 6(5), 7017–7025. <https://doi.org/10.1021/acssuschemeng.8b00853>
- Magallanes, G., Kärkäs, M. D., Bosque, I., Lee, S., Maldonado, S., & Stephenson, C. R. J. (2019a). Selective C-O Bond Cleavage of Lignin Systems and Polymers Enabled by Sequential Palladium-Catalyzed Aerobic Oxidation and Visible-Light Photoredox Catalysis. *ACS Catalysis*, 9(3), 2252–2260. <https://doi.org/10.1021/acscatal.8b04172>

- Magallanes, G., Kärkäs, M. D., Bosque, I., Lee, S., Maldonado, S., & Stephenson, C. R. J. (2019b). Selective C-O Bond Cleavage of Lignin Systems and Polymers Enabled by Sequential Palladium-Catalyzed Aerobic Oxidation and Visible-Light Photoredox Catalysis. *ACS Catalysis*, *9*(3), 2252–2260. <https://doi.org/10.1021/acscatal.8b04172>
- Maghraby, Y. R., El-Shabasy, R. M., Ibrahim, A. H., & Azzazy, H. M. E. S. (2023). Enzyme Immobilization Technologies and Industrial Applications. In *ACS Omega* (Vol. 8, Issue 6, pp. 5184–5196). American Chemical Society. <https://doi.org/10.1021/acsomega.2c07560>
- Magnusson, A. O., Szekrenyi, A., Joosten, H. J., Finnigan, J., Charnock, S., & Fessner, W. D. (2019). nanoDSF as screening tool for enzyme libraries and biotechnology development. *FEBS Journal*, *286*(1), 184–204. <https://doi.org/10.1111/febs.14696>
- Malanovic, N., & Lohner, K. (2016). Gram-positive bacterial cell envelopes: The impact on the activity of antimicrobial peptides. *Biochimica et Biophysica Acta - Biomembranes*, *1858*(5), 936–946. <https://doi.org/10.1016/j.bbamem.2015.11.004>
- Manoel, E. A., dos Santos, J. C. S., Freire, D. M. G., Rueda, N., & Fernandez-Lafuente, R. (2015). Immobilization of lipases on hydrophobic supports involves the open form of the enzyme. *Enzyme and Microbial Technology*, *71*, 53–57. <https://doi.org/10.1016/j.enzmictec.2015.02.001>
- Marrazza, G. (2014). Piezoelectric biosensors for organophosphate and carbamate pesticides: A review. In *Biosensors* (Vol. 4, Issue 3, pp. 301–317). MDPI. <https://doi.org/10.3390/bios4030301>
- Martinelle, M., Holmquist, M., & Hult, K. (1995). On the interfacial activation of *Candida antarctica* lipase A and B as compared with *Humicola lanuginosa* lipase. In *Biochimica et Biophysica Acta* (Vol. 1258).
- Mateo, C., Torres, R., Ferna, G., Ortiz, C., Fuentes, M., Hidalgo, A., Lo, F., Abian, O., Palomo, J. M., Betancor, L., Pessela, B. C. C., Guisan, M., & Ferna, R. (2003). *Epoxy-Amino Groups: A New Tool for Improved Immobilization of Proteins by the Epoxy Method*. 772–777.
- Mendes, A. A., Soares, C. M. F., & Tardioli, P. W. (2023). Recent advances and future prospects for biolubricant base stocks production using lipases as environmentally friendly catalysts: a mini-review. In *World Journal of Microbiology and Biotechnology* (Vol. 39, Issue 1). Springer Science and Business Media B.V. <https://doi.org/10.1007/s11274-022-03465-4>
- Meryam Sardar, R. A. (2015). Enzyme Immobilization: An Overview on Nanoparticles as Immobilization Matrix. *Biochemistry & Analytical Biochemistry*, *04*(02). <https://doi.org/10.4172/2161-1009.1000178>
- Miranda, A. S. De, Miranda, L. S. M., & Souza, R. O. M. A. De. (2015). Lipases: Valuable catalysts for dynamic kinetic resolutions. *Biotechnology Advances*. <https://doi.org/10.1016/j.biotechadv.2015.02.015>
- Mochida, M., & Kawamura, K. (2004). Hygroscopic properties of levoglucosan and related organic compounds characteristic to biomass burning aerosol particles. *Journal of Geophysical Research D: Atmospheres*, *109*(21). <https://doi.org/10.1029/2004JD004962>

- Molton, P., & Demmitt, T. (1977). *Reaction mechanisms in cellulose pyrolysis: a literature review*. <https://doi.org/10.2172/7298596>
- Nakatsubo, F., Kamitakahara, H., & Hori, M. (1996). Cationic Ring-Opening Polymerization of 3,6-Di- O -benzyl- α -D-glucose 1,2,4-Orthopivalate and the First Chemical Synthesis of Cellulose. *Journal of the American Chemical Society*, *118*(7), 1677–1681. <https://doi.org/10.1021/ja953286u>
- Nimz, H. (1974). Beech Lignin—Proposal of a Constitutional Scheme. *Angewandte Chemie International Edition in English*, *13*(5), 313–321. <https://doi.org/10.1002/anie.197403131>
- Nioi, C., Destrac, P., & Condoret, J. S. (2019). Lipase esterification in the Centrifugal Partition Reactor: Modelling and determination of the specific interfacial area. *Biochemical Engineering Journal*, *143*(December 2018), 179–184. <https://doi.org/10.1016/j.bej.2019.01.006>
- Nobles, D. R., Romanovicz, D. K., & Brown, J. (2001). Cellulose in cyanobacteria. Origin of vascular plant cellulose synthase? *Plant Physiology*, *127*(2), 529–542. <https://doi.org/10.1104/pp.010557>
- Octave, S., & Thomas, D. (2009). Biorefinery: Toward an industrial metabolism. *Biochimie*, *91*(6), 659–664. <https://doi.org/10.1016/j.biochi.2009.03.015>
- Ortiz, C., Ferreira, M. L., Barbosa, O., dos Santos, J. C. S., Rodrigues, R. C., Berenguer-Murcia, Á., Briand, L. E., & Fernandez-Lafuente, R. (2019). Novozym 435: the “perfect” lipase immobilized biocatalyst? *Catalysis Science & Technology*, *9*(10), 2380–2420. <https://doi.org/10.1039/C9CY00415G>
- Ortiz, C., Ferreira, M. L., Barbosa, O., Dos Santos, J. C. S., Rodrigues, R. C., Berenguer-Murcia, Á., Briand, L. E., & Fernandez-Lafuente, R. (2019). Novozym 435: The “perfect” lipase immobilized biocatalyst? *Catalysis Science and Technology*, *9*(10), 2380–2420. <https://doi.org/10.1039/c9cy00415g>
- Otto, R. T., Bornscheuer, U. T., Syldatk, C., & Schmid, R. D. (1998). Lipase-catalyzed synthesis of arylaliphatic esters of β -D(+)-glucose, n-alkyl- and arylglucosides and characterization of their surfactant properties. *Journal of Biotechnology*, *64*(2–3), 231–237. [https://doi.org/10.1016/S0168-1656\(98\)00125-4](https://doi.org/10.1016/S0168-1656(98)00125-4)
- Oudenhoven, S. R. G., Westerhof, R. J. M., Aldenkamp, N., Brillman, D. W. F., & Kersten, S. R. A. (2013). Demineralization of wood using wood-derived acid: Towards a selective pyrolysis process for fuel and chemicals production. *Journal of Analytical and Applied Pyrolysis*, *103*, 112–118. <https://doi.org/10.1016/j.jaap.2012.10.002>
- Palomo, J. M., Fuentes, M., Fernández-Lorente, G., Mateo, C., Guisan, J. M., & Fernández-Lafuente, R. (2003). General trend of lipase to self-assemble giving bimolecular aggregates greatly modifies the enzyme functionality. *Biomacromolecules*, *4*(1), 1–6. <https://doi.org/10.1021/bm025729+>
- Palomo, J. M., Ortiz, C., Fuentes, M., Fernandez-Lorente, G., Guisan, J. M., & Fernandez-Lafuente, R. (2004). Use of immobilized lipases for lipase purification via specific lipase-lipase interactions. *Journal of Chromatography A*, *1038*(1–2), 267–273. <https://doi.org/10.1016/j.chroma.2004.03.058>

- Pandey, D. S., Katsaros, G., Lindfors, C., Leahy, J. J., & Tassou, S. A. (2019). Fast pyrolysis of poultry litter in a bubbling fluidised bed reactor: Energy and nutrient recovery. *Sustainability (Switzerland)*, *11*(9). <https://doi.org/10.3390/su11092533>
- Papamichael, E. M., Foukis, A., Papamichael, E. M., Gkini, O. A., & Stergiou, P.-Y. (2019). The mechanism of lipase-catalyzed synthesis of food flavoring ethyl butyrate in a solvent-free system. *Journal of Food Nutrition and Metabolism*, *1*–7. <https://doi.org/10.31487/j.jfnm.2019.03.01>
- Parambath Kootery, K., Jiang, H., Kolusheva, S., Vinod, T. P., Ritenberg, M., Zeiri, L., Volinsky, R., Malferrari, D., Galletti, P., Tagliavini, E., & Jelinek, R. (2014). Poly(methyl methacrylate)-supported polydiacetylene films: Unique chromatic transitions and molecular sensing. *ACS Applied Materials and Interfaces*, *6*(11), 8613–8620. <https://doi.org/10.1021/am501414z>
- Park, K. M., Lee, S. J., Yu, H., Park, J. Y., Jung, H. S., Kim, K., Lee, C. J., & Chang, P. S. (2018). Hydrophilic and lipophilic characteristics of non-fatty acid moieties: significant factors affecting antibacterial activity of lauric acid esters. *Food Science and Biotechnology*, *27*(2), 401–409. <https://doi.org/10.1007/s10068-018-0353-x>
- Park, N., & Walsh, M. K. (2021). Microbial inhibitory properties of maltodextrin fatty acid esters against food-related microorganisms. *LWT*, *147*(April), 111664. <https://doi.org/10.1016/j.lwt.2021.111664>
- Patwardhan, P. R., Dalluge, D. L., Shanks, B. H., & Brown, R. C. (2011). Distinguishing primary and secondary reactions of cellulose pyrolysis. *Bioresource Technology*, *102*(8), 5265–5269. <https://doi.org/10.1016/j.biortech.2011.02.018>
- PAUL BECHER. (1988). *Encyclopedia of Emulsion Technology: Basic Theory, Measurement, Applications* (MARCEL DEK, Vol. 3).
- Pawar, S. V., & Yadav, G. D. (2015). Kinetics and mechanism of regioselective monoacetylation of 3-aryloxy-1,2-propanediols using immobilized *Candida antarctica* lipase. *Journal of Industrial and Engineering Chemistry*, *31*, 335–342. <https://doi.org/10.1016/j.jiec.2015.07.007>
- Pereira, E. B., De Castro, H. F., De Moraes, F. F., & Zanin, G. M. (2001). Kinetic Studies of Lipase from *Candida rugosa*. *Twenty-Second Symposium on Biotechnology for Fuels and Chemicals*, *91*, 739–752. https://doi.org/10.1007/978-1-4612-0217-2_62
- Pérez-Venegas, M., Tellez-Cruz, M. M., Solorza-Feria, O., López-Munguía, A., Castillo, E., & Juaristi, E. (2020). Thermal and Mechanical Stability of Immobilized *Candida antarctica* Lipase B: an Approximation to Mechanochemical Energetics in Enzyme Catalysis. *ChemCatChem*, *12*(3), 803–811. <https://doi.org/10.1002/cctc.201901714>
- Petkova, N. (2021). Ultrasound-Assisted Synthesis of Antimicrobial Inulin and Sucrose Esters with 10-Undecylenic Acid. *Biointerface Research in Applied Chemistry*, *11*(4), 12055–12067. <https://doi.org/10.33263/BRIAC114.1205512067>
- Piskorz, J., StAG RADLEIN, D., Scott, D. S., & Czernik, S. (1989). PRETREATMENT OF WOOD AND CELLULOSE FOR PRODUCTION OF SUGARS BY FAST PYROLYSIS. In *Journal of Analytical and Applied Pyrolysis* (Vol. 16).

- Pollard, A. S., Rover, M. R., & Brown, R. C. (2012a). Characterization of bio-oil recovered as stage fractions with unique chemical and physical properties. *Journal of Analytical and Applied Pyrolysis*, 93, 129–138. <https://doi.org/10.1016/j.jaap.2011.10.007>
- Pollard, A. S., Rover, M. R., & Brown, R. C. (2012b). Journal of Analytical and Applied Pyrolysis Characterization of bio-oil recovered as stage fractions with unique chemical and physical properties. *Journal of Analytical and Applied Pyrolysis*, 93, 129–138. <https://doi.org/10.1016/j.jaap.2011.10.007>
- Pulido, R., & Gotor, V. (1994). Towards the selective acylation of secondary hydroxyl groups of carbohydrates using oxime esters in an enzyme-catalyzed process. *Carbohydrate Research*, 252(C), 55–68. [https://doi.org/10.1016/0008-6215\(94\)90005-1](https://doi.org/10.1016/0008-6215(94)90005-1)
- Punekar, N. S. (2018). ENZYMES: Catalysis, Kinetics and Mechanisms. In *ENZYMES: Catalysis, Kinetics and Mechanisms*. Springer Singapore. <https://doi.org/10.1007/978-981-13-0785-0>
- Puterka, G. J., Farone, W., Palmer, T., & Barrington, A. (2003). Structure-Function Relationships Affecting the Insecticidal and Miticidal Activity of Sugar Esters. In *J. Econ. Entomol* (Vol. 96, Issue 3). <https://academic.oup.com/jee/article/96/3/636/2217752>
- Rabaron, A., Cavé, G., Puisieux, F., & Seiller, M. (1993). Physical methods for measurement of the HLB of ether and ester non-ionic surface-active agents: H-NMR and dielectric constant. *International Journal of Pharmaceutics*, 99(1), 29–36. [https://doi.org/10.1016/0378-5173\(93\)90319-B](https://doi.org/10.1016/0378-5173(93)90319-B)
- Radt, S. (2018). Perspective of Recent Progress in Immobilization of Enzymes. *Mnemosyne*, 71(1), 41–57. <https://doi.org/10.1163/1568525X-12342362>
- Reshmy, R., Paulose, T. A. P., Philip, E., Thomas, D., Madhavan, A., Sirohi, R., Binod, P., Kumar Awasthi, M., Pandey, A., & Sindhu, R. (2022). Updates on high value products from cellulosic biorefinery. *Fuel*, 308. <https://doi.org/10.1016/j.fuel.2021.122056>
- Rgen Pleiss, J., Fischer, M., & Schmid, R. D. (1998). Anatomy of lipase binding sites: the scissile fatty acid binding site. In *Chemistry and Physics of Lipids* (Vol. 93).
- Rhee, J. S., Kwon, S. J., & Han, J. J. (2003). Water Activity Control for Lipase-Catalyzed Reactions in Nonaqueous Media. In *Enzymes in Nonaqueous Solvents* (Vol. 15, Issue 11, pp. 135–150). Humana Press. <https://doi.org/10.1385/1-59259-112-4:135>
- Rinaldi, R., & Schüth, F. (2009). Acid hydrolysis of cellulose as the entry point into biorefinery schemes. *ChemSusChem*, 2(12), 1096–1107. <https://doi.org/10.1002/cssc.200900188>
- Rocha, I. M., Galvão, T. L. P., Sapei, E., Ribeiro Da Silva, M. D. M. C. M. A. V., & Ribeiro Da Silva, M. D. M. C. M. A. V. (2013). Levoglucosan: A calorimetric, thermodynamic, spectroscopic, and computational investigation. *Journal of Chemical and Engineering Data*, 58(6), 1813–1821. <https://doi.org/10.1021/je400207t>
- Romero-Fernández, M., & Paradisi, F. (2020). Protein immobilization technology for flow biocatalysis. *Current Opinion in Chemical Biology*, 55, 1–8. <https://doi.org/10.1016/j.cbpa.2019.11.008>

- Ronzetti, M., Baljinnyam, B., Jalal, I., Pal, U., & Simeonov, A. (n.d.). *Application of biophysical methods for improved protein production and 1 characterization: a case study on an HtrA-family bacterial protease 2 Utpal Pal Running Title: Biophysical methods for HtrA protein production and characterization*. <https://doi.org/10.1101/2022.01.27.477556>
- Rosa, T. R., Rodrigues, J. G. A., & Ferreira, R. de Q. (2016). USE OF EXPERIMENTAL PLANNING FOR OPTIMIZATION OF A PROCEDURE FOR SIMULTANEOUS VOLTAMMETRIC DETERMINATION OF METALS Zn, Cd, Pb AND Cu FREE IN COCONUT WATER. *Química Nova*, 39(2), 8–14. <https://doi.org/10.5935/0100-4042.20160004>
- Roth, S., & Spiess, A. C. (2015). Laccases for biorefinery applications: a critical review on challenges and perspectives. In *Bioprocess and Biosystems Engineering* (Vol. 38, Issue 12, pp. 2285–2313). Springer Verlag. <https://doi.org/10.1007/s00449-015-1475-7>
- Rotticci, D. (2000). *Understanding and Engineering the Enantioselectivity of Candida antarctica Lipase B towards sec -Alcohols*.
- Rover, M. R., Aui, A., Wright, M. M., Smith, R. G., & Brown, R. C. (2019). Production and purification of crystallized levoglucosan from pyrolysis of lignocellulosic biomass. *Green Chemistry*, 21(21), 5980–5989. <https://doi.org/10.1039/c9gc02461a>
- Rover, M. R., Johnston, P. A., Jin, T., Smith, R. G., Brown, R. C., & Jarboe, L. (2014). Production of clean pyrolytic sugars for fermentation. *ChemSusChem*, 7(6), 1662–1668. <https://doi.org/10.1002/cssc.201301259>
- Rover, M. R., Johnston, P. A., Whitmer, L. E., Smith, R. G., & Brown, R. C. (2014). The effect of pyrolysis temperature on recovery of bio-oil as distinctive stage fractions. *Journal of Analytical and Applied Pyrolysis*, 105, 262–268. <https://doi.org/10.1016/j.jaap.2013.11.012>
- S. Souza, R. Almeida, G. Garcia, R. Leão, J. Bassut, R. S. and I. I. J. b. (2017). Immobilization of lipase B from *Candida antarctica* on epoxy- functionalized silica: characterization and improving biocatalytic parameters. *Journal of Chemical Technology and Biotechnology*. <https://doi.org/10.1002/j>
- Sahoo, D., Awasthi, A., Dhyani, V., Biswas, B., Kumar, J., Reddy, Y. S., Adarsh, V. P., Puthiyamadam, A., Mallapureddy, K. K., Sukumaran, R. K., Ummalyma, S. B., & Bhaskar, T. (2019). Value-addition of water hyacinth and para grass through pyrolysis and hydrothermal liquefaction. *Carbon Resources Conversion*, 2(3), 233–241. <https://doi.org/10.1016/j.crcon.2019.08.001>
- Sameni, J., Krigstin, S., & Sain, M. (2017). Solubility of Lignin and Acetylated Lignin in Organic Solvents. *BioResources*, 12(1), 1548–1565. https://ojs.cnr.ncsu.edu/index.php/BioRes/article/view/BioRes_12_1_1548_Sameni_Solubility_Lignin_Acetylated_Lignin_Organic_Solvents/5048
- Samra, H. S., & He, F. (2012). Advancements in high throughput biophysical technologies: Applications for characterization and screening during early formulation development of monoclonal antibodies. In *Molecular Pharmaceutics* (Vol. 9, Issue 4, pp. 696–707). <https://doi.org/10.1021/mp200404c>
- Sanderson, K. (2011). Lignocellulose: A chewy problem. *Nature*, 474(7352), S12–S14. <https://doi.org/10.1038/474S012a>

- Saravanan, A., Hemavathy, R. V., Sundararaman, T. R., Jeevanantham, S., Kumar, P. S., & Yaashikaa, P. R. (2019). Solid waste biorefineries. In *Refining Biomass Residues for Sustainable Energy and Bioproducts: Technology, Advances, Life Cycle Assessment, and Economics* (pp. 3–17). Elsevier. <https://doi.org/10.1016/B978-0-12-818996-2.00001-6>
- Scelsi, E., Angelini, A., & Pastore, C. (2021). Deep Eutectic Solvents for the Valorisation of Lignocellulosic Biomasses towards Fine Chemicals. *Biomass*, 1(1), 29–59. <https://doi.org/10.3390/biomass1010003>
- Schummer, C., Delhomme, O., Appenzeller, B. M. R., Wennig, R., & Millet, M. (2009). Comparison of MTBSTFA and BSTFA in derivatization reactions of polar compounds prior to GC/MS analysis. *Talanta*, 77(4), 1473–1482. <https://doi.org/10.1016/j.talanta.2008.09.043>
- Segel, I. H. (2013). Enzyme Kinetics. In *Encyclopedia of Biological Chemistry: Second Edition* (2nd ed., Vol. 2). Elsevier Inc. <https://doi.org/10.1016/B978-0-12-378630-2.00012-8>
- Sharma, P., Iqbal, H. M. N., & Chandra, R. (2022). Evaluation of pollution parameters and toxic elements in wastewater of pulp and paper industries in India: A case study. *Case Studies in Chemical and Environmental Engineering*, 5. <https://doi.org/10.1016/j.cscee.2021.100163>
- Shen, Q., Yang, R., Hua, X., Ye, F., Zhang, W., & Zhao, W. (2011). Gelatin-templated biomimetic calcification for β -galactosidase immobilization. *Process Biochemistry*, 46(8), 1565–1571. <https://doi.org/10.1016/j.procbio.2011.04.010>
- Shuai, L., & Luterbacher, J. (2016). Organic Solvent Effects in Biomass Conversion Reactions. *ChemSusChem*, 9(2), 133–155. <https://doi.org/10.1002/cssc.201501148>
- Shu-Lai Mok, W., Jerry Antal, M., & Varhegyi, G. (1992). Aerosol Formation by a Reversible Chemical Reaction: Laser-induced NH_4NO_3 Aerosol Formation in a Tubular Reactor. In *J. Colloid Interface Sci* (Vol. 31). Diehl, H. Efficiency of Chemical Desiccants.
- Sirisha, V. L., Jain, A., & Jain, A. (2016). Enzyme Immobilization: An Overview on Methods, Support Material, and Applications of Immobilized Enzymes. In *Advances in Food and Nutrition Research* (1st ed., Vol. 79). Elsevier Inc. <https://doi.org/10.1016/bs.afnr.2016.07.004>
- S-I Mok, W., & Antal, M. J. (1983). EFFECTS OF PRESSURE ON BIOMASS PYROLYSIS. II. HEATS OF REACTION OF CELLULOSE PYROLYSIS. In *Thermochrmrca Acta* (Vol. 165). Elsevier Science Publishers B.V.
- Solange I. Mussatto. (2016). *Biomass Fractionation Technologies for a Lignocellulosic Feedstock Based Biorefiner*.
- Sousa, R. R., Silva, A. S. A., Fernandez-Lafuente, R., & Ferreira-Leitão, V. S. (2021). Solvent-free esterifications mediated by immobilized lipases: A review from thermodynamic and kinetic perspectives. In *Catalysis Science and Technology* (Vol. 11, Issue 17, pp. 5696–5711). Royal Society of Chemistry. <https://doi.org/10.1039/d1cy00696g>
- Speight, J. G. (2020). Non-fossil fuel feedstocks. In *The Refinery of the Future* (pp. 343–389). Elsevier. <https://doi.org/10.1016/b978-0-12-816994-0.00010-5>

- Sun, S., & Hu, B. (2017). A novel method for the synthesis of glyceryl monocaffeate by the enzymatic transesterification and kinetic analysis. *Food Chemistry*, 214, 192–198. <https://doi.org/10.1016/j.foodchem.2016.07.087>
- Sun, S., & Tian, L. (2018). Novozym 40086 as a novel biocatalyst to improve benzyl cinnamate synthesis. *RSC Advances*, 8(65), 37184–37192. <https://doi.org/10.1039/c8ra08433e>
- Sun, Y. E., Xia, W., Tang, X., He, Z., & Chen, J. (2009). Effects of fatty acid chain length and degree of unsaturation on the surface activities of monoacyl trehaloses. *Frontiers of Chemical Engineering in China*, 3(4), 407–412. <https://doi.org/10.1007/s11705-009-0255-9>
- Sutili, F. K., Ruela, H. S., Leite, S. G. F., Miranda, L. S. D. M., Leal, I. C. R., & De Souza, R. O. M. A. (2013). Lipase-catalyzed esterification of steric hindered fructose derivative by continuous flow and batch conditions. *Journal of Molecular Catalysis B: Enzymatic*, 85–86, 37–42. <https://doi.org/10.1016/j.molcatb.2012.08.004>
- Suuberg, E. M., Milosavljevic, I., & Oja, V. (1996a). *TWO-REGIME GLOBAL KINETICS OF CELLULOSE PYROLYSIS: THE ROLE OF TAR EVAPORATION*.
- Suuberg, E. M., Milosavljevic, I., & Oja, V. (1996b). *TWO-REGIME GLOBAL KINETICS OF CELLULOSE PYROLYSIS: THE ROLE OF TAR EVAPORATION*.
- Tamborini, L., Fernandes, P., Paradisi, F., & Molinari, F. (2018). Flow Bioreactors as Complementary Tools for Biocatalytic Process Intensification. *Trends in Biotechnology*, 36(1), 73–88. <https://doi.org/10.1016/j.tibtech.2017.09.005>
- Tang, S. L. Y., Smith, R. L., & Poliakoff, M. (2005). Principles of green chemistry: PRODUCTIVELY. *Green Chemistry*, 7(11), 761. <https://doi.org/10.1039/b513020b>
- Thompson, M. P., Peñafiel, I., Cosgrove, S. C., & Turner, N. J. (2019). Biocatalysis using immobilised enzymes in continuous flow for the synthesis of fine chemicals. *Organic Process Research and Development*, 23(1), 9–18. <https://doi.org/10.1021/acs.oprd.8b00305>
- Torres-Gavilán, A., Castillo, E., & López-Munguía, A. (2006). The amidase activity of *Candida antarctica* lipase B is dependent on specific structural features of the substrates. *Journal of Molecular Catalysis B: Enzymatic*, 41(3–4), 136–140. <https://doi.org/10.1016/j.molcatb.2006.06.001>
- Trevan, M. D. (1988). *Chapter 37 Enzyme Immobilization by Covalent Bonding*.
- T.sriwong, K., & Matsuda, T. (2022). Recent Advances in Enzyme Immobilization Utilizing Nanotechnology for Biocatalysis. *Organic Process Research & Development*. <https://doi.org/10.1021/acs.oprd.1c00404>
- Uriarte, I., Écija, P., Lozada-García, R., Çarçabal, P., & Cocinero, E. J. (2018). Investigating the Conformation of the Bridged Monosaccharide Levoglucosan. *ChemPhysChem*, 19(6), 766–773. <https://doi.org/10.1002/cphc.201701242>
- van Spronsen, J., Cardoso, M. A. T., Witkamp, G. J., de Jong, W., & Kroon, M. C. (2011). Separation and recovery of the constituents from lignocellulosic biomass by using ionic liquids and acetic acid as co-solvents for mild hydrolysis. *Chemical Engineering and*

- Veld, M. A. J., Fransson, L., Palmans, A. R. A., Meijer, E. W., & Hult, K. (2009). Lactone size dependent reactivity in *Candida antarctica* lipase B: A molecular dynamics and docking study. *ChemBioChem*, 10(8), 1330–1334. <https://doi.org/10.1002/cbic.200900128>
- Venderbosch, R. H., & Prins, W. (2010). Fast pyrolysis technology development. In *Biofuels, Bioproducts and Biorefining* (Vol. 4, Issue 2, pp. 178–208). <https://doi.org/10.1002/bbb.205>
- Vicentini, F. C., Figueiredo-Filho, L. C. S., Janegitz, B. C., Santiago, A., Pereira-Filho, E. R., & Fatibello-Filho, O. (2011). Planejamento fatorial e superfície de resposta: Otimização de um método voltamétrico para a determinação de Ag(I) empregando um eletrodo de pasta de nanotubos de carbono. *Química Nova*, 34(5), 825–830.
- Vo, T. K., Kim, S. S., & Kim, J. (2022). Pyrolysis characteristics and quantitative kinetic model of microalgae *Tetraselmis* sp. *Korean Journal of Chemical Engineering*, 39(6), 1478–1486. <https://doi.org/10.1007/s11814-022-1064-9>
- Wallace Cleland, W. (1989). Enzyme kinetics revisited: a commentary on “The kinetics of enzyme-catalyzed reactions with two or more substrates or products” by W.W. Cleland *Biochim. Biophys. Acta* 67 (1963) 104 ff. with *Biochim. Biophys. Acta* 67 (1963) 173, 188 (summaries). *Biochimica et Biophysica Acta (BBA) - General Subjects*, 1000, 209–221. [https://doi.org/10.1016/S0006-3002\(89\)80019-8](https://doi.org/10.1016/S0006-3002(89)80019-8)
- Wang, P. Y., Tsai, S. W., & Chen, T. L. (2008). Improvements of enzyme activity and enantioselectivity via combined substrate engineering and covalent immobilization. *Biotechnology and Bioengineering*, 101(3), 460–469. <https://doi.org/10.1002/bit.21916>
- Wang, Q., Song, H., Pan, S., Dong, N., Wang, X., & Sun, S. (2020). Initial pyrolysis mechanism and product formation of cellulose: An Experimental and Density functional theory(DFT) study. *Scientific Reports*, 10(1). <https://doi.org/10.1038/s41598-020-60095-2>
- Wang, S., Dai, G., Yang, H., & Luo, Z. (2017). Lignocellulosic biomass pyrolysis mechanism: A state-of-the-art review. In *Progress in Energy and Combustion Science* (Vol. 62, pp. 33–86). Elsevier Ltd. <https://doi.org/10.1016/j.peccs.2017.05.004>
- Wang, W., Zhou, W., Li, J., Hao, D., Su, Z., & Ma, G. (2015). Comparison of covalent and physical immobilization of lipase in gigaporous polymeric microspheres. *Bioprocess and Biosystems Engineering*, 38(11), 2107–2115. <https://doi.org/10.1007/s00449-015-1450-3>
- Wang, X., & Rinaldi, R. (2013). A route for lignin and bio-oil conversion: Dehydroxylation of phenols into arenes by catalytic tandem reactions. *Angewandte Chemie - International Edition*, 52(44), 11499–11503. <https://doi.org/10.1002/anie.201304776>
- Wang, Z., McDonald, A. G., Westerhof, R. J. M., Kersten, S. R. A., Cuba-Torres, C. M., Ha, S., Pecha, B., & Garcia-Perez, M. (2013). Effect of cellulose crystallinity on the formation of a liquid intermediate and on product distribution during pyrolysis. *Journal of Analytical and Applied Pyrolysis*, 100, 56–66. <https://doi.org/10.1016/j.jaap.2012.11.017>
- Waziu, D. D., & Sharzadeh, F. (1982a). SOME ESTERIS OF LEVOGLUCOSAN. In *Carbohydrate Research* (Vol. 108).

- Waziu, D. D., & Sharzadeh, F. (1982b). SOME ESTER'S OF LEVOGLUCOSAN. In *Carbohydrate Research* (Vol. 108).
- Westerhof, R. J. M., Oudenhoven, S. R. G., Marathe, P. S., Engelen, M., Garcia-Perez, M., Wang, Z., & Kersten, S. R. A. (2016). The interplay between chemistry and heat/mass transfer during the fast pyrolysis of cellulose. *Reaction Chemistry and Engineering*, 1(5), 555–566. <https://doi.org/10.1039/c6re00100a>
- Wong Sak Hoi, L., & Martincigh, B. S. (2013). Sugar cane plant fibres: Separation and characterisation. *Industrial Crops and Products*, 47, 1–12. <https://doi.org/10.1016/j.indcrop.2013.02.017>
- Woodcock, L. L., Wiles, C., Greenway, G. M., Watts, P., Wells, A., & Eyley, S. (2008). Enzymatic synthesis of a series of alkyl esters using novozyme 435 in a packed-bed, miniaturized, continuous flow reactor. *Biocatalysis and Biotransformation*, 26(6), 466–472. <https://doi.org/10.1080/10242420802456571>
- Wu, S. (1987). Formation of dispersed phase in incompatible polymer blends: Interfacial and rheological effects. *Polymer Engineering and Science*, 27(5), 335–343. <https://doi.org/10.1002/pen.760270506>
- Xu, A., Guo, X., Zhang, Y., Li, Z., & Wang, J. (2017a). Efficient and sustainable solvents for lignin dissolution: Aqueous choline carboxylate solutions. *Green Chemistry*, 19(17), 4067–4073. <https://doi.org/10.1039/c7gc01886j>
- Xu, A., Guo, X., Zhang, Y., Li, Z., & Wang, J. (2017b). Efficient and sustainable solvents for lignin dissolution: Aqueous choline carboxylate solutions. *Green Chemistry*, 19(17), 4067–4073. <https://doi.org/10.1039/c7gc01886j>
- Yadav, G. D., & Lathi, P. S. (2003). Kinetics and mechanism of synthesis of butyl isobutyrate over immobilised lipases. *Biochemical Engineering Journal*, 16(3), 245–252. [https://doi.org/10.1016/S1369-703X\(03\)00026-3](https://doi.org/10.1016/S1369-703X(03)00026-3)
- Yadav, G. D., & Trivedi, A. H. (2003). Kinetic modeling of immobilized-lipase catalyzed transesterification of n-octanol with vinyl acetate in non-aqueous media. *Enzyme and Microbial Technology*, 32(7), 783–789. [https://doi.org/10.1016/S0141-0229\(03\)00064-4](https://doi.org/10.1016/S0141-0229(03)00064-4)
- Yang, H., Yan, R., Chen, H., Lee, D. H., & Zheng, C. (2007). Characteristics of hemicellulose, cellulose and lignin pyrolysis. *Fuel*, 86(12–13), 1781–1788. <https://doi.org/10.1016/j.fuel.2006.12.013>
- Yang, M., Wei, T., Wang, K., Jiang, L., Zeng, D., Sun, X., Liu, W., & Shen, Y. (2022). Both levoglucosan kinase activity and transport capacity limit the utilization of levoglucosan in *Saccharomyces cerevisiae*. *Biotechnology for Biofuels and Bioproducts*, 15(1). <https://doi.org/10.1186/s13068-022-02195-x>
- Yang, X., Li, Z., Liu, H., Ma, L., Huang, X., Cai, Z., Xu, X., Shang, S., & Song, Z. (2020). Cellulose-based polymeric emulsifier stabilized poly(N-vinylcaprolactam) hydrogel with temperature and pH responsiveness. *International Journal of Biological Macromolecules*, 143, 190–199. <https://doi.org/10.1016/j.ijbiomac.2019.12.019>

- You, C., & Xu, C. (2017). *Review of Levoglucosan in Glacier Snow and Ice studies: Recent Progress and Future Perspectives*.
- Zahirinejad, S., Hemmati, R., Homaei, A., Dinari, A., Hosseinkhani, S., Mohammadi, S., & Vianello, F. (2021). Nano-organic supports for enzyme immobilization: Scopes and perspectives. In *Colloids and Surfaces B: Biointerfaces* (Vol. 204). Elsevier B.V. <https://doi.org/10.1016/j.colsurfb.2021.111774>
- Zaidi, A., Gainer, J. L., Carta, G., Mrani, A., Kadiri, T., Belarbi, Y., & Mir, A. (2002). Esterification of fatty acids using nylon-immobilized lipase in n-hexane: kinetic parameters and chain-length effects. In *Journal of Biotechnology* (Vol. 93). www.elsevier.com/locate/jbiotec
- Zaini, I. N., Sophonrat, N., Sjöblom, K., & Yang, W. (2021). Creating values from biomass pyrolysis in Sweden: Co-production of H₂, biocarbon and bio-oil. *Processes*, 9(3), 1–21. <https://doi.org/10.3390/pr9030415>
- Zakzeski, J., Bruijninx, P. C. A., Jongerius, A. L., & Weckhuysen, B. M. (2010). The catalytic valorization of lignin for the production of renewable chemicals. *Chemical Reviews*, 110(6), 3552–3599. <https://doi.org/10.1021/cr900354u>
- Zdráhal, Z., Oliveira, J., Vermeylen, R., Claeys, M., & Maenhaut, W. (2002). Improved method for quantifying levoglucosan and related monosaccharide anhydrides in atmospheric aerosols and application to samples from urban and tropical locations. *Environmental Science and Technology*, 36(4), 747–753. <https://doi.org/10.1021/es015619v>
- Zhang, C., Liang, X., Abdo, A. A. A., Kaddour, B., Li, X., Teng, C., & Wan, C. (2021). Ultrasound-assisted lipase-catalyzed synthesis of ethyl acetate: process optimization and kinetic study. *Biotechnology and Biotechnological Equipment*, 35(1), 255–263. <https://doi.org/10.1080/13102818.2020.1868331>
- Zhang, H., Liu, X., Li, J., Jiang, Z., & Hu, C. (2018). Performances of Several Solvents on the Cleavage of Inter- and Intramolecular Linkages of Lignin in Corncob Residue. *ChemSusChem*, 11(9), 1494–1504. <https://doi.org/10.1002/cssc.201800309>
- Zhang, J., Nolte, M. W., & Shanks, B. H. (2014). Investigation of primary reactions and secondary effects from the pyrolysis of different celluloses. *ACS Sustainable Chemistry and Engineering*, 2(12), 2820–2830. <https://doi.org/10.1021/sc500592v>
- Zhang, K., Pei, Z., & Wang, D. (2016). Organic solvent pretreatment of lignocellulosic biomass for biofuels and biochemicals: A review. In *Bioresource Technology* (Vol. 199, pp. 21–33). Elsevier Ltd. <https://doi.org/10.1016/j.biortech.2015.08.102>
- Zhang, P., Cheng, Q., Xu, W., & Tang, K. (2019). Simulation and optimization of Novozym 40086 kinetic resolution of α -cyclopentylphenylacetic acid enantiomers. *Journal of Chemical Technology and Biotechnology*, 94(11), 3595–3605. <https://doi.org/10.1002/jctb.6163>
- Zhang, X., Wei, W., Cao, X., & Feng, F. (2015). Characterization of enzymatically prepared sugar medium-chain fatty acid monoesters. *Journal of the Science of Food and Agriculture*, 95(8), 1631–1637. <https://doi.org/10.1002/jsfa.6863>

- Zhang, X., Yang, W., & Dong, C. (2013). Levoglucosan formation mechanisms during cellulose pyrolysis. *Journal of Analytical and Applied Pyrolysis*, *104*, 19–27. <https://doi.org/10.1016/j.jaap.2013.09.015>
- Zoghalmi, A., & Paës, G. (2019). Lignocellulosic Biomass: Understanding Recalcitrance and Predicting Hydrolysis. In *Frontiers in Chemistry* (Vol. 7). Frontiers Media S.A. <https://doi.org/10.3389/fchem.2019.00874>

ANNEX A

A1. Hydrolytic Activity Assay

Table A1: Immobilization efficiency of the new biocatalysts compared to that of N435

Biocatalyst Immobilized	Amount of protein (mg/g of support)	IPC (%) ^a	H _A (U.g ⁻¹ of support) ^b	S _A (U.mg ⁻¹ of protein) ^c
N435 ¹²	15.0	-	248.0	16.53
CalB_Epoxy	9.0	>99	372.0	41.33

^aIPC: immobilized protein concentration; ^b Hydrolytic activity; ^c Specific activity

$$^a \text{IPC (\%)}: \left(\frac{P_0 - P_f}{P_0} \right) * 100$$

P₀ and P_f are the initial and final time protein concentrations in the supernatant (mg.mL⁻¹), respectively.

$$^b \text{Hydrolytic activity (H}_A\text{)}: \frac{(V - V_b)}{t * V_a} * M * 1000$$

Where, **V** and **V_b** are the volume (mL) of NaOH solution used for sample and blank titration, respectively; **t** is the reaction time (min); **M** is the molarity (mmol.mL⁻¹) and **V_a** is the sample volume (mL).

$$^c \text{Specific activity (S}_A\text{)}: \frac{U}{\text{milligrams of protein}}$$

A2. Hydrolytic activity of different lipases

Table A2: Hydrolytic activity of different lipases.

Lipases	Description	Hydrolytic activity (U.mg ⁻¹)
Free	<i>Candida Rugosa</i> from <i>Rhizomucor miehei</i> (CR)	2.4
	<i>Candida antarctica</i> B, recombinant from <i>Aspergillus oryzae</i> (CalB)	1.1
Immobilized	Novozym®435 (N435)	0.3
	Novozym®40086 (N40086)	1.9

A3. Calibration curve

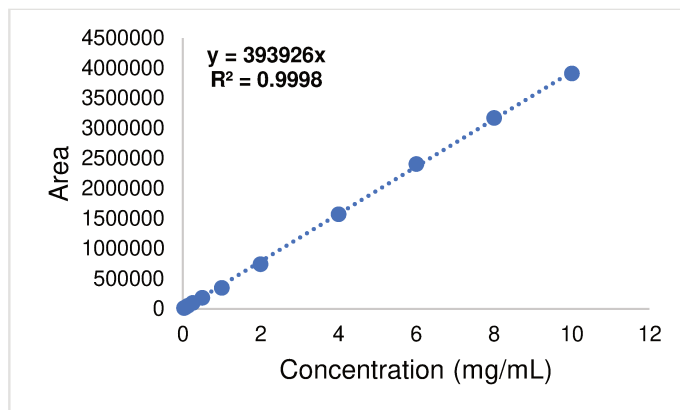


Figure S1: Calibration curve for different concentration of levoglucosan.

ANNEX B

B1. Analytical Methods

$^1\text{H-NMR}$, $^{13}\text{C-NMR}$; COSY, NOEDIFF, HMBC, HSQC and Dept135 spectra were recorded on a Bruker Advance 400 and 500 MHz spectrometer. Reported chemical shifts (δ) are expressed in parts per million (ppm) down field from tetra methyl silane (TMS) and the coupling constant (J) in Hz.

GC analysis was performed on a Shimadzu CG2010 – SLB-5MS capillary column 30 m, 0.25 mm ID, 0.25 μm film thickness (MS) and with helium used as the carrier gas. The injector and detector temperatures were 250°C, and the oven was maintained at 80 °C for 4 min, increased to 200 °C at a rate of 6 °C/min for 10 min, increased to 310 °C at a rate of 8 °C/min, when it was held constant for 4 min, totalling 51.75 min. High Resolution Mass Spectrometric Analysis (HRMS).

Infrared spectra were obtained in KBr pellets (complexes), in NICOLET MAGNA FTIR-760 (4000-400 cm^{-1}) spectrophotometer.

B1.1. GC-MS and FID

In this section, we will show the illustrative chromatograms obtained in the steps of higher product conversions with their respective mass spectra, in the transesterification reactions with ethyl laurate, ethyl palmitate, ethyl stearate and ethyl oleate for the synthesis of levoglucosan esters.

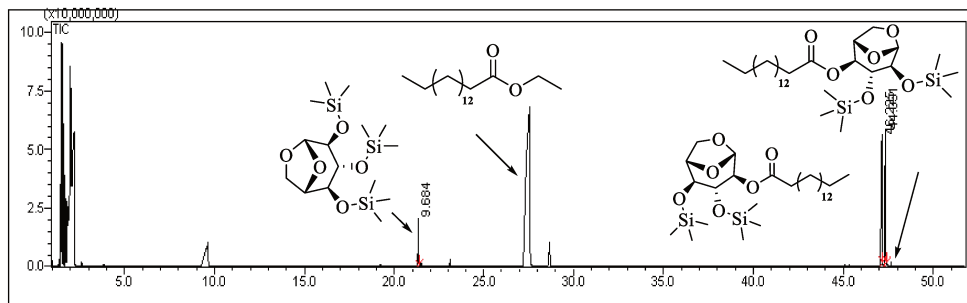


Figure S2: Chromatogram of levoglucosan reaction medium with ethyl palmitate using N435 (derivatized) 55 °C. Peak with retention time at 9.2 for excess BSTFA.

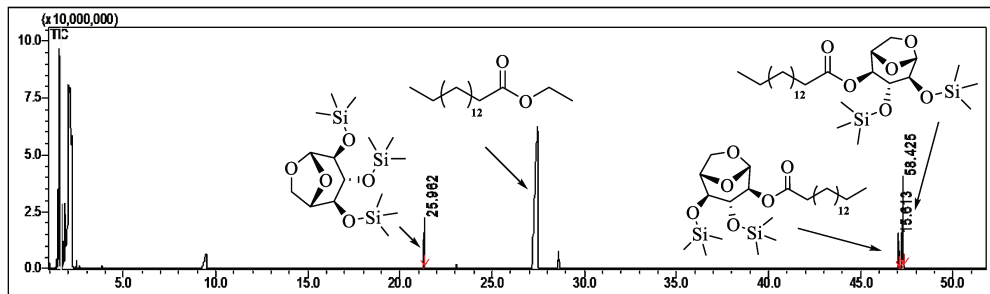


Figure S3: Chromatogram of levoglucosan reaction medium with ethyl palmitate using PS IM (derivatized) 55 °C. Peak with retention time at 9.2 for excess BSTFA.

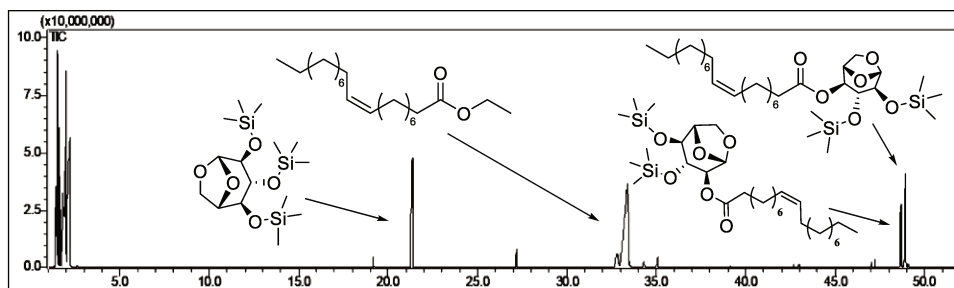


Figure S4: Chromatogram of levoglucosan reaction medium with ethyl oleate using calb_epoxy (derivatized) 55 °C.

B.1.1.1. Solubility test for BoE in different organic solvent

Table B1: Insoluble; 2: Partially soluble and 3: Totally soluble.

Solvents	Temperature		
	50 °C	55°C	60°C
Acetonitrile	1	2	2
CPME	1	1	2
Cyrene	1	2	2

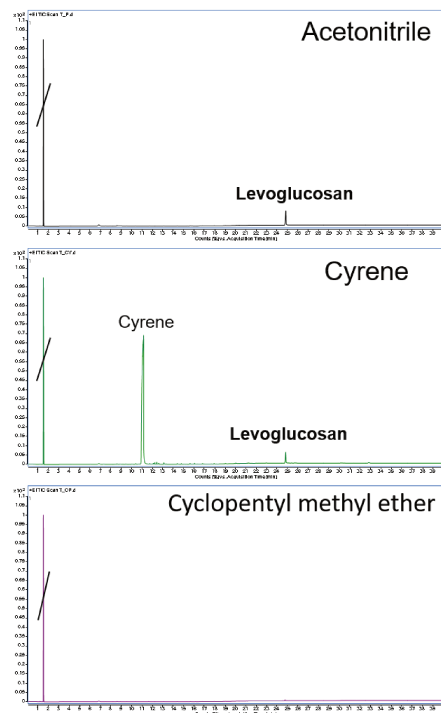
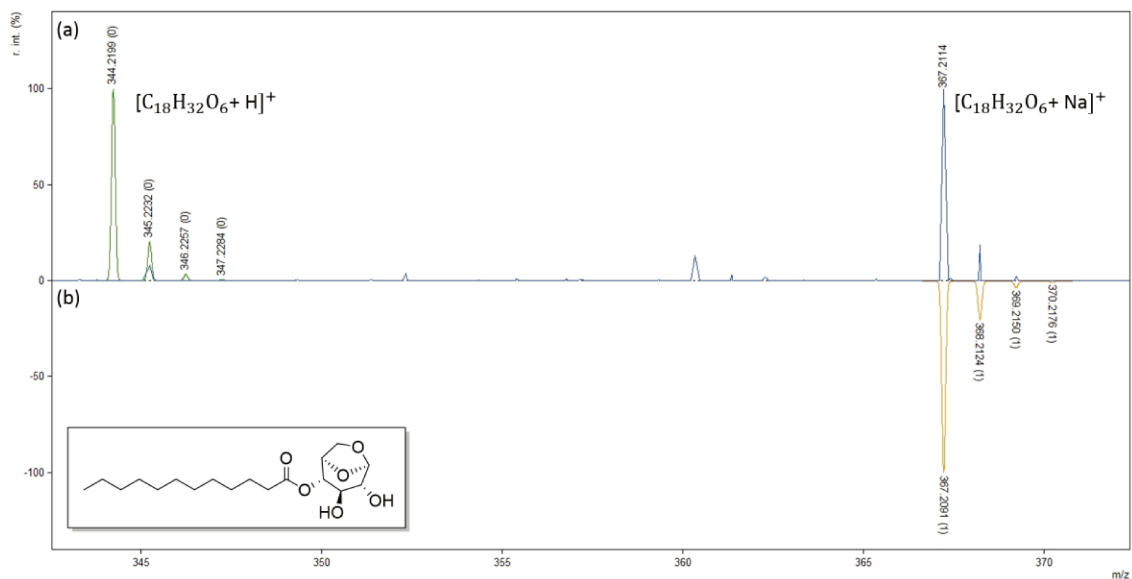


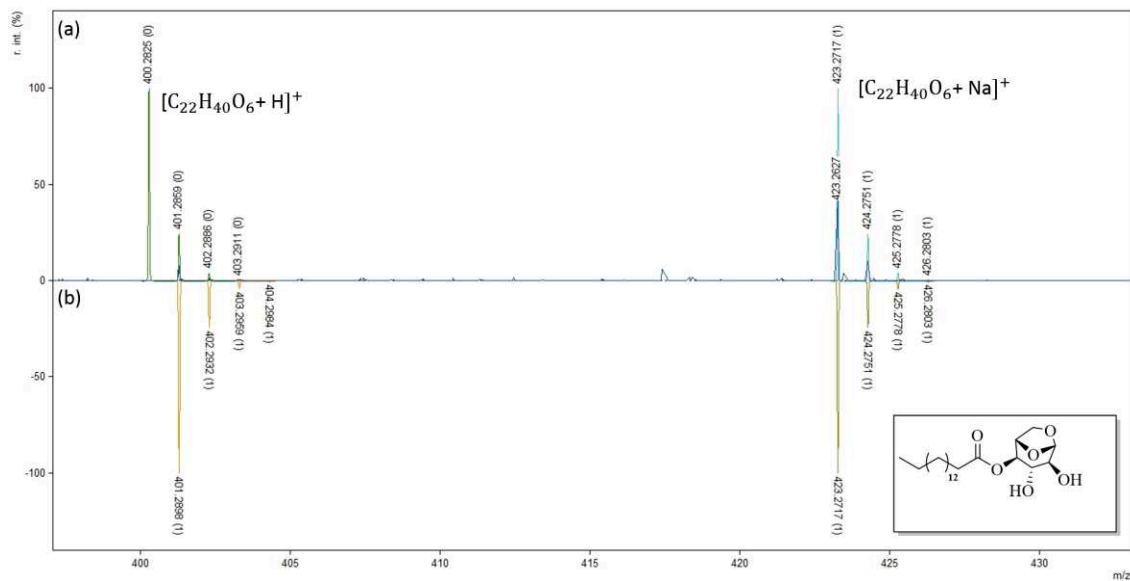
Figure S5: Chromatogram of BoE in different organic solvents at 55 °C.

B.1.2. HRMS

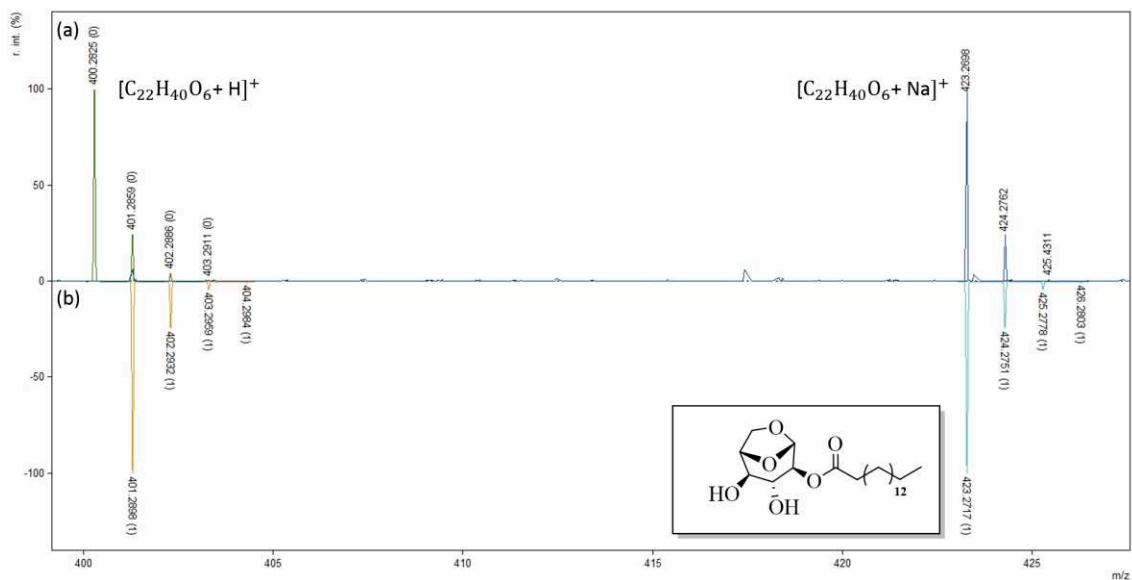
High Resolution Mass Spectrometric Analysis (HRMS) for 4-O-Lauryl-1,6-anhydroglucopyranose, where a) found and b) calculated.



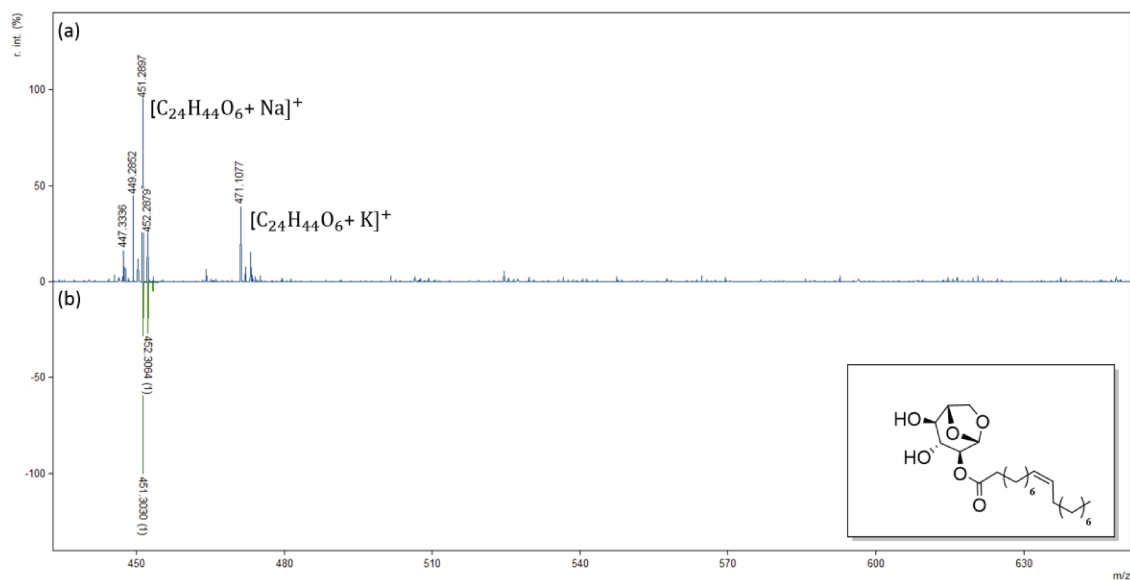
High Resolution Mass Spectrometric Analysis (HRMS) for 4-O-Palmitoyl-1,6-anhydroglucopyranose, where a) found and b) calculated.



High Resolution Mass Spectrometric Analysis (HRMS) for 2-O-Palmitoyl-1,6-anhydroglucopyranose, where a) found and b) calculated.



High Resolution Mass Spectrometric Analysis (HRMS) for 2-O-Oleoyl-1,6-anhydroglucopyranose, where a) found and b) calculated.



B.1.3. Fourier Transform Infrared Spectroscopy (FTIR)

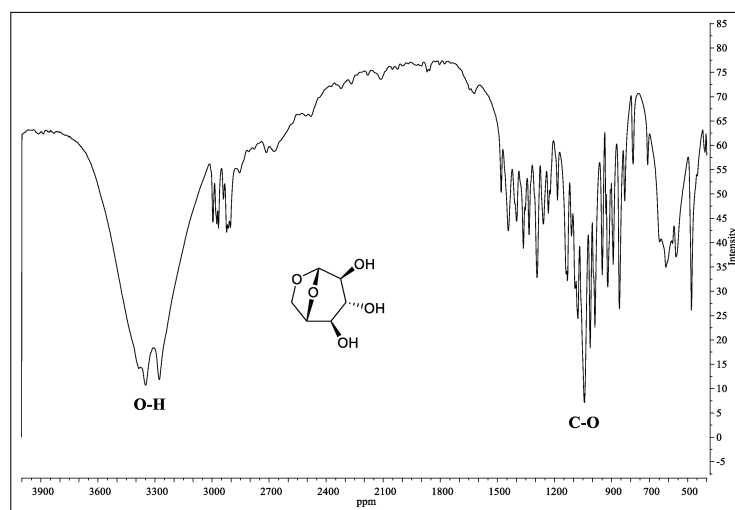


Figure S6: Infrared spectrum of levoglucosan.

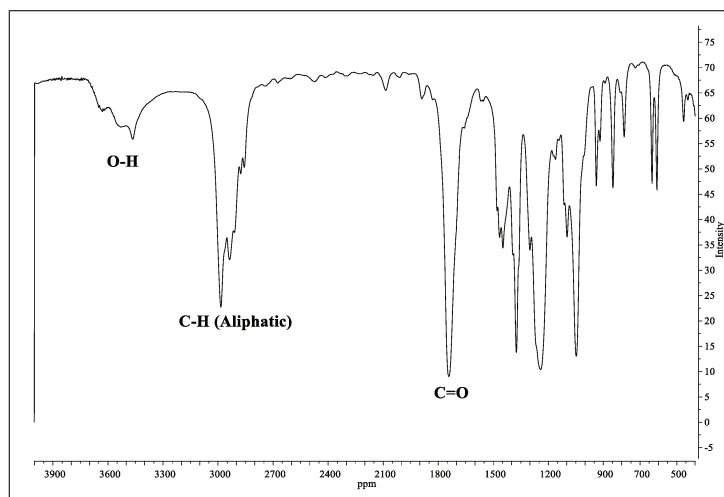


Figure S7: Infrared spectrum of the transesterification reaction of levoglucosan with ethyl oleate.

B.1.4. Nuclear Magnetic Resonance (NMR)

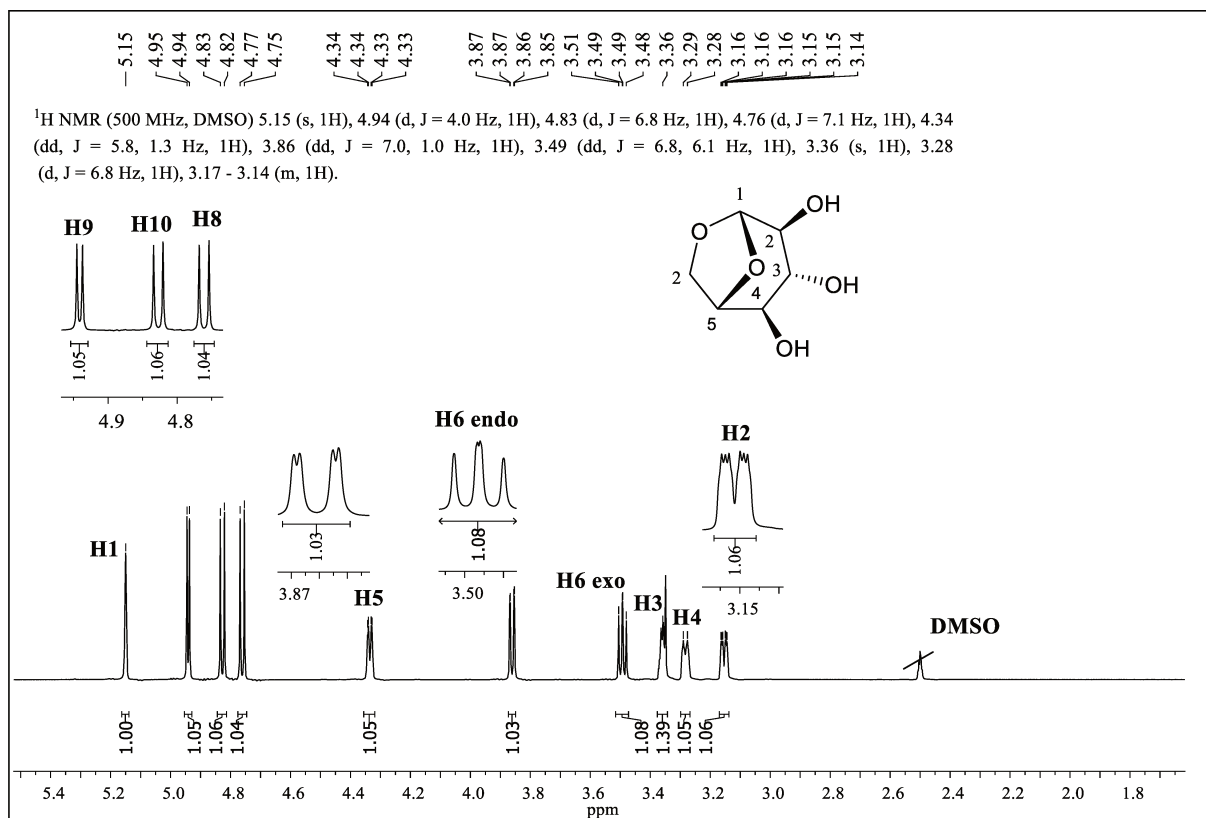


Figure S8: ¹H-NMR spectrum for levoglucosan (DMSO).

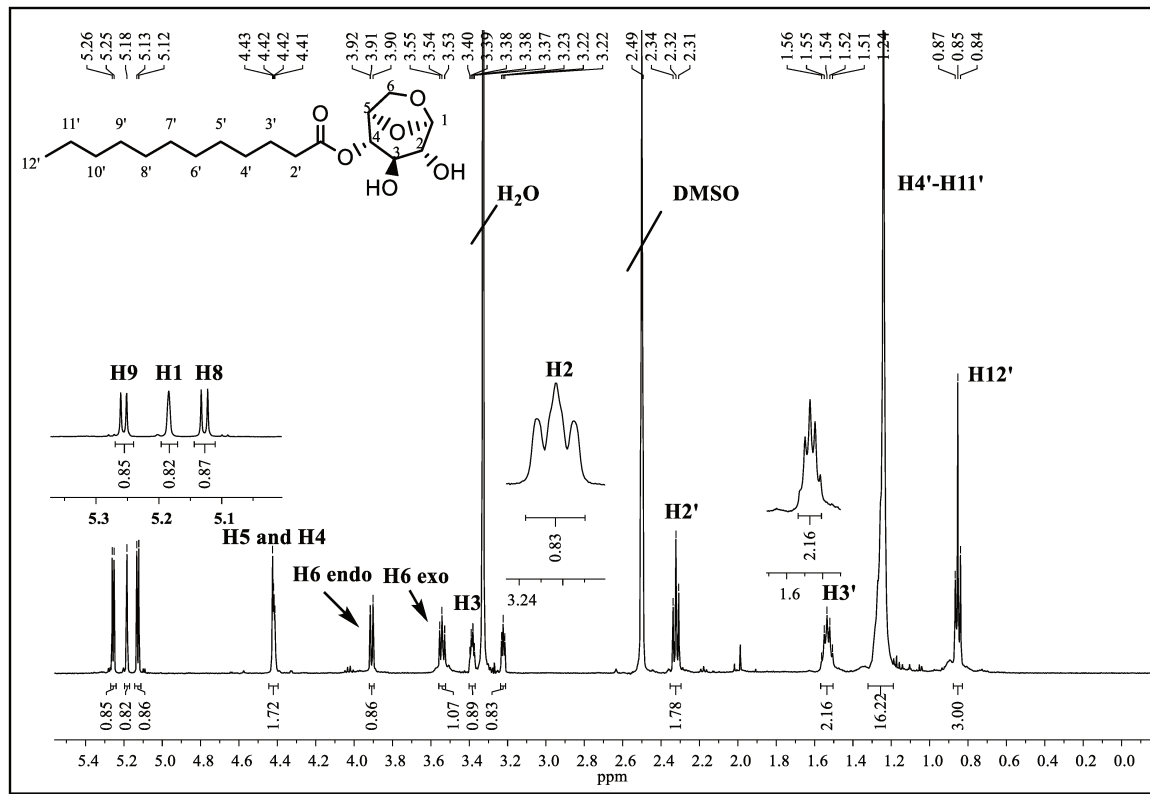


Figure S9: $^1\text{H-NMR}$ Spectrum for 4-O-Lauryl-1,6-anhydroglucopyranose (CDCl_3).

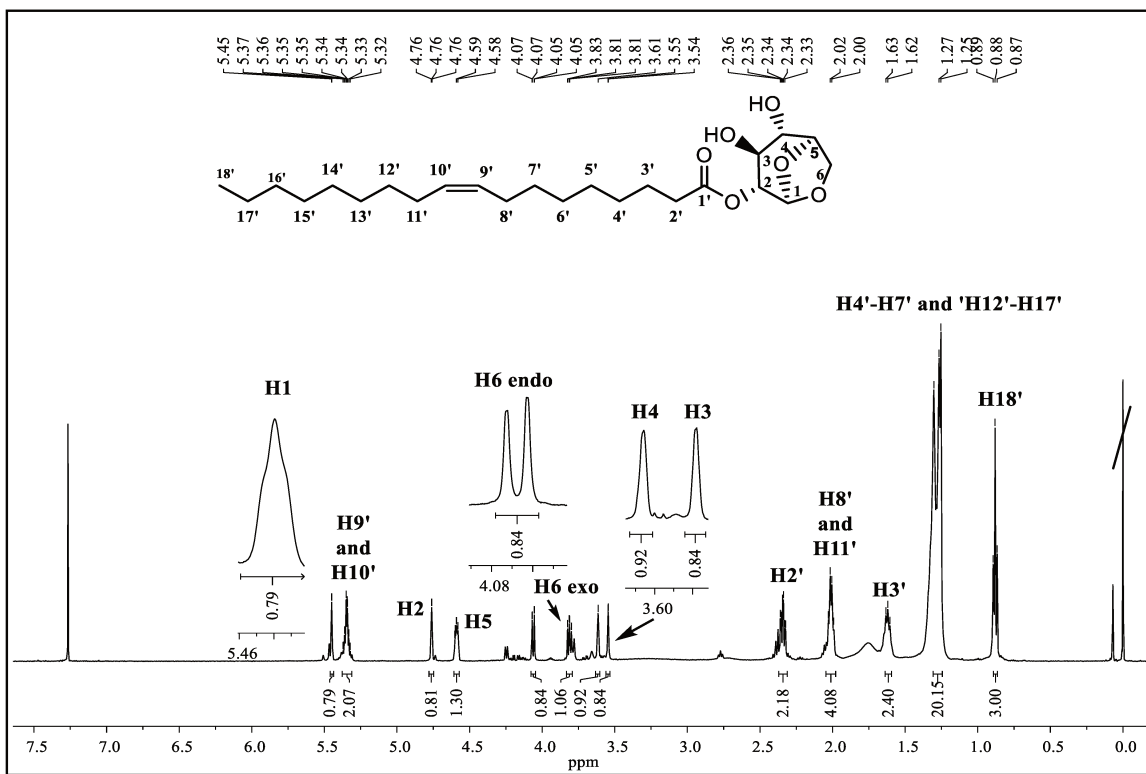


Figure S10: ¹H-NMR Spectrum for 2-O-Oleoyl-1,6-anhydroglucopyranose (CDCl₃).

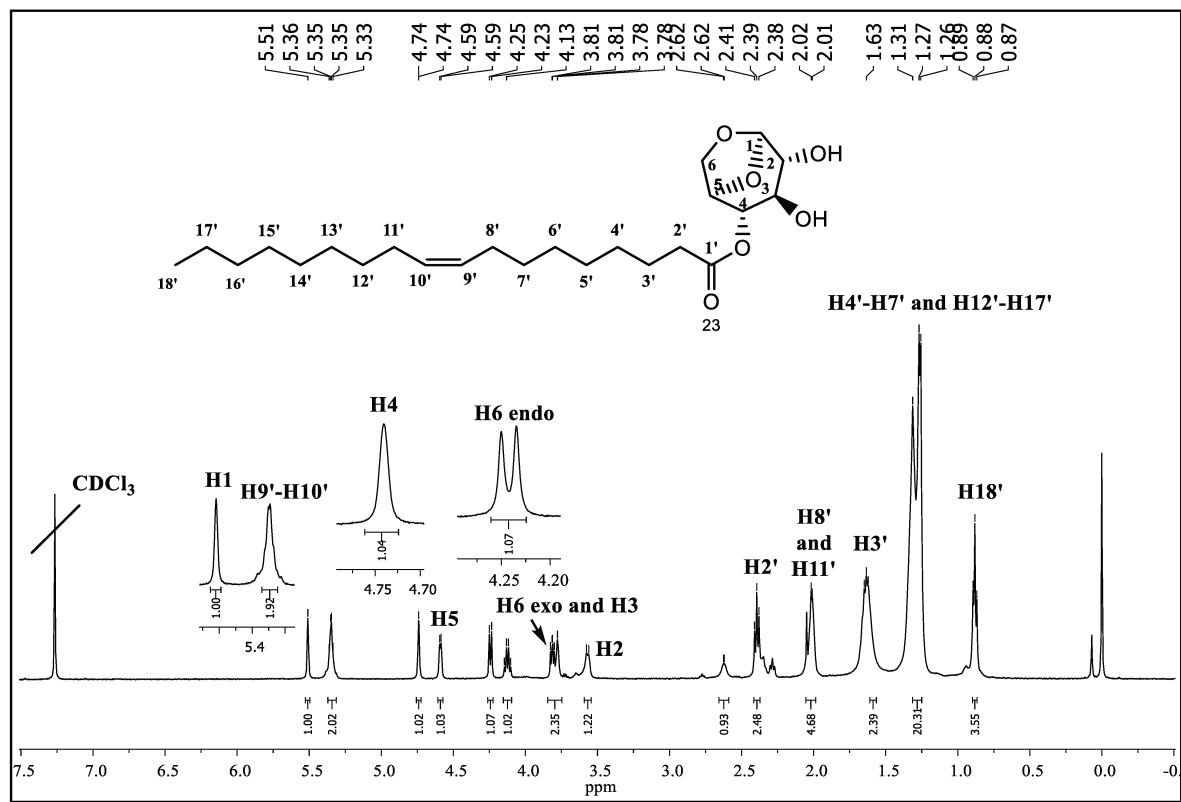


Figure S11: ¹H-NMR Spectrum for 4-O-Oleoyl-1,6-anhydroglucopyranose (CDCl₃).

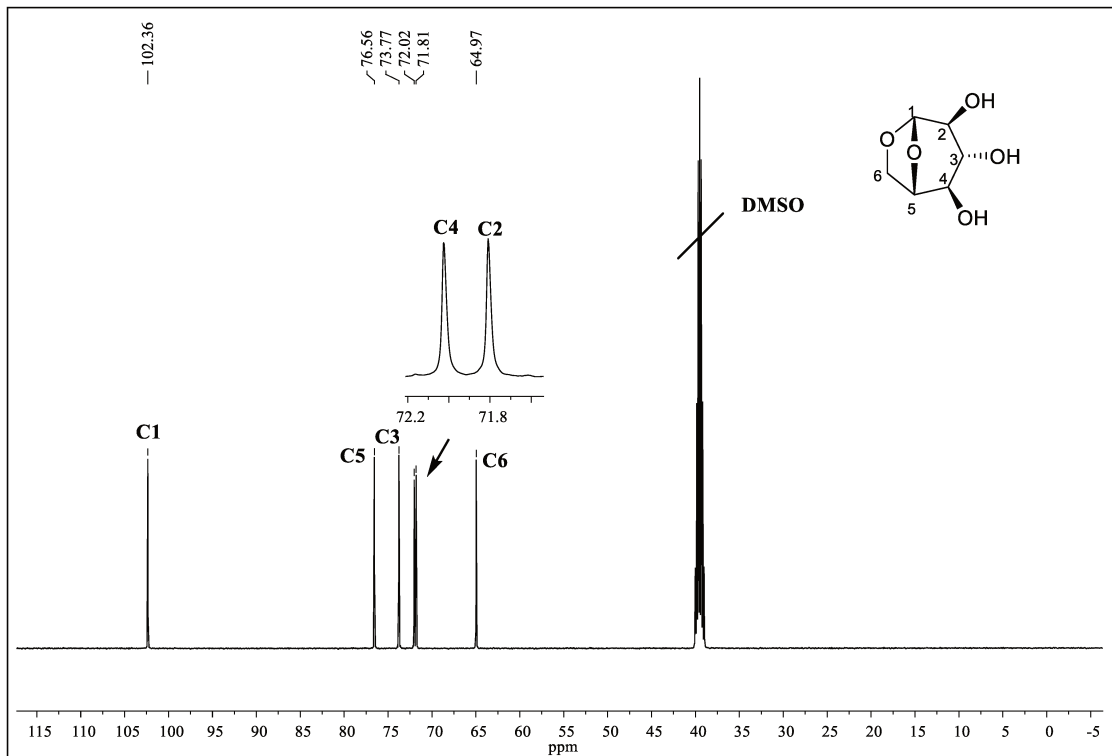


Figure S12: ^{13}C -NMR Spectrum for levoglucosan (DMSO).

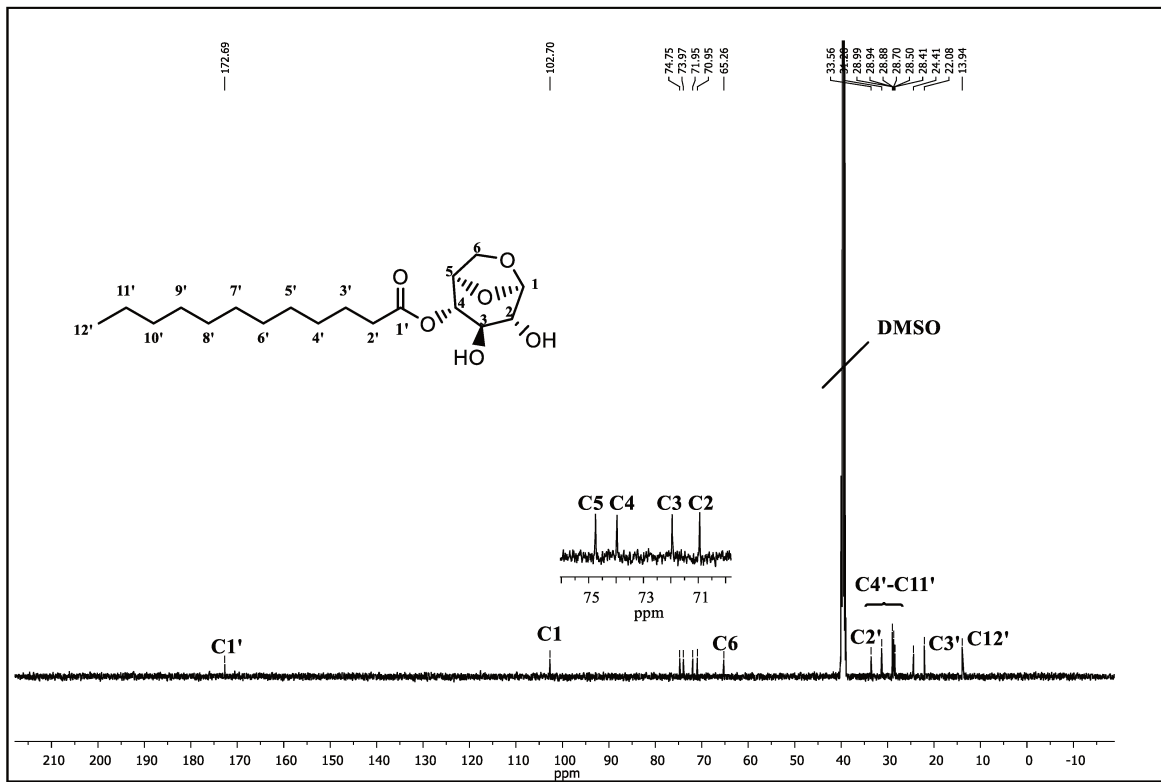


Figure S13: ^{13}C -NMR Spectrum for 4-O-Lauryl-1,6-anhydroglucopyranose (CDCl_3).

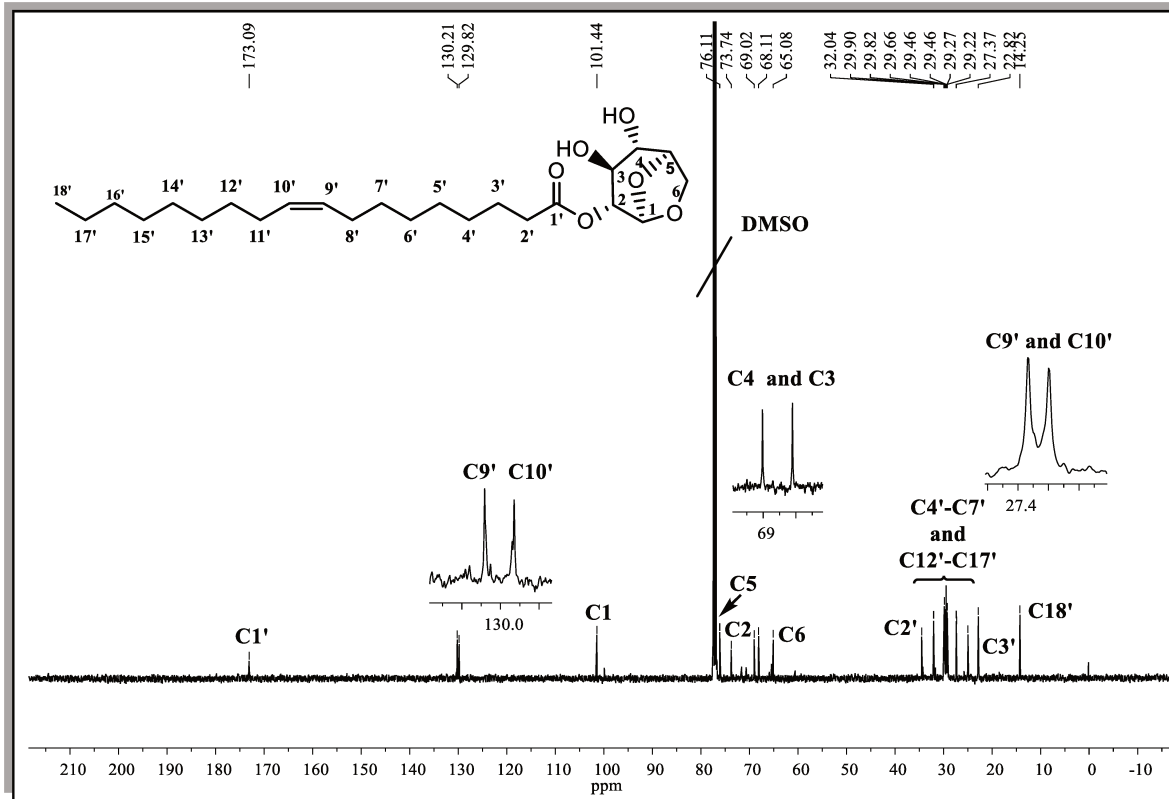


Figure S14: ^{13}C -NMR Spectrum for 2-O-Oleoyl-1,6-anhydroglucopyranose (CDCl_3).

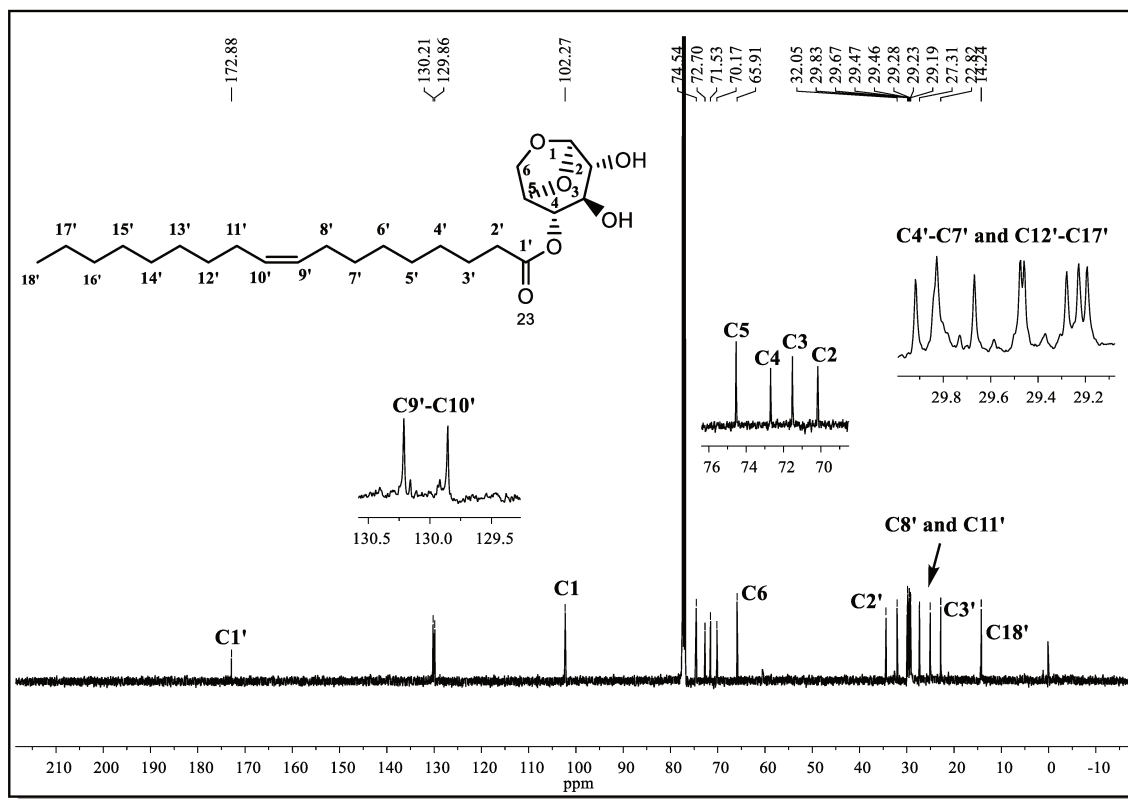


Figure S15: ^{13}C -NMR Spectrum for 4-O-Oleoyl-1,6-anhydroglucopyranose(CDCl_3).

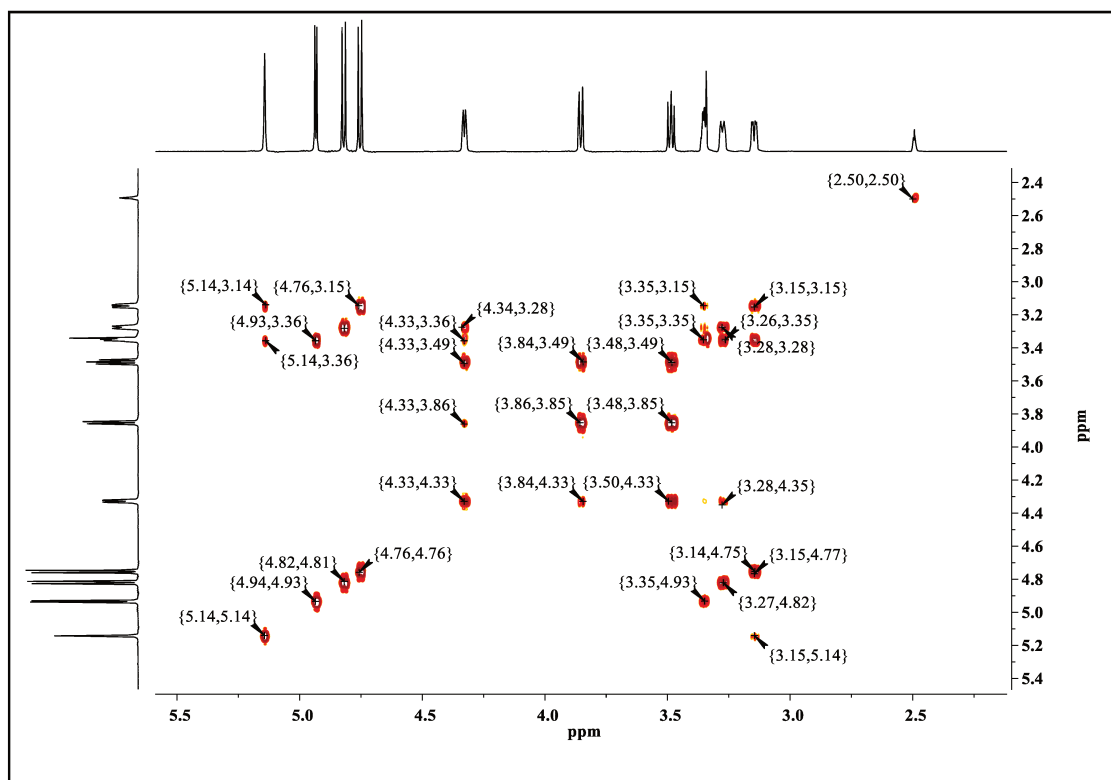


Figure S16: ^1H , ^1H COSY for levoglucosan (DMSO).

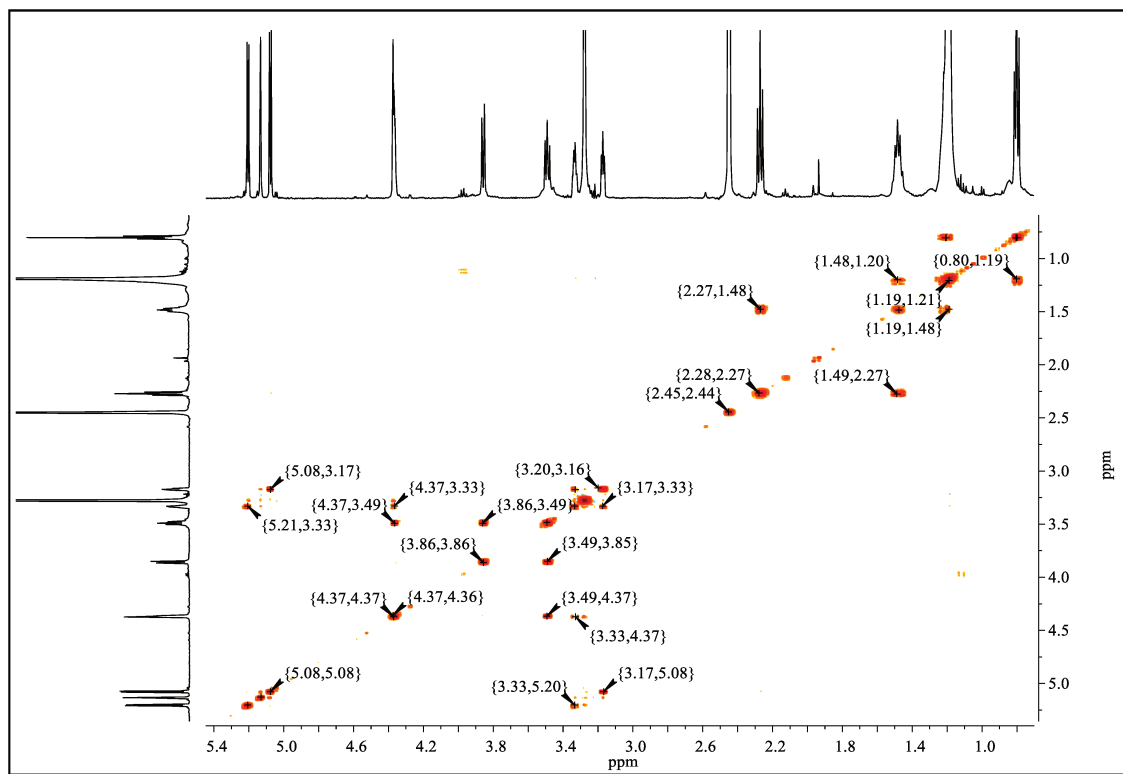


Figure S17: ^1H , ^1H COSY for 4-O-Lauryl-1,6-anhydroglucopyranose (CDCl_3).

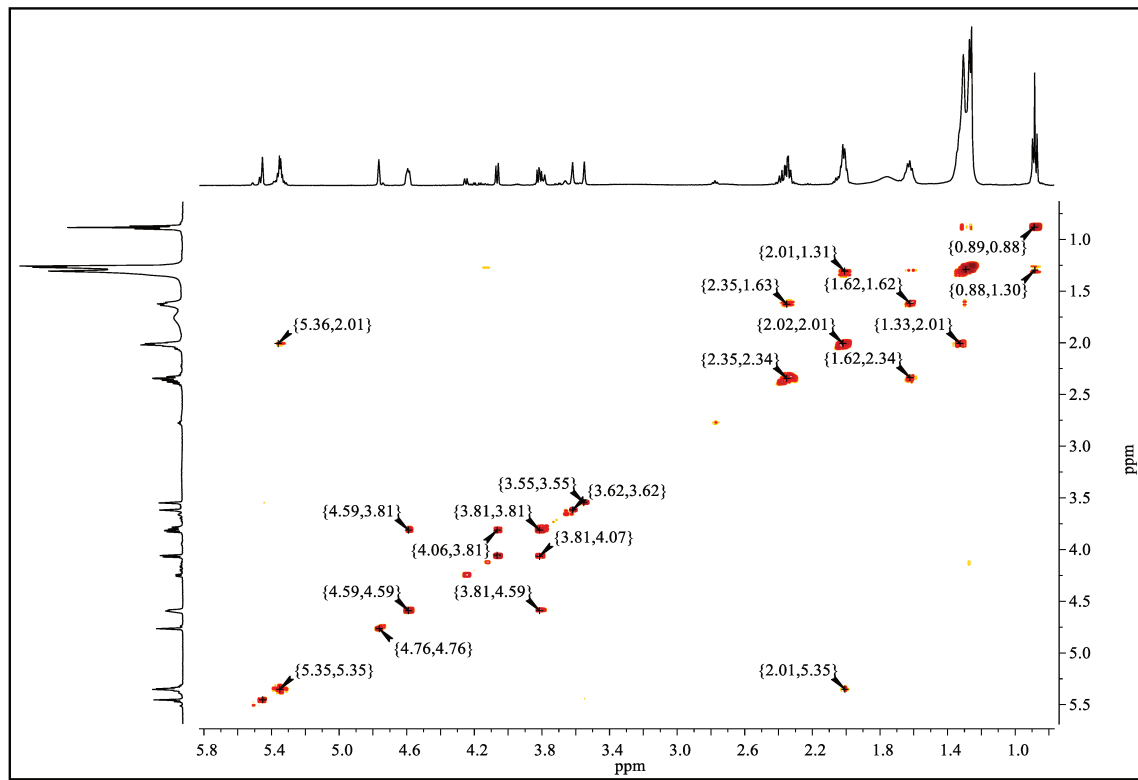


Figure S18: ^1H , ^1H COSY for 2-O-Oleoyl-1,6-anhydroglucopyranose (CDCl_3).

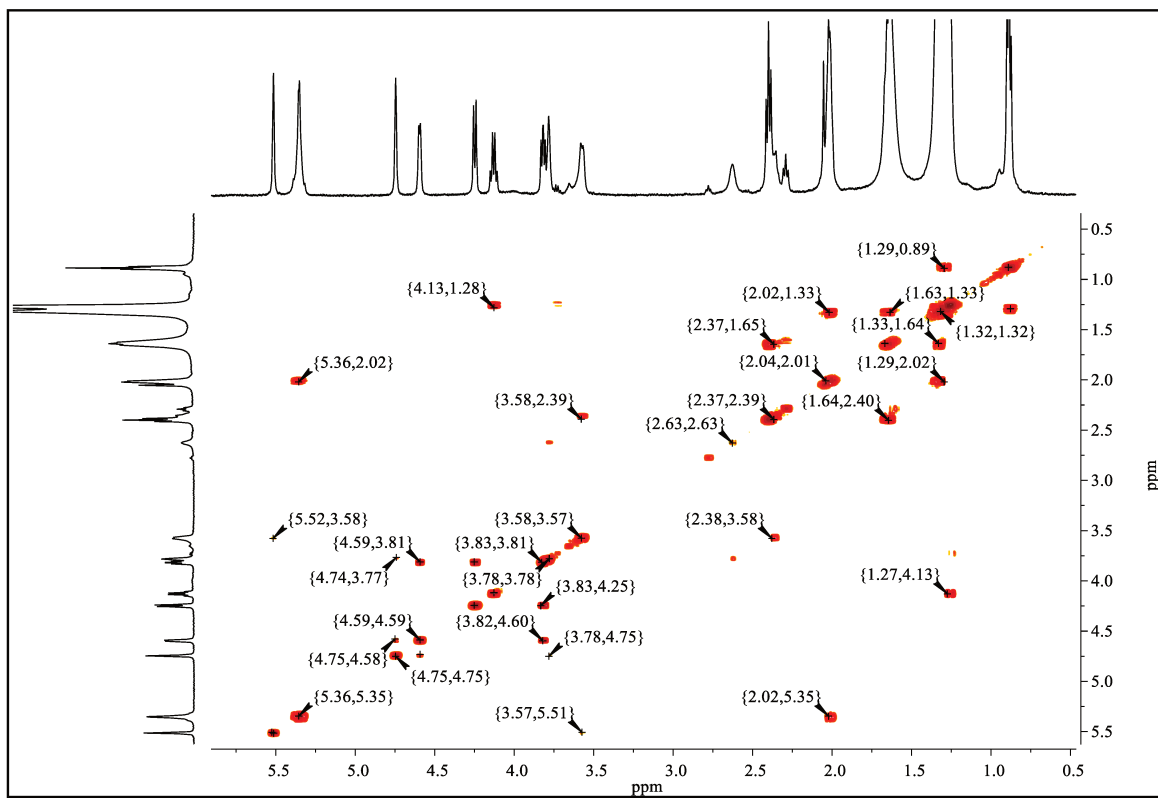


Figure S19: ^1H , ^1H COSY for 4-O-Oleoyl-1,6-anhydroglucopyranose (CDCl_3).

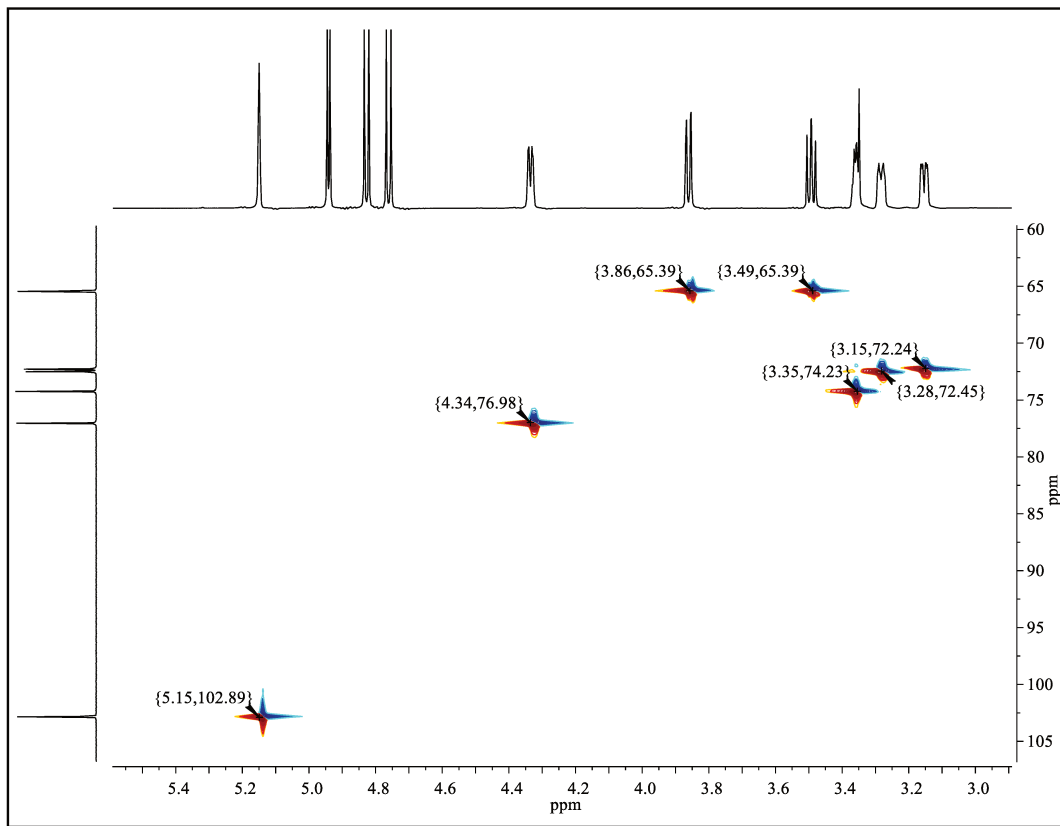


Figure S20: HSQC for levoglucosan (DMSO).

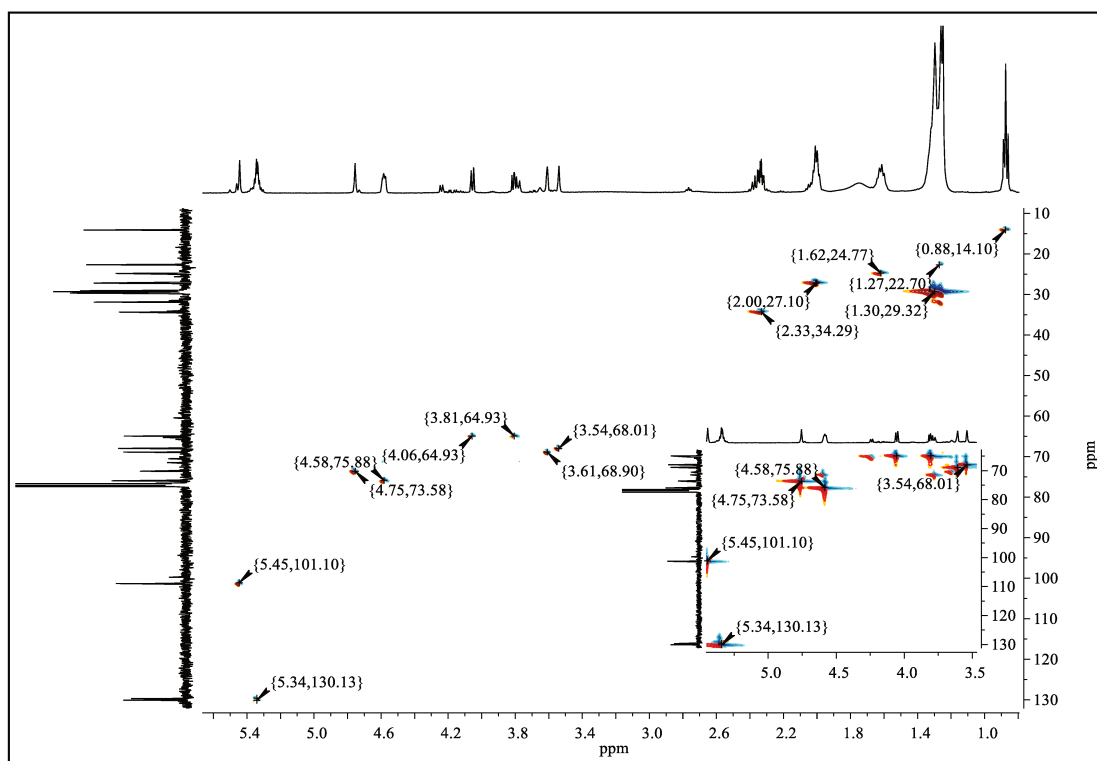


Figure S21: HSQC for 2-O-Oleoyl-1,6-anhydroglucopyranose (CDCl₃).

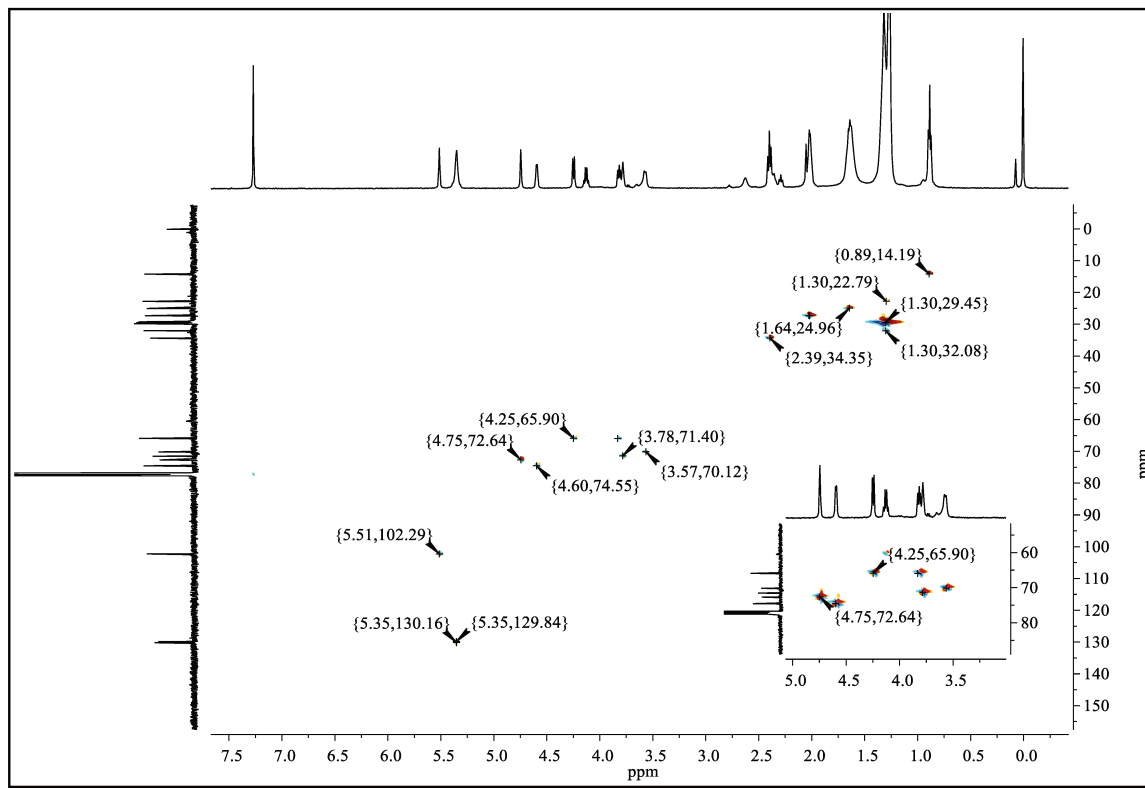


Figura S22: HSQC for 4-O-Oleoyl-1,6-anhydroglucopyranose (CDCl_3).

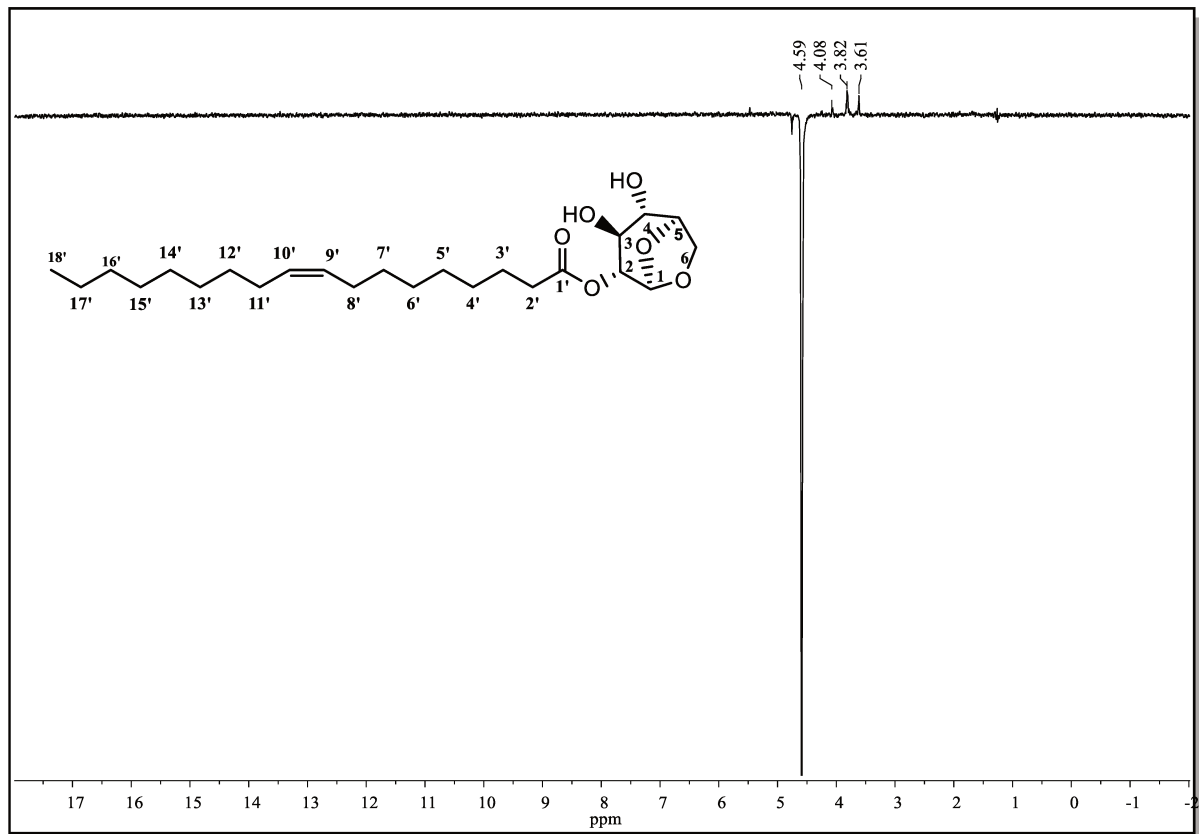


Figura S23: n.O.e difference spectra for irradiation in the H-5 compound 2-O-Oleoyl-1,6-anhydroglucopyranose (CDCl_3).

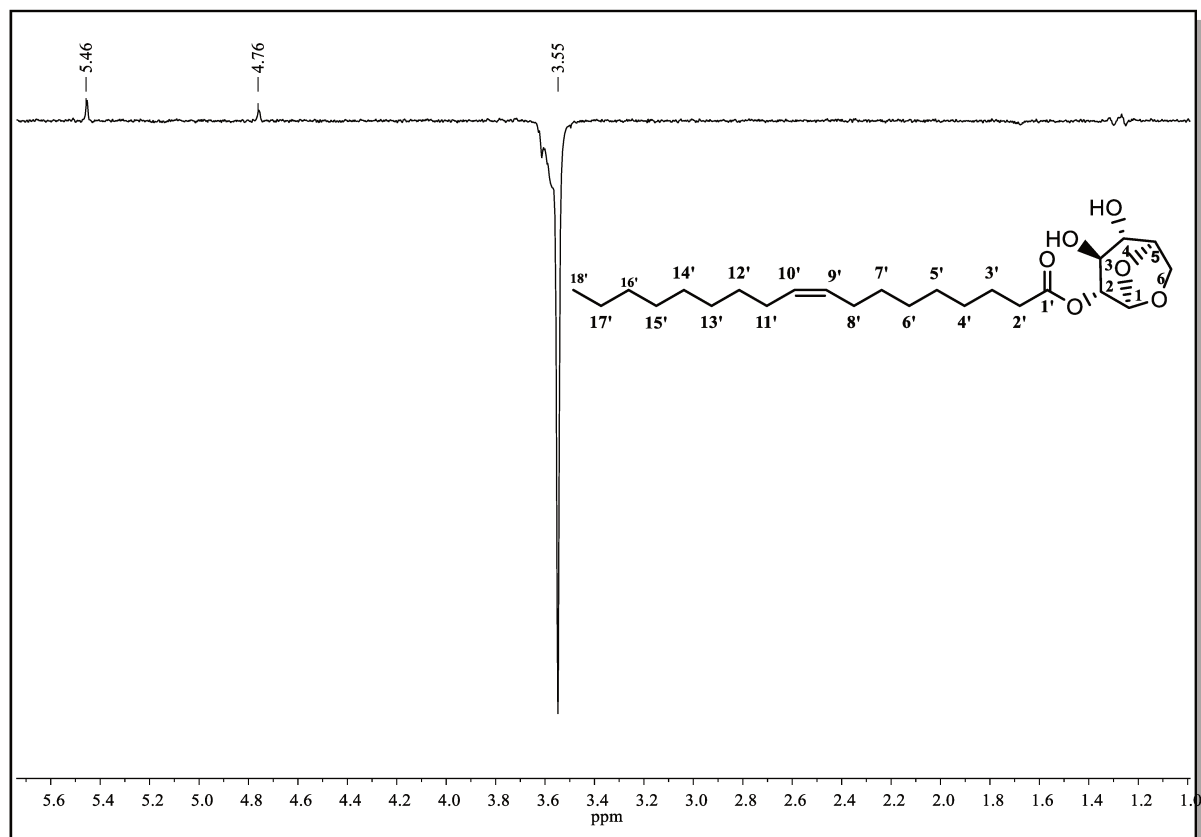


Figura S24: n.O.e difference spectra for irradiation in the H-3 compound 2-O-Oleoyl-1,6-anhydroglucopyranose (CDCl_3).

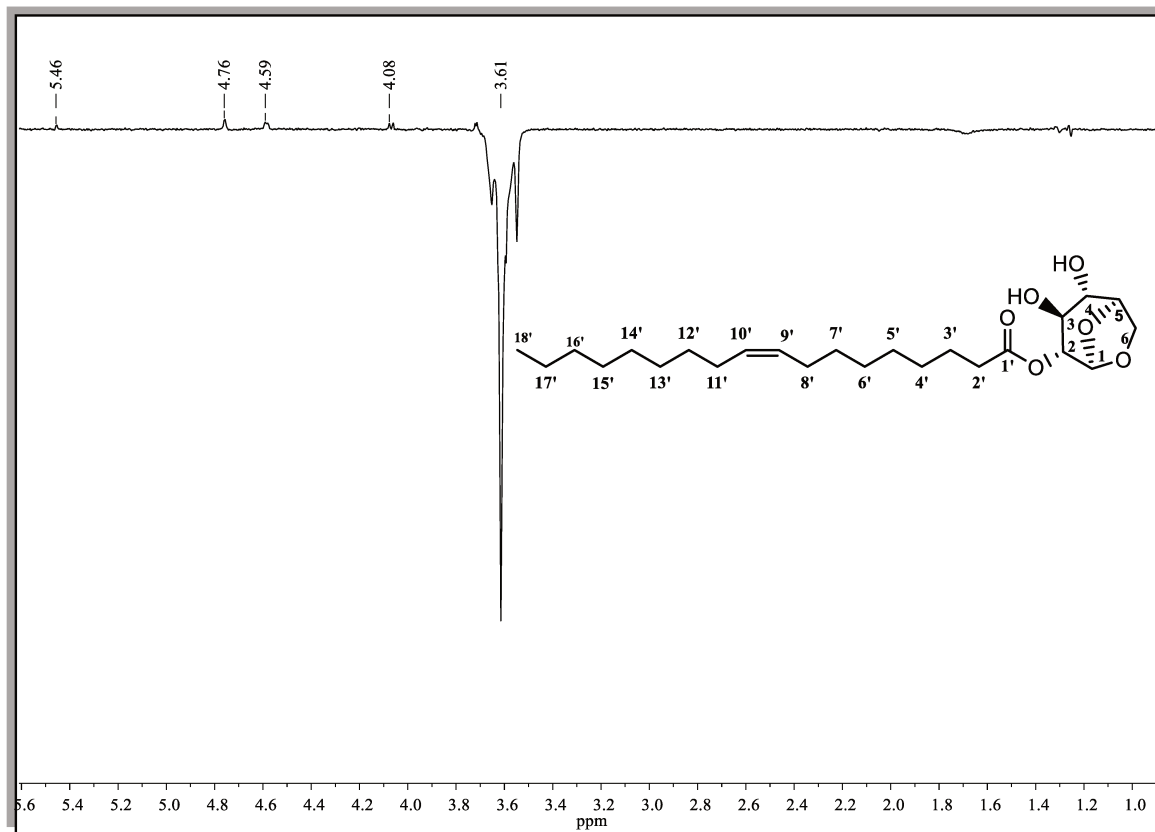


Figure S25: n.o.e difference spectra for irradiation in the H-4 compound 2-O-Oleoyl-1,6-anhydroglucopyranose (CDCl₃).

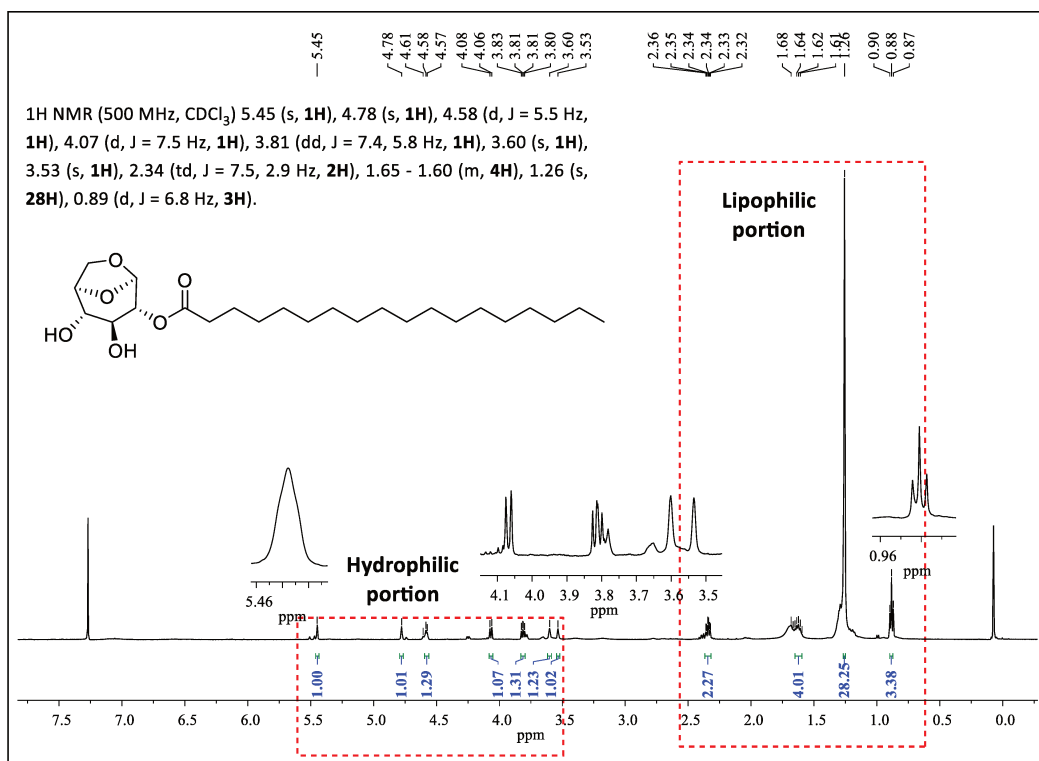


Figure S26: ¹H-NMR Spectrum for 2-O-Estearyl-1,6-anhydroglucopyranose (CDCl₃).

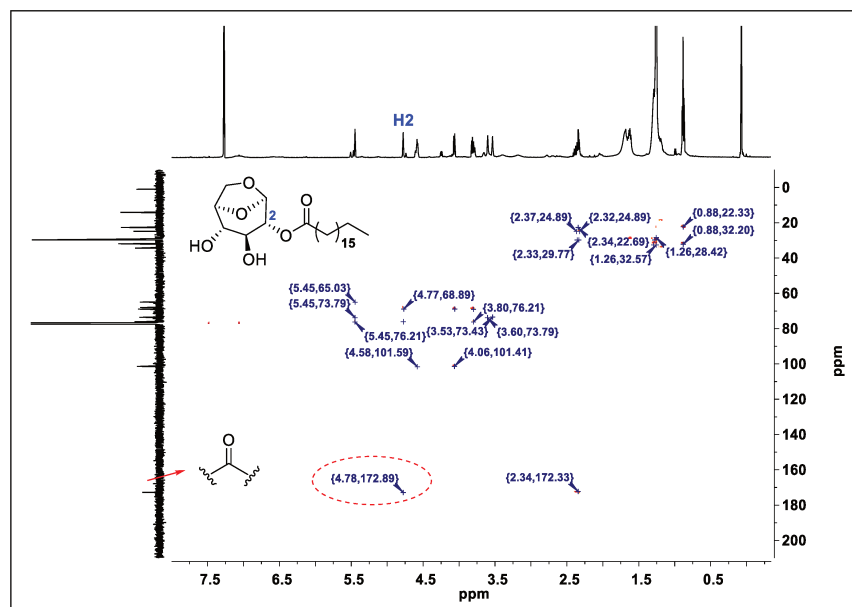


Figure S27: HMBC for 2-O-Estearyl-1,6-anhydroglucopyranose (CDCl₃).

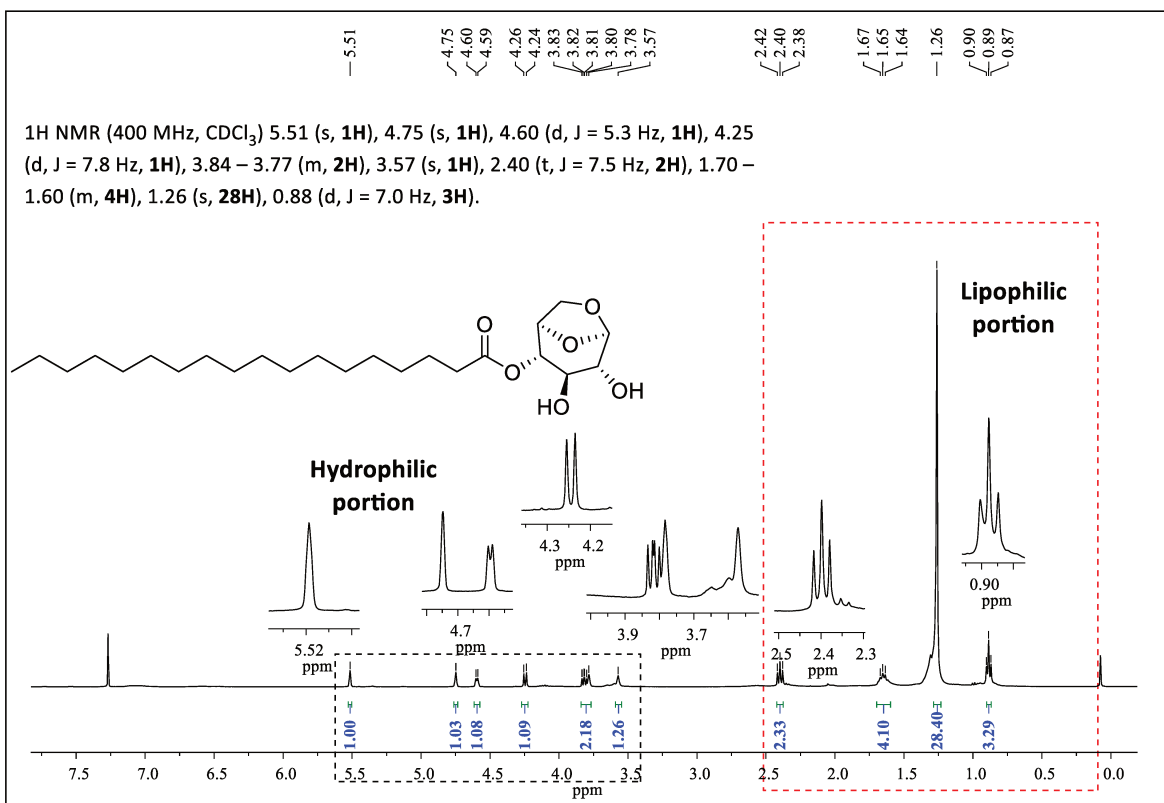


Figure S28: ^1H -NMR Spectrum for 4-O-Estearyl-1,6-anhydroglucopyranose (CDCl_3).

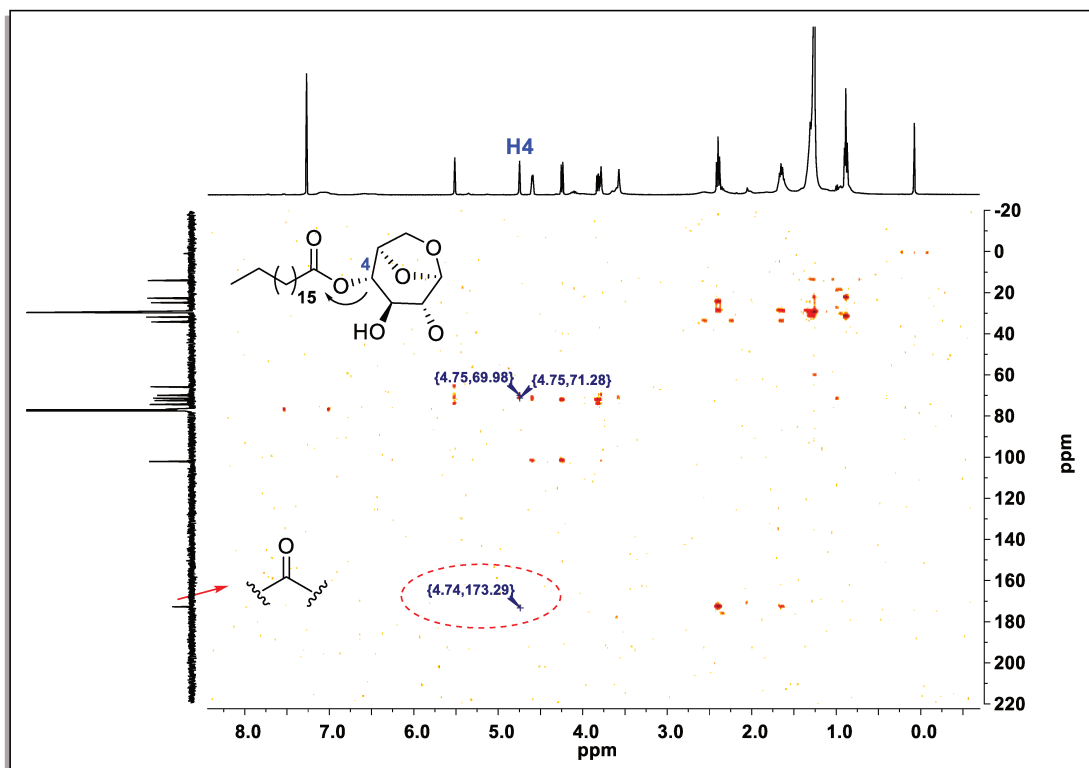


Figure S29: HMBC for 4-O-Estearyl-1,6-anhydroglucopyranose (CDCl₃).

ANNEX C

C1. Reaction optimization in continuous flow

C.1.1. Experimental setup

C1. Solubility tests of levoglucosan and acyl donors in acetonitrile

Levoglucosan and acyl donors vinyl laurate, ethyl laurate, lauric acid, vinyl stearate, vinyl oleate and vinyl palmitate were subjected to solubility tests. 40 and 100 mM solutions were prepared in a total volume of 500 mL of acetonitrile. The temperatures tested were 45, 50 and 55 °C and shaken at 200 rpm in an orbital shaker incubator for 30 min. The numbers below have been assigned in relation to the solubility of the reagents:

- 1 – Insoluble: turbid solution and background body;
- 2 – Partially soluble: turbid solution;
- 3 – Completely soluble: Clear solution.

Table C1: Solubility tests of levoglucosan and acyl donors in acetonitrile

Reagent	Temperature (°C)					
	45		50		55	
	40 mM	100 mM	40 mM	100 mM	40 mM	100 mM
Levoglucosan	1	1	1	1	3	3
Lauric acid	3	3	3	3	3	3
Ethyl laurate	2	2	2	2	2	2
Vinyl laurate	2	2	3	3	3	3
Vinyl stearate	2	2	3	3	3	3
Vinyl palmitate	3	3	3	3	3	3
Vinyl oleate	3	3	3	3	3	3

C.2. CCD planning matrix

Table C2: CCD planning matrix for two variables real and normalized levels and the response obtained.

EXP	X ₁	X ₂	Conversão %
1	(-1)	(-1)	31
2	(1)	(-1)	38
3	(-1)	(1)	50
4	(1)	(1)	54
5	(-1,42)	(0)	26
6	(1,42)	(0)	36
7	(0)	(-1,42)	28
8	(0)	(1,42)	54
9	(0)	(0)	54
10	(0)	(0)	54
11	(0)	(0)	56

C3. Reaction Optimization

The reaction of levoglucosan (**1**) and aliphatic esters (laurate, palmitate, stearate and olete, respectively) was optimized for the formation of products with respect to different biocatalysts (N435, Calb_epoxy and PSIM) and incubation temperature.

Table C3: Regioselectivity in the enzymatic acetylation of levoglucosan in CH₃CN with ethyl aliphatic esters. Analyses were performed in a GC-MS.

$\text{1} + \text{R}-\text{C}(=\text{O})-\text{O}-\text{CH}_2-\text{CH}_3 \xrightarrow[\text{Acetonitrile, 50-65 } ^\circ\text{C, 120 h}]{\text{Biocatalyst 0.8 \% (v/v)}} \text{3-I} + \text{3-II} + \text{3-III} + \text{4}$

$\text{2 a: R}=\text{CH}_3(\text{CH}_2)_{10}$
 $\text{b: R}=\text{CH}_3(\text{CH}_2)_{14}$
 $\text{c: R}=\text{CH}_3(\text{CH}_2)_{16}$
 $\text{d: R}=\text{CH}_3(\text{CH}_2)_7\text{CHCH}(\text{CH}_2)_7$

Entry	Biocatalyst ¹	AcylDonor ²	Regioselective (%)								
			50°C			55°C			65°C		
			3-I	3-II	3-III	3-I	3-II	3-III	3-I	3-II	3-III
1	N435	a	99	-	-	48	-	52	51	-	49
2		b	46	-	54	50	-	50	50	-	50
3		c	23	23	54	51	-	49	60	-	40
4		d	72	-	28	68	-	32	66	-	34
5	Calb_epoxy	a	73	-	27	64	-	36	99	-	-
6		b	51	-	49	73	-	27	94	-	6
7		c	-	-	-	78	-	22	81	-	19
8		d	99	-	-	99	-	-	99	-	-
9	PSIM	a	99	-	-	87	-	13	95	5	-
10		b	90	-	10	79	-	21	99	-	-
11		c	72	28	-	43	14	43	-	-	-
12		d	74	-	26	97	-	3	99	-	-

¹ N435 = Novozym 435 (*Candida antarctica* lipase B), immobilized on macroporous acrylic type ion exchange resin; Calb_epoxy = *Candida antarctica* lipase B immobilized on epoxy support by our research group and PSIM = lipase from *Pseudomonas cepacea* immobilized on ceramic particles.

² 2 equivalents, **a** = ethyl laurate, **b** = ethyl palmitate, **c** = ethyl stearate and **d** = ethyl oleate.

ANNEX D

D1. Determination of surface activity

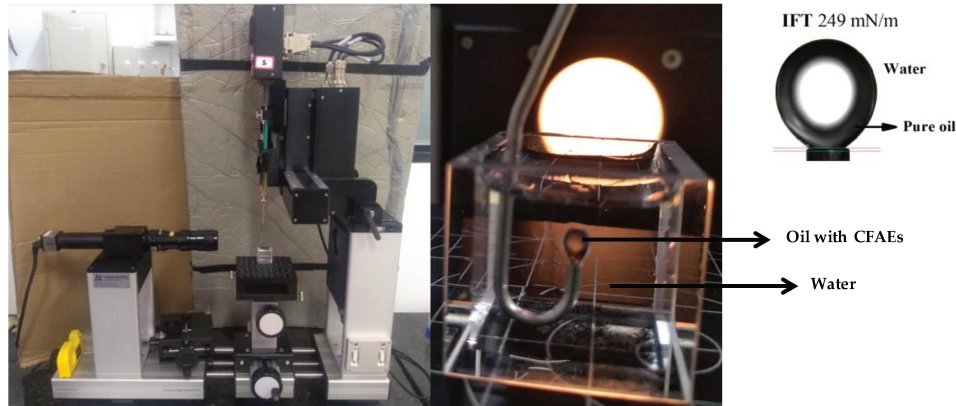


Figure S31: Evaluation of pendant drop method using Goniometer OCA25 (DataPhysic Instruments, Germany)

Table D1: Variation of the interface tension with the concentration of CFAEs: MONLAU, MONPAL, MONEST and MONOLE in oil at 25 °C

Compound	CONCENTRATION (mM)											
	0	5	10	20	30	40	50	60	75	100	120	150
	IFT[mN/m]											
MONLAU	249,39	176,6	166,9333	137,1033	115,3817	111,8117	96,39	88,71833	90,55667	90,55667	90,49333	89,97667
MONPAL	249,39	184,85	155,966	133,252	121,818	105,58	88,214	88,53	86,576	89,48	88,356	86,346
MONEST	249,39	226,435	222,73	212,1933	200,3917	178,6117	177,4317	171,5917	141,16	135,56	140,1933	139,655
MONOLE	249,39	237,5083	198,1483	188,79	158,9	148,5333	134,6317	102,4817	105,3367	104,0533	103,1367	105,6033

Table D2: Variation of the interface tension with the concentration of MONLAU in oil at 25 °C

Compound	CONCENTRATION (mM)										
	5	10	20	30	40	50	60	75	100	120	150
	IFT[mN/m]										
MONLAU	175,6	168,13	136,85	114,99	111,95	96,87	89,31	90,58	91,3	90,78	91,14
	176,47	167,52	136,77	115,16	111,98	96,78	89,14	90,8	91,17	90,52	89,14
	177,91	166,94	136,75	115,21	111,8	95,49	88,73	91,14	91,17	89,91	88,73
	177,24	166,34	136,7	115,9	111,4	96,77	88,53	90,02	90,58	90,42	90,52
	176,31	166,12	137,69	115,36	111,83	95,9	88,43	90,78	89	90,91	89,91
	176,07	166,55	137,86	115,67	111,91	96,53	88,17	90,02	90,12	90,42	90,42
Average	176,6	166,9333	137,1033	115,3817	111,8117	96,39	88,71833	90,55667	90,55667	90,49333	89,97667
Sd	0,837568	0,766385	0,525268	0,341843	0,213112	0,565084	0,435266	0,452975	0,885362	0,348578	0,905951

Sd: Standard deviation

Table D3: Variation of the interface tension with the concentration of MONPAL in oil at 25 °C

Compound	CONCENTRATION (mM)										
	5	10	20	30	40	50	60	75	100	120	150
	IFT[mN/m]										
MONPAL	185,71	154,56	134,59	123,12	106,58	89,39	88,34	87,11	89,76	88,9	86,17
	184,15	155,57	134,41	121,98	106,01	88,95	87,91	86,17	89,63	88,52	86,06
	184,4	155,95	132,51	121,66	105,55	88,88	87,87	86,06	89,48	88,11	86,06
	184,28	156,79	131,9	121,7	105,28	87,05	89,36	86,05	89,36	88,34	86,05
	185,71	156,96	132,85	120,63	104,48	86,8	89,17	87,49	89,17	87,91	87,39
Average	184,85	155,966	133,252	121,818	105,58	88,214	88,53	86,576	89,48	88,356	86,346
Sd	0,790032	0,974797	1,190722	0,890461	0,788321	1,196089	0,699035	0,676077	0,229891	0,381615	0,585688

Sd: Standard deviation

Table D4: Variation of the interface tension with the concentration of MONEST in oil at 25 °C

Compound	CONCENTRATION (mM)										
	5	10	20	30	40	50	60	75	100	120	150
	IFT[mN/m]										
MONEST	225,68	221,57	211,57	200,04	177,94	178,01	171,7	142,56	136,51	137,8	141,25
	227,78	221,45	210,91	200,71	177,92	177,36	171,37	142,25	136,27	139,01	141,36
	226,61	223,17	213,17	199,72	181,39	176,78	170,87	138,66	133,18	142,56	140,88
	225,87	222,59	212,59	200,66	176,82	177,31	171,9	141,25	136,14	142,25	137,09
	227,44	225,4	211,75	200,58	179,85	178,43	171,47	141,36	135,42	138,66	135,47
	225,23	222,2	213,17	200,64	177,75	176,7	172,24	140,88	135,84	140,88	141,88
Average	226,435	222,73	212,1933	200,3917	178,6117	177,4317	171,5917	141,16	135,56	140,1933	139,655
Sd	1,018916	1,456503	0,927053	0,411165	1,68135	0,679865	0,471568	1,380188	1,225186	1,989067	2,683123

Sd: Standard deviation

Table D5: Variation of the interface tension with the concentration of MONLAU in oil at 25 °C

Compound	CONCENTRATION (mM)										
	5	10	20	30	40	50	60	75	100	120	150
	IFT[mN/m]										
MONOLE	238,53	198	187,84	158,84	152,43	134,95	102,67	107,41	102,94	103,4	105,85
	237,96	198,18	188,69	157,61	147,96	134,53	103,88	107,12	103,66	102,67	107,41
	237,79	197,36	187,67	161,79	148,21	135,48	102,21	104,61	104,33	103,88	107,12
	236,89	199,73	190,55	160,04	147,95	134,67	101,69	104,97	104,02	102,21	104,61
	236,67	197,66	191,98	158,04	147,34	134,29	101,77	102,94	103,4	101,69	104,97
	237,21	197,96	186,01	157,08	147,31	133,87	102,67	104,97	105,97	104,97	103,66
Average	237,5083	198,1483	188,79	158,9	148,5333	134,6317	102,4817	105,3367	104,0533	103,1367	105,6033
Sd	0,707288	0,827053	2,152626	1,753362	1,943097	0,553115	0,80415	1,674511	1,055683	1,196021	1,468982

Sd: Standard deviation

D2. Antibacterial Assays

Table D6: Strains used in the antibacterial assays.

Bacterial species	Code	Isolation source	Susceptibility profile
<i>Staphylococcus aureus</i> subsp. <i>aureus</i> Rosenbach	ATCC 29213	Injury	Sensitive to methicillin
	ATCC 33591	Clinical isolate	Resistant to methicillin
	ATCC 25933	Clinical isolate	Sensitive to methicillin
<i>Staphylococcus aureus</i>	517	Blood	Resistant to methicillin

ANNEX E

In this section, all the publications resulting from this work are attached.



Article

Regioselective Acylation of Levoglucosan Catalyzed by *Candida Antarctica* (CaLB) Lipase Immobilized on Epoxy Resin

Marcelo Azevedo do Nascimento ¹, Larissa Ester Gotardo ¹, Eduardo Miguez Bastos ², Fabio C. L. Almeida ³, Raquel A. C. Leão ^{3,4}, Rodrigo O. M. A. de Souza ¹, Robert Wojcieszak ^{5,6} andIVALDO IBAIANA JR. ^{5,*}

- ¹ BCCS Group—Biocatalysis and Organic Synthesis Group, Chemistry Institute, Federal University of Rio de Janeiro, Rio de Janeiro 21941-909, Brazil; marceloavelar@id.uff.br (M.A.d.N.); gotardolarissa@gmail.com (L.E.G.); capelaleao@gmail.com (R.A.C.L.); souzarrod@gmail.com (R.O.M.A.d.S.)
 - ² Instituto de Macromoléculas Professora Eliete Mano, Federal University of Rio de Janeiro, CEP 21941-908, Brazil; emiguez54@gmail.com
 - ³ Center of Structural Biology and Biomaging 1 (CENABIO 1), Federal University of Rio de Janeiro, Rio de Janeiro 21941-905, Brazil; lalmeida@biogmed.uff.br
 - ⁴ Pharmacy School, Federal University of Rio de Janeiro, Rio de Janeiro 21941-170, Brazil
 - ⁵ Univ. Lille, CNRS, Centrale Lille, ENSCI, Univ. Artois, UMR 8181-UCCS-Unité de Catalyse et Chimie des Solides, F-59000 Lille, France; robert.wojcieszak@univ-lille.fr
 - ⁶ Department of Biochemical Engineering, School of Chemistry, Federal University of Rio de Janeiro, Rio de Janeiro 21941-910, Brazil
- * Correspondence: ivaldo@eq.uff.br

Received: 17 September 2019; Accepted: 18 October 2019; Published: 31 October 2019



Abstract: Every year, a large amount of residual agroindustrial waste has been generated and only around 10% is in fact reused. The development of new strategies for biomass valorization is important to add value to these commodities, since biomass is an excellent alternative feedstock to obtain chemicals of interest from renewable resources. The major compound of pyrolytic treatment of lignocellulosic biomass is levoglucosan (1,6-anhydroglucopyranose), an anhydro-sugar that can be transformed into glucose and is greatly valued in the most diverse industrial sectors as a surfactant, emulsifier, or even a lubricant. In this work, levoglucosan was acylated by lipase-catalyzed transesterification in acetonitrile with great conversions and selectivities with different acyl donors such as ethyl esters of lauric, palmitic, stearic, and oleic acids prepared in situ in an integrated strategy mediated by commercial lipases Novozym435 (N435), PSIM, and the home-made biocatalyst CaLB_epoxy. As a result, all biocatalyst generated mostly monoesters, with N435 being more selective to produce lauric esters (99% at 50 °C) and PSIM to produce oleic esters (97% at 55 °C) while CaLB_epoxy was more selective to produce oleic esters of levoglucosan (83% at 55 °C). This is the first report in the literature on the production of high selectivity levoglucosan esters.

Keywords: levoglucosan; CaLB; lipase; immobilization; NOEdiff; transesterification; esters

1. Introduction

Biotechnology has focused its attention on the development of sustainable processes. The Twelve Principles of Green Chemistry reflect the need for actions in the development of bioprocesses both at universities and in industries [1]. In this context, the availability of cheap raw materials and renewable energy is the basis for global sustainability, where strategies for the development of clean technologies for chemical processes has aimed to balance economic and environmental aspects [2]. In this trend, the

CRITICAL REVIEW

View Article Online

DOI: 10.1039/C5GC00149G


 Cite this: *Green Chem.*, 2016, **18**, 5859

Levoglucosan: a promising platform molecule?

 Ivaildo Itabiana Junior,^a  [✉] Marcelo Avelar do Nascimento,^b Rodrigo Octavio Mendonça Alves de Souza,^c  [†] Anthony Dufour  [‡] and Robert Wojcieszak  ^{✉*}

Lignocellulosic biomass is the most abundant carbon source and it is a base of the whole biorefinery concept. Levoglucosan (1,6-anhydro- β -D-glucopyranose) (LG) is an anhydro sugar formed as a major product during pyrolysis of cellulose. LG might be a promising chemical platform. It can be converted to different high added-value chemicals such as levoglucosone, 5-hydroxymethylfurfural and styrene directly or through a glucose intermediate via chemical, catalytic and biochemical processes. In this critical review we focus not only on the pyrolytic methods for the synthesis of levoglucosan, but above all also on the recent scientific progress in the chemical and biochemical transformation of levoglucosan to highly valued compounds. The catalytic performances of the heterogeneous and enzymatic catalytic systems used for different reactions of LG conversion are reviewed. Specific properties of the active sites, roles of additives, and solvents and conditions are discussed in detail. We conclude our recommendations to further improve LG conversion to high added-value products.

 Received 20th April 2016
Accepted 7th June 2016
DOI: 10.1039/C5GC00149G
www.rsc.org/greenchem

^aUnité UMR, CNRS, Centre-Lille, Des. Actus, 59650 RUMILLY-LES-VALLÉES – Institut de Catalyse et Chimie du Solide, F-69626 LILLÉ, FRANCE.

E-mail: Robert.wojcieszak@univ-lille.fr

^bDepartment of Biomedical Engineering, School of Chemistry, Federal University of Rio de Janeiro, 21941-910 Rio de Janeiro, Brazil

^cBIOT Group – Biocatalysis and Organic Synthesis Group, Chemistry Institute, Federal University of Rio de Janeiro, 21941-910 Rio de Janeiro, Brazil

[†]UMR, CNRS, Université de Lorraine, 54002, 1 rue Grandville, 54000 Nancy, France

1. Introduction

The need for natural resources has influenced the development of human society throughout history. Due to the increase of life expectancy, the world population has been growing alarmingly, bringing as immediate consequences the increase of industrial and agricultural activities as a way to supply the energy and food demands.^{1,2} As a direct consequence of this



Ivaildo Itabiana Junior

Professor Ivaildo Itabiana Junior obtained his PhD in pharmaceutical science from the Federal University of Rio de Janeiro, Brazil where he is now a full professor. He has experience in biocatalysis, biotransformation and the use of biomass for the production of bio-products of industrial interest. He has extensive collaboration with CNRS Lille, France working on the development of a new concept of

hybrid catalysis for the transformation of biomass residues, such as pyrolysis oils, lignin and microbial hydrolysis derivatives into products with higher added value. His research interests are biocatalysis, enzymatic biotechnology (lipases, oxidoreductases, lactases), enzyme immobilization and drug delivery.



Marcelo Avelar do Nascimento

MSc Marcelo Avelar is graduated in Applied Chemistry at the Federal Fluminense University (UFF, 2016) and obtained his master's degree in Chemistry in 2016 from the Program of Post-Graduation in Chemistry (PGQ) from the Federal University of Rio de Janeiro (UFRJ). He is currently a PhD student at INQa and is supervised by professors Ivaildo Itabiana Jr. and Rodrigo M. A. de Souza. Marcelo has experience in the biocatalysis of levoglucosan and the immobilization of enzymes for application in batch and continuous flow systems.



Cite this: RSC Adv., 2022, 12, 3027

Lipase-catalyzed acylation of levoglucosan in continuous flow: antibacterial and biosurfactant studies†

Marcelo A. do Nascimento,^{a*} Juan P. C. Vargas,^b Jose G. A. Rodrigues,^c Raquel A. C. Leão,^d Patricia H. B. de Moura,^e Ivana C. R. Leal,^e Jonathan Baisuf,^f Rodrigo O. M. A. de Souza,^{g*} Robert Wojcieszak^h and Valdo Itabiana Jr.^{g,††}

Studies involving the transformation of lignocellulosic biomass into high value-added chemical products have been intensively conducted in recent years. Its matrix is mainly composed of cellulose, hemicellulose and lignin, being therefore, an abundant and renewable source for obtaining several platform molecules, with levoglucosan (LG) standing out. This anhydrous carbohydrate can be acylated to obtain carbohydrate fatty acid esters (CFAEs). Here, these compounds were obtained via enzymatic acylation of LG, commercially obtained (Stari BioScience®), with different acyl donors in continuous flow. Through the experimental design using a model reaction, it was possible to optimize the reaction conditions, temperature and residence time, obtaining a maximum conversion at 61 °C and 77 min. In addition, there was a productivity gain of up to 100 times in all comparisons made with the batch system. Finally, CFAEs were applied in tests of interfacial tension and biological activity. For a mixture of 4- and 2-O-lauryl-1,6-anhydroglucopyranose (MONLAU), the minimum interfacial tension (IFT^{min}) obtained was 96 mN m⁻¹ and the critical micelle concentration (CMC) was 50 mM. Similar values were obtained for a mixture of 4- and 2-O-palmitoyl-1,6-anhydroglucopyranose (MONPAL), not yet reported in the literature, of 88 mN m⁻¹ in 50 mM. For a mixture of 4- and 2-O-stearoyl-1,6-anhydroglucopyranose (MONEST) and 4- and 2-O-decyl-1,6-anhydroglucopyranose (MONDEC), CMC was higher than 60 mM and IFT^{min} of 141 mN m⁻¹ and 102 mN m⁻¹, respectively. Promising data were obtained for minimal inhibitory concentration (MIC) and minimal bactericidal concentration (MBC) of MONLAU against *Staphylococcus aureus* strains at 0.25 mM.

Received 5th November 2021

Accepted 12th January 2022

DOI: 10.1039/D2RA00011G

rsc.advances

Introduction

Carbohydrates, also called sugars, are the most abundant organic substances in the biological world that make up more than 50% of the dry weight of the earth's biomass, being

essential for life.^{1–3} These compounds can be partially acylated via chemo or enzymatic reactions in batch or continuous flow conditions with different acyl donors to access a variety of mono- or oligosaccharide esters which may have valuable properties with wide applications in the food, pharmaceutical, detergent, agricultural, fine chemical and personal care industries.^{4,5}

In this scenario, levoglucosan (1,6-anhydro-β-D-glucopyranose) (LG) might be a promising chemical platform for the synthesis of carbohydrate fatty acid esters, denoted as CFAEs. LG is a major product of cellulose pyrolysis and it can be converted to different high added-value chemicals such as glucose, 5-hydroxymethylfurfural, furfural, sorbitol, levoglucosone and, as highlighted in this work, CFAEs (Fig. 1).⁶

The structure-activity relationship of CFAEs depends on the degree of substitution of the hydroxyl groups, in addition to the size and amount of unsaturation in the alkyl chains,^{6a} which can generate compounds with a hydrophobic-lipophilic balance (HLB) of great industrial interest as emulsifying agents, stabilizers in conventional systems and also promising biological activities as already mentioned.^{6a} It is important to

^aBioactivity and Organic Synthesis Group, Chemistry Institute, Federal University of Rio de Janeiro, CEP 219-098, Brazil

^bNanochemistry Engineering Program, COPPE, Universidade Federal do Rio de Janeiro, CEP Rio de Janeiro, Brazil

^cInstitute of Chemistry, Federal University of Rio de Janeiro, University City, 21941-909, Rio de Janeiro, Brazil

^dLaboratory of Natural Products and Biological Assays, Department of Natural Products and Food, Pharmacy Faculty, Federal University of Rio de Janeiro, 21941-902, Rio de Janeiro, Brazil

^eUnité L6E, CNRS, Centre de Recherche sur les Biomolécules, 2007-2009 de Courcouronnes, 77300, France

^fLaboratory of Biotechnological Biochemistry and Biocatalysis, Department of Biochemical Engineering, School of Chemistry, Federal University of Rio de Janeiro, 21941-909, Rio de Janeiro, Brazil. Email: rba@ciq.ufrj.br

† Electronic supplementary information (ESI) available: See ESI, 10.1039/D2RA00011G





A new approach for the direct acylation of bio-oil enriched with levoglucosan: Kinetic study and lipase thermostability

Marcelo A. do Nascimento^{a,c}, Raquel A.C. Leão^a, Rénato Froidevaux^b, Robert Wojcieszak^c,
Rodrigo O.M. A. de Souza^a,IVALDO IZABELA JR.^{a,c,d,*}

^a BOD Group - Biocatalysis and Organic Synthesis Group, Chemistry Institute, Federal University of Rio de Janeiro, Brazil

^b UMR 7048 BioAlgo (UMR 7118, Institut Charles Villiers, INRAE, Agropar Interactions/Biocatalyse et Enzymes - Université de Lille, Millepied Polytech/Life, CNRS, Sorbonne, FRESY Villesaveur d'Alain, France

^c Univ. Lille, CNRS, Centrale Lille, Univ. Artois, UMR 8381 - UCCS - Unité de Catalyse et Chimie du Solide, Lille, France

^d Department of Biochemical Engineering, School of Chemistry, Federal University of Rio de Janeiro, Brazil

ARTICLE INFO

Keywords:
Lipases
Levoglucosane
Pyrolysis of biomass
Kinetics
Thermostability

ABSTRACT

Lignocellulosic biomass can be valorized by fast pyrolysis, generating a bio-oil with levoglucosane (LGL), anhydrous sugar applied as building block for several compounds of great industrial interest. In this work we demonstrated for the first time the direct transesterification of LGL with different acyl donors by free and immobilized lipases. Influence of acetonitrile (ACN) and cyrene (CYE) in the stability of lipases from *Candida rugosa* and *Candida antarctica* B by differential scanning Nano fluorimetry (NanoDSF), at substrate concentrations of 20–300 mM as well as the alkyl chain effect for synthesis of the carboxylate fatty acid esters (CFAs) were carried out at 55 °C. Best results were obtained with Novozym® 435 in ACN and ethyl octanoate (EO) with 76% of conversion against 58% in CYE and ethyl palmitate (EP). In general it was observed that increasing on hydrophobicity of acyl donor contributed to greater regioselectivity for the hydroxyl bound to carbon 4 with up to 87% for C16 in ACN. Thermostability profile of GR1 and CR suggested higher stability in CYE with values of $T_{50} = 61$ °C for GR1 and $T_{50} = 53$ °C for CR. Finally, the kinetic parameters were obtained through the Michaelis-Menten constants generated by the double-reciprocal plot and indicated an inhibition by the L1 substrate. Moreover, catalytic efficiency data suggest higher enzyme-substrate affinity in CYE.

1. Introduction

As the world population's life expectancy increases, the consumption of fossil reserves has increased to meet increased energy demands. It is estimated that between 2015 and 2040, energy consumption will increase by 28% [1]. As a result of this high population growth and disorderly consumption of both raw materials and consumer goods, global warming and different types of pollution are evident, which reinforces both in academia and in industry, the search for renewable energy sources and the establishment of more sustainable protocols to reduce greenhouse gas emissions and increase energy efficiency [2].

In this context, lignocellulosic biomass has been emerging as an auspicious and renewable source, as it is abundant and able to replace fossil materials in several applications and contribute to 10% of the global energy supply [3]. Its composition ranges from 40% to 50% cellulose, 20–30% hemicellulose, 20–25% lignin, and 1.5–3% ash [4].

However, different protocols have been designed to convert this material into high value-added products, it is still estimated that 182 billion tons of residual biomass is generated each year and only around 10% is reused [4]. In this trend, the development of new platforms for the valorization of these resources is essential to promote a circular economy [5].

Several approaches have been applied for the valorization of biomass [6]. Among them, thermochemical routes have gained prominence in recent years. It is highlighted, the pyrolysis has generally been used because it involves a single-step process, does not use any solvents or enzymes to depolymerization, facilitating the efficient conversion of most biochemical constituents of raw biomass into useful energy products [7], where fast pyrolysis has been the most interesting, since different derivative molecules can be obtained in a short time and dispersed in the three main fractions, gas fraction, which can be charred and generate several derivative molecules, biochar, which can

* Corresponding author at: Univ. Lille, CNRS, Centrale Lille, Univ. Artois, UMR 8381 - UCCS - Unité de Catalyse et Chimie du Solide, Lille, France.
E-mail address: ivaldo@ag.uqj.fr (I. Izabela Jr.).

<https://doi.org/10.1016/j.bej.2023.108913>

Received 4 February 2023; Received in revised form 30 March 2023; Accepted 26 March 2023

Available online 29 March 2023

1369-703X/ Published by Elsevier B.V.

Collaborations unrelated to the thesis



Immobilized lipase screening towards continuous-flow kinetic resolution of (\pm)-1,2-propanediol

Anderson R. Aguilón^a, Marcelo N. Avelar^a, Larissa E. Gotardo^a, Stefania P. de Souza^a, Raquel A.C. Leão^{a,b},IVALDO ITABAIANA JR.^a, Leandro S.M. Miranda^a, Rodrigo O.M.A. de Souza^{a,b}



Show more

Add to Mendeley Share Cite

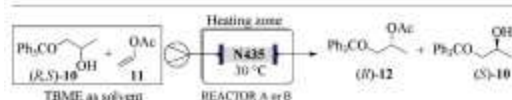
<https://doi.org/10.1016/j.mcat.2019.01.034>

Get rights and content

Abstract

Here, we report a flow chemistry approach for kinetic resolution of (\pm)-1,2-propanediol protected by trityl group using the packed-bed reactor filled with different immobilized enzymes. It was investigated the performance of 16 immobilized lipases, including commercial Lipozyme TL, Novozym 51032, Novozym 435 (N435) and lipases immobilized by our group. Based on the values of conversion and enantioselectivity, batch experiments were then translated to the continuous-flow environment. Continuous flow (CF) reactors allowed reaction time reduction, from 6 h in batch to 7 min, keeping the values of conversion (up to 50%) and selectivity (E value >200) during the reaction procedure using the commercial enzyme Novozym 435. In addition, continuous flow conditions increased the productivity of kinetic resolution 3 times when compared to conventional batch reactor, after its optimization.

Graphical abstract



Download Download full-size image



Synthesis and characterization of a magnetic hybrid catalyst containing lipase and palladium and its application on the dynamic kinetic resolution of amines

Clara A. Ferraz^a, Marcelo A. do Nascimento^b, Rhudson F.O. Almeida^b, Gabriella G. Sergio^a, Aldo A.L. Junior^a, Gisele Dalmónico^a, Richard Caraballo^a, Priscilla V. Finotelli^a, Raquel A.C. Leão^{a,b}, Robert Wojcieszak^a, Rodrigo O.M.A. de Souza^a,IVALDO ITABAIANA JR.^a

Show more

Add to Mendeley Share Cite

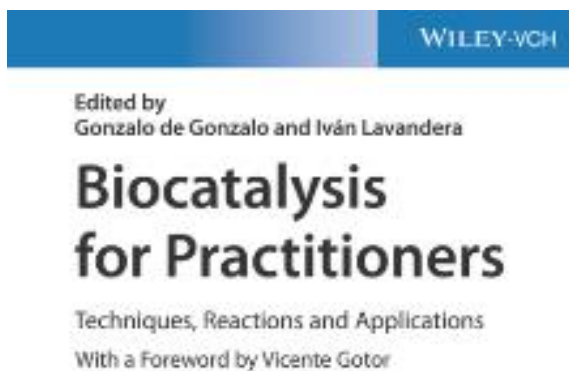
<https://doi.org/10.1016/j.mcat.2020.111106>

Get rights and content

Abstract

Recent papers estimates that about 40 % of drugs present chiral amines in their structure and their synthesis in a sustainable and cost-competitive way still a challenge for the industry. Kinetic resolution is one of the most applied method to produce these desired compounds where the association with lipase as a catalyst is a good alternative. However the use of separate racemization catalyst and enzymes in the reaction medium still limits recovery, recycling and can occasionally be responsible for decreasing in selectivity for the desired product. In this work we proposed the synthesis and characterization of a hybrid magnetic catalyst composed containing lipase Cal. B and Pd immobilized on the same recovered nanometric magnetic support for the application on Dynamic Kinetic Resolution of (*rac*)-1-phenylethylamine both in batch and continuous flow conditions. As results it was possible to achieve 99 % of conversion, with 95 % of selectivity and 93 % of enantiomeric excess after 12 h in batch. For a continuous flow system, it was possible to achieve 95 % of conversion with 71 % of selectivity and *ee* > 99 % after 60 min of reaction. The hybrid catalyst had around 50–100 nm with nanoparticulated Pd (5–10 nm) on its surface, presented a superparamagnetic behavior without remaining magnetization and 22 emu/g of saturation magnetization.

Book Chapter



Voies biotechnologiques pour l'obtention de composés à haute valeur ajoutée à partir de la biomasse résiduelle

RÉSUMÉ

Chaque année, des milliards de tonnes de biomasse lignocellulosique sont générées, et seule une petite partie est réutilisée, couramment utilisée comme nourriture et/ou à des fins énergétiques et matérielles. Par conséquent, de nouvelles stratégies sont nécessaires pour valoriser ces matières premières, car la biomasse est une excellente matière première alternative pour obtenir des produits chimiques d'intérêt à partir de ressources renouvelables. Dans cette tendance, une autre alternative prometteuse est l'application d'enzymes en conjonction avec la chimie synthétique pour explorer de nouveaux produits d'intérêt industriel. Parmi les produits de la pyrolyse rapide se trouve le bio-huile, dont le composant principal est le lévoglucosane (1,6 anhydroglucopyranose), un sucre anhydre utilisé comme élément de base pour divers composés d'intérêt industriel. Dans cette étude, du lévoglucosane commercial (LGCom) et du lévoglucosane obtenu à partir de la pyrolyse de la cellulose (BoE) ont été acylés par transestérification / estérification en utilisant divers donneurs d'acyl dans des systèmes en continu et en batch catalysés par des lipases libres et immobilisées en présence de différents solvants organiques. Enfin, les CFAE ont été testés pour la tension interfaciale et l'activité biologique. Des données prometteuses ont été obtenues pour la concentration inhibitrice minimale (CIM) et la concentration bactéricide minimale (CBM) de MONLAU contre les souches de *Staphylococcus aureus* à 0,25 mM.

Mots-clefs: Lipase, Transestérification, Glucides et Biomasse.

Biotechnological Routes for Obtaining High-Added Value Compounds from Residual Biomass

ABSTRACT

Every year, billions of tons of lignocellulosic biomass are generated, and only a small portion is reused, commonly used as food and/or for energy and material purposes. Therefore, new strategies are needed to valorize these raw materials, as biomass is an excellent alternative feedstock for obtaining chemicals of interest from renewable resources. In this trend, another promising alternative is the application of enzymes in conjunction with synthetic chemistry to explore new products of industrial interest. Among the products of fast pyrolysis is bio-oil, whose main component is levoglucosane (1,6 anhydroglucopyranose), an anhydrous sugar used as a base for various industrially relevant compounds. As a result, all biocatalysts mainly produced carbohydrate fatty acid esters (CFAEs) with different selectivities. In the batch reaction using BoE, the best results were obtained with N435 in ACN, with the acyl donor ethyl octanoate (C8) achieving a conversion of 74%. The thermal stability profiles of CalB and CR suggested increased stability in CYE, with protein melting point (T_m) values of 61°C for CalB and 53°C for CR. From the kinetic parameters obtained from the Michaelis-Menten constants, substrate inhibition by LG was indicated. Finally, CFAEs were tested for interfacial tension and biological activity. Promising data were obtained for the minimum inhibitory concentration (MIC) and minimum bactericidal concentration (MBC) of MONLAU against *Staphylococcus aureus* strains at 0.25 mM.

Key words: Lipase, Transesterification, Carbohydrate and Biomass.